

FORMAZANS

A Structural and Spectroscopic Study

of

3-Substituted-1,5-Diphenylformazans



Presented in partial fulfilment for the degree
of Doctor of Philosophy in Chemistry
at Victoria University of Wellington
by

Christopher William Cunningham

December, 1988.

STATEMENT

The work presented in this thesis is wholly the work of the author except where indicated in the text. Co-authors of papers are acknowledged as such in the respective chapter. This work was undertaken at the Chemistry Department of Victoria University under the supervision of Dr Gary R. Burns between August, 1983 and December, 1988 on a part-time basis.

Some practical work was completed at the Chemistry Division and Physics and Engineering Laboratory of the Department of Scientific and Industrial Research, Gracefield. X-ray crystal structures were solved at the University of Canterbury, Christchurch.

ABSTRACT

A series of thirteen isomeric 1,5-diphenylformazans have been structurally characterised both in the solid state and in solution by the combined techniques of x-ray crystallography, nuclear magnetic resonance, Raman, mass and absorption spectroscopies.

1,5-Diphenylformazan is known to exist in the *anti,s-trans* configuration in the solid state and this is shown to be the solution dominant species. In aprotic solvents an equilibrium involving the *anti,s-trans* and *syn,s-cis* configurations is evidenced.

3-Methyl-1,5-diphenylformazan has been characterised by an x-ray crystal analysis. $C_{14}H_{14}N_4$ belongs to the monoclinic space group $P2_1/c$, $a = 8.133(1)$, $b = 19.085(4)$, $c = 9.364(2)$ Å, $\beta = 105.93^\circ$, $U = 1397.6(5)$ Å³, $Z = 4$. The *anti,s-trans* configuration of the solid state is also preferred in solution where it is in equilibrium with the *syn,s-cis* configuration.

3-Ethyl-1,5-diphenylformazan exists in two isomers in the solid state, both of which have been characterised by an x-ray crystal analysis. The red isomer of 3-ethyl-1,5-diphenylformazan belongs to the orthorhombic space group $P2_12_12_1$ and adopts the *syn,s-trans* configuration in the solid state. The orange, light stable isomer of 3-ethyl-1,5-diphenylformazan belongs to the monoclinic space group $P2_1/c$ and adopts the *anti,s-trans* configuration in the solid state. The rate of return of the photo-activated orange isomer to the dark-stable red isomer follows first order kinetics dependent upon the total concentration of the formazan and the water content of the solvent.

3-Tertiary-butyl-1,5-diphenylformazan has been characterised by an x-ray crystal analysis. $C_{17}H_{20}N_4$ belongs to the monoclinic space group $P2_1/c$, $a = 11.235(3)$, $b = 20.117(5)$, $c = 14.176(3)$ Å, $\beta = 92.14(2)^\circ$, $U = 3202(1)$ Å³, $Z = 8$. The *syn,s-cis* configuration of the solid state is maintained in solution.

1,3,5-Triphenylformazan is shown to exist in two red forms in the solid state. The *syn,s-cis* and *syn,s-trans* isomers are both present in the crystalline sample. These isomers are also evident in solution with the *syn,s-trans* configuration becoming more dominant in aprotic solvents.

1,5-Diphenylformazan reacts with bromine in solution in a single reaction to give di(3-bromo-1,5-diphenyltetrazolium)-decabromide and 3-bromo-1,5-di-*para*-phenylformazan, both of which have been characterised by an x-ray crystal analysis. $C_{13}H_{10.6}N_4Br_{5.3}$ belongs to the triclinic space group $P1$, $a = 8.572(1)$, $b = 9.711(1)$, $c = 14.166(3)$ Å, $\alpha = 75.18(1)$,

$\beta = 89.84(1)$, $\gamma = 70.42(1)^\circ$, $Z = 2$. Stacks of anti-parallel pairs of 3-bromo-1,5-diphenyltetrazolium cations are interleaved by pairs of Br_{10}^{2-} anions. The polybromide represents a new type of polyhalogen network for bromine, Br_{10}^{2-} , the Raman spectrum of which has been recorded for the first time. $\text{C}_{13}\text{H}_9\text{N}_4\text{Br}_3$ belong to the orthorhombic space group $Pnma$, $a = 7.343(2)$, $b = 32.793(12)$, $c = 5.912(1)$ Å, $Z = 4$. The formazan adopts the *anti,s-trans* configuration in the solid state.

3-Chloro-1,5-diphenylformazan has been characterised by an x-ray crystal analysis. Preliminary results indicate that the formazan adopts the *anti,s-trans* configuration in the solid state.

3-Mercapto-1,5-diphenylformazan is shown to exist in the *anti,s-trans* configuration in CDCl_3 solution.

3-Methylthio-1,5-diphenylformazan is shown to exist in an equilibrium mixture of *syn,s-trans* and *anti,s-trans* configurations in solution. The ratio of the two isomers is approximately equal.

3-Ethylthio-1,5-diphenylformazan exists in two isomers in the solid state, one of which has been characterised by an x-ray crystal analysis. Preliminary results indicate that the orange isomer of 3-ethylthio-1,5-diphenylformazan. $\text{C}_{15}\text{H}_{16}\text{N}_4\text{S}$ belongs to the monoclinic space group $P2_1$, $a = 11.027(6)$, $b = 8.627(7)$, $c = 15.487(8)$ Å, $\beta = 93.70(5)^\circ$, $U = 1470$ Å³, $Z = 4$, and exists in the *anti,s-trans* configuration on the solid state. The orange and red isomers are both present in an equilibrium mixture in solution. The red isomer is shown to exist in the *syn,s-trans* configuration in the solid.

3-isopropylthio-1,5-diphenylformazan is shown to exist in an equilibrium mixture of *anti,s-trans* and *syn,s-trans* configurations in solution.

1-Methyl-1,5-diphenylformazan has been characterised by an x-ray crystal analysis. $\text{C}_{14}\text{H}_{14}\text{N}_4$ belongs to the monoclinic space group $I2_1$, $a = 28.402(7)$, $b = 5.640(1)$, $c = 15.688(4)$ Å, $\beta = 97.34^\circ$, $U = 2493(1)$ Å³, $Z = 8$. The formazan adopts the *anti,s-trans* configuration in the solid state. The formazan retains its configurational integrity in both protic and aprotic solutions. The excitation profile of the Raman active phonons based upon coupled vibrations of the formazan backbone indicate a maximum corresponding to the absorption spectra in both the solid state and in solution.

Preliminary results of a kinetic investigation of some primary metal dithizonates indicate that the thermal-path return is strictly first order. The mechanism would appear to be essentially similar to that operating in 3-ethyl-1,5-diphenylformazan.

The mass spectra of the series of formazan follow similar splitting schemes irrespective of the solid-state configuration.

ACKNOWLEDGEMENTS

Although only one name appears as the author of this thesis, it is truly the culmination of a sustained and continuous effort of countless many. As a proof of this statement I offer my gratitude to a selection of those countless individuals.

Firstly, and mostly, I thank my Mother, Father, my family and especially Joanne for their encouragement, support and interest.

My supervisor, Gary Burns, suggested the project and the collaboration with Dr Vickie McKee, Dr Ward Robinson, Dr Gerald Smith, Dr Roger Newman, Dr Keith Morgan, Dr Graham Bowmaker and Dr Herbert Wong, all of whom have generously contributed their spectroscopic expertise to myself and this project.

I am indebted to the Maori Education Foundation and Education Department for the awarding of a Maori and Polynesian Scholarship for Higher Education, Queen Elizabeth II Post Graduate Scholarship, Ti Maru Scholarship and Grants and Travel Awards given over the course of my University career; the Internal Research Committee of VUW; the Royal Society of New Zealand; the Wellington Branch of NZIC and the UGC for assistance during my Ph.D. enrolment.

I acknowledge the considerable technical assistance I have received with much gratitude to those professionals at VUW, the DSIR and other Universities.

Finally, I am grateful for the many friends I have made in the course of this Ph.D. - those in the Labs (Raj, Dugald, Victor, Suki, Li, Sally, Alan Freeman, Robyn, Joanne, Murray), those at work (Izabella, Ian, Viv, Priyanthi, Romani, David², Emmanuel, Eric, Eddie, Sheila, Rosalind, Raj, Rhyl, Susan) and those at play (Dennis, Paul, Sarah, Chi, Brian, Rob, Gordon, Douglas, and Teresa).

ABBREVIATIONS

nmr	nuclear magnetic resonance
Å	angstroms
o.d.	outside diameter
MAS	magic angle spinning
CP	cross polarisation
TOSS	toss out spinning sidebands (nmr software)
GASPE	gated spin echo (nmr software)
DEPT	Bruker software package
SSB	spinning side band
DMSO-d ₆	dimethyl sulphoxide, deuterated
lit.	literature

PREFACE

This investigation had as its aim the identification of the solid state structures of a series of isomeric 3-substituted formazans. This primary goal was envisaged in order to substantiate the solution and solid state structures proposed in the literature and to ultimately identify the thermally and photochemically promoted species available in the formazan equilibrium. The structures of these species are still the subject of considerable controversy. 1,5-Diphenylformazans were the compounds of choice as the effect of various 3-substituents differing both sterically and electronically could be studied.

X-ray crystallography is the definitive technique in the solid state where single crystals are available. The availability of new analytical techniques (solid state nmr and Raman spectroscopy) also affords the identification of individual isomers even in the absence of single crystals. However, the major advantage of magnetic resonance, vibrational and electronic spectroscopies is their ability to span the phases and, in particular, bridge the gap between solid state and solution structures.

In Chapter 1 formazans are introduced with the conventions of nomenclature. A summary of the literature is also given in the context of an historical survey. Proposed atomic and molecular structures and physical properties are introduced together with a brief description of the photochromic and thermochromic interconversions. The compounds chosen for study are also listed.

In Chapter 2 general experimental procedures are described. Particular experiments are detailed in the chapter where the results are discussed.

In Chapter 3 a brief review is given summarising the major results of previous spectroscopic studies. The results of the spectroscopic studies of this thesis and the discussion of the corresponding results are presented in a compoundwise manner. Compounds which either compare well or contrast well are grouped and presented in the rigorous format of a scientific paper. This approach has been adopted as the bulk of the work encompassed by this study is of a publishable nature. Reprints or preprints of papers therefore form the basis of this chapter. For the

compounds where no publication of results is imminent this format is also adopted for consistency. This style necessarily results in the replication of some information of a procedural nature, however, this style also results in the omission of data which is either not unique in the literature or is of a more routine nature. Data which fall into this category include Fourier transform infrared, mass and ^1H nmr spectra as well as synthetic details.

In Chapter 4 an overall summary of trends in the series as they relate to the structural and spectroscopic studies and an overall conclusion is given.

In Chapter 5 areas of appropriate future research are indicated.

Editorial Style.

References are included at the end of each section and are not numbered consecutively for the whole thesis. Figures and tables are also not numbered consecutively throughout the whole thesis, however a list of tables, figures and plates is included in the contents pages. Chapter headings are clearly labelled at the foot of each page to further assist the reader.

TABLE OF CONTENTS

Statement	i
Abstract	ii
Acknowledgements	iv
Abbreviations	v
Preface	vi
Table of Contents	viii
Table of Figures	xii
Table of Tables	xvii

Chapter 1 Introduction

1.1	Definition of Formazans.....	2
1.2	Nomenclature.....	2
1.3	Literature Survey.....	3
1.4	Historical Survey.....	3
1.5	Physical Properties of Formazan.....	5
1.6	Molecular Structures.....	8
1.7	Tautomerism and Isomerism.....	8
1.7.1	Tautomerism.....	9
1.7.2	Isomerism.....	9
1.8	Preparation of the Formazans.....	11
1.8.1	Mechanism of Formazan Formation.....	12
1.9	Photochromism and Thermochromism.....	12
1.9.1	The Action of Light.....	12
1.9.2	Thermochromism.....	16
1.10	Compounds of Study.....	17
	References.....	18

Chapter 2 Experimental Techniques

2.1	General Procedures.....	21
2.2	Experimental Techniques.....	21
	Reference.....	23

Chapter 3 Results and Discussion

3.0.1	Electronic Absorption Spectra.....	24
3.0.2	Vibrational Spectra.....	24
3.0.3	X-Ray Crystal Structure Analysis.....	24
3.0.4	Mass Spectra.....	24
3.0.5	Nuclear Magnetic Resonance Spectra.....	24

	References.....	26
3.1	The Aromatic Formazans.....	27
	Properties.....	27
	Experimental.....	28
	Results and Discussion.....	28
	X-Ray Crystal Structures.....	28
	Nuclear Magnetic Resonance.....	29
	Absorption Spectra.....	33
	Raman Spectra.....	34
	Conclusion.....	37
	References.....	38
3.2	3-Ethyl-1,5-Diphenylformazan.....	39
	Experimental.....	40
	Results and Discussion.....	42
	Crystal Structures.....	42
	Raman Spectra.....	43
	Infrared Spectra.....	43
	¹³ C Nmr Spectra.....	44
	References.....	45
	Solid state ¹³ C Nmr Spectra.....	46
	Kinetic Studies.....	47
	Discussion.....	49
	References.....	50
3.3	3-Methyl-1,5-diphenylformazan and 3- <i>tertiary</i> - butyl-1,5-diphenylformazan.....	51
	Introduction.....	53
	Experimental.....	54
	Results and Discussion.....	56
	Crystal Structures.....	56
	¹³ C Nmr Spectra.....	64
	Raman Spectra.....	68
	Conclusion.....	70
	References.....	71
3.4	3-Halogenated-1,5-diphenylformazans.....	72
	Introduction.....	74
	Experimental.....	75
	Results.....	77
	Di(3-bromo-1,5-diphenyltetrazolium)- decabromide.....	78
	The Crystal Structure.....	79
	The Raman Spectrum.....	80
	3-Bromo-1,5-di- <i>para</i> -bromophenyl- formazan.....	82

	Discussion.....	83
	Di(3-bromo-1,5-diphenyltetrazolium)- decabromide.....	83
	The Cation.....	83
	The Anion.....	84
	Raman Spectra.....	86
	3-bromo-1,5-di- <i>para</i> -bromophenyl- formazan.....	88
	Crystal Structures.....	88
	References.....	89
	3-Chloro-1,5-diphenylformazan and 3-iodo- 1,5-diphenylformazan.....	91
	Properties.....	91
	Experimental.....	91
	X-Ray Crystal Structures.....	92
	References.....	94
3.5	3-Alkylthio-1,5-diphenylformazans.....	95
	Introduction.....	96
	Properties.....	97
	Experimental.....	98
	Results and Discussion.....	99
	X-Ray Crystal Structures.....	99
	Raman Spectra.....	104
	Nmr Spectra.....	107
	Absorption Spectra.....	113
	Conclusion.....	115
	References.....	116
3.6	1-Methyl-1,5-diphenylformazan.....	117
	Introduction.....	119
	Experimental.....	120
	Results and Discussion.....	122
	Crystal Structure.....	122
	Raman Spectra.....	125
	Nmr Spectra.....	129
	Conclusions.....	131
	References.....	132
3.7	Metal Dithizonates.....	133
	Introduction.....	134
	The Structures of Dithizonate Complexes.....	134
	The Dithizone Residue.....	136
	Photochromism.....	137
	Experimental.....	138
	Results.....	139

The Effect of Water.....	139
Discussion.....	141
References.....	142

Chapter 4 Summary of Results

Introduction.....	145
Isomerism in Formazans.....	146
Experimental.....	148
X-Ray Crystal Structures.....	150
¹³ C Solid State Nuclear Magnetic Resonance Spectra.....	154
Vibrational Spectroscopy.....	158
Assignment of the Raman Bands.....	158
Mass Spectra.....	164
Solution Nmr and Absorption Spectra.....	165
Conclusion.....	167
References.....	169

Summary

Summary.....	171
--------------	-----

Future Study

Future Study.....	172
-------------------	-----

TABLE OF FIGURES

Chapter 1 Introduction

Figure 1	Hypothetical Formazan (1).....	2
Figure 2	Resonance Structures for Formazans.....	5
Figure 3	Triphenyltetrazolium chloride as first prepared by von Pechmann in 1894.....	6
Figure 4	Leucoverdazyls as discovered by Kuhn and Trischmann.....	6
Figure 5	Potassium Dithizonate.....	7
Figure 6	Mercury(II) Dithizonate Complex.....	7
Figure 7	Carbohydrate Formazans.....	8
Figure 8	The Four Principal Isomers of 1,5-Diphenylformazan and its Derivatives.....	9
Figure 9	The Standard Procedure for the Preparation of Formazans (Nineham's A1 Method).....	11
Figure 10	Species in the Photochromism of 1,3,5-Triphenylformazan.....	12
Figure 11	Scheme Proposed by Kuhn and Weitz.....	14
Figure 12	Scheme as Proposed by Langbein and Grummt.....	15

Chapter 3.1 The Aromatic Formazans

Figure 1	X-Ray Crystal Structure of 1,5-diphenylformazan by O'melchenko <i>et al.</i>	29
Figure 2	The Solid state ¹³ C MAS Nmr Spectra for 1,5-diphenylformazan.....	30
Figure 3	The Solid state ¹³ C MAS Nmr Spectra for 1,3,5-triphenylformazan.....	30
Figure 4	Short Contact Time Solid-state ¹³ C MAS Nmr Spectrum for 1,5-diphenylformazan	31
Figure 5	The Ultra violet-visible Absorption Spectrum of 1,5-diphenylformazan.....	34
Figure 6	The Ultra violet-visible Absorption Spectrum of 1,3,5-triphenylformazan.....	34
Figure 7	Raman Spectrum of 1,5-diphenylformazan	36
Figure 8	Raman Spectrum of	

1,3,5-triphenylformazan.....	36
------------------------------	----

Chapter 3.2 3-Ethyl-1,5-Diphenylformazan

Figure 1	Molecular structures and atomic nomenclature of orange (1) and red (2) 3-ethyl-1,5-diphenylformazan.....	42
Figure 2	Unit-cell projection of orange (1) 3-ethyl-1,5-diphenylformazan.....	43
Figure 3	Unit-cell projection of red (2) 3-ethyl-1,5-diphenylformazan.....	43
Figure 4	Raman spectra of orange (1) and red (2) 3-ethyl-1,5-diphenylformazan.....	43
Figure 5	I.r. spectra of orange (1) and red (2) 3-ethyl-1,5-diphenylformazan.....	44
Figure 6	U.v.-visible absorption spectra of 3-ethyl-1,5-diphenylformazan.....	44
Figure 7	The Solid State ^{13}C MAS Nmr Spectrum of the Orange Isomer of 3-ethyl-1,5-diphenylformazan.....	46
Figure 8	The Solid State ^{13}C MAS Nmr Spectrum of the Red Isomer of 3-ethyl-1,5-diphenylformazan.....	46
Figure 9	The Ultra violet-visible Absorption Spectra of the Return of the Photo-activated Species to the Dark Stable Species of 3-ethyl-1,5-diphenylformazan.....	47

Chapter 3.3 3-Methyl-1,5-diphenylformazan and 3-tertiary-butyl-1,5-diphenylformazan.

Figure 1	The Principal Isomers in the Formazan System.....	53
Figure 2	Molecular Structure and Atomic Nomenclature for 3-methyl-1,5-diphenylformazan.....	57
Figure 3	Molecular Structures and Atomic Nomenclature for 3-tertiary-butyl-1,5-diphenylformazan.....	57
Figure 4	A Projection of the Unit Cell for 3-methyl-1,5-diphenylformazan.....	61
Figure 5	A Projection of the Unit Cell for 3-tertiary-butyl-1,5-diphenylformazan.....	63
Figure 6	The Solid state ^{13}C MAS Nmr Spectrum	

	for 3-methyl-1,5-diphenylformazan.....	66
Figure 7	The Solid state ^{13}C MAS Nmr Spectrum for 3- <i>tertiary</i> -butyl-1,5-diphenylformazan..	66
Figure 8	The Ultra-violet Absorption Spectrum of 3-methyl-1,5-diphenylformazan.....	67
Figure 9	The Ultra-violet Absorption Spectrum of 3- <i>tertiary</i> -butyl-1,5-diphenylformazan.....	67
Figure 10	The Raman Spectrum of 3-methyl-1,5-diphenylformazan.....	68
Figure 11	The Raman Spectrum of 3- <i>tertiary</i> -butyl-1,5-diphenylformazan.....	68

Chapter 3.4 3-Halogenated-1,5-diphenylformazans

Figure 1	A Stereoview of the Unit Cell of 3-bromo-1,5-diphenyltetrazolium- decabromide (2).....	80
Figure 2	Raman Spectrum of Br_{10}^{2-}	80
Figure 3	A Description of the Unit Cell for 3-bromo-1,5-di- <i>para</i> -bromophenylformazan.	83
Figure 4	Molecular Structure and Atomic Nomenclature for Di(3-bromo-1,5-diphenyltetrazolium)- decabromide.....	83
Figure 5	Molecular Structure and Atomic Nomenclature for the Decabromide of 3-bromo-1,5-diphenyltetrazolium- decabromide.....	85
Figure 6	Molecular Structure and Atomic Nomenclature for 3-bromo-1,5-di- <i>para</i> - bromophenylformazan.....	88

3-Chloro-1,5-diphenylformazan and 3-iodo-1,5-diphenylformazan

Figure 7	Molecular Structure and Atomic Nomenclature for 1-methyl-1,5- diphenylformazan.....	92
Figure 8	A Description of the Unit Cell for 1-methyl-1,5-diphenylformazan.....	93

Chapter 3.5 3-Alkylthio-1,5-Diphenylformazans

Figure 1	S-Alkyl-Dithizones.....	96
Figure 2	The Eight Probable Configurations of	

	3-Alkyl-dithizones.....	97
Figure 3	The X-Ray Crystal Structure of Dithizone (1) as shown by Laing.....	100
Figure 4	The X-Ray Crystal Structure of 3-methylthio-1,5-diphenylformazan (2) as shown by Preuss and Gieren.....	101
Figure 5	Molecular Structure and Atomic Nomenclature for the Orange Isomer of 3-ethylthio-1,5-diphenylformazan.....	102
Figure 6	A Description of the Unit Cell for the Orange Isomer of 3-ethylthio-1,5-diphenylformazan.....	102
Figure 7	The X-Ray Crystal Structure of 3-isopropylthio-1,5-diphenylformazan (5) as shown by Guillerez <i>et al.</i>	104
Figure 8	The Solid state ^{13}C MAS Nmr Spectrum for Dithizone (1).....	108
Figure 9	The Solid state ^{13}C MAS Nmr Spectrum for 3-methylthio-1,5-diphenylformazan.....	108
Figure 10	The Solid state ^{13}C MAS Nmr Spectrum for orange 3-ethylthio-1,5-diphenylformazan.....	109
Figure 11	The Solid state ^{13}C MAS Nmr Spectrum for red 3-ethylthio-1,5-diphenylformazan.....	109
Figure 12	The Solid state ^{13}C MAS Nmr Spectrum for 3-isopropylthio-1,5-diphenylformazan..	110
Figure 13	The Ultra violet-visible Absorption Spectra of 3-methylthio-1,5-diphenylformazan.....	114
Figure 14	The Ultra violet-visible Absorption Spectra of Orange 3-ethylthio-1,5-diphenylformazan.....	114
Figure 15	The Ultra violet-visible Absorption Spectra of Red 3-methylthio-1,5-diphenylformazan.....	115
Figure 16	The Ultra violet-visible Absorption Spectra of 3-isopropylthio-1,5-diphenylformazan.....	115

Chapter 3.6 1-Methyl-1,5-Diphenylformazan

Figure 1	The Principal Isomers in the Formazan System.....	120
Figure 2	Molecular Structure and Atomic Nomenclature for	

	1-methyl-1,5-diphenylformazan (1).....	122
Figure 3	A Projection of the Unit Cell for 1-methyl-1,5-diphenylformazan (1).....	125
Figure 4	The Raman Spectra of Crystalline and Solution Samples of 1-methyl-1,5-diphenylformazan.....	126
Figure 5	The U.v.-visible Electronic Absorption Spectra and Diffuse Reflectance Spectrum of 1-methyl-1,5-diphenylformazan (1).....	128
Figure 6	The Solid state ^{13}C MAS Nmr Spectrum for 1-methyl-1,5-diphenylformazan (1).....	129

Chapter 3.7 Metal Dithizonates

Figure 1	The Thiol-Thione Equilibrium for Dithizone.....	134
Figure 2	Mercury(II) Dithizonate Complex.....	135

Chapter 4 Summary of Results

Figure 1	The Principal Configurations of Isomeric 1,5-Diphenylformazans.....	146
Figure 2	The Orange and Red Isomers of 3-ethyl-1,5-diphenylformazan.....	152
Figure 3	The <i>E</i> and <i>Z</i> Isomers of (1,3-diphenyl-5- (1',2'-dihydro-2'-methyl-4'-chloro-1'- phthalazinylidene) formazan) as shown by Espenbetov <i>et al.</i>	153
Figure 4	Solid state ^{13}C Nmr Spectra for 3-methyl-, 3-tertiary-butyl- and the Red Isomer of 3-ethylthio-1,5-diphenylformazan	155
Figure 5	Chemical Shift vs C=N Bond Length.....	156
Figure 6	The Raman Spectra of 1,5-diphenylformazan (I) and 1-methyl- 1,5-diphenylformazan (VII).....	160
Figure 7	The Raman Spectra of 1,5-diphenylformazan (II) and 3-methyl- and the Orange Isomer of 3-ethyl- 1,5-diphenylformazan (III).....	161
Figure 8	The Raman Spectra of the Red Isomer of 3-ethyl-1,5-diphenylformazan (V) and 3-tertiary-butyl-1,5-diphenylformazan (V)..	162
Figure 9	Splitting Scheme for 1,5-diphenylformazans	164

TABLE OF TABLES

Chapter 1 Introduction

Table 1	Published Structures for the Formazans.....	10
---------	---	----

Chapter 3.1 The Aromatic Formazans

Table 1	Resonances for ^{13}C Nmr Spectra of 1,5-diphenylformazan and 1,3,5- triphenylformazan	32
Table 2	Raman Bands for 1,5-diphenylformazan and 1,3,5-triphenylformazan.....	35

Chapter 3.2 3-Ethyl-1,5-diphenylformazan

Table 1	Crystal Data for 3-ethyl- 1,5-diphenylformazan Isomers.....	41
Table 2	Atomic Co-ordinates and Temperature Factors for the Orange Isomer.....	41
Table 3	Atomic Co-ordinates and Temperature Factors for the Red Isomer.....	41
Table 4	A Comparison of Bond Lengths and Bond Angles for the -N=N-C=N-NH- Backbone of the Orange and Red Isomers.....	42
Table 5	Raman Bands Observed for the Orange and Red Isomers in the Solid State.....	43
Table 6	Infrared Spectra of Orange and Red 3-ethyl- 1,5-diphenylformazan.....	44
Table 7	Calculated Rate Constants for the Return of the Activated Orange Form to the Dark Stable Red Form of 3-ethyl-1,5-diphenylformazan...	49

Chapter 3.3 3-Methyl-1,5-diphenylformazan and 3-tertiary-butyl-1,5-diphenylformazan

Table 1	Fractional Atomic Co-ordinates and Temperature Factors for 3-methyl-1,5-diphenylformazan.....	58
Table 2	Fractional Atomic Co-ordinates and Temperature Factors for 3-tertiary-butyl-1,5-diphenylformazan.....	58

Table 3	Bond Lengths and Bond Angles for 3-methyl-1,5-diphenylformazan.....	59
Table 4	Bond Lengths and Bond Angles for 3- <i>tertiary</i> -butyl-1,5-diphenylformazan.....	59
Table 5	A Comparison of Selected Bond Angles and Bond Lengths for Formazan -N=N-C=N-NH- Backbones.....	60
Table 6	Selected Inter- and Intramolecular Distances and Bond Angles for 3-methyl-1,5-diphenylformazan.....	62
Table 7	Selected Inter- and Intramolecular Distances for 3- <i>tertiary</i> -butyl-1,5-diphenylformazan.....	63
Table 8	Nuclear Magnetic Resonance Spectra of 3-methyl-1,5-diphenylformazan.....	64
Table 9	Nuclear Magnetic Resonance Spectra of 3- <i>tertiary</i> -butyl-1,5-diphenylformazan.....	65
Table 10	Band Centre Wavenumbers for the Raman Spectra of 3-methyl-1,5-diphenylformazan and 3- <i>tertiary</i> -butyl-1,5-diphenylformazan.....	69

Chapter 3.4 3-Halogenated-1,5-diphenylformazans

Table 1	Bond Lengths and Bond Orders for the Anion and Cation of Di(3-bromo-1,5-diphenyltetrazolium)- decabromide.....	78
Table 2	Bond Angles for the Anion and Cation of Di(3-bromo-1,5-diphenyltetrazolium)- decabromide.....	78
Table 3	Atomic Co-ordinates and Temperature Factors for Di(3-bromo-1,5-diphenyltetrazolium)- decabromide.....	79
Table 4	Raman Bands Observed for Bromine, and Some Crystalline Di-, Tri- and Penta- bromides.....	81
Table 5	Bond Lengths for 3-bromo-1,5-di- <i>para</i> -bromo- phenylformazan.....	82
Table 6	Bond Angles for 3-bromo-1,5-di- <i>para</i> -bromo- phenylformazan.....	82
Table 7	Atomic Co-ordinates and Temperature Factors for 3-bromo-1,5-di- <i>para</i> -bromo- phenylformazan.....	82
Table 8	Br-Br Distances for Br ₂ and Some Br ₃ ⁻ and Br ₄ ²⁻ Anions.....	86
Table 9	Bond Lengths and Bond Angles for 3-chloro-1,5-diphenylformazan.....	93

Chapter 3.5 3-Alkylthio-1,5-diphenylformazans

Table 1	Bond Lengths and Bond Angles for the Orange Isomer of 3-ethylthio-1,5-diphenylformazan..	103
Table 2	Raman Bands for 3-Alkylthio-1,5-diphenylformazans.....	105
Table 3	Resonances for the Solid state ^{13}C Nmr Spectra of the 3-Alkylthio-1,5-diphenylformazans.....	107
Table 4	Resonances for the Solution ^{13}C Nmr Spectra of 3-mercapto-1,5-diphenylformazan.....	111
Table 5	Resonances for the Solution ^{13}C Nmr Spectra of 3-methylthio-1,5-diphenylformazan.....	111
Table 6	Resonances for the Solution ^{13}C Nmr Spectra of 3-ethylthio-1,5-diphenylformazan.....	112
Table 7	Resonances for the Solution ^{13}C Nmr Spectra of 3-isopropylthio-1,5-diphenylformazan.....	113

Chapter 3.6 1-Methyl-1,5-diphenylformazan

Table 1	Fractional Atomic Co-ordinates and Temperature Factors for 1-methyl-1,5-diphenylformazan.....	123
Table 2	Bond Lengths and Bond Angles for 1-methyl-1,5-diphenylformazan.....	124
Table 3	Band Centre Wavenumbers for the Raman Spectra of 1-methyl-1,5-diphenylformazan...	127
Table 4	^{13}C Nmr Resonances for 1-methyl-1,5-diphenylformazan.....	130

Chapter 3.7 Metal Dithizonates

Table 1	Half Lives for Metal Dithizonates.....	140
---------	--	-----

Chapter 4 Summary of Results

Table 1	1,5-Diphenylformazans Studied.....	147
Table 2	Elemental Analyses and Synthetic Methods..	149
Table 3	Crystal Structure Data for 1,5-Diphenylformazans.....	151
Table 4	Resonances for the Solid State ^{13}C MAS Nmr Spectra of Isomeric 1,5-Diphenylformazans	157
Table 5	Band Centre Wavenumbers for the Raman	

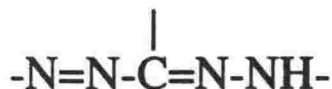
	Spectra of Isomeric 1,5-Diphenylformazans	159
Table 6	Ion Abundances for 1,5-Diphenylformazans	164
Table 7	¹³ C Nmr Spectra in Various Solvents for Some 1,5-Diphenylformazans.....	166

Photochromic materials are of interest for their potential use in information storage and other related optical devices. Of the numerous materials known to be photochromic some are inorganic compounds, where their photochromism can be attributed to the formation of colour centres or to some other charge transfer mechanism. In organic and organometallic compounds photochromism usually involves a photoinduced isomerisation or dissociation which gives rise to the differently coloured metastable species. There are advantages in using organometallic and organic photochromes in that their optical properties can be tuned by making small structural adjustments to the molecular species and that they show more favourable changes in optical density when compared with inorganic photochromes. The main disadvantage is that they show a greater tendency to fatigue on recycling than do inorganic photochromes. Consequently, it is important to identify causes of fatigue in a photochromic system if that system is to be improved. This presupposes an understanding of the structures of the chromophores and the conditions which govern these structures.

As a class of photochromic material the formazans provide both organic and organometallic [1] examples, with the latter being the more widely investigated to date. While the mechanisms of the photochromic and thermochromic changes have been investigated they are still the subject of considerable controversy. The interpretation of formazan behaviour has suffered due to a lack of definitive structural information on the chromophores involved. Neither has the link between the solid state and solution structures been established by a convenient or routine spectroscopic technique.

1.1 Definition of Formazans.

Formazans are compounds containing the characteristic azohydrazone group:



In general the two substituent groups attached to the nitrogen atoms are aromatic. Compounds which are unsaturated at both the terminal 1 and 5 positions, and also 1,5-dialkylformazans are so far unknown. Compounds unsaturated at either the 1 or 5 positions are known. The 3-carbon position (the *meso*-position) can contain various substituents (hydrogen, aliphatic, aromatic, heteroaromatic, halogen, pseudo-halogen, sugar etc.).

The aromatic formazans, 1,5-diphenyl- and 1,3,5-triphenyl-derivatives, were first described by von Pechmann and Bamberger in 1892 [2,3], who first used the term *formazyl* compound. However, the chemistry of formazans and the tetrazolium salts obtained from them did not develop vigorously until the 1940s when Kuhn and Jerchel [4] found applications for tetrazolium salts in biochemistry and histology as indicators for oxidation-reduction processes. The successful use of formazans as dyes [3,5], ligands in complex formation reactions [6-11], and analytical reagents [5] played an important role in the development of formazan containing systems.

1.2 Nomenclature.

The early literature of this field is very confusing since different systems of nomenclature developed amongst the British, German and American workers. However, with increasing use and modernisation, the German system [12], would now seem to be the most readily accepted. This system takes as its fundamental unit the hypothetical compound (1):

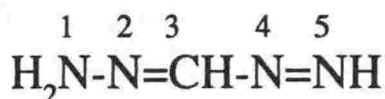


Figure 1: Hypothetical Formazan (1).

and calls it formazan. The numbering, 1 through 5, may be applied

arbitrarily from either end but this does not lead to confusion. This method of naming the series is presently accepted by the *Journal of the Chemical Society* [13].

"Formazan" is a *Chemical Abstracts* recognised keyword and has the registry number 504-65-4.

1.3 Literature Survey.

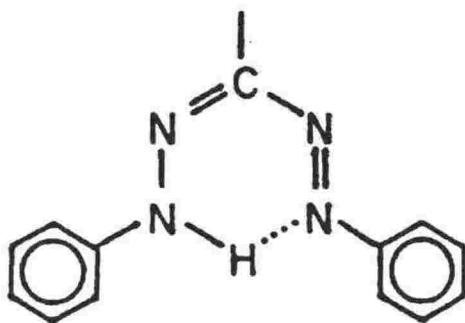
Several excellent reviews have been written on the formazans as well as the related tetrazolium salts and verdazyls. In 1955 Nineham [14] gave a comprehensive and definitive review on the chemistry of the formazans and tetrazolium salts up to that date. Mester [15] gave a review in 1958 on the formazan reaction as it applied in carbohydrate chemistry. This was followed in 1969 by Hooper [16] who reviewed more than 800 articles which had appeared in the intervening time. In 1975 an English translation of a Russian Chemical Review by Bednyagina *et al.* [17] on heteroaromatic formazans (hetarylformazans) gave an informative summary of that class of formazan as well as an insight into the wealth of Russian work on formazans previously unavailable in the western literature. Since the last published review, more than 100 papers have appeared in the literature.

Often treated as a distinct class of its own, dithizone (diphenylthiocarbazone) has featured prominently in the literature, particularly as a reagent for inorganic analyses [18]. Metal dithizonate complexes are known to be photochromic [19], principally as a result of the formazan ligand. In 1977, Irving [20] produced a monograph on dithizone which summarised well the literature on the class up to that date. A continuing series of articles have been published by him until his death [21] and articles [22] on the photochromism of metal dithizonates have appeared. Some 150 new papers have been published since the last major review.

1.4 Historical Survey.

Formazan chemistry is generally regarded as beginning in 1892 when independent preparations by von Pechmann [2] and Bamberger and Wheelwright [23] gave the first representatives of this class of compound. The earliest recorded preparation of a formazan was that of Fries [24], reported in 1875. He regarded his product, which was formed by the

reaction of benzene-diazonium nitrate with nitromethane, as phenylazomethane. The condensation products of phenylhydrazine were also studied [25,26,27]. Some formazans had also been prepared by Fischer [28], Fischer and Besthorn [26] and Heller [29], but their formazan structure was only established subsequently. Shortly thereafter, the action of diazonium salts in alkaline solutions on various aliphatic compounds containing active methylene groups was studied, leading Claisen [30] in 1892 to suggest a structure for the class:



The problem of the structure was elucidated independently by von Pechmann [2] and Bamberger [23] who jointly proposed the name "formazyl" for the equivalent described above.

Von Pechmann [31] listed general methods for the preparation of compounds of this type. Further work followed on their tautomerism [32,33,34] and on their products of oxidation [34,35]. These latter compounds were subsequently described as "tetrazolium compounds".

The chemistry of 1,5-diphenylformazans bearing 3-amino-, 3-nitro- and 3-mercapto- groups was clarified to a great extent by the work of Bamberger, Padova and Ormerod [36] in 1925. The tautomerism of formazans, initially described by Wedekind [37], was studied by Lapworth [38]. Although his results were inconclusive, Lapworth led Hunter and Roberts [39] in 1941 to establish conclusively that for several pairs of formazans that the individuals in each pair, previously described as tautomeric, were identical. They suggested that formazans were resonance hybrids with a chelated hydrogen-bridge structure as exemplified by 1,3,5-triphenylformazan in Figure 2.

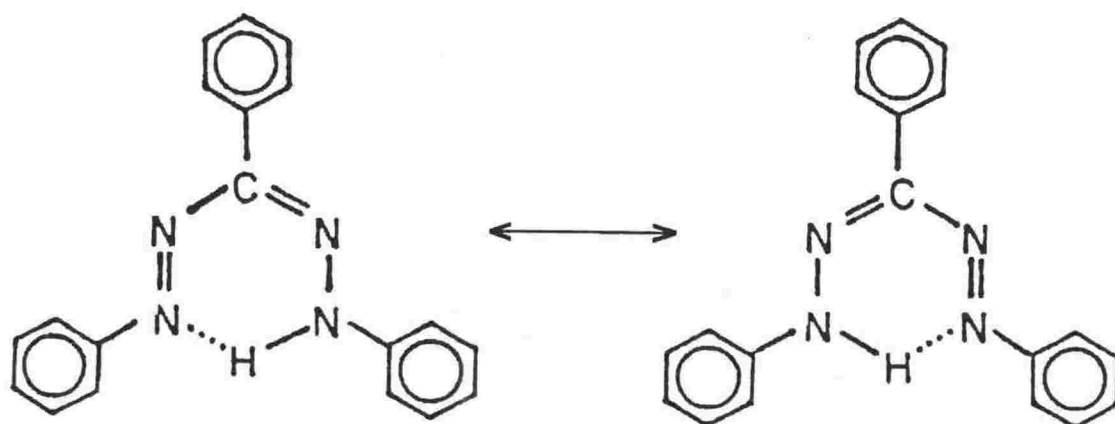


Figure 2: Resonance Structures for Formazans.

This formulation requires that the double bonds are not exactly located. This view was advanced at about the same time by Kuhn and Jerchel [4] who confirmed the mesomeric character of formazans.

The foundations of modern interest in formazan chemistry, both practical and theoretical, were laid in the early forties by these highly significant works of Kuhn and his co-workers; this interest has become ever-widening. Extensive studies have now been carried out in a number of important areas of formazan chemistry and these are summarised in the sub-sections which follow.

1.5 Physical Properties of Formazans.

Formazans generally are solids of relatively low melting point for the size of the molecule; most triaryl-formazans tend to melt in the range 70-215° C. They are characterised by intense colours ranging from yellow-orange through most of the visible region to an intense purplish-black. At the same time they show brilliant reflex colours and their appearances are very striking.

The influence of substituents on the colour of the formazan follows rules in line with many dyestuffs. Formazans with aliphatic substituents (hydrogen, methyl, carboxyl, etc.) attached to the 3-carbon have lighter (yellow-orange) colours and a greater solubility in common organic solvents than do the aryl derivatives whose colours are deep red. Water solubility is negligible, except where specifically solubilising functionality has been introduced into the molecule. Ciba-Geigy have patented some of these as dyes for use with natural silk [40]. Most formazans are soluble to some extent in a wide range of common organic solvents; some

biformazans of high molecular weight seem to have no appreciable solubility in any solvent but nitrobenzene [41].

Formazans may behave as weak acids and weak bases; both of the resulting salts may be hydrolysed in the cold.

Characteristic reactions of formazans include reversible oxidation/reduction to tetrazolium salts:

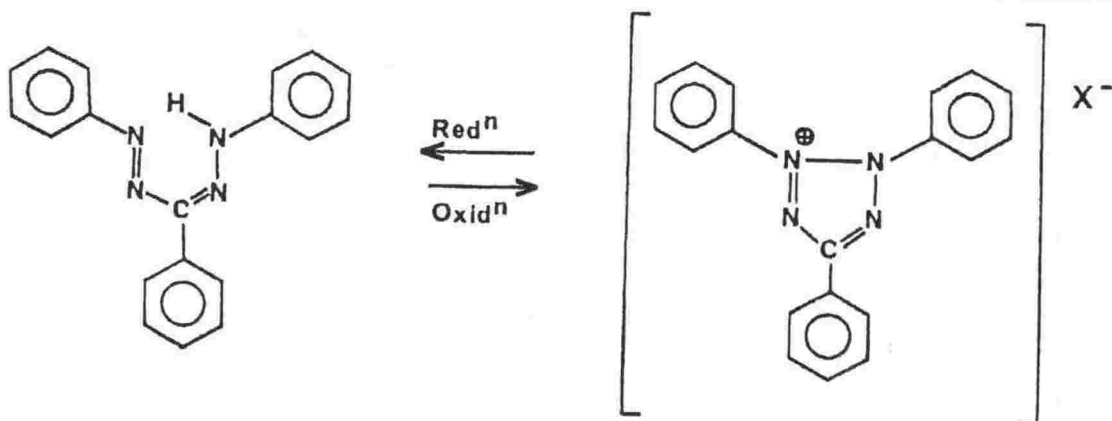


Figure 3: Triphenyltetrazolium chloride as first prepared by von Pechmann in 1894. [31]

which may be effected by various means [4,34,35,42-48]; alkylation and conversion to verdazyl radicals:

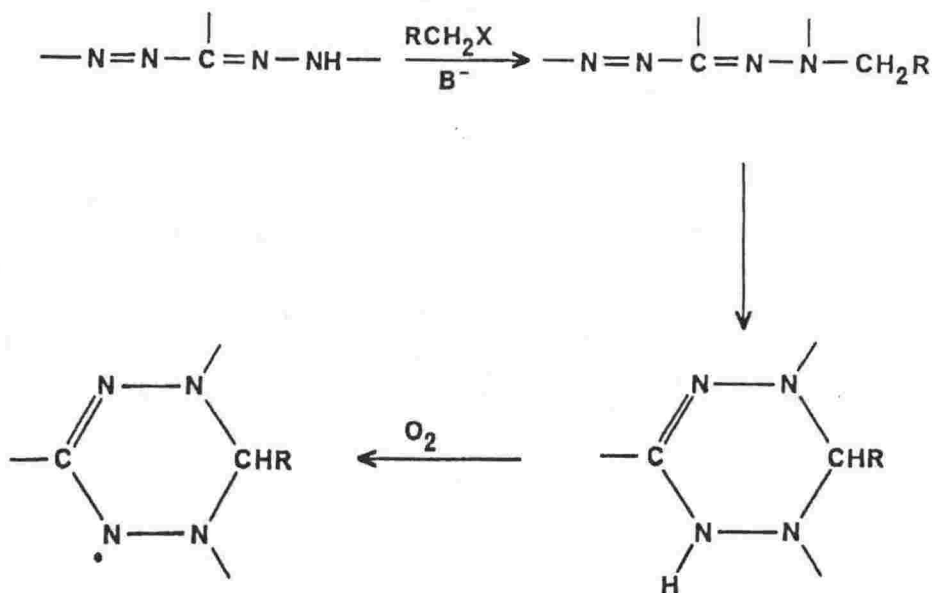


Figure 4: Leucoverdazyls as discovered by Kuhn and Trischmann. [49]

and salt and complex formation with metal ions:

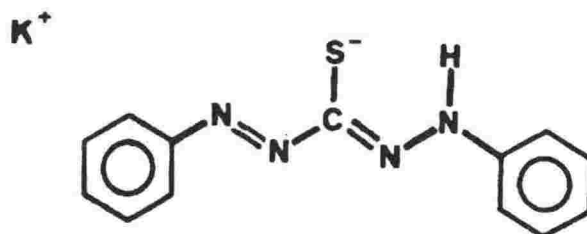


Figure 5: Potassium Dithizonate.

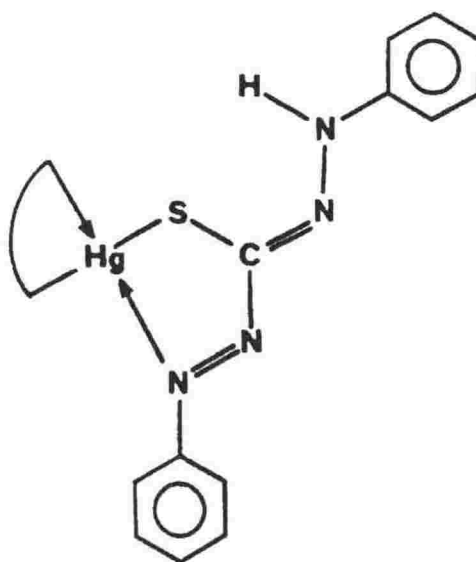


Figure 6: Mercury(II) Dithizonate Complex.

IUPAC: Bis-(1,5-diphenylthiocarbazonato-*N,S*-)mercury(II).

The continuing keen interest in coordination chemistry has resulted in an increasing number of reports dealing with formazans coordinated to metal atoms [20].

Sugar formazans have also been studied. The recovery of aldoses from their formazans can be conveniently effected [50] and the formation of osotriazoles by the elimination of aniline has been investigated by Mester [51]. The synthesis of sugar formazans provides a convenient

method of distinguishing aldoses from ketoses as the latter do not yield formazans because they contain no active methine groups.

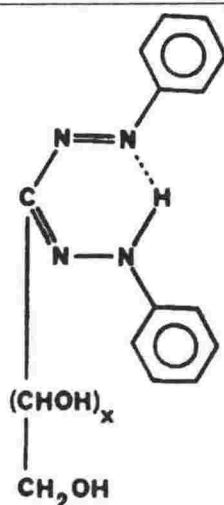


Figure 7: Carbohydrate Formazans.

1.6 Molecular Structures.

The structures of formazans have been of interest to research workers from the outset. A number of studies have been made on the tautomerism, stereoisomerism and the state of the hydrogen bond in arylformazans [52-59]. Special studies have been carried out on the infrared spectroscopy of arylformazans [60-70]. The relationship between the colour of formazans and their structure has been studied and quantum mechanical calculations on the π -electron system and electronic spectra of formazans have been published [71-76]. ^1H and ^{13}C nmr have featured, however these have mostly concerned carbohydrate formazans with the emphasis on the carbohydrate rather than the formazan moiety. Some studies of ^{15}N -labelled formazans have yielded valuable information on the tautomerism. Some Raman and resonance Raman studies of formazans have appeared [79,80], although a comprehensive study has not been undertaken. These studies have all been valuable in the determination of the molecular structures of the formazans.

1.7 Tautomerism and Isomerism.

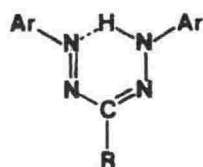
The isomerism of diphenylformazans presupposes the existence of three tautomeric and four stereoisomeric (Figure 8) forms.

1.7.1 Tautomerism: The two 1,5-diphenylformazans previously described in Figure 2 are indistinguishable. Nineham [14], in summarising the early literature on this question, cited evidence which enabled him to conclude that:

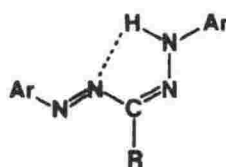
"when all three substituents in a molecule are alike only one formazan can be synthesised. When two of the three groups are the same only two isomers can be prepared; one with the odd group attached to the carbon, the other with the odd group attached to nitrogen. When all three substituents are different, three isomers can be prepared"

Most of the additional data which have appeared up to 1970 have agreed with the classical viewpoint. These data have come from spectroscopic work: infrared, ultra violet and nuclear magnetic resonance. Schiele *et al.* [79] maintained that, in certain cases at least, the formazan is more truly represented by a hybrid involving the chelate structure as well.

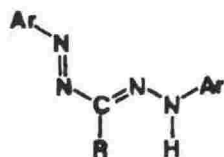
1.7.2 Isomerism: Formazans can, in principle, adopt any one of sixteen possible geometric isomers due to isomerisation about the double bonds. In practice, however, isomers which are unlikely to occur due to serious steric crowding may be ignored. This leaves four structures (Figure 8) as a result of *syn-anti* isomerisation about the C-N single bond designated



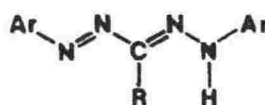
(a) *syn, s-cis*



(b) *syn, s-trans*



(c) *anti, s-cis*



(d) *anti, s-trans*

Figure 8: The Four Principal Isomers of 1,5-Diphenylformazan and its Derivatives.

s-cis and *s-trans*.

The structure of the formazan chain is influenced significantly by the substituent R in the *meso*-position (3-position). Phenyl and *tertiary*-butyl groups promote the fixation of the chelate form. Alkyl substituents weaken the hydrogen bridge thus leading to the opening of the chelate ring, while hydrogen stabilises the *anti,s-trans* structure. Otting and Neugebauer [80,81] have concluded that in solution the red and yellow formazans represent *syn,s-cis* and *anti,s-trans* isomers. In the solid state the formazans crystallise as red or orange/yellow solids, with the *syn,s-cis* [82] or *syn,s-trans* [83,84] configurations if red and the *anti,s-trans* [85-88] if orange/yellow. A comprehensive x-ray crystallographic study has never been published; neither have the red and orange/yellow isomers of a single photochromic formazan been obtained and characterised in terms of their solid-state structure. The crystal structures published to date are summarised and presented in Table 1.

Table 1: Published Structures for the Formazans.

<i>anti,s-trans</i>	Ref
1,5-diphenylformazan	[85]
1,5-diphenyl-3-mercapto-1,5-diphenylformazan	[86]
3-isopropylthio-1,5-diphenylformazan	[87]
3-methylthio-1,5-di-(<i>o</i> -tolyl)-phenylformazan	[88]
potassium dithizonate	[89]
<i>syn,s-trans</i>	
3-methylthio-1,5-diphenylformazan	[83]
3-carboxymethylthio-1,5-diphenylformazan	[84]
<i>syn,s-cis</i>	
1,5-bis(2,6-dimethylphenyl)-3-nitroformazan	[82]

1.8 Preparation of the Formazans.

In his excellent general survey of the chemistry of the formazans, Nineham [14] mentioned some 500 formazans; this number has subsequently increased. He has given a comprehensive account (24 pages) of the classical syntheses. While there have been few significant additions to these general methods, details have been refined allowing the range and yield of compounds to increase.

The most generally applicable method (Nineham's A1) is the coupling of diazonium salts with aldehyde or glyoxylic acid arylhydrazones in the presence of caustic alkalis or sodium acetate. The aldehyde arylhydrazone method is the standard procedure for the preparation of triaryl formazans.

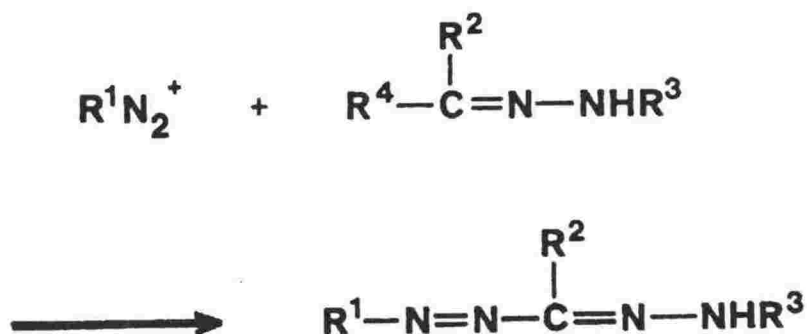


Figure 9: The Standard Procedure for the Preparation of Formazans (Nineham's A1 Method). [14]

The general experimental procedure for this method of preparation of formazans has also been reviewed by von Pechmann [31]. The only notable modern improvement in the technique has been the use of pyridine as the coupling medium. This appears to have been as a result of the experiences gained of the value of pyridine as a promoter in the dyestuffs industry.

Another useful method involves the action of diazonium salts on compounds containing active methylene or methine groups (Nineham's A2). Malonic acid and its derivatives have proven particularly useful. The reaction of arylhydrazines with a variety of compounds such as ethyl formate, imino ethers and halogenohydrazines is also generally applicable.

An obvious, but sometimes overlooked, method of preparation involves the simple modification of substituents already present in formazans. Using 1,5-diphenylformazan as a building block many 3- and/or 5- substituted derivatives can be made by simple treatment with

nucleophiles.

There have been very few additions to the synthetic methods available in recent years.

Mester [15] has described the synthetic approaches in carbohydrate research and Bednyagina *et al.* [17] have described the preparation of hetarylformazans. The general methods apply in both reviews.

1.8.1 Mechanism of Formazan Formation: The mechanism of the reaction which provides the principal route to, and also the greatest variety of, formazans, the coupling of diazonium salts and arylhydrazones (Nineham's A1, Figure 9), has been the subject of some controversy [90]. This controversy has centred mainly about the initial position of attack on the diazonium ion, whether it occurs at the methine carbon or at the amino nitrogen, and about the role of base catalysis.

Formazan formation is a two-step reaction [90], the first step involving electrophilic attack by diazonium ion at the methine carbon, the second a tautomeric shift of the hydrogen from carbon to nitrogen giving the stabilized cyclic formazan structure. The first step is facilitated by electron-donating and the second by electron-withdrawing substituents.

Pyridine has been shown to be a powerful specific catalyst [91] in diazo coupling reactions due to the acceleration of the loss of a proton from the intermediate. The reaction of arylhydrazones with diazonium salts may yield different products depending on the pH of the solution. In acidic solution, when the pH is maintained below about 3, ring substitution products are obtained [92]. When the reaction is carried out at pH 3-8, an unstable, light yellow intermediate may be isolated, which rapidly isomerises to the formazan - even in the solid state. Above pH's of 9 (depending to some extent on the reactants involved) only the formazan may be isolated.

1.9 Photochromism and Thermochromism.

Aryl- and hetaryl-formazans can, in many cases, isomerise by photoinduction or thermoinduction, with proton transfer, which entail a change in the chromophoric system and the colour of the compound.

1.9.1 The Action of Light: Hausser, Jerchel and Kuhn [53] have observed that in benzene solution the red isomer of 1,3,5-triphenylformazan is transformed into a yellow form which is stable only while being irradiated, and which, in darkness, is retransformed to the red formazan. Many formazans, previously thought to be single substances, can be obtained in red and yellow forms. The structural interpretation of this change has been hampered by the fact that definitive structural data

for a formazan isolated in both the red and yellow forms has not been observed.

Kuhn and his co-workers [53] suggested two possible explanations for the fact that some formazans can be converted from a red form to a yellow form by irradiation with visible light and that the reverse reaction occurs in darkness. Hausser [56] measured the quantum yields of the red-yellow change in triphenylformazan irradiated by light of wavelength 490 nm. His results showed that this change involved a photochemical intermediate which was reconverted back to the red form after a half-life of 17 s^{-1} .

Such measurements showed a cycle of events involving two yellow

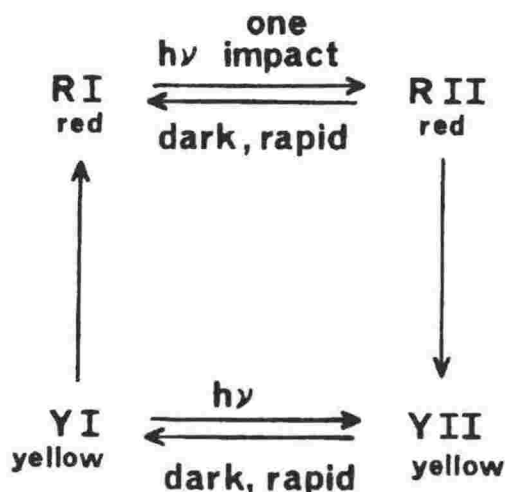


Figure 10: Species in the Photochromism of 1,3,5-Triphenylformazan. [56]

and two red forms as shown in the following scheme (Figure 10):

The red form, R I, which is stable in the solid state, is converted to a short-lived red form, R II, which is converted by another quantum of light to the yellow form, Y II. Y II is also a very short lived species and rapidly passes in darkness to the more stable form, Y I. This reverts to the R I form slowly in darkness; catalysts influence the change strongly. The absorption spectra of the short-life intermediates R II and Y II show only small differences from those of R I and Y I, respectively.

Following this study, Kuhn and Weitz [57] then discussed the precise allocation of these four experimentally observed forms. As discussed

above, the classical spatial arrangement of a formazan molecule allows the existence of four probable structures, with the possibilities of tautomerism being ignored for the moment. They assumed that the observed changes were due to the interconversions of the geometrical isomers. These changes were accompanied by opening or closing of the chelated hydrogen bridge.

By analogy with the changes in light absorption of the geometrical isomers of certain azo compounds, they assigned the stable red form R I to the *syn,s-trans* form and the unstable red form R II to the *syn,s-cis* form. Therefore, the first change on illumination ($R\ I \rightarrow R\ II$) involves a change of configuration about the $-N=N-$ system from *trans*- to *cis*- without rupturing the hydrogen bridge. In the change from red to yellow

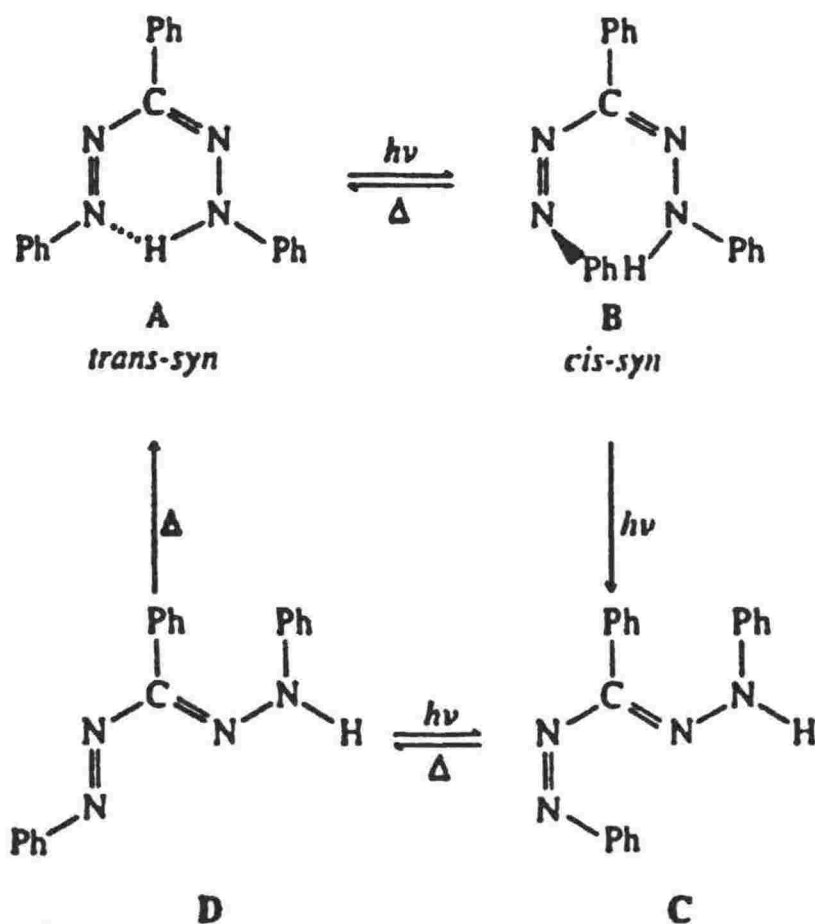


Figure 11: Scheme Proposed by Kuhn and Weitz. [57]

($R\ II \leftrightarrow Y\ II$), the chelation is destroyed (together with the resonance in the molecule) when the $-C=N-$ bond assumes a *trans*- or *anti*-configuration. The yellow form, Y II, is the *anti,s-cis* form and the more stable yellow form, Y I, is the *anti,s-trans* form. The rapid dark reactions are *cis-trans* conversions and the slow dark reaction is an *anti-syn* change.

The cyclic process in light can therefore be rewritten in terms of the isomeric structures as described in Figure 11. Indirect confirmation of

these theories is found in the classical *cis-trans* conversion in azobenzene [57].

Langbein [93] subsequently attempted to modify this scheme after considering the results of irradiation experiments at different temperatures. He demonstrated that only the *trans-cis* isomerisation of the azo group proceeds both photochemically and thermochemically. Langbein and Grummt [94] then studied the system by flash photolysis and proposed the modified scheme shown in Figure 12.

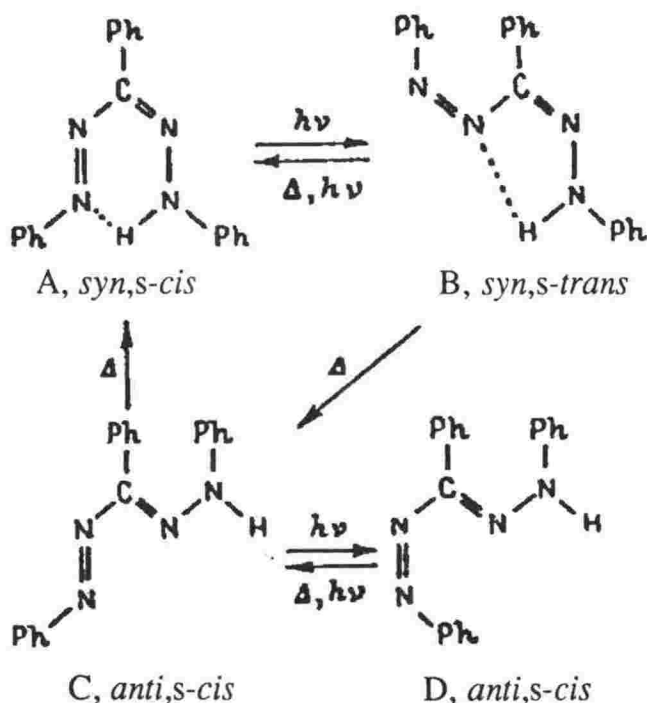


Figure 12: Scheme as Proposed by Langbein and Grummt. [94]

Their results indicate that the stable red form A is converted through a photochemical *trans-cis* isomerisation about the N=N double bond into isomer B which is also red but has a smaller molar absorption coefficient than A. Increased conjugation in the azohydrazone part of the molecule through the formation of a weak five membered, cyclic hydrogen bonded interaction in the B isomer was held to account for the comparatively long wavelength of absorption seen. According to this modified scheme, B may revert to the original isomer A by a photochemical and thermal path. A competing reaction to form isomer C by a thermal path occurs at a comparable rate at room temperature. Isomer D is formed photochemically from C. The reverse reaction occurs both photochemically and thermally.

Despite the obvious differences between the schemes of Kuhn *et al.* [57] and Langbein *et al.* [94] both clearly suggest that under continuous

irradiation a photostationary state involving D and C should be achieved.

Further investigations of the transitions by infrared and Raman spectroscopy [95] by Lewis and Sandorfy have led to a series of contradictory conclusions about the structures of specific isomers and the sequence of mutual transformations. A recent investigation of the same system by Kovalenko *et al.* [96] has shown that two red forms (A and B) exist in the solid state and demonstrated the possibility of a purely thermal interconversion between the two. While they were able to determine the kinetic parameters for interconversions in benzene solution they did not offer any new evidence contradicting or supporting the previously proposed structures of the species involved.

Negative red-yellow photochromism of this type has also been observed for analogues of triphenylformazan [97]. *Negative* photochromism is when the absorption of the species eventually generated by means of a photo-initiated first event is characterised by a band at **higher** energy than the initial molecular species. Most photochemical species exhibit the opposite effect.

The photochromism of 1-benzimidazolyl-5-phenylformazans which occurs in chloroform or carbon tetrachloride solutions, is of a different kind than triphenylformazan [98,99]. Here, positive red-blue photochromism with a large (up to 200 nm) bathochromic photochromic shift is observed. The reverse dark transition is difficult, but the initial form can be quantitatively isolated when a more polar solvent is added to a solution of the blue form. The ease of the reconversion into the initial formazan, the change in the nature of the infrared spectrum of the irradiated form, and steric hindrance by the *ortho*-substituent in the 5-phenyl group suggested [98] that photoinduction is accompanied by intermolecular proton transfer and the formation of dimeric structures.

The photochromism of mercury and zinc dithizonates, which has been described [100,101], can also be accounted for by a change in the chromophoric system of the ligand (isomerism and proton transfer). The isomerism of the formazan chain similarly explains the photochromism of S-alkyldithizones. [102,103].

1.9.2 Thermochromism: Substances exhibiting both negative [104,105] and positive [104,106] thermochromism have been found among the benzazolyformazans. The group of 1-benzothiazoyl-5-nitrophenylformazans has been studied in greater detail. It has been established that the repeated reversible thermochromic transitions of alcoholic solutions from the initial red form to the thermally induced blue form are due to the dissociation and conversion into the anionic form, whose spectrum is identical with that of the sodium salt of the formazan.

All of the studies to date have concentrated upon the physical properties, syntheses and molecular or atomic structures of formazans. However, apart from the review articles which have appeared, no comprehensive study of a series of formazans has been published. Many studies have been applied to a variety of individual formazans over the last 15 years and a review of these results is well overdue!

1.10 The Compounds of Study.

The following 1,5-diphenylformazans were chosen to be studied:

- 1,5-diphenylformazan
- 3-methyl-1,5-diphenylformazan
- 3-ethyl-1,5-diphenylformazan
- 3-*tertiary*-butyl-1,5-diphenylformazan
- 1,3,5-triphenylformazan
- 3-mercapto-1,5-diphenylformazan
- 3-methylthio-1,5-diphenylformazan
- 3-ethylthio-1,5-diphenylformazan
- 3-*isopropyl*-1,5-diphenylformazan
- 1-methyl-1,5-diphenylformazan
- 3-chloro-1,5-diphenylformazan
- 3-bromo-1,5-di-*para*-phenylformazan
- 3-iodo-1,5-diphenylformazan.

References

- 1 Brown, G. H., "Techniques of Chemistry, Vol III, Photochromism", Wiley-Interscience, New York (1971).
- 2 von Pechmann, H., *Chem. Ber.*, **25**, 3175 (1892).
- 3 Bamberger, E., *Chem. Ber.*, **25**, 3547 (1892).
- 4 Kuhn, R. and Jerchel, D., *Chem. Ber.*, **74**, 941 (1941); Kuhn, R. and Jerchel, D., *Chem. Ber.*, **74**, 949 (1941).
- 5 Price, R., "Chemistry of Synthetic Dyes", *Izd. Khimiya, Leningrad*, 2013 (1974). (Translation).
- 6 Hunter, L. and Roberts, L.B., *J. Chem. Soc.*, **1941**, 820; Hunter, L. and Roberts, L.B., *J. Chem. Soc.*, **1941**, 823.
- 7 Wizinger, R. and Biro, V., *Helv. Chim. Acta*, **32**, 901 (1949).
- 8 Wizinger, R., *Z. Naturforsch.*, **9b**, 729 (1954).
- 9 Irving, H., Gill, J.B. and Cross, W.R., *J. Chem. Soc.*, **1960**, 2087.
- 10 Tabel, H.R. and Wizinger, R., (see Ref. 5, p 495).
- 11 Wizinger, R. *Chimia (Switz.)*, *Supple*, **82** (1968).
- 12 Bilstein, Introduction, 4th Edition, **16** (1933).
- 13 Ashley, J.N., Davis, B.M., Nineham, A.W. and Slack, R., *J. Chem. Soc.*, **1953**, 3881.
- 14 Nineham, A.W., *Chem. Rev.*, **55**, 355 (1955).
- 15 Mester, L., *Adv. Carbohydrate Chem.*, **13**, 105 (1958).
- 16 Hooper, W.D., *Rev. Pure and Appl. Chem.*, **19**, 221 (1969).
- 17 Bednyagina, N.P., Postovskii, I.Ya., Garnovskii, A.D. and Osipov, O.A., *Russ. Chem. Rev. (Engl. Transl.)* **44**, 493 (1975).
- 18 Vogel, A.I., "Quantitative Inorganic Analysis", William Clowes, London (1981).
- 19 Irving, H., Andrew, G. and Ridson, E.J., *J. Chem. Soc.*, **1949**, 541.
- 20 Irving, H.M.N.H., "Dithizone, Analytical Sciences Monographs 5", John Wright and Sons, London (1977).
- 21 Irving, H.M.N.H., *Crit. Rev. Anal. Chem.*, **9**, 321 (1980) and references contained therein; Irving, H.M.N.H., *Anal. Chim. Acta.*, **141**, 311 (1982).
- 22 Geosling, C., Adamson, A.W. and Gutierrez, A.R., *Inorg. Chim. Acta*, **29**, 279 (1978).
- 23 Bamberger E. and Wheelwright, E.W., *Chem. Ber.*, **25**, 3201 (1892).
- 24 Frieze, P., *Chem. Ber.*, **8**, 1078 (1875).
- 25 Fischer, E., *Chem. Ber.*, **22**, 1930 (1889).
- 26 Fischer, E. and Besthorn, K., *Liebigs Ann. Chem.*, **212**, 316 (1882).
- 27 Freund, M., *Chem. Ber.*, **24**, 4178 (1891).
- 28 Fischer, E., *Liebigs Ann. Chem.*, **190**, 67 (1878).
- 29 Heller, G., *Liebigs Ann. Chem.*, **263**, 269 (1891).
- 30 Claisen, L., *Liebigs Ann. Chem.*, **287**, 360 (1895).
- 31 von Pechmann, H., *Chem. Ber.*, **27**, 320 (1894).
- 32 von Pechmann, H., *Chem. Ber.*, **27**, 1679 (1894).
- 33 von Pechmann, H., *Chem. Ber.*, **28**, 876 (1895).
- 34 von Pechmann, H. and Runge, P., *Chem. Ber.*, **27**, 323 (1894).
- 35 von Pechmann, H. and Runge, P., *Chem. Ber.*, **27**, 2920 (1894).
- 36 Bamberger, E., Padova, R. and Ormerod, E., *Liebigs Ann. Chem.*, **446**, 260 (1925).
- 37 Wedekind, E., *Chem. Ber.*, **31**, 479 (1898).
- 38 Lapworth, A., *J. Chem. Soc.*, **83**, 1125 (1903).
- 39 Hunter, L. and Roberts, C.B., *J. Chem. Soc.*, **1941**, 820; Hunter, L. and Roberts, C.B., *J. Chem. Soc.*, **1941**, 822.
- 40 Ciba Ltd., Swiss P.: 246 475 (1947); I.R. Geigy A.G., Belg. P.: 650 328 (1965); French P.: 1 560 653 (1969).
- 41 Eadie, M.J., Tyrer, J.H., Kukums, J.R. and Hooper, W.D., see *Rev. Pure and Appl. Chem.*, **19**, 221 (1969).
- 42 Fichter, F. and Schiess, E., *Chem. Ber.*, **33**, 747 (1900).
- 43 Matson, A.M., Jensen, C.O. and Dutcher, R.A., *J. Am. Chem. Soc.*, **76**, 1695 (1954).
- 44 Hirsch, B., *Liebigs Ann. Chem.*, **648**, 151 (1963).
- 45 Kuhn, R. and Munzing, W., *Chem. Ber.*, **86**, 858 (1953).
- 46 Benson, F.R., Otten, E.A. and Schachat, R.E., *J. Am. Chem. Soc.*,

- 76, 1695 (1954).
- 47 Ashley, J.N., Davis, B.M., Nineham, A.W. and Slack, R.J., *J. Chem. Soc.*, **1953**, 3881.
- 48 Reid, W., *Angew. Chem.*, **64**, 391 (1952).
- 49 Kuhn, R. and Trischmann, H., *Angew. Chem.*, **75**, 294 (1963).
- 50 Mester, L., *Chem. Ber.*, **93**, 1684 (1960).
- 51 Mester, L. and Weygand, F., *Bull. Soc. Chim. Fr.*, 381 (1962).
- 52 Ermakova, M.I., Krylov, E.I. and Postovskii, I.Ya, *Zh. Obshch. Khim.*, **30**, 849 (1960).
- 53 Hausser, J., Jerchel, D. and Kuhn, R., *Chem. Ber.*, **82**, 195 (1949).
- 54 Hausser, J., Jerchel, D. and Kuhn, R., *Chem. Ber.*, **82**, 515 (1949).
- 55 Hausser, J., Jerchel, D. and Kuhn, R., *Chem. Ber.*, **84**, 651 (1951).
- 56 Hausser, K., *Naturwissenschaften*, **36**, 313 (1949).
- 57 Kuhn, R. and Weitz, H., *Chem. Ber.*, **86**, 1199 (1959).
- 58 Shulte-Frolinde, D., Kuhn, R. Munzig, W. and Otting, W., *Liebigs Ann. Chem.*, **622**, 43 (1959).
- 59 Burns, G.R. and Duncan J.F., *J. Chem. Soc., Chem. Commun.*, **4**, 116 (1966).
- 60 Jerchel, D. and Edler, W., *Chem. Ber.*, **88**, 1287 (1955).
- 61 Le Fevre, R.J., Sousa, J.B. and Werner, R.L., *Aust. J. Chem.*, **9**, 151 (1956).
- 62 Foffani, A., Pecile, C. and Ghersetti, S., *Tetrahedron Lett.*, 16 (1959).
- 63 Foffani, A., Pecile, C. and Ghersetti, S., *Adv. Mol. Spectroscopy*, **2**, 769 (1962).
- 64 Schiele, C., *Liebigs Ann. Chem.*, **689**, 197 (1965).
- 65 Schiele, C. and Arnold, G., *Tetrahedron Lett.*, 4103 (1966).
- 66 Arnold, G. and Schiele, C., *Spectrochim. Acta*, **25A**, 671 (1969).
- 67 Arnold, G. and Schiele, C., *Spectrochim. Acta*, **25A**, 685 (1969).
- 68 Arnold, G. and Schiele, C., *Spectrochim. Acta*, **25A**, 697 (1969).
- 69 Kukushkina, I.I., Yurchenko, E.N. Ermakova, M.I. and Latosh, N.I., *Zh. Fiz. Khim.*, **46**, 176 (1972); *Russian J. Phys. Chem. (Engl. Transl.)*, **1** (1972).
- 70 Kukushkina, I.I., Yurchenko, E.N., Arkhipenko, D.V. and Orekhov, B.A., *Zh. Fiz. Khim.*, **46**, 1677 (1972); *Russian J. Phys. Chem. (Engl. Transl.)*, **7**, (1972).
- 71 Bednyagina, N.P., Lipunova, G.N., Novikova, A.P., Zeif, A.P. and Shchegoleva, L.N., *Zh. Org. Khim.*, **6**, 619 (1970).
- 72 Zeif, A.P., Shchegoleva, N.N., Lipunova, G.N., Novikova, A.P. and Bednyagina, N.V., *Zh. Org. Khim.*, **6**, 1332 (1970).
- 73 Zeif, A.P., Lipunova, G.N., Bednyagina, N.P. Shchegoleva, L.N. and Cheryavskii, L.I., *Zh. Org. Khim.*, **6**, 2590 (1970).
- 74 Lipunova, G.N., Zeif, A.P., Bednyagina, N.P. and Shchegoleva, L.N., *Zh. Org. Khim.*, **8**, 1757 (1972).
- 75 Yurchenko, E.N. and Kukushkina, I.I., *Zh. Strukt. Khim.*, **10**, 706 (1960).
- 76 Kukushkina, I.I., Yurchenko, E.N., Ermakova, M.I., Sadakova, G.P. and Latosh, N.I., *Zh. Strukt. Khim.*, **11**, 341 (1971).
- 77 Lewis, J.W. and Sandorfy, C., *J. Phys. Chem.*, **87**, 4885 (1983); Igarashi, T., Sugihari, J., Ochiai, K., Kaneko, N. and Takahashi, H., VIII International Conference on Raman Spectroscopy, Bordeaux, 137 (1982).
- 78 Burns, G.R. and Clark, R.J.H., *Inorg. Chim. Acta.*, **88**, 83 (1984).
- 79 Schiele, C., Halfar, K. and Arnold, G., *Tetrahedron*, **23**, 2693 (1967).
- 80 Otting, W. and Neugebauer, F.A., *Z. Naturforsch., Teil B*, **23**, 1064 (1968).
- 81 Otting, W. and Neugebauer, F.A., *Chem. Ber.*, **102**, 2520 (1969).
- 82 Dijkstra, E., Hutton, A.T., Irving, H.M.N.H. and Nassimbeni, L.R., *Acta Crystallogr., Sect B*, **38**, 535 (1982).
- 83 Preuss, J. and Gieren, A., *Acta Crystallogr., Sect B*, **38**, 535 (1982).
- 84 Hutton, A.T., Irving, H.M.N.H., Nassimbeni, L.R. and Gafner, G., *Acta Crystallogr., Sect B*, **35**, 1354 (1979).
- 85 Omel'chenko, Yu.A., Kondrashev, Yu.D., Ginzburg, S.L. and Neiganz, M.G., *Kristallografiya*, **19**, 522 (1974).
- 86 Laing, M., *J. Chem. Soc., Perkin Trans. 2*, **1977**, 1248.
- 87 Guillerez, J., Pascard, C. and Prange, T., *J. Chem. Res.*, (S) 308 (1978); (M) 3934 (1978).
- 88 Hutton, A.T., Irving, H.M.N.H. and Nassimbeni, L.R., *Acta Crystallogr., Sect B*, **36**, 2071 (1980).
- 89 Noda, H., Engelhardt, L.M.,

- Harrowfield, J.MacB., Pakawatchai, C., Patrick, J.M. and White, A.H., *Bull. Chem. Soc. Jpn.*, **58**, 2385 (1985).
- 90 Hegarty, A.F. and Scott, F.L., *Chem. Commun.*, 662 (1966); *J. Org. Chem.*, **32**, 1957 (1967).
- 91 Wittwer, C. and Zollinger, H., *Helv. Chim. Acta*, **37**, 1954 (1954).
- 92 Hauptmann, H. and Perisse, A.C. de M., *Chem. Ber.*, **89**, 1081 (1956); *Experientia*, **10**, 60 (1954).
- 93 Langbein, H., *J. Prak. Chem.*, **321**, 655 (1979).
- 94 Grummt, U.W. and Langbein, H., *J. Phot.*, **15**, 329 (1981).
- 95 Lewis, J.W. and Sandorfy, C., *Can. J. Chem.*, **61**(5), 809 (1983).
- 96 Kovalenko, M.F., Kurapov, P.B. and Grandberg, I.I., *Zh. Org. Khim.*, **23**(5), 1070 (1987).
- 97 Sidorova, L.P., Bednyagina, N.P. and Koznetsova, T.A., *Khim. Geterotsikl. Soedin.*, 1136 (1971).
- 98 Bednyagina, N.P. and Lipunova, G.N., *Khim. Geterotsikl. Soedin.*, 877 (1969).
- 99 Bednyagina, N.P., Lipunova, G.N. and Mokrushina, G.A., USSR Patent 241 442; *Byul. Izobret.*, 14 (1969).
- 100 Meriwether, L.S., Breitner, E.S. and Sloan, C.L., *J. Am. Chem. Soc.*, **87**, 4441 (1965).
- 101 Meriwether, L.S., Breitner, E.S. and Colthup, N.B., *J. Am. Chem. Soc.*, **87**, 4448 (1965).
- 102 Pel'kis, P.S. and Dubenko, R.G., *Dokl. Akad. Nauk. SSSR*, **110**, 798 (1956).
- 103 Pel'kis, P.S. and Dubenko, R.G., *Ukr. Khim. Zh.*, **23**, 64 (1957).
- 104 Rybakova, Yu.A., Lipunova, G.N. and Bednyagina, N.P., USSR Patent 296 791; *Byul. Izobret.*, 9 (1971).
- 105 Rybakova, Yu.A. and Bednyagina, N.P., *Khim. Geterotsikl. Soedin.*, 970 (1971).
- 106 Lipunova, G.N., Gulemina, N.N., Zeif, A.P. and Bednyagina, N.P., *Khim. Geterotsikl. Soedin.*, 493 (1974).

EXPERIMENTAL TECHNIQUES

In the following chapter general experimental techniques and equipment are described. Modifications to existing standard methods are noted.

2.1 General Procedures.

All solvents were either analytical grade or purified by standard methods [1].

A refrigerated cold bath was used for all diazotisations and some of the subsequent couplings. Water:Ethylene glycol was used in a 1:1 ratio and was stirred while being cooled by a commercial refrigeration coil. Temperatures less than -20°C were thus easily maintained.

2.2 Experimental Techniques.

X-Ray Crystal Structures:

Precession photographs were taken with a Nonius Graf Y924 camera using $\text{Co-K}\alpha$ radiation.

Crystal data were collected at -100°C with a Nicolet R3m four circle diffractometer using graphite monochromated $\text{Mo-K}\alpha$ radiation. Data sets were solved with the assistance of Dr Vickie McKee and Dr Ward Robinson, both from the University of Canterbury. For all structures solved in this study lists of bond angles, bond lengths, cartesian coordinates and thermal parameters have been deposited at the Cambridge Crystallographic Data Centre.

Raman Spectra:

Unless otherwise stated, Raman spectra were recorded using a SPEX 1401 spectrometer equipped with a Thorn EMI 6256 photomultiplier used in the photon counting mode. A Spectra-Physics 164-01 Krypton ion laser was used as the Raman scattering source operating at wavelengths between *ca.* 400 and 700 nm. Band wavenumbers were calibrated using the emission spectrum of neon and typical slit widths of 200 μm were employed giving a bandpass of 2 cm^{-1} at 647 nm. Samples were studied as crystals, thin films sublimed onto glass substrates or pressed discs diluted in KBr so as to reduce self-absorption and fluorescence. Divided discs, incorporating a suitable standard, were made for the resonance Raman intensity experiments. Spectra were recorded at room temperature using laser powers of less than 50 mW at the sample to avoid photo-

decomposition. Formazans are particularly susceptible to photo-degradation by blue or higher energy radiation.

Infrared Spectra:

Infrared spectra were recorded on samples prepared as KBr discs using a Digilab FTS-80 Fourier transform infrared spectrometer equipped with a globar source, KBr beamsplitter and a TGS pyroelectric detector. The optical bench was purged with air recycled through a molecular sieve air drier.

Ultra Violet-Visible Spectra:

Electronic absorption spectra were recorded with a Shimadzu model 160 ultra violet-visible spectrophotometer. Solvents were either spectroscopic grade or purified by standard methods. Diffuse reflectance spectra were recorded with a Pye Unicam SP700 spectrometer using MgCO_3 as a reference.

Nuclear Magnetic Resonance:

Solid state ^{13}C nmr spectra were recorded at 50.3 MHz on a Varian Associates XL-200 spectrometer using a standard CP/MAS probe. Powdered samples (*ca.* 300 mg) were packed in Kel-F rotors and spun using MAS frequencies of up to 10 kHz. The combined techniques of high power proton decoupling and single contact cross polarisation (CP) were employed. Typical contact times of 50 μs were used using delays of 1.2 s. The number of transients acquired was typically of the order of 1000.

Solution ^{13}C nmr spectra were recorded at 20.00 MHz with a Varian Associates FT-80A spectrometer employing proton decoupling. In all cases either deuterated solvents or D_2O capillary tubes provided the spin-lock. Typical spectral parameters employed were: spectral width 5000 Hz; acquisition time 1.023 s; pulse width 4 μs . Samples of *ca.* 200 mg were used in 5 mm o.d. tubes with tetramethylsilane as the internal standard. Precautions were taken to protect the spectroscopic solutions from the adverse effects of light and heat.

Microanalyses:

These were performed by Professor A.D. Campbell, Dr R.G. Cunninghame and associates of the University of Otago.

Mass Spectra:

These were recorded on a Micromass mass spectrometer with an ionising voltage of 70 eV. The temperature of the sample cell was 200°C.

Reference.

- 1 Perrin, D.D., Armarego, W.L.F. and Perrin, D.R., "*Purification of Laboratory Chemicals*", Pergamon Press, (1980).

RESULTS AND DISCUSSION

3.0.1 Electronic Absorption Spectra.

Most formazans absorb fairly intensively at wavelengths in the red and violet bands of the spectrum; this gives rise to their characteristic intense colours. They also absorb strongly in the ultra violet at *ca.* 250-300 nm. The former band(s) correspond to an $n - \pi^*$ transition originating in the lone pair of electrons of the nitrogen atoms present in the formazan system [1] and the latter band is due to absorptions of the phenyl groups attached to the formazan system.

Spectral data is scattered throughout the literature dealing mainly with the observation of the photochromic properties of the formazans. Some authors have discussed the relationship between colour and chemical constitution [2]. The energies and intensities of electron transitions have been calculated for dithizone by the method of molecular orbitals which has allowed the assignment of the configurational forms corresponding to the spectra [3]. However, the corresponding studies for other formazans have not appeared.

In this study solid state diffuse reflectance and solution absorption spectra have been recorded. For the solid state data band edges only are reported. For the solution data absorption maxima are indicated.

3.0.2 Vibrational Spectra.

Spectral data is again scattered throughout the literature [2] dealing mainly with the synthesis and characterisation of new formazans. There have been a number of specifically spectral studies correlating spectral measurements with the reactivity of formazan systems. Le Fevre [4] and Foffani [5] have studied the hydrogen bonding in the formazan system. Infrared spectra can be used as convincing evidence that red formazans are generally intramolecularly hydrogen bonded whereas orange formazans are generally intermolecularly hydrogen bonded.

In this study infrared spectra have been recorded, however, as several [6] comprehensive infrared spectral studies have already appeared in the literature the spectra are not reproduced herein.

Few Raman spectra have appeared in the literature for formazans although some studies of dithizone and metal dithizonates [7] have been

published.

In this study Raman and some resonance Raman spectra have been recorded and band centre wavenumbers together with the assignment of major bands are reported for solid state and some solution samples. Solid state spectra at reduced temperatures have also been recorded and are reported.

3.0.3 X-Ray Crystal Structure Analyses.

Several x-ray crystallographic analyses for the formazans have appeared in the literature. Crystal data are reported for all structures so far known for 1,5-diphenylformazans.

In this study the structures of several 1,5-diphenylformazans have been solved. A full description is given for those structures determined during the course of this study and a brief summary only is given for those structures determined by other authors.

Precession photographs have been taken for all of the structures determined herein.

3.1.4 Mass Spectra.

Some studies of the mass spectra of dithizone and its metal complexes have been published [8]. It has been shown that all of the dithizonates share a similar splitting scheme.

In this study the results of the mass spectra of formazans are presented.

3.1.5 Nuclear Magnetic Resonance Spectra.

Several magnetic resonance studies have appeared in the literature, but these have mostly concerned carbohydrate formazans, with the emphasis on the sugar, rather than the formazan, moiety [9].

Nmr has been used to investigate the keto-enol equilibrium of dithizone [10]. ^1H and ^{13}C nmr spectra have been used in association with ^{15}N -labelling to correctly predict the thione structure of dithizone and the equivalence of the imino protons, substantiated by an x-ray crystal analysis.

^{15}N -H coupling in 1,3,5-triphenylformazan derivatives has been shown to demonstrate that these compounds are not resonance hybrids but tautomeric pairs. The position of the equilibrium is dependent upon the substituents present in the 1,5-phenyl rings and tautomerism is rapid on the timescale of the nmr experiment.

No comprehensive nmr studies of formazans have appeared in the literature, neither have any solid state nmr spectra been recorded and reported in the literature.

In this study solid state and solution ^{13}C nmr spectral data are reported. Resonances in ppm and the assignments of major bands are given.

References.

- 1 Veas-Arancibia, C., Ph.D. Thesis, Louisiana State University and Agricultural and Mechanical College, 1986.
- 2 Hooper, W.D., *Rev. Pure and Appl. Chem.*, **19**, 221 (1969).
- 3 Spevacek, V. and Spevackova, V., *J. Inorg. Nucl. Chem.*, **38**, 1299 (1976).
- 4 Schiele, C., *Ber. Bunsenges. Physik. Chem.*, **69**, 308 (1965).
- 5 Foffani, A., Pecile, C. and Ghersetti, S., *Proc. Intern. Meeting Mol. Spectroscopy*, 4th; Bologna 1959; **2**, 769 (1962).
- 6 Jerchel, D. and Edler, W., *Chem. Ber.*, **88**, 1287 (1955); Le Fevre, R.J., Sousa, J.B. and Werner, R.L., *Aust. J. Chem.*, **9**, 151 (1956); Foffani, A., Pecile, C. and Ghersetti, S., *Tetrahedron Lett.*, **16** (1956); Foffani, A., Pecile, C. and Ghersetti, S., *Adv. Mol. Spectrosc.*, **2**, 769 (1962); Schiele, C., *Leibigs Ann. Chem.*, **689**, 197 (1965); Schiele, C. and Arnold, G., *Tetrahedron Lett.*, 4103 (1966); Arnold, G. and Schiele, C., *Spectrochim. Acta*, **25A**, 671 (1969); Arnold, G. and Schiele, C., *Spectrochim. Acta*, **25A**, 685 (1969); Arnold, G. and Schiele, C., *Spectrochim. Acta*, **25A**, 697 (1969); Kukushkina, I.I., Yurchenko, E.N., Ermakova, M.I. and Latosh, N.I., *Zh. Fiz. Khim.*, **46**, 176 (1972), *Russ. J. Phys. Chem.*, **1** (1972) (Engl. Trans.); Kukushkina, I.I., Yurchenko, E.N., Arkhipenko, D.V. and Orekhov, B.A., *Zh. Fiz. Khim.*, **46**, 1677 (1972), *Russ. J. Phys. Chem.*, **7** (1972) (Engl. Trans.); Lewis, J.W. and Sandorfy, C., *Can. J. Chem.*, **61**, 809 (1983); Otting, W. and Neugebauer, F.A., *Z. Naturforsch.*, **B**, **23**, 1064 (1968).
- 7 Takahashi, H., Yamada, O., Isaka, H., Igarashi, T. and Kaneko, N., *J. Raman Spectrosc.*, **19**, 305 (1988).
- 8 Alsop, P.A. and Irving, H.M.N.H., *Anal. Chim. Acta*, **65**, 202 (1973).
- 9 Kettrup, A. and Grote, M., *Z. Naturforsch.*, **B**, **31**, 1689 (1976); Tiers, V.D., Kansas State University, Ph.D. Thesis, 1959; Tiers, V.D., Plován, S. and Searles, S., *J. Org. Chem.*, **25**, 285 (1960).
- 10 Hutton, A.T. and Irving, H.M.N.H., *J. Chem. Soc., Chem. Commun.*, **1981**, 735; Coleman, R.A., Foster W.H. and Mason, M., *J. Org. Chem.*, **35**, 2039 (1970).

Chapter 3.1

The Aromatic Formazans.

In this chapter the results of the study of the following two formazans are given:

1,5-diphenylformazan (1)

1,3,5-triphenylformazan (2)

The aromatic formazans, 1,5-diphenylformazan (1) and 1,3,5-triphenylformazan (2) were first described by von Pechmann and Bamberger in 1892 [1].

For many years (1) was thought to be the simplest formazan available, closest to the hypothetical formazan molecule, and therefore invaluable as a 'building block' for the synthesis of more highly substituted formazans. However, formazans with only one aromatic ring are now available [2].

The triaromatic formazan (2) has been the subject of considerable study over the years. Following the observation that metal complexes were readily formed with (2) considerable effort has been devoted to developing formazan dyestuffs [3]. More importantly, however, the study of the photochromic nature of (2) has captured much interest [4]. On irradiation with visible light a red solution of (2) in toluene turns yellow. When left in the dark the colour reverts back to red. Several interconversion schemes have been proposed [4].

Properties.

The formazan (1) crystallises as either deep black/red or red crystals. The existence of a monohydrated species (red) accounts for the varying reports of the colour of the compound in the literature. Storage *in vacuo* over CaCl_2 effectively removes the water.

The formazan (2) crystallises as deep red plates with a brilliant green reflex. The formazan is very stable and may be kept, in a stoppered vessel in the dark, almost indefinitely.

Experimental.

Syntheses: (1) was prepared following the methods of von Pechmann [5] and Irving, Gill and Cross [6] with modifications.

The preparation of (1) by the coupling of malonic acid with benzenediazonium chloride was found to depend upon reaction conditions. It was essential to keep the temperature well below 0° C and the pH above 9 during the coupling.

To a diazonium solution prepared from aniline (23 g), concentrated hydrochloric acid (82 ml), water (100 ml) and sodium nitrite (18 g) was added sodium acetate (50 g) in water (100 ml). The whole was cooled to below -5° C and added over ten minutes to a stirred solution, also below -5° C, of malonic acid (26 g) and hydrated sodium acetate (50 g) in water (300 ml). The mixture was not allowed to rise above -3° C during the addition. After being stirred for a further 2 hours the mixture was left in the ethylene glycol bath, maintained at -10° C overnight. The flocculant red precipitate was collected and dried *in vacuo* over CaCl₂. A further crop of crystals was obtained from the mother liquor. After drying, the dark red crystals had a violet reflex. Melting Point: 115-117° C.

1,3,5-Triphenylformazan was prepared following the method of Todd [7].

Benzaldehyde phenylhydrazone was first prepared by placing benzaldehyde (10.6 g) in ethanol (50 ml). Over one minute and in an ambient waterbath, phenylhydrazine (10.6 g) in ethanol (25 ml) was added. The mush of crystals which resulted was warmed on a steambath, cooled and washed with a little cold ethanol. The pure white product was air-dried overnight.

Aniline was diazotised on a 0.02 mol scale. Firstly pyridine (15 ml) then ethanol (25 ml) were added to the phenylhydrazone (3.9 g, 0.02 mol). The diazonium solution was added to the swirled phenylhydrazone in squirts. The formazan precipitated with the addition of water as a deep red precipitate.

Triphenylformazan was recrystallised as deep red plates with a green reflex. Melting Point: 170-172° C.

Results and Discussion.

X-Ray Crystal Structures: The x-ray crystal structure of (1) has been solved by O'melchenko *et al.* in 1973 [8]. C₁₃H₁₂N₄ crystallises in the monoclinic space group *C2/c*, *a*=25.278(5), *b*=7.085(2), *c*=20.645(5) Å, *β*=139.50(10)°, *V*=2358 Å³, *Z*=8.

The formazan adopts the *anti,s-trans* configuration in the solid state.

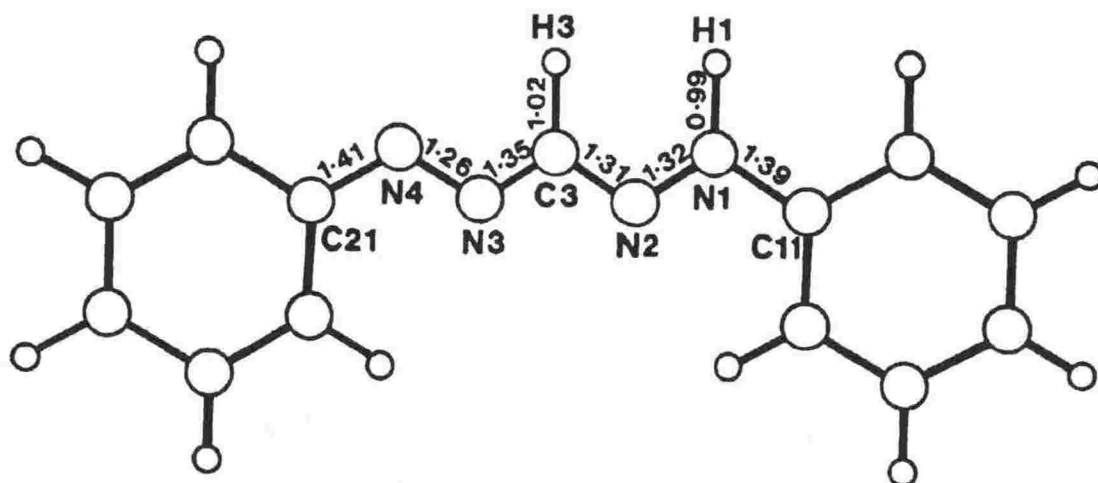


Figure 1: X-Ray Crystal Structure of 1,5-diphenylformazan by O'melchenko *et al.* [8]

In the free state the molecule would seem to be planar but in the crystal the phenyl rings are rather expanded in relation to each other. The angle between their respective planes is 17.24° .

There is an intermolecular hydrogen bond between N1-H1...N'4 atoms in adjacent diphenylformazan molecules causing the formation of infinite spirals along a two-fold helical axis. The packing of the spirals obeys the principle of densest packing. The intermediate values of the N-N and C-N bonds (between a double and a single bond) and the inequality of the two N-N bond distances for what seems to be a fairly symmetrical molecule indicate an appreciable delocalisation of electrons along the formazan backbone. The structure closely parallels that seen for other orange formazans although the average C-N bond distance is shorter than is usual.

The crystal structure of (2) remains undetermined.

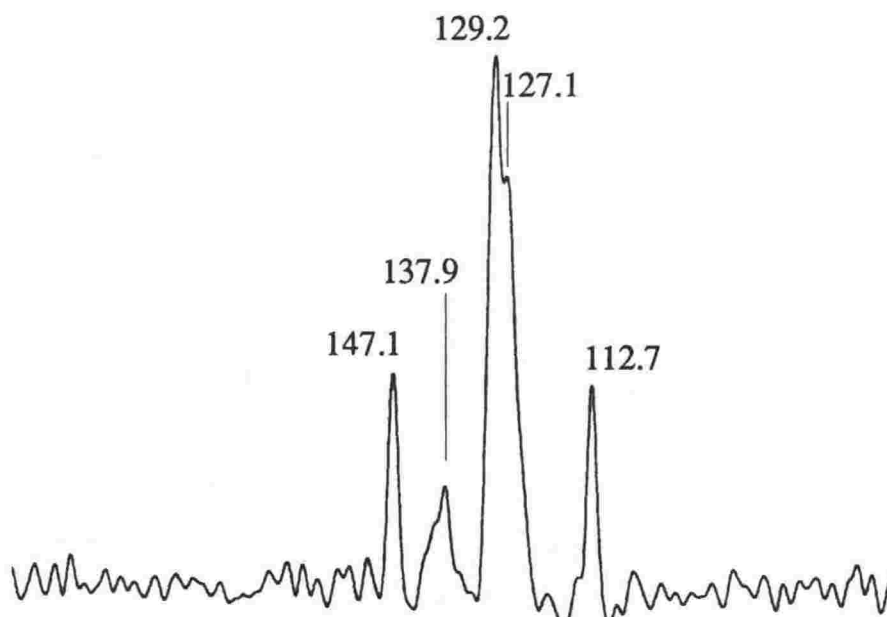
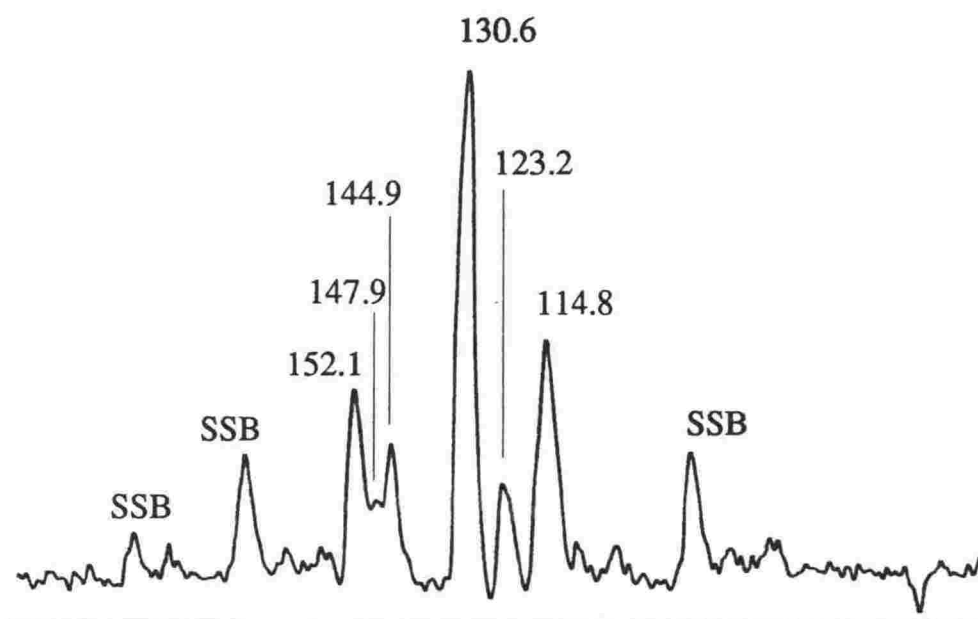
Nuclear Magnetic Resonance: The solid state ^{13}C and solution ^{13}C nmr spectra in several solvents have been observed and are summarised in Table 1. The solid state spectra for (1) and (2) are shown in Figures 2 and 3. The short contact time spectrum for (1) is shown in Figure 4.

Assignments in the solid state are based on the use of short contact times, to identify quaternary carbon signals, TOSS experiments and multiple and fast spinner speeds to remove spinning sidebands.

Assignments in solution are based on GASPE or DEPT experiments. In the solid state some of the motional degrees of freedom are quenched allowing the identification of different isomers and configurations.

The solid state ^{13}C nmr confirm that (1) and (2) exist in different configurations from each other.

For (1) discrete signals for C11 and C21 are observed (at 147.9 and 144.9 ppm) confirming their non-equivalence. The attitude of the phenyl rings in (1) is such that they are twisted out of the plane of the molecule rather more than in comparable orange formazans and this feature, together with the effect of the 1-H substituent, is manifest.



Figures 2 and 3: The Solid State ^{13}C MAS Nmr Spectra for 1,5-diphenylformazan (1), top, and 1,3,5-triphenylformazan (2) bottom.

For (2) a broad signal at *ca.* 138 ppm is observed and this is assigned to the C11 and C21 phenyl carbon atoms. The broadening of this signal can be attributed to the proximity of the quadrupolar (nitrogen) nucleus, a slight inequivalence of environment or a mixture of configurations. The signal would appear to be broader than that observed in other 1,5-diphenylformazans. The pattern of resonances for the three phenyl groups would seem to indicate that the 1- and 5- phenyl rings are in very similar environments and that the 3-phenyl ring is in a dissimilar environment. The most marked effect would be expected in the signals for the quaternary phenyl carbon signals. This observation in respect of the 1- and 5- phenyl carbon resonances parallels that seen for 3-*tertiary* butyl-1,5-diphenylformazan and importantly contrasts that for red isomers of 3-ethylthio- and 3-ethyl-1,5-diphenylformazan.

The short contact time spectrum for (1) utilises the fact that carbon nuclei with directly bonded protons relax faster than do quaternary carbon to assist in the assignment of phenyl and quaternary carbon resonances.

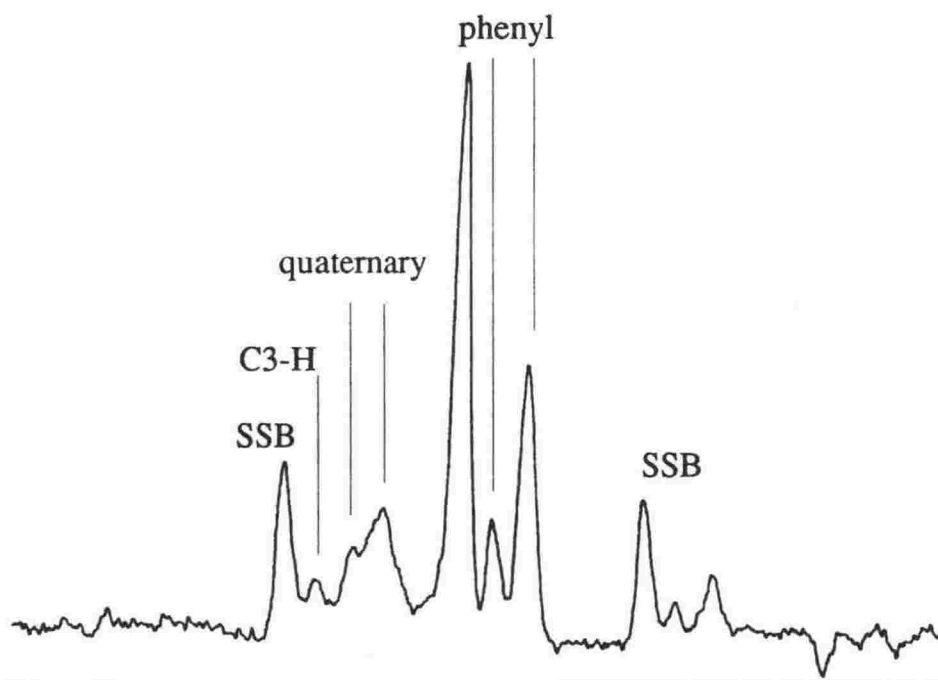


Figure 4: Short Contact Time Solid State ^{13}C MAS Nmr Spectrum for 1,5-diphenylformazan (1).

In solution the *anti,s-trans* and *syn,s-cis* configurations yield equivalent aromatic carbon resonances as tautomerism is fast on the timescale of the nmr experiment.

For (1) the solution spectrum in $\text{DMSO}-d_6$ agrees closely with the solid state spectrum. Signals are observed for all carbon atoms although the C3 and C21 signals are coincident at 147 ppm. In CDCl_3 however, the spectrum differs importantly in that the C3 signal has shifted from *ca.*

Table 1: Resonances (δ ppm) for ^{13}C Nmr Spectra of 1,5-diphenylformazan (1) and 1,3,5-triphenylformazan (2).

State	C3	C11	C21	C phenyl
1,5-diphenylformazan				
Solid	151.2	147.9	144.9	130.6 123.2 114.8
DMSO- d_6	147.95	149.84	147.95	129.31 126.12 117.81
CDCl_3	140.50	150.15	148.14	129.37 127.01 118.62
1,3,5-triphenylformazan				
Solid	147.1	137.9		129.2 127.1 112.7
CDCl_3	147.88	141.09	137.43	129.43 128.41 127.65 127.50 125.82 118.79
C_6D_6	148.24	141.65	138.09	129.62 129.51 129.05 128.72 128.34 128.13 128.02 127.87 127.70 127.53 126.41 119.16
$(\text{CD}_3)_2\text{CO}$	148.87	138.05		129.28 128.57 128.49 126.80 119.75
1,5-Diphenyl and 1,3,5-Triphenylformazans.				

148 to *ca.* 140 ppm. The pattern of resonances for the phenyl rings indicates that they are in equivalent chemical environments.

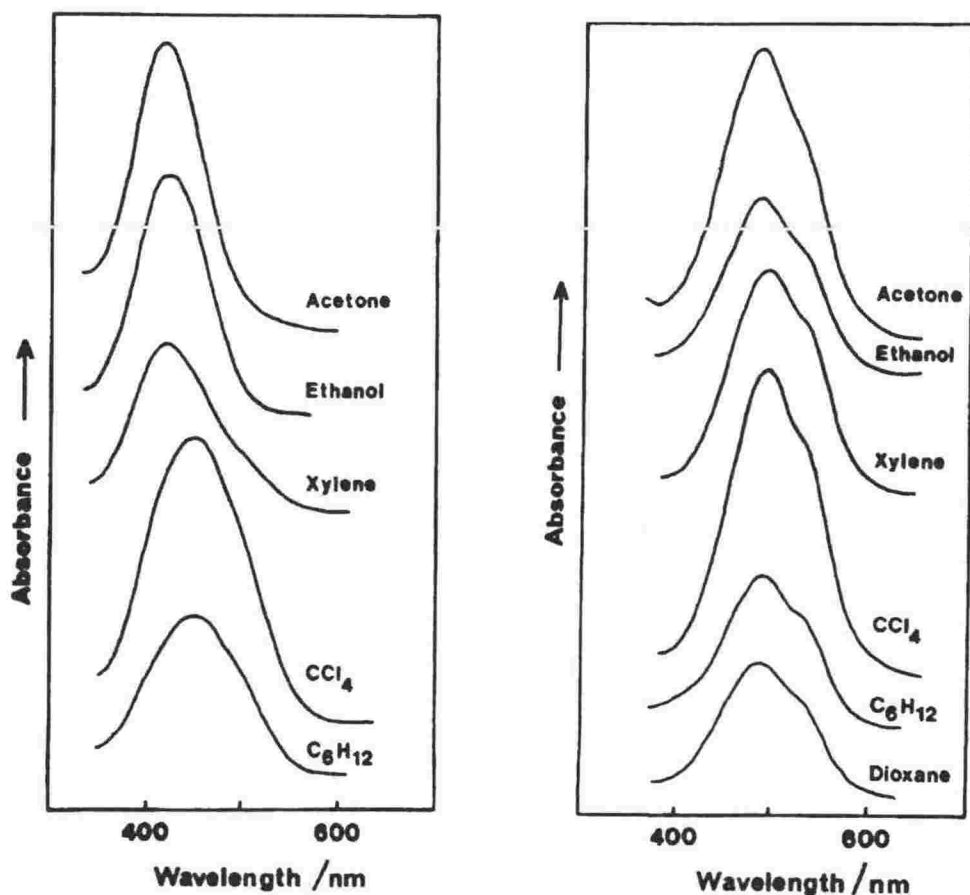
These observations indicate that in DMSO- d_6 the stable configuration of (1) is the same as that observed in the solid state. The small shifts in signals arise from solution effects and tautomerism in solution. The $CDCl_3$ configuration is not the *anti,s-trans* of the solid state but is a symmetric red formazan. It is apparent that each configuration becomes dominant over the period of the experiment (several hours) in the respective solvent.

For (2) the resonances observed in solution for the $(CD_3)_2CO$ spectrum agrees closely with the solid state spectrum. Only one signal is observed coincident at 138.05 ppm for C11 and C21. The C3 signal occurs at 148.87 ppm and five phenyl peaks, for the 1- and 5-phenyl rings and the phenyl C3 substituent are observed. The solution spectra for $CDCl_3$ and C_6D_6 compare favourably with each other but differ importantly from the solid state and hexadueteroacetone spectrum. Two signals are observed for C11 and C21 at *ca.* 141 and 138 ppm respectively. The C3 signal occurs at *ca.* 148 ppm and a well defined multiplet of signals occurs between 129 and 118 ppm for the three phenyl groups. A close analysis of these peaks shows that there are more peaks than could possibly be accounted for by one configuration of 1,3,5-triphenylformazan. Even an asymmetric configuration would only result in a maximum of 12 signals, and it is unlikely that all of these peaks could be resolved. In C_6D_6 we can resolve 15 peaks - the obvious explanation is that two configurations are present and that these are most likely to be *syn,s-cis* and *syn,s-trans* red formazans.

Absorption Spectra: Further evidence for the existence of an equilibrium comes from the electronic absorption spectra shown in Figures 5 and 6.

For (1) these spectra clearly demonstrate that both an orange and a red form are present in differing concentrations dependent upon the solvent.

In the electronic absorption spectra of unirradiated solutions of (2) there are two bands with maxima of 495 and 546 nm respectively. During irradiation with visible light the red chelate form isomerises to the yellow open form with absorption maximum 405 nm. Ultra violet-visible and kinetics studies have variously ascribed the bands to different species [9]. According to published data [9] the first maximum is due to $\pi-\pi^*$ transition of the conjugated system while the second transition corresponds to $n-\pi^*$ transitions in fragments of the $\ddot{N}=$ type. A recent investigation by Kovalenko *et al.* [10] has established that these two bands are, in fact, attributable to two individual red triphenylformazan isomers, presumably *syn,s-cis* and *syn,s-trans*. These results also indicated the possibility of a purely thermal transition between these two red isomers in the solid state.



Figures 5 and 6: The Ultra violet-visible Absorption Spectra of 1,5-diphenylformazan (1), left, and 1,3,5-triphenylformazan (2), right.

The electronic absorption spectra confirm the existence of two red isomers in all of the solvents studied. In all cases the species absorbing at 495 nm exceeds the concentration of the species absorbing at 546 nm.

Raman Spectra: The band centre wavenumbers for the Raman active phonons of (1) and (2) are given in Table 2. Raman spectra are shown in Figures 7 and 8. Assignments are based on the symmetry coordinate whose contribution to the normal coordinate is greatest, although it is clear that the vibrations of the formazan backbone are largely coupled.

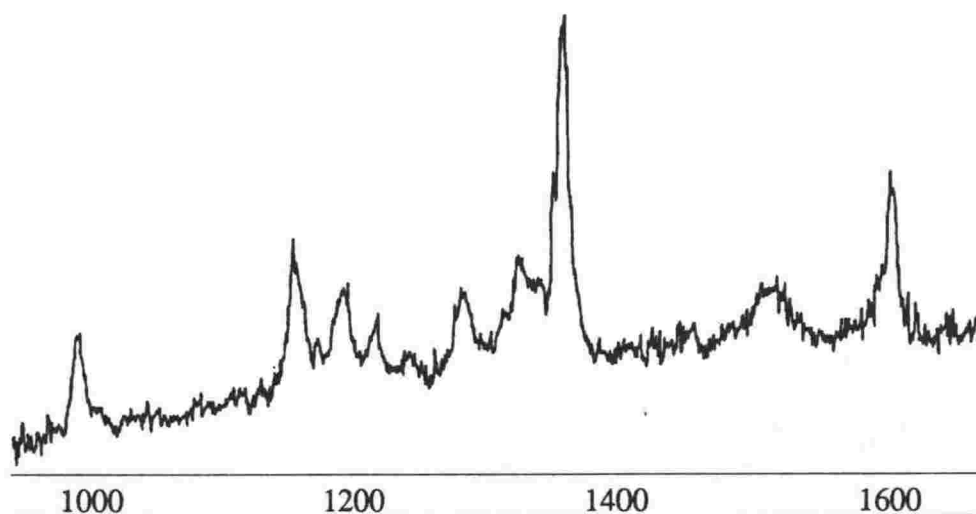
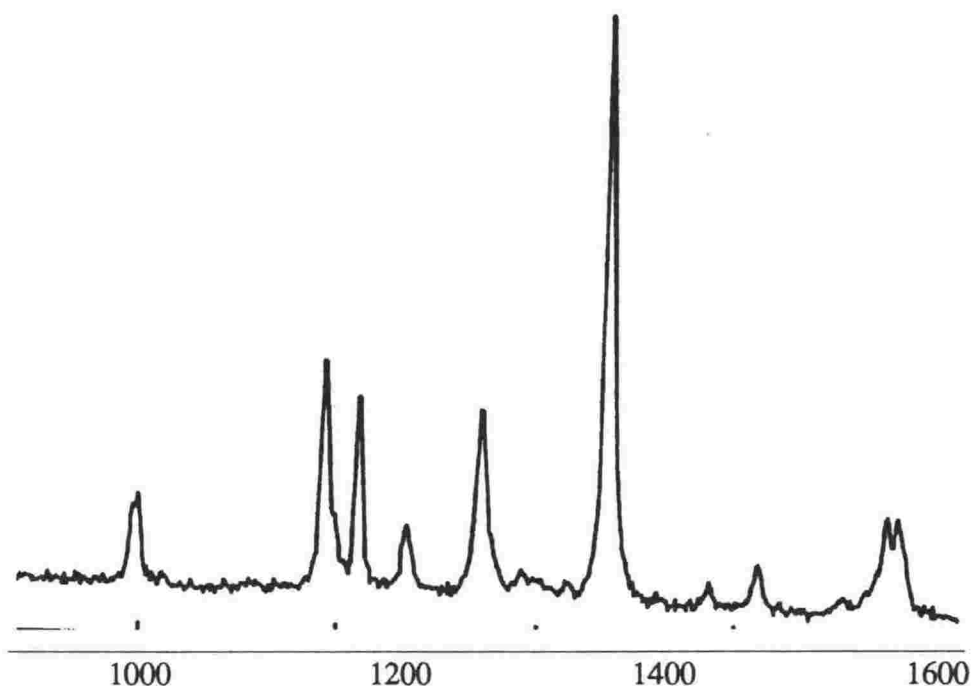
For (1) the Raman spectrum closely resembles those for other orange *anti,s-trans* formazans.

The most intense band in the spectrum of (1) occurs at 1379 cm^{-1} and for (2) occurs at 1349 cm^{-1} . While these bands are assigned principally to vibrations of the N=N group there must be a significant contribution from the C3-N3 fragment of the formazan. When compared with the spectra of other orange formazans this vibration occurs some 35 cm^{-1} lower than either 3-methyl- or the orange isomer of 3-ethyl-1,5-diphenylformazan. The major difference in the molecular structures of these three *anti,s-trans* formazans is the C3-N3 bond length. This band is

**Table 2: Raman Bands (cm^{-1}) for
1,5-diphenylformazan (1) and 1,3,5-triphenylformazan (2).**

1,5-diphenylformazan	1,3,5-triphenylformazan
1600	1598
1592	
1557	
1487	1510
1450	
1379	1349
	1334
	1321
	1305
1275	1271
1234	
1218	1204
1178	1181
1159	1147
1151	
1023	
1000	983
995	

seen to be a marker band for the configurations of 1,5-diphenylformazans with *syn,s-trans* and *anti,s-trans* occurring at *ca.* 1400 cm^{-1} while *syn,s-cis* occurs at *ca.* 1350 cm^{-1} .



**Figures 7 and 8: Raman Spectra
of 1,5-diphenylformazan (1), top,
and 1,3,5-triphenylformazan (2), bottom.**

Conclusion.

1,5-Diphenylformazan exists in the *anti,s-trans* configuration in the solid state. In methanol solution this configuration is maintained but in aprotic solvents this configuration is in equilibrium with the *syn,s-cis* configuration. This behaviour does not typify that of other orange formazans which generally equilibrate with the *syn,s-trans* configuration. The only significant difference is in the bond length of the C3-N3 fragment of the formazan with the result that the average bond length of the N-N-C-N-N backbone equals 1.30(5) Å compared with 1.35(5) Å in 3-methyl- and 3-ethyl-1,5-diphenylformazan. This average distance corresponds closely to the *aromatic distance* of 1.31 Å.

The H substituent is clearly the feature which determines the open *anti,s-trans* configuration of (1) in the solid state allowing the open configuration which is further stabilised by an intramolecular hydrogen bond.

In solution the formation of an equilibrium involving the closed red structure is evidenced by nmr and absorption spectra. The closed structure is clearly, but atypically, *syn,s-cis*. The lower average bond length of the formazan backbone and, in particular, the unusually shortened C3-N3 distance and the very small 3-substituent must be held to account for this observation. The only other 3-H substituted formazan structurally characterised is 1-methyl-1,5-diphenylformazan in which an intramolecular hydrogen bond is precluded from occurring by the 1-substituent. The orange configuration would seem to be the thermodynamically preferred one and is apparent in appreciable concentration even in aprotic solvents in the dark.

The formazan (2) has long been assumed to exist in the *syn,s-cis* configuration in the solid state. Kinetics studies and absorption spectra have established the existence of two thermodynamically stable red forms in the solid state and a possible thermal path between them for their interconversion.

The result of nmr, Raman and electronic absorption studies confirm the existence of two red forms. In the solid state, the Raman spectrum is characteristic of *syn,s-cis* configuration and closely parallels that seen for 3-*tertiary*-butyl-1,5-diphenylformazan which has been structurally characterised in the *syn,s-cis* configuration. The observed spectrum, however, shows much weaker scattering than other formazans due to considerable self-absorption. The spectrum also possesses several broadened signals which may indicate the existence of the second, *syn,s-trans*, configuration in the solid state. The photochromic interconversion for red to yellow triphenylformazan has been monitored in the solid state in thin films. The lifetime of the yellow species is short ($k < 0.1$ s) and

so this species is unlikely to contribute to the Raman spectrum of (2).

The solid state nmr spectrum also indicates a degree of mixing of two red configurations. While the concentration of the respective configurations cannot be accurately gauged it is certain that the formazan does not exist in one pure red configuration.

The solution behaviour of (2) is more convincing. The absorption spectra clearly indicate the existence of two isomers in all the solvents studied (both protic and aprotic). The solution nmr spectra confirm this observation that the *syn,s-trans* configuration is appreciable and may in fact be dominant in aprotic solvents. The reason for this is unclear. On this basis one may assign the 495 nm band in the ultra violet-visible absorption spectrum to the *syn,s-trans* configuration and the 546 nm band to the *syn,s-cis* configuration.

References.

- | | | | |
|---|--|----|--|
| 1 | von Pechmann, H., <i>Chem. Ber.</i> , 25 , 3175 (1892); Bamberger, E., <i>Chem. Ber.</i> , 25 , 3547 (1892). | 6 | Irving, H.M.N.H., Gill, J.B. and Cross, W.R., <i>J. Chem. Soc.</i> , 1960 , 2087. |
| 2 | Buzykin, B.I., Sysoeva, L.P., Espenbetov, A.A., Struchkov, Yu.T. and Kitaev, Yu.P., <i>Zh. Org. Khim.</i> , 22 , 2277 (1986). | 7 | Todd, D., " <i>Experimental Organic Chemistry</i> ", Prentice-Hall Inc., New Jersey, 1979, p251. |
| 3 | Nineham, A.W., <i>Chem. Rev.</i> , 55 , 355 (1955). | 8 | Omel'chenko, Yu.A., Kondrashev, Yu.D., Ginzburg, S.L. and Neiganz, M.G., <i>Kristallografiya</i> , 19 , 522 (1974). |
| 4 | Lewis, J.W. and Sandorfy, C., <i>Can. J. Chem.</i> , 61 (5), 809 (1983). | 9 | Veas-Arancibia, C., Louisiana State University and Agricultural and Mechanical College, Ph.D. Thesis, 1986. |
| 5 | von Pechmann, H., <i>Chem. Ber.</i> , 27 , 320 (1894); von Pechmann, H., <i>Chem. Ber.</i> , 27 , 1679 (1894); von Pechmann, H., <i>Chem. Ber.</i> , 28 , 876 (1895). | 10 | Kovalenko, M.F., Kurapov, P.B. and Grandberg, I.I., <i>Zh. Org. Khim.</i> , 23 (5), 1070 (1987). |

Chapter 3.2

3-Ethyl-1,5-Diphenylformazan.

In this chapter the results of studies of the following two formazans are given:

- | | |
|-------------------------------------|-----|
| orange 3-ethyl-1,5-diphenylformazan | (1) |
| red 3-ethyl-1,5-diphenylformazan | (2) |

The first section of this chapter consists of the preparation and characterisation of the two isomers of a formazan equilibrium. The results of the study have been published and a reprint of a paper entitled "Photochromic Formazans: Raman Spectra, X-Ray Crystal Structures, and ^{13}C Magnetic Resonance Spectra of the Orange and Red Isomers of 3-Ethyl-1,5-diphenylformazan" which has appeared in the *Journal of the Chemical Society, Perkin Transactions 2*, **1988**, 1275, forms the basis of this section.

The second section of this chapter includes the actual solid state nmr spectra which are described for completeness.

The third section of this chapter consists of some preliminary investigations on the kinetics of the interconversions of the two isomers.

Photochromic Formazans: Raman Spectra, X-Ray Crystal Structures,[†] and ¹³C Magnetic Resonance Spectra of the Orange and Red isomers of 3-Ethyl-1,5-diphenylformazan

Gary R. Burns* and Christopher W. Cunningham

Chemistry Department, Victoria University, Private Bag, Wellington, New Zealand
Vickie McKee

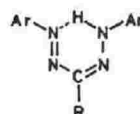
Chemistry Department, University of Canterbury, Christchurch 1, New Zealand

The X-ray crystal structures of the two isomers of a photochromic formazan have been determined. Red 3-ethyl-1,5-diphenylformazan belongs to the orthorhombic space group $P2_12_12_1$ and adopts a *syn,s-trans*-configuration. The orange, light-stable isomer, belongs to the monoclinic space group $P2_1/c$ and adopts an *anti,s-trans*-configuration. Raman and ¹³C n.m.r. spectra for the orange isomer both in the solid state and in solution confirm that the solution species retains the structure established for the solid state. The Raman spectrum for the red isomer in the solid state shows the shift to lower wavenumber for the azo group stretching vibration characteristic of the *syn,s-trans*-configuration.

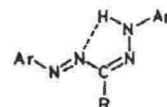
Photochromic materials are potentially useful for information storage and in various optical devices. The photochromism of inorganic compounds can be attributed to the formation of colour centres or to some other charge-transfer mechanism, whereas in organic and organometallic compounds photochromism usually involves a photoinduced isomerisation or dissociation which gives rise to differently coloured metastable species. There are advantages in using organometallic and organic photochromes in that their optical properties can be 'tuned' by making small structural adjustments, and they show greater changes in optical density than inorganic photochromes. However, they also show a greater tendency to fatigue on recycling. Consequently it is important to identify causes of fatigue in a photochromic system if that system is to be improved.

The formazans provide both organic and organometallic examples of photochromism;¹ the latter have been the more widely investigated. The Hg^{II} dithizonet complex is one of a small number of commercially exploited organic photochromes.

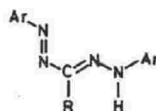
Apart from isomers which are unlikely because of serious steric crowding, the formazans can in principle adopt any of four possible structures (a)–(d) corresponding to *syn-anti* isomerisation about the C=N double bond and isomerisation about the C–N single bond (*s-cis/s-trans*). Otting and Neugebauer^{2,3} have concluded that in solution the red and yellow formazans are, respectively, *syn,s-cis*- and *anti,s-trans*-isomers. In the solid state the formazans crystallise as red or orange-yellow solids, with the *syn,s-cis*⁴ or *syn,s-trans*^{5,6} configuration if red and the *anti,s-trans*^{7–10} configuration if orange-yellow. However, no single photochromic formazan has yet been reported where both the red and the orange-yellow isomers have been obtained in the solid state and their structures established. Consequently, attempts to correlate photochromic behaviour with the nature of the substituents on C(1), C(3), and C(5) suffer from the absence of definitive



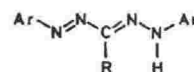
(a) *syn,s-cis*



(b) *syn,s-trans*



(c) *anti,s-cis*



(d) *anti,s-trans*

structural information for both red and yellow isomers of a single photochromic formazan.

We have been able to isolate the orange and the red conformers of 3-ethyl-1,5-diphenylformazan and now describe their X-ray crystal structures together with the results of i.r., Raman, and n.m.r. spectroscopic studies.

Experimental

Orange 3-Ethyl-1,5-diphenylformazan (I).—This was prepared by the method of Todd¹¹ and crystallised from 1:1 ethanol–water as orange needles, m.p. 96–98 °C (Found: C, 71.1; H, 6.5; N, 22.5. C₁₅H₁₆N₄ requires C, 71.4; H, 6.4; N, 22.2%).

Crystal structure analysis. An irregularly shaped crystal of dimensions 0.30 × 0.15 × 0.075 mm was used. Intensity data were collected at –150 °C with a Nicolet R3m four-circle diffractometer using graphite-monochromated Mo-K_α radiation. The unit-cell parameters (Table I) were determined by least-squares refinement of 25 accurately centred reflections (24 < 2θ < 26°); 2 020 reflections were collected using the θ–2θ scan technique (3 < 2θ < 50°) and variable scan rate (4.88–58.6° min^{–1}). Crystal stability was monitored by recording three standard reflections every 100 reflections; no significant variation was observed. Data reduction gave 1 800 unique reflections of which 1 372 had I > 3[σ(I)] and these

[†] Supplementary data (see section 5.6.3 of Instructions for Authors, in the January issue). Full lists of bond lengths and angles, H-atom coordinates, and thermal parameters have been deposited at the Cambridge Crystallographic Data Centre.

[‡] Bis-(1,5-diphenylthiocarbazono-N,S)-mercury(II).

Table 1. Crystal data for 3-ethyl-1,5-diphenylformazan isomers

	Orange (1)	Red (2)
Formula	$C_{15}H_{14}N_4$	$C_{15}H_{14}N_4$
M_r	252.4	252.4
Crystal system	Monoclinic	Orthorhombic
$a/\text{\AA}$	9.281(1)	5.211(11)
$b/\text{\AA}$	17.986(2)	9.835(12)
$c/\text{\AA}$	8.474(1)	25.950(60)
$\alpha/^\circ$	90	90
$\beta/^\circ$	104.07(1)	90
$\gamma/^\circ$	90	90
$V/\text{\AA}^3$	1 373.2(3)	1 329.9(4)
$R(000)$	535.86	535.86
$\mu(\text{Mo-K}\alpha)/\text{cm}^{-1}$	0.71	0.73
$\lambda(\text{Mo-K}\alpha)/\text{\AA}$	0.710 69	0.710 69
$D_c/\text{g cm}^{-3}$	1.21	1.25
Z	4	4
Obs. refl.	1 372	515
R/R_w	0.0486/0.0625	0.059/0.067
Space group	$P2_1/c$	$P2_12_12_1$

Table 2. Atomic co-ordinates ($\times 10^4$) and temperature factors ($\text{\AA}^2 \times 10^3$) for the orange isomer (1)

Atom	x	y	z	U^a
C(1)	6 722(2)	2 801(1)	2 063(3)	36(1)
C(2)	5 707(2)	2 171(1)	2 333(2)	26(1)
C(3)	4 570(2)	1 995(1)	798(2)	23(1)
N(1)	2 914(2)	2 858(1)	1 168(2)	26(1)
N(2)	3 307(2)	2 329(1)	246(2)	24(1)
N(3)	4 799(2)	1 450(1)	-299(2)	23(1)
N(4)	5 999(2)	1 090(1)	200(2)	25(1)
C(11)	6 214(2)	505(1)	-848(2)	25(1)
C(12)	5 161(2)	267(1)	2 222(2)	29(1)
C(13)	5 493(3)	-331(1)	-3 098(3)	35(1)
C(14)	6 844(3)	-683(1)	-2 641(3)	40(1)
C(15)	7 889(3)	-455(1)	-1 271(3)	40(1)
C(16)	7 568(2)	137(1)	-369(3)	32(1)
C(21)	1 559(2)	3 231(1)	632(2)	25(1)
C(22)	674(2)	3 139(1)	-937(2)	29(1)
C(23)	-603(2)	3 558(1)	-1 431(3)	36(1)
C(24)	-1 024(2)	4 053(1)	-387(3)	44(1)
C(25)	-161(2)	4 129(1)	1 186(3)	43(1)
C(26)	1 131(2)	3 721(1)	1 696(3)	32(1)

^a Equivalent isotropic U defined as one third of the trace of the orthogonalised U_{ij} tensor.

were used for the structure determination. Intensities were corrected for Lorentz-polarisation effects but no absorption correction was applied ($\mu = 0.71 \text{ cm}^{-1}$). Systematic absences uniquely specified the space group as $P2_1/c$.

The structure was solved by direct methods using the program SOLV,¹² which revealed the positions of all the non-hydrogen atoms. Isotropic refinement using blocked cascade least-squares methods converged at $R = 0.109$. The non-hydrogen atoms were then refined anisotropically. Hydrogen atoms were included at calculated positions except H(1), which was located from a difference map. They were refined by using the riding model with thermal parameters of $1.2U$ of their carrier atoms [$d(\text{C-N-C-H}) = 0.96 \text{ \AA}$]. The structure converged with $R = 0.0486$ and $R_w = 0.0625$. The function minimised was $\sum w(|F_o| - |F_c|)^2$, where $w = [\sigma^2(F_o) + 0.0009 4F_o^2]^{-1}$; a final difference map showed no peaks greater than 0.25 e \AA^{-3} .

Red 3-Ethyl-1,5-diphenylformazan (2).—Crystals were grown by dissolving pure orange (1) (1 g) in light petroleum (500 cm^3 ;

Table 3. Atomic co-ordinates ($\times 10^4$) and temperature factors ($\text{\AA}^2 \times 10^3$) for the red isomer (2)

Atom	x	y	z	U
C(1)	4 432(2)	3 680(10)	689(4)	32(3)
C(2)	6 780(22)	2 715(11)	660(4)	31(3)
C(3)	6 780(24)	1 709(12)	1 102(5)	26(3)
N(1)	5 519(17)	903(9)	1 869(4)	26(3) ^a
N(2)	5 337(18)	1 804(8)	1 473(4)	21(3) ^a
N(3)	8 837(18)	688(9)	1 126(4)	21(3) ^a
N(4)	10 252(17)	646(9)	731(4)	23(3) ^a
C(11)	3 704(22)	914(11)	2 261(4)	22(3)
C(12)	3 962(22)	-91(11)	2 648(4)	24(3)
C(13)	2 233(24)	-128(11)	3 058(4)	28(3)
C(14)	220(24)	805(11)	3 092(4)	31(3)
C(15)	13(23)	1 767(12)	2 701(4)	31(3)
C(16)	1 694(19)	1 830(11)	2 290(4)	18(3)
C(21)	12 161(23)	-378(11)	755(4)	24(3)
C(22)	12 555(23)	-1 253(10)	1 159(5)	27(3)
C(23)	14 534(25)	-2 237(11)	1 147(4)	36(4)
C(24)	16 028(22)	-2 330(12)	726(4)	28(3)
C(25)	15 626(23)	-1 465(10)	390(4)	30(3)
C(26)	13 714(22)	-493(11)	325(4)	27(3)

^a Equivalent isotropic U defined as one third of the trace of the orthogonalised U_{ij} tensor.

b.p. 40–60 $^\circ\text{C}$) and allowing the solution to equilibrate in the dark. The volume was reduced to ca. 200 cm^3 using a vacuum oven; after 3 days at 0 $^\circ\text{C}$ the resulting solution had deposited red needles in low yield; m.p. 73–74 $^\circ\text{C}$.

Crystal structure analysis. A small crystal (0.86 \times 0.13 \times 0.063 mm) of high mosaicity was used. Intensity data were collected at -150 $^\circ\text{C}$ with a Nicolet R3m four-circle diffractometer. The unit-cell parameters (Table 1) were determined by least-squares refinement of 18 accurately centred reflections with $14 < 2\theta < 19^\circ$; 1 122 reflections were collected using the θ - 2θ scan technique ($3 < 2\theta < 45^\circ$) and variable scan rate (4.0–29.3 $^\circ \text{ min}^{-1}$). Crystal stability was monitored by recording three standard reflections every 100 measurements and no significant variation was observed. Data reduction gave 1 062 unique reflections of which 515 having $I > 3[\sigma(I)]$ were used in the subsequent structure analysis. The intensities were corrected for Lorentz-polarisation effects but no absorption correction was applied ($\mu = 0.73 \text{ cm}^{-1}$). Systematic absences uniquely specified the space group as $P2_12_12_1$.

The structure was solved by direct methods using the program RANT which revealed the positions of all the non-hydrogen atoms. Isotropic refinement converged with $R = 0.089$. Hydrogen atoms were inserted at calculated positions on appropriate carbon atoms, using the riding model with thermal parameters equal to $1.2U$ of their carrier atoms [$d(\text{CH}) = 0.96 \text{ \AA}$]. The position of H(1), bound to N(1), was located from a difference map and not further refined. The four nitrogen atoms were refined anisotropically and the structure converged with $R = 0.059$, $R_w = 0.067$. The function minimised was $\sum w(|F_o| - |F_c|)^2$ where $w = [\sigma^2(F_o) + 0.0005 7F_o^2]^{-1}$; a final difference map showed no features greater than 0.3 e \AA^{-3} . All the programs used for data reduction and structure solution are included in the SHELXTL (Version 4.0)¹² package.

General Methods.—Raman spectra were recorded with a Spex 1401 spectrometer equipped with a Thorn EM1 6256 photomultiplier tube used in the photon counting mode. A Spectra Physics 164-01 Krypton ion laser was used as the Raman scattering source, operating at 647 and 676 nm. Band wavenumbers were calibrated by using the emission spectrum of neon, and typical slit widths of 200 μm were employed, giving a

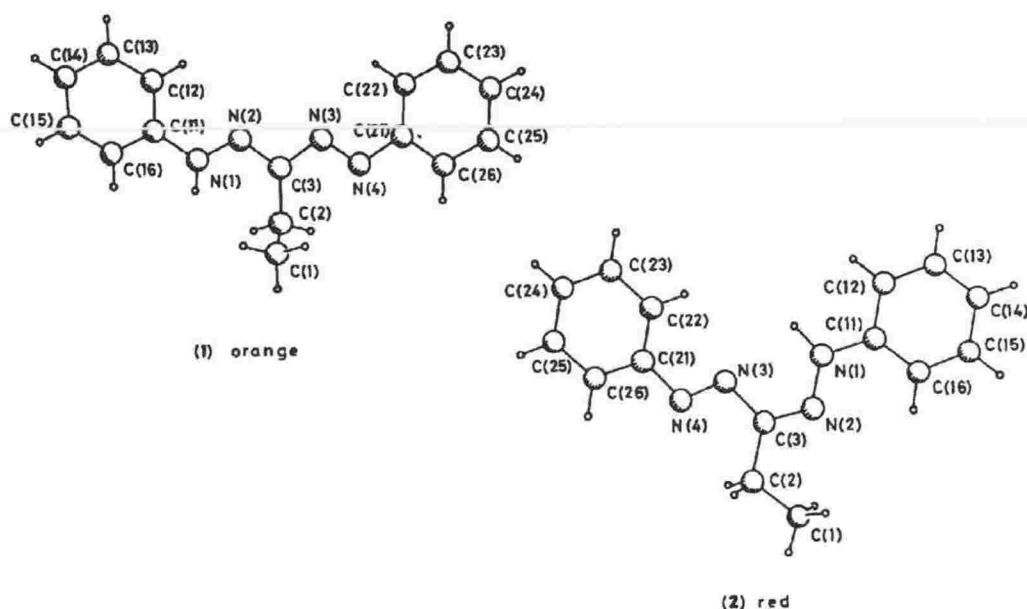


Figure 1. Molecular structures and atomic nomenclature of orange (1) and red (2) 3-ethyl-1,5-diphenylformazan

Table 4. A comparison of bond lengths and bond angles for the $-N=N-C=N-N-$ backbone of the orange (1) and red (2) isomers

Bond lengths (Å)	Bond angles (°)	
	Orange (1)	Red (2)
C(1)–C(2)	1.525(3)	1.515(16)
C(2)–C(3)	1.496(2)	1.520(17)
C(3)–N(2)	1.298(2)	1.308(15)
C(3)–N(3)	1.403(2)	1.379(15)
N(1)–N(2)	1.337(2)	1.361(13)
N(1)–C(11)	1.400(2)	1.389(15)
N(3)–N(4)	1.269(2)	1.265(13)
N(4)–C(21)	1.422(3)	1.417(15)
Bond angles (°)		
C(1)C(2)C(3)	111.0(2)	114.4(10)
C(2)C(3)N(2)	126.8(2)	116.8(10)
C(2)C(3)N(3)	122.4(2)	124.5(10)
N(2)C(3)N(3)	110.7(1)	118.6(10)
N(2)N(1)C(11)	120.2(1)	120.0(9)
C(3)N(2)N(1)	118.0(1)	117.5(9)
C(3)N(3)N(4)	113.5(1)	112.6(9)
N(3)N(4)C(21)	114.5(1)	113.3(9)
N(4)C(21)C(22)	124.9(2)	125.9(10)
N(4)C(21)C(26)	115.1(2)	115.6(10)
N(1)C(11)C(12)	121.9(2)	116.7(10)
N(1)C(11)C(16)	118.1(2)	124.1(10)

bandpass of 2 cm^{-1} at 647 nm . Samples were studied as crystals and as thin films sublimed onto glass substrates. Spectra were recorded at room temperature using laser powers of less than 50 mW so as to avoid sample decomposition.

I.r. spectra were recorded for KBr discs using a Bomem DA3 FTIR spectrometer.

Solid-state ^{13}C n.m.r. spectra were recorded at 50.3 MHz with a Varian Associates XL-200 spectrometer using a standard CP/MAS probe. Powdered samples (*ca.* 300 mg) were packed in rotors made of Kel-F and spun using MAS frequencies of $2-3\text{ kHz}$. The combined techniques of high-power proton decoupling and single-contact cross polarisation (CP) were employed. Typical contact times of 50 ms were used, with recycle delays of 1.2 s . The number of transients acquired was of the order of 1000 .

Solution n.m.r. spectra were recorded at 20.00 MHz with a Varian Associates FT-80A spectrometer employing proton decoupling. In all cases either deuterated solvents or a D_2O capillary insert provided the spin lock. Typical spectral parameters employed were: spectral width 5000 Hz , acquisition time 1.023 s , pulse width $4\text{ }\mu\text{s}$, number of transients $10000-15000$. Quaternary carbon signals were identified by using pulse delays of up to 4 s . In some cases spin relaxation was assisted by the addition of chromium acetylacetonate to the spectroscopic solution. Samples of *ca.* 200 mg were used in 5 mm o.d. tubes with tetramethylsilane as internal standard.

Microanalyses were performed by Professor A. D. Campbell of the University of Otago.

Results and Discussion

Crystal Structures.—The molecular structures and atomic nomenclature for the orange (1) and red (2) isomers are shown in Figure 1. The final fractional atomic co-ordinates are given in Tables 2 and 3 and the bond lengths and angles for the $-N=N-C=N-N-$ backbone are compared in Table 4. As found for all orange-yellow formazans in the solid state,⁷⁻¹⁰ the orange isomer (1) adopts the *anti,s-trans* configuration whereas the red isomer (2) adopts the *syn,s-trans* configuration observed previously for the red crystals of 3-methylthio-1,5-diphenylformazan⁵ and 3-carboxymethylthio-1,5-diphenylformazan.⁶ No significant change is observed for the azo bond length in going from orange (1) to red (2) but there are significant changes in the remainder of the backbone. An increase in the mean $\text{C}=\text{N}$

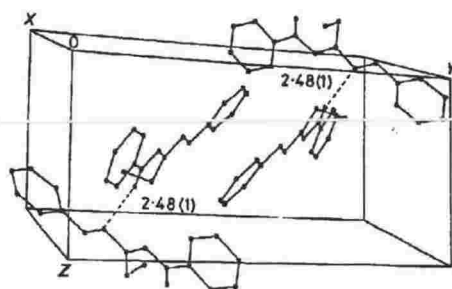


Figure 2. Unit-cell projection of orange (1) 3-ethyl-1,5-diphenylformazan. Bond length in Å

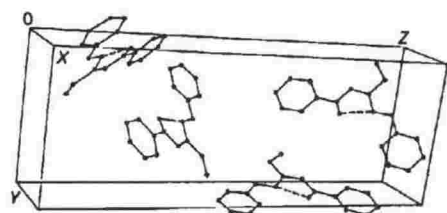


Figure 3. Unit-cell projection of red (2) 3-ethyl-1,5-diphenylformazan

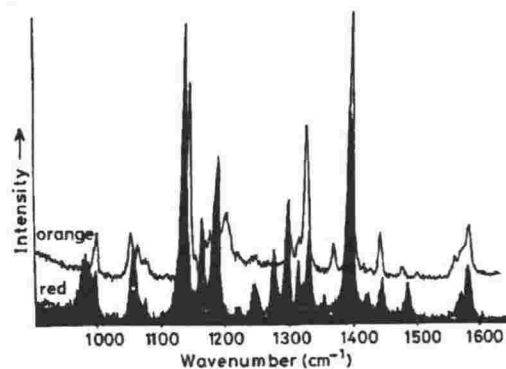


Figure 4. Raman spectra of orange (1) and red (2) 3-ethyl-1,5-diphenylformazan

bond length and an increase in the hydrazinyl N-N bond length accompany the orange *anti,s-trans* to red *syn,s-trans* change in configuration.

There is a rather long intermolecular hydrogen bond between H(1) and N(3) of adjacent molecules for orange (1) (see Figure 2) and a somewhat shorter intramolecular H(1) to N(3) bond length for red (2) (see Figure 3). The lower m.p. observed for red (2) is in accord with these observations.

The ethyl substituent on C(3) clearly represents a borderline functional group in that for formazans with small C(3) substituents such as -H, -CH₃, and -S, the orange *anti,s-trans* configuration is favoured whereas for formazans with the bulkier C(3) substituents, -Bu^t, -NO₂, -Ph, and -SMc either the *syn,s-trans* or the *syn,s-cis* configuration is thermodynamically more stable in the solid state at room temperature. It appears that the steric effect of the C(3) substituent is the most important factor in determining the configuration adopted by a particular

Table 5. Raman bands (wavenumbers) observed for the orange (1) and red (2) isomers in the solid state

Orange (1)	Red (2)
1 603	1 600
1 591	1 590
1 583	
1 519	
1 500	1 504
1 461	1 461
1 411	1 408
1 372.5	
1 331.3	1 339
1 323.9	
1 306	1 306
	1 285
1 242	
1 208	
1 179	1 192
1 172	1 170
1 147	1 141
1 076	
1 059	1 062
1 051	
998.3	
993.8	

formazan in the solid state. The electronic properties of the C(3) substituents and the effects of intra- or inter-molecular hydrogen bonding appear to play a secondary role.

Raman Spectra.—Raman spectra for the light-stable structure (1) were obtained in solution and in the solid state, whereas for the dark-stable structure (2) the solution species was found to be unstable and only solid-state Raman data could be measured. Typical spectra for each structure are shown in Figure 4 with the band wavenumbers listed in Table 5.

The two most intense bands shift from 1 408 and 1 141 cm⁻¹ in (2) to 1 411 and 1 147 cm⁻¹ in (1). The bands at 1 408 and 1 411 cm⁻¹ can be assigned to $\bar{\nu}_{N-N}$ and the shift to higher wavenumber for the *anti,s-trans* structure parallels the change reported¹³ for a Hg^{II} formazan complex. The bands at 1 141 and 1 147 cm⁻¹ are assigned to a mode involving $\bar{\nu}_{N-N}$. The substantial increase in the N-N bond order in (1) supports this assignment. Changes in the C-N bond order are reflected in the shift of the band at 1 339 cm⁻¹ in (2) to bands at 1 372, 1 331, and 1 324 cm⁻¹ in (1). The increase in the mean C-N bond order for (2) can account for the increase in wavenumber for the intense band at 1 331 cm⁻¹ in the orange isomer (1) to 1 339 cm⁻¹ in the red isomer (2). The increased bond order for the isolated C=N bond in the orange isomer (1) may explain the increased intensity for the band at 1 603 cm⁻¹. The other differences in the Raman spectra are the presence of bands at 1 242, 1 208, 1 076, and 1 051 cm⁻¹ for (1) and a band at 1 285 cm⁻¹ for (2).

I.r. Spectra.—The only difference detected in the i.r. absorption spectra of the red and orange isomers is the appearance of a weak band assigned as $\bar{\nu}_{N-H}$ (see Figure 5) at 3 337 cm⁻¹ for (2). Otherwise both structures appear to have identical i.r. spectra in the solid state, in contrast with the number of significant changes observed for their solid-state Raman spectra.

The appearance of a band at high wavenumber for the red isomer (2) parallels the earlier observation¹⁴ of a band at 3 334 cm⁻¹ for a fresh chloroform solution of 3-methylthio-1,5-diphenylformazan. Over a period of time in this solution the formation of the yellow isomer was observed, with the

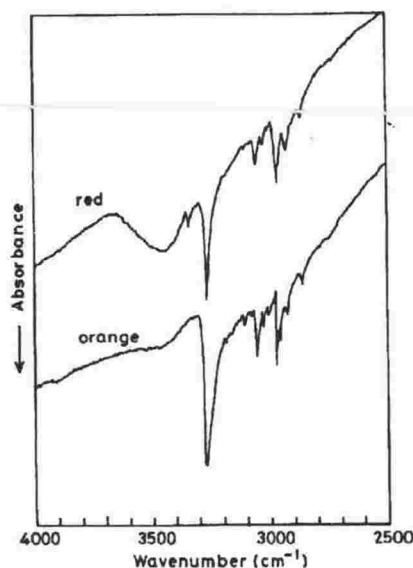


Figure 5. I.r. spectra of orange (1) and red (2) 3-ethyl-1,5-diphenylformazan

Table 6. ^{13}C N.m.r. bands (p.p.m.) for the orange (1) and red (2) isomers in the solid state and in solution; relative intensities in parentheses

State	CH_2	CH_3	$\text{C}(3)$	$\text{C}(11)$	$\text{C}(21)$
Solid					
orange (1)	15.4	10.6	159.9	152.9	144.8
red (2)	22.5	10.1	153.3	149.2	144.2
Solution					
C_6D_6	23.7(15)	11.4(15)	156.0(3)	148.7(23)	149.9(11)
CDCl_3	23.3(17)	11.3(15)	159.0(3)*	148.5(14)	149.9(10)
	14.2(4)	9.5(4)		148.3(12)	
$(\text{CD}_3)_2\text{CO}$	23.3(11)	13.4(12)		149.4(14)	150.5(5)
	14.8(4)	9.5(3)		149.4(14)*	
EtOH	[Masked by solvent]			147.0(18)	
MeOH	18.4(11)	10.5(11)	157.0(2)	149.8(30)	

* Only one peak observed. ^b Peaks superimposed and assigned to both isomers.

appearance of a strong band at 3240 cm^{-1} . This corresponds to the strong band observed at 3268 cm^{-1} for the orange isomer (1).

^{13}C N.m.r. Spectra.—The ^{13}C n.m.r. resonances for the two isomers in the solid state are listed in Table 6. Assignments are based on the use of short contact times to identify quaternary carbon signals, TOSS experiments, and multiple spinner speeds to remove sidebands. Resonances for solution spectra are given for comparison.

In the solid spectra three signals for quaternary carbon are observed. The large shift in the $\text{C}(3)$ signal in going from intramolecularly hydrogen bonded red (2) to intermolecularly bonded orange (1) reflects differences in the mean $\text{C}=\text{N}$ bond order, $r_{\text{C}=\text{N}}$, with the greater electron density of (2) giving the expected lower-field resonance as compared with (1). A corresponding shift is noted for the ethyl resonances. Signals are

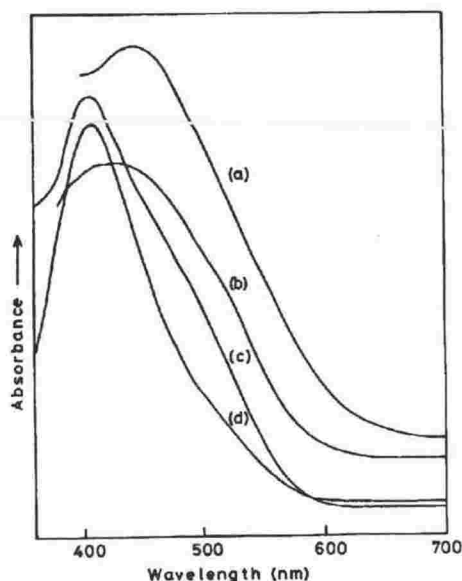


Figure 6. U.v.-Visible absorption spectra of 3-ethyl-1,5-diphenylformazan. Solvents (a) C_6D_6 ; (b) CDCl_3 ; (c) $(\text{CD}_3)_2\text{CO}$; (d) ethanol

observed for each of the quaternary aromatic carbon atoms $\text{C}(21)$ and $\text{C}(11)$. The differences are a reflection of the magnitude of shift expected for a carbon atom in proximity to an $-\text{N}-\text{H}$ group. The $\text{C}(11)-\text{N}-\text{H}$ resonances show a small conformation-dependent shift in going from (2) to (1) whereas the $\text{C}(21)-\text{N}-\text{H}$ resonances are the same in both forms.

The ethyl group resonances provide a means of establishing the solvent dependence of the equilibrium between (1) and (2). The red isomer (2) is the dominant dark-stable species in C_6D_6 , with the orange isomer becoming increasingly important as the solvent changes from CDCl_3 to hexadeuterioacetone and finally to ethanol. U.v. and visible absorption spectra measured on the actual samples used for the ^{13}C n.m.r. experiments (see Figure 6) confirm these conclusions. Data for the solution in hexadeuteriobenzene show that the red isomer is the major species, whereas in ethanol the orange isomer predominates.

In solution, rapid tautomerisation of the orange isomer (1) results in the collapse of the discrete signals for the aromatic quaternary carbon atoms into an averaged one. For the red isomer (2), the intramolecular hydrogen bond apparently inhibits such tautomerisation and signals for each of the aromatic quaternary carbon atoms are seen. When the two isomers are both present signals are observed for each isomer; CDCl_3 solutions yield three distinct signals for the quaternary aromatic carbon atoms of (1) and (2). The resonance for the third quaternary carbon atom, $\text{C}(3)$, is more difficult to observe in solution; no evidence has been found for two distinct signals arising from the two isomers.

These same trends have been observed for all formazans of known crystal structure and will be outlined in a more comprehensive paper.¹⁵

Acknowledgements

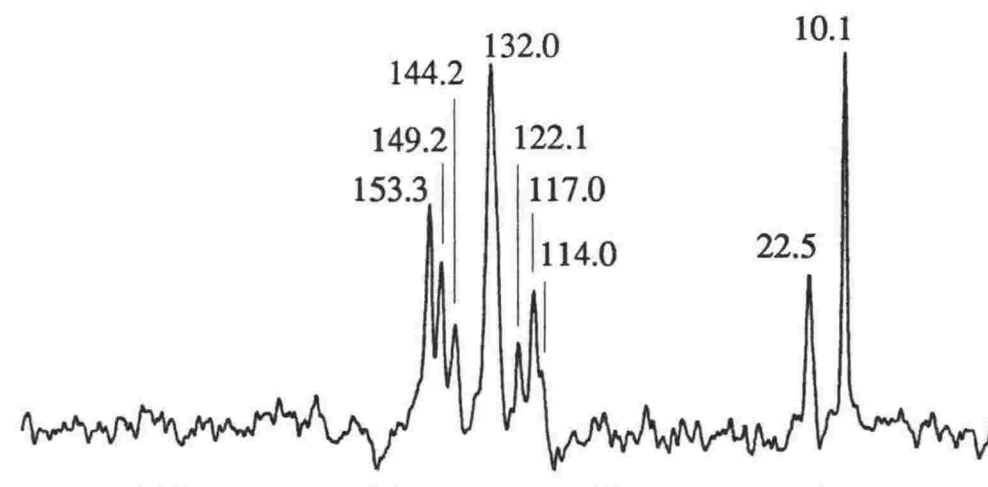
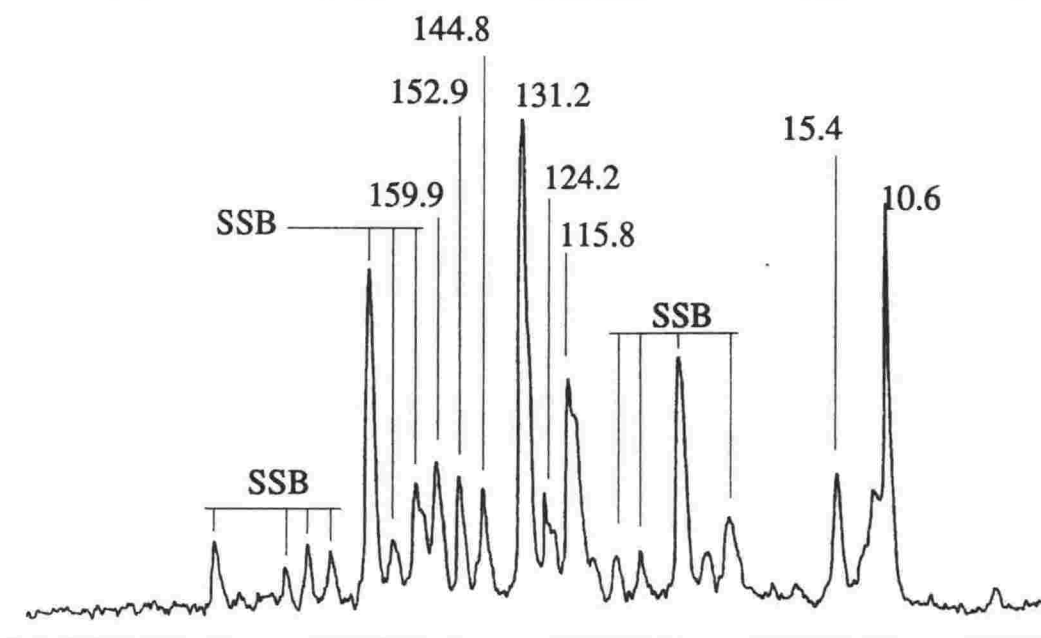
One of the authors (C. W. C.) thanks the Maori Education Foundation for a Queen Elizabeth II Post-Graduate Scholarship.

References

- 1 G. H. Brown, 'Techniques of Chemistry, Vol. III, Photochromism,' Wiley-Interscience, New York, 1971.
- 2 W. Otting and F. A. Neugebauer, *Z. Naturforsch., Teil B*, 1968, **23**, 1064.
- 3 W. Otting and F. A. Neugebauer, *Chem. Ber.*, 1969, **102**, 2520.
- 4 E. Dijkstra, A. T. Hutton, H. M. N. H. Irving, and L. R. Nassimbeni, *Acta Crystallogr., Sect. B*, 1982, **38**, 535.
- 5 J. Preuss and A. Gieren, *Acta Crystallogr., Sect. B*, 1975, **31**, 1276.
- 6 A. T. Hutton, H. M. N. H. Irving, L. R. Nassimbeni, and G. Gafner, *Acta Crystallogr., Sect. B*, 1979, **35**, 1354.
- 7 Yu. A. Mel'chenko, Yu. D. Kondrashev, S. L. Ginzburg, and M. G. Neiganz, *Kristallografiya*, 1974, **19**, 522.
- 8 M. Laing, *J. Chem. Soc., Perkin Trans. 2*, 1977, 1248.
- 9 J. Guillerez, C. Pascard, and T. Prange, *J. Chem. Res.*, 1978, (S) 308; (M), 1978, 3934.
- 10 A. T. Hutton, H. M. N. H. Irving, and L. R. Nassimbeni, *Acta Crystallogr., Sect. B*, 1980, **36**, 2071.
- 11 D. Todd, 'Experimental Organic Chemistry,' Prentice-Hall Inc., New Jersey, 1979, p. 251.
- 12 G. A. Sheldrick, 'SHELXTL User Manual, Revision 4,' Nicolet XJ.D Corp., Madison, Wisconsin.
- 13 G. R. Burns and R. J. H. Clark, *Inorg. Chim. Acta*, 1984, **88**, 83.
- 14 G. R. Burns and J. F. Duncan, *Chem. Commun.*, 1966, 116.
- 15 C. Cunningham, G. R. Burns, and R. H. Newman, unpublished work.

Received 1st October 1987; Paper 7/1758

The solid-state nmr spectra described in the paper are shown below. The resonances are listed in Table 6 of the paper.



Figures 7 and 8: The Solid State ^{13}C MAS Nmr Spectra of the Orange Isomer (top) and the Red Isomer (bottom) of 3-ethyl-1,5-diphenylformazan.

Kinetic Studies.

The characterisation of the solid state structures of the orange and red isomers of 3-ethyl-1,5-diphenylformazan and the realisation of the corresponding structures in solution make the system an ideal one in which to investigate the kinetics of the photochromic equilibrium in diphenylformazans. Therefore, (1) and (2) in benzene or toluene solutions were chosen as a model because they were significantly soluble in benzene and the return rate of the photochromic change in this solvent was measurably slow at room temperature.

The return reaction of the photochromic change was followed spectrophotometrically by the disappearance of the absorption band of the activated orange form at 405 nm. A description of the absorption spectrum of (1) and (2) in benzene is shown in Figure 9.

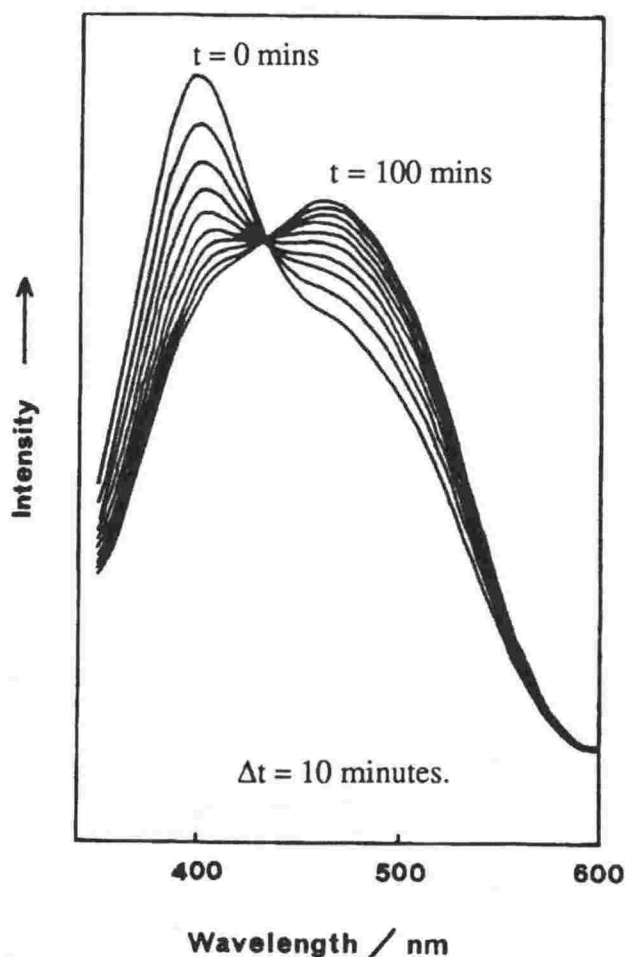


Figure 9: The Ultra violet-visible Absorption Spectra of the Return of the Photo-activated Species to the Dark Stable Species of 3-ethyl-1,5-diphenylformazan.

It can be seen that the red isomer is the dominant species in the spectrum in the dark with an absorption maximum of 475 nm. When illuminated with a broad band quartz-halogen lamp, the orange activated species is promoted with an absorption maximum of 405 nm. These maxima do not differ if either (1) or (2) is dissolved in benzene and allowed to equilibrate in the dark. However, when the absorption spectrum of (1) in benzene is measured immediately upon dissolving, the spectrum gives a broad maximum between 405 and 475 nm as it equilibrates towards the red form. Evidence for the existence of only two absorbing species in this system come from the appearance of an isosbestic point at 440 nm. However, initial studies seem to indicate that the pseudo first order rate constants calculated for the disappearance of the 405 nm band and the re-appearance of the 475 nm band do not concur.

The rate of return of the activated orange form (1) to the dark stable red form (2) in benzene, toluene, light petroleum and cyclohexane follows first order kinetics. The pseudo first order rate constants observed would seem to be functions of:

- i) the total concentration of the compound
- ii) the water content.

Calculated rate constants are listed below in Table 7. As the dependence of the return rate is known to depend upon the water content of the system, measurements were made on solutions saturated in water by allowing them to stand over water for *ca.* 24 hours. The solubility of water in benzene at 25 °C is 0.039 mol dm⁻³. Solutions of (1) or (2) in benzene which was not saturated with water showed an increase in their rate of return as they aged. As the return is thought to be a thermal process, the temperature for a standard concentration solution was varied and the rate constant for the return measured.

The rate constants above were calculated following the method of Guggenheim [16], as described by Frost and Pearson [17], for calculating k_{obs} where D_{∞} (the optical density at time = ∞) is unknown, which is often the case for photochromic systems.

Table 7: Calculated Rate Constants for the Return of the Activated Orange form to the Dark Stable Red Form of 3-ethyl-1,5-diphenylformazan.

Solvent	Concentration /10 ⁻⁴ mol dm ⁻³	Temperature /°C	k(obs.) /10 ⁻² s ⁻¹
benzene	1.98	25	2.17 ± 0.07
benzene	0.99	25	3.01 ± 0.03
benzene	0.44	25	3.64 ± 0.04
toluene	1.66	25	9.95
toluene	0.79	25	11.23
toluene	0.44	25	28.98
benzene	0.44	25	1.65 ± 0.08
benzene	0.44	20	1.25 ± 0.08
benzene	0.44	15	0.82 ± 0.08

Discussion.

The orange and red isomers of 3-ethyl-1,5-diphenylformazan have been identified in solution and they have the *anti,s-trans* and *syn,s-trans* configurations respectively. While photochromic systems have been proposed for 1,3,5-triphenylformazan, the four-specied system seems inappropriate as a starting point for this system. The simple two specied system below is therefore proposed:



A may be assigned as the orange *anti,s-trans* isomer and B as the red *syn,s-trans* isomer. The photochemically promoted reaction $B \rightarrow A$ is relatively rapid and that under high illumination a relatively steady state of the photo-excited species A can be formed. The thermal back-reaction

A → B is observed to be:

- i) measurably slow at room temperature;
- ii) dependent upon the water content of the solvent/solute;
- iii) dependent upon the total concentration of solute;
- iv) first order;
- v) not reproducible from one preparation to the next.

All of these findings parallel similar observations for triphenylformazan [18] and some primary dithizonate complexes studied in a flash photolytic study [19].

While the scheme proposed is, perhaps, an over simplification the variation in the observed rate was too great to allow for mechanistic conclusions. Similar patterns have been observed by other authors studying the photochromism of formazans and the closely related metal dithizonates [20] and a full explanation awaits further investigation.

References.

- | | | | |
|----|--|----|---|
| 16 | Guggenheim, E.A., <i>Phil. Mag.</i> , 2 538 (1926). | 20 | Geosling, C., Adamson, A.W. and Gutierrez, A.R., <i>Inorg. Chim. Acta</i> , 29 , 279 (1978); Meriwether, L.S., Breitner, E.S. and Sloan, C.L., <i>J. Am. Chem. Soc.</i> , 87 , 4441 (1965); Meriwether, L.S., Breitner, E.S. and Colthup, N.B., <i>J. Am. Chem. Soc.</i> , 87 , 4448 (1965). |
| 17 | Frost, A.A. and Pearson, R.G., " <i>Kinetics and Mechanism</i> ", John Wiley and Sons, Inc., New York, 1961. | | |
| 18 | Cunningham, C.W. Victoria University of Wellington, B.Sc.(Hons.) Thesis, 1982. | | |
| 19 | see Chapter 3.7, page 133. | | |
-

Chapter 3.3

3-Methyl-1,5-diphenylformazan and 3-*tertiary*-butyl-1,5-diphenylformazan.

In this chapter the results of studies of the following two formazans are given:

- | | |
|--|-----|
| 3-methyl-1,5-diphenylformazan | (1) |
| 3- <i>tertiary</i> -butyl-1,5-diphenylformazan | (2) |

The following chapter consists of a preprint of a paper entitled "Photochromic Formazans: X-Ray Crystal Structure, Magnetic Resonance and Raman Spectra of 3-methyl-1,5-diphenylformazan and 3-*tertiary*-butyl-1,5-diphenylformazan." which has been accepted for publication in *The Journal of The Chemical Society, Perkin Transactions 2*, 1989.

Proofs to: Dr Gary R Burns,
Chemistry Department,
Victoria University of Wellington,
P.O. Box 600,
Wellington,
NEW ZEALAND.

**Photochromic Formazans: X-ray Crystal Structure,
Magnetic Resonance and Raman Spectra of
3-methyl-1,5-diphenylformazan and
3-*tertiary*-butyl-1,5-diphenylformazan.**

Christopher W. Cunningham and Gary R. Burns,
Chemistry Department,
Victoria University of Wellington,
P.O.Box 600,
Wellington, New Zealand.,

and

Vickie McKee,
Department of Chemistry,
University of Canterbury,
Christchurch 1, New Zealand.

Abstract

The X-ray crystal structures of 3-methyl-1,5-diphenyl-formazan (1) and 3-*tertiary* butyl-1,5-diphenylformazan (2) have been determined. Magnetic resonance spectra, in both the solid state and in solution, and Raman spectra have been studied. $C_{14}H_{14}N_4$ (1) belongs to the monoclinic space group $P2_1/c$, $a = 8.133(1)$, $b = 19.085(4)$, $c = 9.364(2)$ Å, $\beta = 105.93^\circ$, $U = 1397.6(5)$ Å³, $Z = 4$; the *anti,s-trans* configuration found for the solid state is also the thermodynamically preferred configuration in solution equilibrium. $C_{17}H_{20}N_4$ (2) belongs to the monoclinic space group $P2_1/c$, $a = 11.235(3)$; $b = 20.117(5)$; $c = 14.176(3)$ Å; $\beta = 92.14(2)^\circ$;

$U = 3202(1) \text{ \AA}^3$; $Z = 8$; the *syn,s-cis* configuration of the solid state is maintained in solution.

Introduction

Formazans have been known since the late nineteenth century when they were discovered and studied independently by Bamberger and his co-workers [1] and von Pechmann [2]. As a class of photochromic compound, formazans provide both organic and organometallic examples with the latter being the more widely investigated to date. Hg(II) dithizonate remains one of the few commercially exploited photochromes while 1,3,5-triphenylformazan has recently found favour as being a "dramatic yet reliable" example of photo-isomerism for organic chemistry demonstrations [3].

Formazans can in principle adopt four structures (a-d Figure 1) ignoring isomers which are unlikely to occur due to serious steric crowding. This is as a result of *syn-anti* isomerisation about the C=N double bond and isomerisation about the C-N single bond designated *s-cis* and *s-trans*.

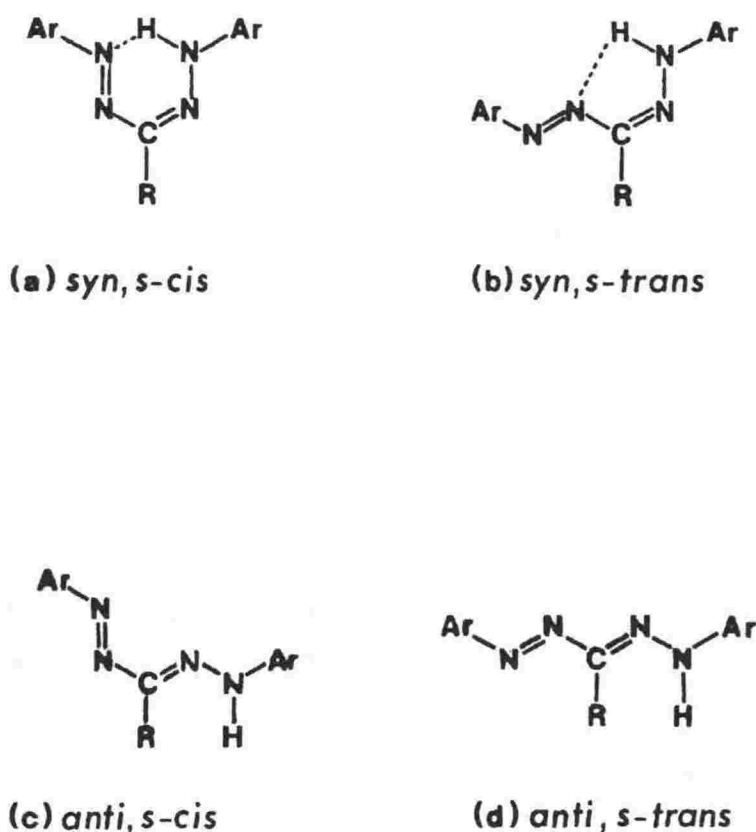


Figure 1: The Principal Isomers in the Formazan System.

Otting and Neugebauer [4,5] have concluded that in solution the red and yellow formazans represent respectively *syn,s-cis* and *anti,s-trans* isomers. In the solid state, formazans crystallise as red or orange-yellow solids, with the *syn,s-cis* [6] or *syn,s-trans* [7,8] configurations if red and the *anti,s-trans* [9-12] configuration if orange-yellow. We have recently determined the structures of a pair of photochromes of a formazan equilibrium [13] which we were able to isolate in the solid-state, as *anti,s-trans* and *syn,s-trans* respectively for the orange and red forms of 3-ethyl-1,5-diphenylformazan (3). In this work we report on 3-methyl-1,5-diphenyl- formazan which crystallises as an orange formazan and 3-*tertiary* butyl-1,5-diphenylformazan which crystallises as a red formazan.

By 1955 [14] over 500 formazans were known and this total has since increased to the present count of over a thousand formazans. However, only eight formazans have had their crystal structures determined [6-13], and this present study is only the second in which the *syn,s-cis* configuration has been established. It is the first formazan with unsubstituted aromatic groups to have the *syn,s-cis* conformation unequivocally determined. Although the structure has been assumed to exist for half a century it is important, as we seek to explain why formazans adopt different structures on the basis of substitution at the three position, that there be no influence from substitution of the phenyl rings. The structure of (2) provides a useful analogue for 1,3,5-triphenylformazan which has been the subject of much study [15] although its crystal structure remains undetermined. The formazan (2) also provides an opportunity to investigate the quasi-aromatic ring postulated for 3-carboxymethylthio-1,5-diphenylformazan [16] whose solution structure is thought to be *syn,s-cis*.

The 3-methyl-formazan (1) is known to behave similarly to the closely related compound 3-ethyl-1,5-diphenylformazan (3). On irradiation in solution, the orange colour is promoted but it reverts to the red form on standing in the dark. All attempts at crystallising the dark-stable red isomer have been unsuccessful.

We present the crystal structures of (1) and (2) together with their magnetic resonance and Raman spectra.

Experimental.

Syntheses: 3-methyl-1,5-diphenylformazan (1) was prepared following the method of Irving, Gill and Cross [17]. The formazan was recrystallised from hot ethanol by the addition of water yielding orange needles in excellent yield. (Anal. Calcd: C, 70.55; H, 5.92; N, 23.51. Found: C, 70.69; H, 5.79; N, 23.71 %). 3-*Tertiary* butyl-1,5-diphenylformazan (2) was prepared following the method of Neugebauer and Trischmann [18]. The formazan was recrystallised from 1:1

methanol:water as dark red elongated needles with a striking metallic reflex. (Anal. Calcd: C, 72.82; H, 7.19; N, 19.99 %. Found: C, 72.99; H, 7.48; N, 20.22 %).

Crystal Structure Analysis and Data:

3-Methyl-1,5-diphenylformazan (1): An orange, regularly shaped crystal of dimensions 0.22 x 0.22 x 0.22 mm, was used and found to be monoclinic, $a = 8.133(1)$, $b = 19.085(4)$, $c = 9.364(2)$ Å, $\beta = 105.93^\circ$, $U = 1397.6(5)$ Å³, space group $P2_1/c$; $Z = 4$, $F(000) = 503.9$. 1.6° ω -scans at $4.88^\circ \text{ min}^{-1}$ were used to collect 1833 unique reflections in the range ($4 < 2\theta < 45$) and, of these, 1203 having $I < 3(\sigma I)$ were used for the structural analysis.

3-Tertiary butyl-1,5-diphenylformazan (2): A red crystal of irregular shape with dimensions 0.14 x 0.26 x 0.33 mm was used and found to be monoclinic, $a = 11.235(3)$; $b = 20.117(5)$; $c = 14.176(3)$ Å; $\beta = 92.14(2)^\circ$; $U = 3202(1)$ Å³; Space group $P2_1/c$; $Z = 8$, $F(000) = 1007.8$. 1.6° ω -scans at $4.88^\circ \text{ min}^{-1}$ were used to collect 4176 unique reflections, 2015 of these, which had $I < 3(\sigma I)$ were used in the subsequent calculations.

Intensity data for both crystals were collected at -100° C with a Nicolet R3m four-circle diffractometer using graphite monochromated Mo-K α radiation. Cell parameters were determined by least-squares refinement of 13 accurately centred reflections ($2\theta > 15^\circ$). Crystal stability was monitored by recording 3 check reflections every 100 reflections and no significant variations were observed. The data sets were corrected for Lorentz-polarisation effects but no absorption corrections were applied.

Both structures were solved by direct methods, using the program SOLV, and refined by blocked-cascade least squares methods. The refinement of (1) converged with $R = 0.045$ and $R' = 0.066$ while (2) converged with $R = 0.061$ and $R' = 0.091$. All non-hydrogen atoms were refined anisotropically, hydrogen atoms (except H1 in (1) and H11 and H21 in (2)) were inserted at calculated positions using a riding model with thermal parameters equal to 1.2 U of their carrier atoms. H1, H11 and H21 were located from difference Fourier maps, inserted at those positions and not further refined. The function minimised in the refinement was $\sum w(|F_o| - |F_c|)^2$ where $w = [\sigma(F_o) + gF_o]$ and $g = 0.0026$. Final difference maps showed no features greater than ± 0.3 electron Å⁻³.

All programs used for data collection and structure solution are contained in the SHELXTL (Version 4) package¹.

Nuclear Magnetic Resonance Spectra: Solid state ¹³C nmr spectra were recorded at 50.3 MHz with a Varian Associates XL-200 spectrometer using a standard CP/MAS probe. Powdered samples (ca. 300 mg) were packed in Kel-F rotors and spun using MAS frequencies between 2 and 3 kHz for (1) and up to 10 kHz for (2). The combined techniques of high

1 G.M. Sheldrick, SHELXTL User Manual, Revision 4, Nicolet XRD Corporation, Madison, Wisconsin.

power proton decoupling and single contact cross polarisation (CP) were employed. Typical contact times of 50 ms were used, with recycle delays of 1.2 s. The number of transients acquired was of the order of 1000.

Solution spectra were recorded at 20.00 MHz with a Varian Associates FT-80A spectrometer employing proton decoupling. In all cases either deuterated solvents or D₂O capillary tubes provided the spin lock. Typical spectral parameters employed were: spectral width 5000 Hz, acquisition time 1.023 s, pulse width 4 μ s. Samples of ca. 200 mg were used in 5 mm o.d. tubes with tetramethylsilane as the internal standard. Precautions were taken to protect the spectroscopic solutions from the effect of light.

Vibrational Spectra: Raman spectra were recorded using a Spex 1401 spectrometer equipped with a Thorn EMI 6256 photomultiplier tube used in the photon counting mode. A Spectra-Physics 164-01 Krypton Ion laser was used as the Raman scattering source, operating at a wavelength of 647 nm. Band wavenumbers were calibrated using the emission spectrum of neon and typical slit widths of 200 μ m were employed, giving a bandpass of 2 cm⁻¹ at 647 nm. Samples were studied as crystals or in capillary tubes. Pressed discs diluted in potassium bromide were also used effectively to eliminate fluorescence. Spectra were recorded at room temperature using laser powers of less than 50 mW at the sample to avoid photo-decomposition.

Electronic Absorption Spectra: Ultra violet-visible spectra were recorded with a Shimadzu Model 160 ultra violet-visible spectrophotometer. Solvents were spectroscopic grade or purified by standard methods.

Analyses: Microanalyses were performed by Professor A.D. Campbell of the University of Otago.

Results and Discussion.

X-Ray Crystal Structures: The molecular structure and atomic nomenclature for (1) and (2) are given in Figures 2 and 3. The final fractional atomic coordinates are given in Tables 1 and 2. The bond lengths and bond angles are given in Tables 3 and 4.

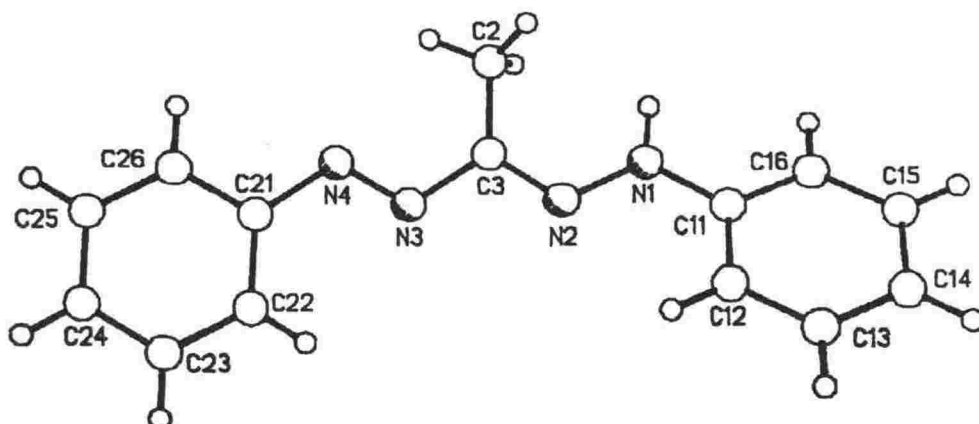


Figure 2: Molecular Structure and Atomic Nomenclature for 3-methyl-1,5-diphenylformazan (1).

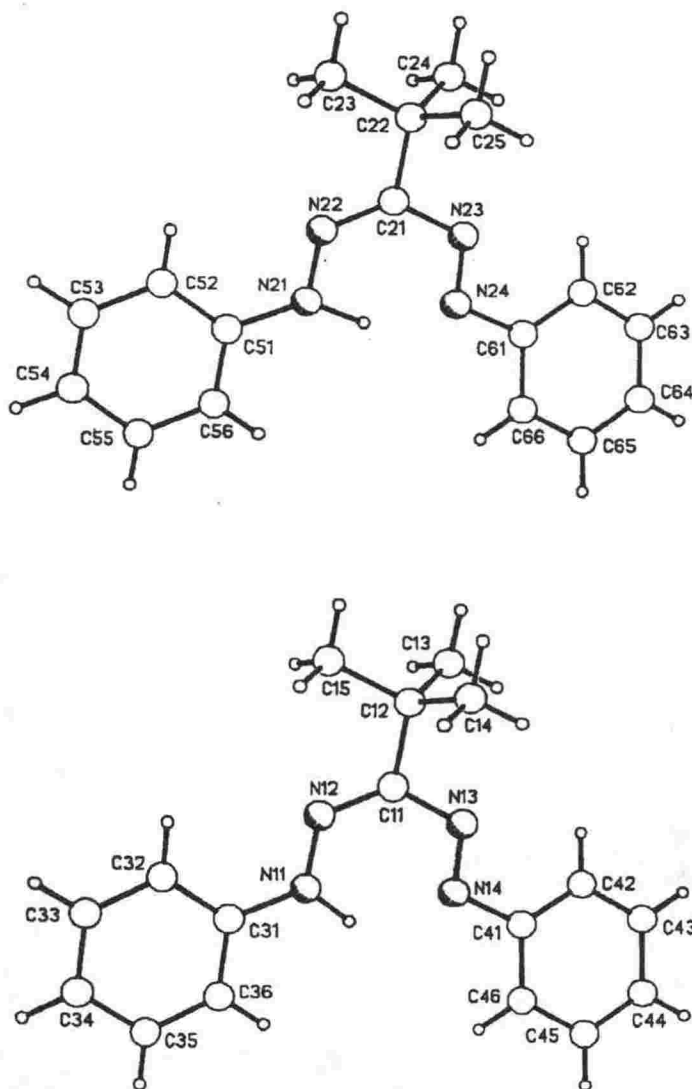


Figure 3: Molecular Structures and Atomic Nomenclature for 3-tertiary-butyl-1,5-diphenylformazan (2).

Table 1. Fractional Atomic Coordinates ($\times 10^4$) and Temperature Factors ($\text{\AA}^2 \times 10^3$) for 3-methyl-1,5-diphenylformazan (1).

Atom	x	y	z	U
C(2)	-3001(4)	1783(2)	-287(4)	58(1)*
C(3)	-1135(3)	1830(1)	408(3)	34(1)*
N(1)	-1348(3)	2706(1)	1979(2)	37(1)*
N(2)	-380(3)	2253(1)	1476(2)	35(1)*
N(3)	76(3)	1419(1)	-19(2)	37(1)*
N(4)	-562(3)	984(1)	-1039(2)	40(1)*
C(11)	-623(3)	3118(1)	3233(3)	31(1)*
C(12)	998(3)	2996(1)	4154(3)	41(1)*
C(13)	1624(4)	3417(2)	5380(3)	48(1)*
C(14)	654(4)	3946(2)	5709(3)	46(1)*
C(15)	-962(4)	4061(1)	4805(3)	44(1)*
C(16)	-1599(3)	3687(1)	3687(3)	39(1)*
C(21)	665(3)	573(1)	-1494(3)	38(1)*
C(22)	2422(4)	680(2)	-1048(3)	53(1)*
C(23)	3485(4)	255(2)	-1575(3)	60(1)*
C(24)	2810(4)	-280(2)	-2549(3)	58(1)*
C(25)	1082(4)	-392(2)	-3004(3)	57(1)*
C(26)	14(4)	40(2)	-2486(3)	55(1)*

* Equivalent isotropic U defined as one third of the trace of the orthogonalised U_{ij} tensor

Table 2. Fractional Atomic Coordinates ($\times 10^4$) and Temperature Factors ($\text{\AA}^2 \times 10^3$) for 3-tertiary-butyl-1,5-diphenylformazan (2).

Atom	x	y	z	U
N(14)	1157(5)	4214(2)	4914(4)	35(2)*
N(13)	339(5)	4173(2)	4266(4)	34(2)*
C(11)	352(5)	4658(3)	3553(4)	29(2)*
C(12)	-590(6)	4538(3)	2766(4)	31(2)*
C(13)	-1812(6)	4476(3)	3184(4)	47(3)*
C(14)	-292(6)	3899(3)	2257(4)	46(3)*
C(15)	-604(6)	5115(3)	2061(4)	43(2)*
N(12)	1084(4)	5162(2)	3459(3)	31(2)*
N(11)	1960(4)	5258(2)	4111(3)	34(2)*
C(41)	1111(6)	3712(3)	5618(4)	29(2)*
C(42)	111(6)	3331(3)	5763(4)	38(2)*
C(43)	143(6)	2853(3)	6471(4)	47(3)*
C(44)	1169(7)	2764(3)	7026(4)	47(3)*
C(45)	2161(7)	3146(3)	6888(4)	46(3)*
C(46)	2127(6)	3630(3)	6187(4)	37(2)*
C(31)	2765(5)	5769(3)	3985(4)	30(2)*
C(32)	2675(6)	6217(3)	3240(4)	35(2)*
C(33)	3542(6)	6704(3)	3147(5)	45(3)*
C(34)	4501(6)	6741(3)	3778(4)	49(3)*
C(35)	4592(6)	6298(3)	4518(4)	44(3)*
C(36)	3741(6)	5818(3)	4621(4)	37(2)*
N(24)	3610(4)	10415(2)	4120(3)	36(2)*
N(23)	4497(4)	10205(2)	3661(3)	33(2)*
C(21)	4655(6)	9513(3)	3629(4)	31(2)*
C(22)	5666(6)	9311(3)	2996(4)	34(2)*
C(23)	5873(6)	8562(3)	3054(5)	49(3)*
C(24)	6816(6)	9684(3)	3279(5)	44(3)*
C(25)	8297(6)	9495(4)	1974(4)	51(3)*
N(22)	4039(5)	9050(2)	4033(3)	32(2)*
N(21)	3124(4)	9204(2)	4565(3)	34(2)*
C(61)	3507(6)	11124(3)	4147(4)	32(2)*
C(62)	4411(6)	11558(3)	3908(4)	38(2)*
C(63)	4208(7)	12235(3)	3993(5)	47(3)*
C(64)	3148(7)	12479(3)	4302(5)	48(3)*
C(65)	2266(6)	12044(3)	4540(4)	43(3)*
C(66)	2437(6)	11364(3)	4474(4)	39(2)*
C(51)	2530(6)	8693(3)	5024(4)	31(2)*
C(52)	2899(6)	8036(3)	4971(4)	39(2)*
C(53)	2282(6)	7555(3)	5444(5)	46(3)*
C(54)	1338(7)	7726(3)	5978(5)	52(3)*
C(55)	950(6)	8377(4)	6022(4)	44(3)*
C(56)	1554(6)	8859(3)	5548(4)	38(2)*

* Equivalent isotropic U defined as one third of the trace of the orthogonalised U_{ij} tensor

Table 3. Bond Lengths (Å) and Bond Angles (°) for 3-methyl-1,5-diphenylformazan.

C(2)-C(3)	1.480(4)	C(3)-N(2)	1.302(3)
C(3)-N(3)	1.400(4)	N(1)-N(2)	1.339(3)
N(1)-C(11)	1.402(3)	N(3)-N(4)	1.264(3)
N(4)-C(21)	1.423(4)	C(11)-C(12)	1.383(4)
C(11)-C(16)	1.382(4)	C(12)-C(13)	1.379(4)
C(13)-C(14)	1.368(5)	C(14)-C(15)	1.372(4)
C(15)-C(16)	1.377(4)	C(21)-C(22)	1.390(4)
C(21)-C(26)	1.381(4)	C(22)-C(23)	1.372(5)
C(23)-C(24)	1.378(5)	C(24)-C(25)	1.368(5)
C(25)-C(26)	1.379(5)		
C(2)-C(3)-N(2)	125.8(3)	C(2)-C(3)-N(3)	123.9(2)
N(2)-C(3)-N(3)	110.2(2)	N(2)-N(1)-C(11)	120.3(2)
C(3)-N(2)-N(1)	118.2(2)	C(3)-N(3)-N(4)	114.1(2)
N(3)-N(4)-C(21)	114.3(2)	N(1)-C(11)-C(12)	122.6(2)
N(1)-C(11)-C(16)	117.8(2)	C(12)-C(11)-C(16)	119.7(2)
C(11)-C(12)-C(13)	119.5(3)	C(12)-C(13)-C(14)	120.9(2)
C(13)-C(14)-C(15)	119.6(3)	C(14)-C(15)-C(16)	120.5(3)
C(11)-C(16)-C(15)	119.9(2)	N(4)-C(21)-C(22)	125.3(2)
N(4)-C(21)-C(26)	115.9(2)	C(22)-C(21)-C(26)	118.9(3)
C(21)-C(22)-C(23)	120.2(3)	C(22)-C(23)-C(24)	120.0(3)
C(23)-C(24)-C(25)	120.7(3)	C(24)-C(25)-C(26)	119.3(3)
C(21)-C(26)-C(25)	121.0(3)		

Table 4. Bond Lengths (Å) and Bond Angles (°) for 3-tertiary-butyl-1,5-diphenylformazan.

N(14)-N(13)	1.279(7)	N(14)-C(41)	1.422(7)
N(13)-C(11)	1.404(7)	C(11)-N(12)	1.316(7)
N(12)-N(11)	1.340(7)	N(11)-C(31)	1.386(8)
C(41)-C(42)	1.382(9)	C(41)-C(46)	1.383(8)
C(42)-C(43)	1.390(9)	C(43)-C(44)	1.383(10)
C(44)-C(45)	1.374(10)	C(45)-C(46)	1.391(9)
C(31)-C(32)	1.389(8)	C(31)-C(36)	1.397(9)
C(32)-C(33)	1.391(9)	C(33)-C(34)	1.376(9)
C(34)-C(35)	1.377(9)	C(35)-C(36)	1.371(9)
N(24)-N(23)	1.282(7)	N(24)-C(61)	1.431(8)
N(23)-C(21)	1.405(8)	C(21)-N(22)	1.305(8)
N(22)-N(21)	1.334(7)	N(21)-C(51)	1.401(8)
C(61)-C(62)	1.390(9)	C(61)-C(66)	1.390(9)
C(62)-C(63)	1.388(9)	C(63)-C(64)	1.375(10)
C(64)-C(65)	1.373(10)	C(65)-C(66)	1.386(9)
C(51)-C(52)	1.388(8)	C(51)-C(56)	1.387(9)
C(52)-C(53)	1.379(9)	C(53)-C(54)	1.370(10)
C(54)-C(55)	1.381(10)	C(55)-C(56)	1.374(9)
N(13)-N(14)-C(41)	114.5(5)	N(14)-N(13)-C(11)	116.5(5)
N(13)-C(11)-N(12)	129.2(5)	C(11)-N(12)-N(11)	119.2(5)
N(12)-N(11)-C(31)	119.0(5)	N(14)-C(41)-C(42)	123.3(5)
N(14)-C(41)-C(46)	116.3(5)	C(42)-C(41)-C(46)	120.3(5)
C(41)-C(42)-C(43)	119.5(6)	C(42)-C(43)-C(44)	119.9(6)
C(43)-C(44)-C(45)	120.7(6)	C(44)-C(45)-C(46)	119.5(6)
C(41)-C(46)-C(45)	120.0(6)	N(11)-C(31)-C(32)	123.4(5)
N(11)-C(31)-C(36)	118.0(5)	C(32)-C(31)-C(36)	118.6(6)
C(31)-C(32)-C(33)	119.8(6)	C(32)-C(33)-C(34)	120.7(6)
C(33)-C(34)-C(35)	119.5(6)	C(34)-C(35)-C(36)	120.3(6)
C(31)-C(36)-C(35)	121.0(6)	N(23)-N(24)-C(61)	114.1(5)
N(24)-N(23)-C(21)	116.4(5)	N(23)-C(21)-N(22)	128.6(5)
C(21)-N(22)-N(21)	121.0(5)	N(22)-N(21)-C(51)	118.9(5)
N(24)-C(61)-C(62)	123.9(5)	N(24)-C(61)-C(66)	115.3(5)
C(62)-C(61)-C(66)	120.8(6)	C(61)-C(62)-C(63)	118.1(6)
C(62)-C(63)-C(64)	121.7(7)	C(63)-C(64)-C(65)	119.5(6)
C(64)-C(65)-C(66)	120.6(6)	C(61)-C(66)-C(65)	119.3(6)
N(21)-C(51)-C(52)	121.7(6)	N(21)-C(51)-C(56)	118.2(5)
C(52)-C(51)-C(56)	120.1(6)	C(51)-C(52)-C(53)	119.0(6)
C(52)-C(53)-C(54)	120.4(6)	C(53)-C(54)-C(55)	121.1(7)
C(54)-C(55)-C(56)	118.9(6)	C(51)-C(56)-C(55)	120.5(6)

The calculated bond lengths reveal a marked delocalisation of electrons over the N-N-C-N-N formazan backbone for (1) and (2). While the formal double bonds are clearly extended in comparison with isolated double bonds, the formal single bonds are noticeably shortened. For comparison, bond lengths and bond angles for the formazans of similar configuration are given, as are those for the *syn,s-trans* red isomer of 3-ethyl-1,5-diphenylformazan, in Table 5.

Table 5. A Comparison of Selected Bond Angles and Bond Lengths

|
for Formazan -N=N-C=N-NH- Backbones.

Bond lengths (Å)						
	3-methyl ⁷ (1)	Orange	3-ethyl ⁸ Red	3-tertiary-butyl ⁹ (2)		3-nitro ¹⁰
				A	B	
C(1)-C(2)		1.525(3)	1.515(16)			
C(2)-C(3)	1.480(4)	1.496(2)	1.520(17)			
C(3)-N(2)	1.302(3)	1.298(2)	1.308(15)	1.316(7)	1.305(8)	1.322(5)
C(3)-N(3)	1.400(4)	1.403(2)	1.379(15)	1.404(7)	1.405(8)	1.346(5)
N(1)-N(2)	1.339(3)	1.337(2)	1.361(13)	1.340(7)	1.334(7)	1.301(5)
N(1)-C(11)	1.402(3)	1.400(2)	1.389(15)	1.386(8)	1.401(8)	1.436(5)
N(3)-N(4)	1.264(3)	1.269(2)	1.265(13)	1.279(7)	1.282(7)	1.298(5)
N(4)-C(21)	1.423(4)	1.422(3)	1.417(15)	1.422(7)	1.431(8)	1.421(5)
Bond angles (°)						
C(1)-C(2)-C(3)	111.0(2)	114.4(10)				
C(2)-C(3)-N(2)	125.8(3)	126.8(2)	116.8(10)			
C(2)-C(3)-N(3)	123.9(2)	122.4(2)	124.5(10)			
N(2)-C(3)-N(3)	110.2(2)	110.7(1)	118.6(10)	129.2(5)	128.6(6)	136.5(5)
N(2)-N(1)-C(11)	120.3(2)	120.2(1)	120.0(9)	119.0(5)	118.8(5)	116.0(5)
C(3)-N(2)-N(1)	118.2(2)	118.0(1)	117.5(9)	119.2(5)	121.0(5)	117.0(5)
C(3)-N(3)-N(4)	114.1(2)	113.5(1)	112.8(9)	116.5(5)	116.4(5)	117.2(5)
N(3)-N(4)-C(21)	114.3(2)	114.5(1)	113.3(9)	114.5(5)	114.1(5)	116.7(5)
N(4)-C(21)-C(22)	125.3(2)	124.9(2)	125.9(10)	123.3(5)	123.9(6)	121.7(5)
N(4)-C(21)-C(26)	115.9(2)	115.1(2)	115.8(10)	116.3(5)	115.3(5)	115.7(5)
N(1)-C(11)-C(12)	122.8(2)	121.9(2)	116.7(10)	123.4(5)	121.7(6)	122.9(5)
N(1)-C(11)-C(16)	117.8(2)	118.1(2)	124.1(10)	118.0(5)	118.2(5)	115.6(5)

⁷ 3-methyl-1,5-diphenylformazan. This Work.

⁸ 3-ethyl-1,5-diphenylformazan. This Work.

⁹ 3-tertiary butyl-1,5-diphenylformazan. This Work.

¹⁰ 1,5-bis(2,6-dimethylphenyl)-3-nitroformazan. Ref [6].

Bond orders have been calculated after the method of Burke-Laing and Laing [19]. For (1) C=N, bond order = 1.8; C-N, 1.2; N=N, 1.8; N-N, 1.4; for (2) C=N, 1.8; C-N, 1.2; N=N, 1.8; N-N, 1.4. It can be seen that while there is extensive delocalisation of the π -electrons for all of these formazans, the double-bond and single-bond character of the skeleton is clearly maintained as the 3-substituent, and therefore the configuration, changes from methyl to ethyl and finally to *tertiary*-butyl. While substitution and configuration do not have a profound effect on the bond orders, the subtle differences which are seen are reflected in the vibrational spectra of the systems.

The structure of (1) closely resembles other orange formazans which assume the *anti,s-trans* configuration [13]. The N-N-C-N-N backbone is planar and the phenyl rings are inclined to this plane [the angle between C11-C16 and the mean plane C21-C26 = 27°]. Delocalisation of electrons extends to the phenyl rings with N-C(phenyl) bond lengths of 1.402 and 1.423 Å which represent bond orders of *ca.* 1.2.

Selected intermolecular distances for (1) are listed in Table 6 and a view of the unit cell is given in Figure 4.

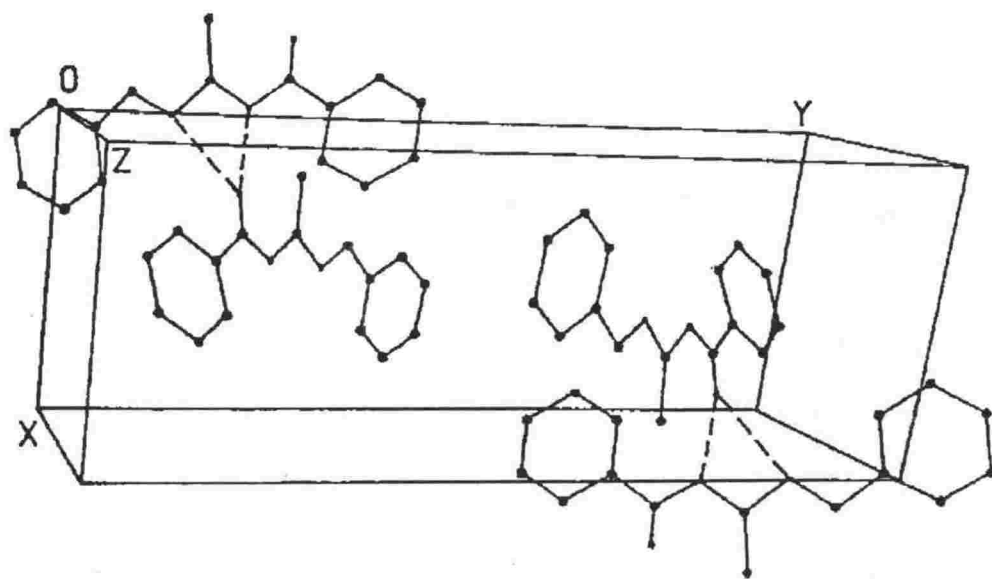


**Figure 4. A Projection of the Unit Cell for
3-methyl-1,5-diphenylformazan (1).**

Table 6: Selected Inter- and Intramolecular Distances (Å) and Bond Angles (°) for 3-methyl-1,5-diphenylformazan.

N1'-H1'	0.960				
N1'-N2'	1.339	119.8			
N1'-C11'	1.402	119.9	120.3		
N1'-N2	3.183	20.3	130.2	106.8	
N1'-N3	3.429	25.5	128.0	106.4	39.0
		H1'	N2'	C11'	N2
H1'-N1'	0.960				
H1'-N2	2.307	151.4			
H1'-N3	2.596	145.3	53.4		
		N1'	N2		

There is a significantly short intermolecular hydrogen bond of 2.31 Å between H1' and N2. This distance is less than the sum of van der Waals radii of Bondi [20] (2.95 Å). The C2-C3 distance of 1.48 Å is clearly a single bond and therefore delocalisation of electrons does not extend into the methyl substituent.

The structure of (2) differs significantly from the only other *syn,s-cis* configuration structurally confirmed for a formazan. Dijkstra *et al.* [6] have reported a mesomeric structure for 1,5-bis(2,6-dimethylphenyl)-3-nitroformazan. However, the structure of (2) can not be described as mesomeric. The two N-N bond lengths are dissimilar as are the two C-N bond lengths. The imino proton is not symmetrically located equidistant from N1 and N5 and it does not share the plane of the N-N-C-N-N backbone. The phenyl rings are inclined to the plane of the backbone. The angle between C41-C46 and the mean plane of C31-C36 = 12.1°; the angle between C61-C66 and the mean plane of C51-C56 = 19.1°. This inclination does not preclude delocalisation of electrons into the phenyl rings and the N-C(phenyl) bond distances of less than 1.43 Å confirm a degree of delocalisation. A corresponding delocalisation into the ring is not seen for the nitro-formazan structure; substitution of the phenyl rings was held to account for the twisting of the phenyl rings out of the plane. The C11-C12 distance of 1.52 Å however, is clearly a single bond indicating that delocalisation of electrons into the backbone and phenyl rings does not extend to the *tertiary*-butyl substituent.

The x-ray analysis shows that there are two unique molecules of (2) in

each unit cell. There are also significant intramolecular hydrogen bonds in the molecules of (2). Selected intramolecular bond distances for (2) are listed in Table 7 and a view of the unit cell is given in Figure 5.

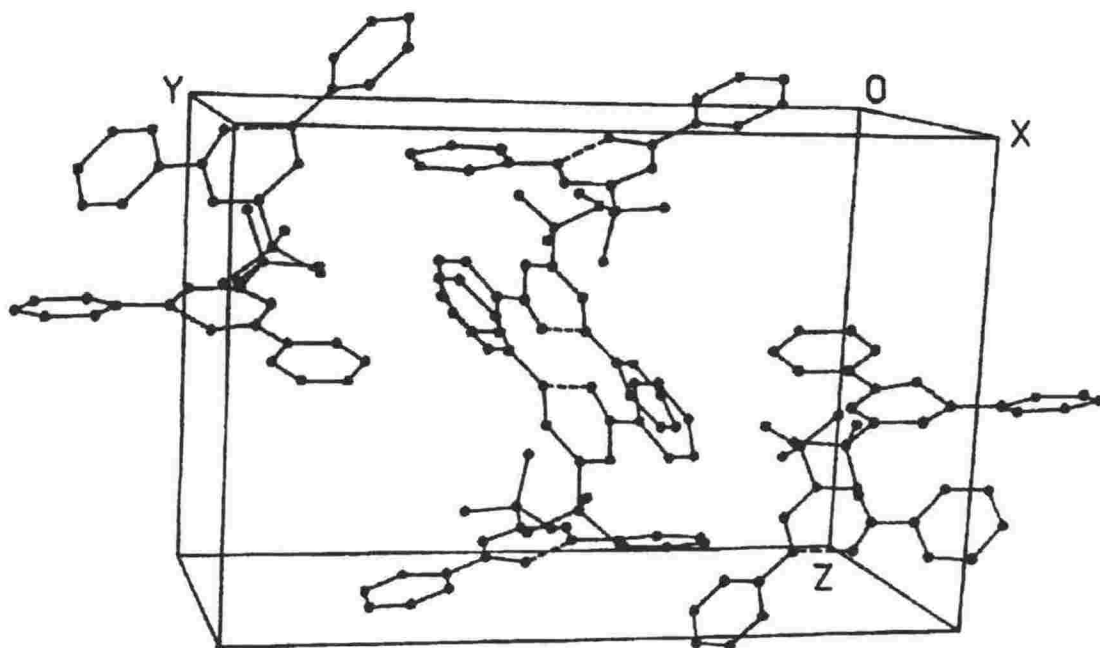


Figure 5. A Projection of the Unit Cell for 3-tertiary-butyl-1,5-diphenylformazan (2).

Table 7: Selected Inter- and Intramolecular Distances (Å) for 3-tertiary-butyl-1,5-diphenylformazan.

H11-N14	1.85
N11-N14	2.57
H21-N24	1.58
N21-N24	2.58

The H11-N14 distance of 1.85 Å and the H21-N24 distance of 1.58 Å are considerably less than the sum of van der Waals radii of Bondi [20] (2.95 Å). The formazan is therefore effectively locked into the *syn,s-cis* configuration.

^{13}C -Nmr Spectra: The ^{13}C nmr resonances in the solid state and in solution for (1) and (2) are listed in Tables 8 and 9. Solid state spectra are shown in Figures 6 and 7. Assignments in the solid-state are based on the use of short contact times to identify quaternary carbon signals, TOSS experiments and multiple spinner speeds to remove sidebands. Assignments in solution are based on gated spin echo (GASPE) and selective decoupling experiments.

In solid-state nmr some of the motional degrees of freedom are quenched allowing the identification of different conformers. The solid-state ^{13}C nmr confirm that, while (1) and (2) each exist in pure configurations, they do not exist in the same one. For (1) discrete signals for C11 and C21 are observed confirming their non-equivalence and only one signal for the methyl substituent is observed for the *anti,s-trans* configuration as established by the x-ray analysis. For (2) only one signal is observed for the quaternary aromatic carbon atoms due to their

**Table 8: Nuclear Magnetic Resonance Spectra
of 3-methyl-1,5-diphenylformazan. (^{13}C δ ppm)**

State	$-\text{CH}_3$	Intensity	C3	C11	C21	Aromatic
Solid	7.8	100	155.8	153.2	144.0	114.7 124.1 130.2
CH_3OH	7.9	100	154.7	149.8		130.1 127.0 119.5
$(\text{CD}_3)_2\text{CO}$	7.4	80	155.0	149.5		129.9 126.9 114.7
	15.5	18		147.5		weak bands
CDCl_3	6.6	58	154.2	149.5		129.3 126.3 118.3
	16.1	42	152.1	147.1	143.2	130.5 129.0 122.9 122.1 114.4
C_6D_6	6.1	33	154.1	148.7		129.4 126.5 118.8 130.5 127.5 123.3 122.2 114.6

Table 9: Nuclear Magnetic Resonance Spectra for 3-*tertiary*-butyl-1,5-diphenylformazan. (^{13}C δ ppm).

State	-C(CH) ₃	Intensity	C3	C11/C21	Aromatic
Solid	38	31	149.8	146.5	129.4 123.8 120.3 114.6
CDCl ₃	38.1	29.9	150.2	148.2	118.4 129.3 126.7
(CD ₃) ₂ CO	38.6	38.6	150.9	149.4	119.2 130.2 127.7

equivalence in the *syn,s-cis* configuration; one set of signals only is seen for the *tertiary*-butyl group. The shift in the C3 signals for (1) and (2) reflects the difference in C=N bond order with the greater electron density of (1) giving the downfield resonance when compared with (2).

In solution both the *anti,s-trans* and *syn,s-cis* configurations yield equivalent aromatic carbon resonances as tautomerism is fast on the nmr timescale. The *syn,s-trans* configuration, however, yields discrete signals for the aromatic carbon atoms as they are not equivalent and are unaffected by tautomerism. The resonances for the 3-substituents also provide a useful method for analysing the conformational integrity of the sample. For (1) two configurations are apparent giving the two 3-methyl resonances between 6 and 16 ppm. The *anti,s-trans* form is in equilibrium with the *syn,s-trans* form as evidenced by the more complicated pattern of phenyl resonances in all of the solvents studied with the exception of the methanol spectrum which emulates the solid-state spectrum - CDCl₃, 129.3, 126.3, 118.3 for *anti,s-trans*; 130.5, 129.0, 122.9, 122.1, 114.4 ppm for *syn,s-trans* (the *para*-phenyl carbon atoms are equivalent in both forms). Isomer ratios can be gauged from the intensities of the methyl signals and these are listed in Table 8.

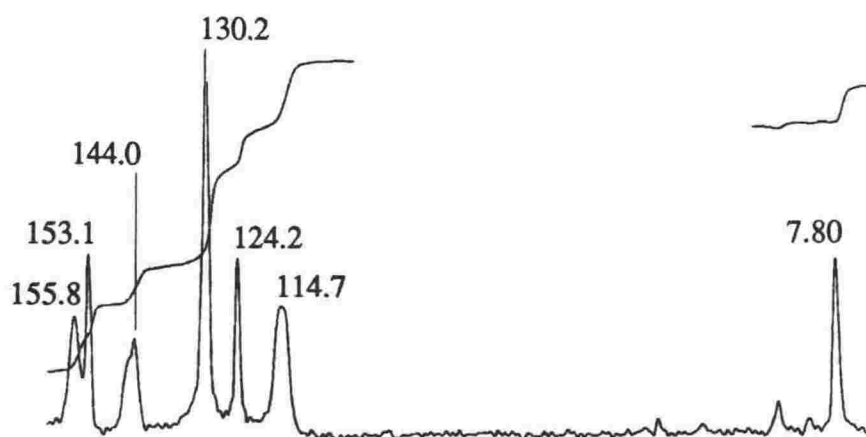


Figure 6: The Solid state ^{13}C MAS Nmr Spectrum for 3-methyl-1,5-diphenylformazan (1).

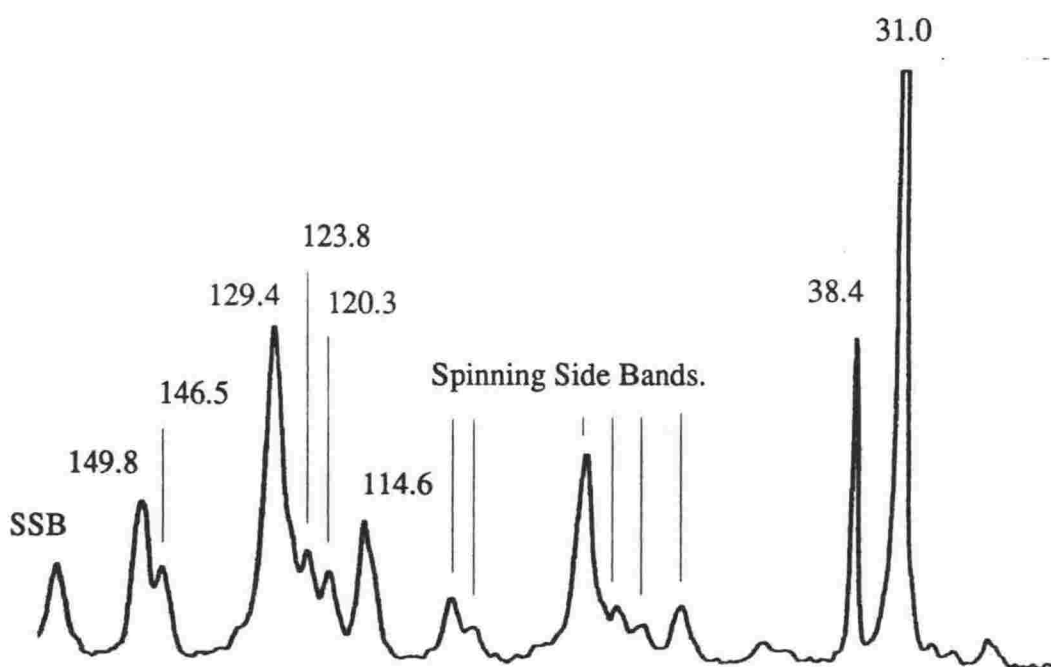
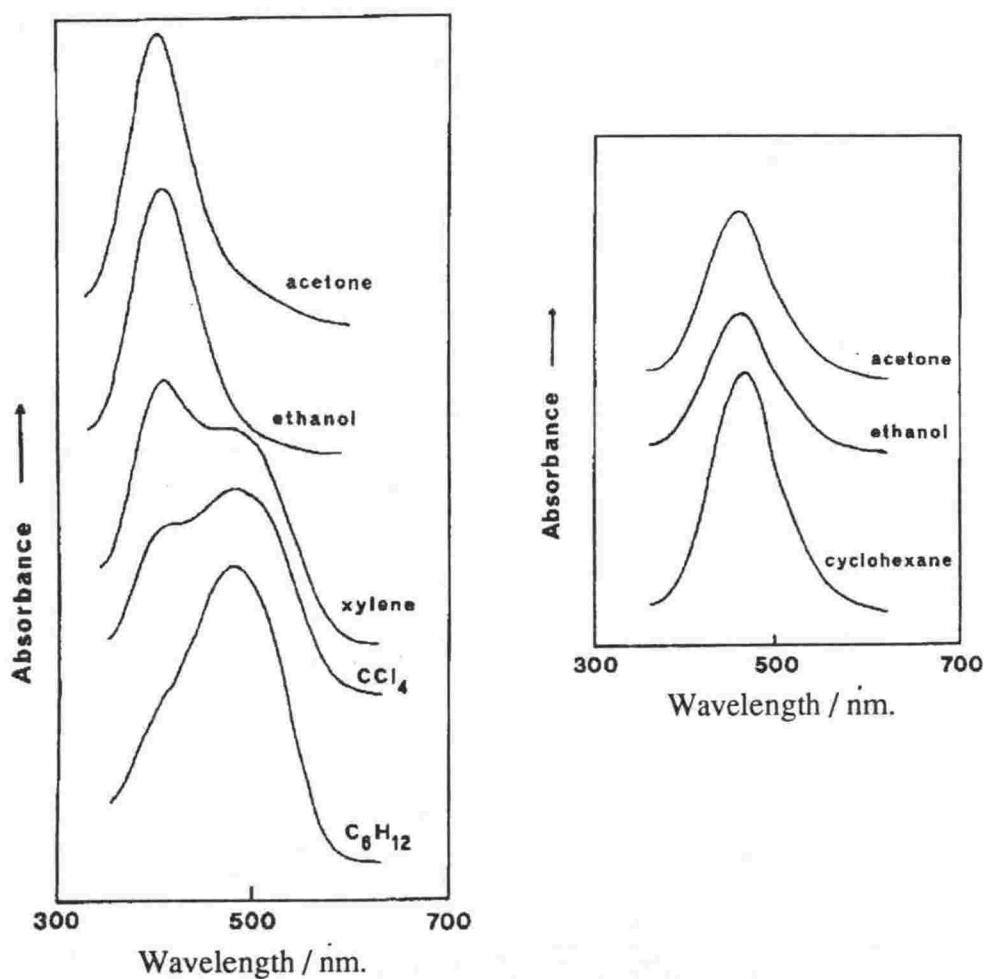


Figure 7: The Solid State ^{13}C MAS Nmr Spectrum for 3-tertiary-butyl-1,5-diphenylformazan (2).

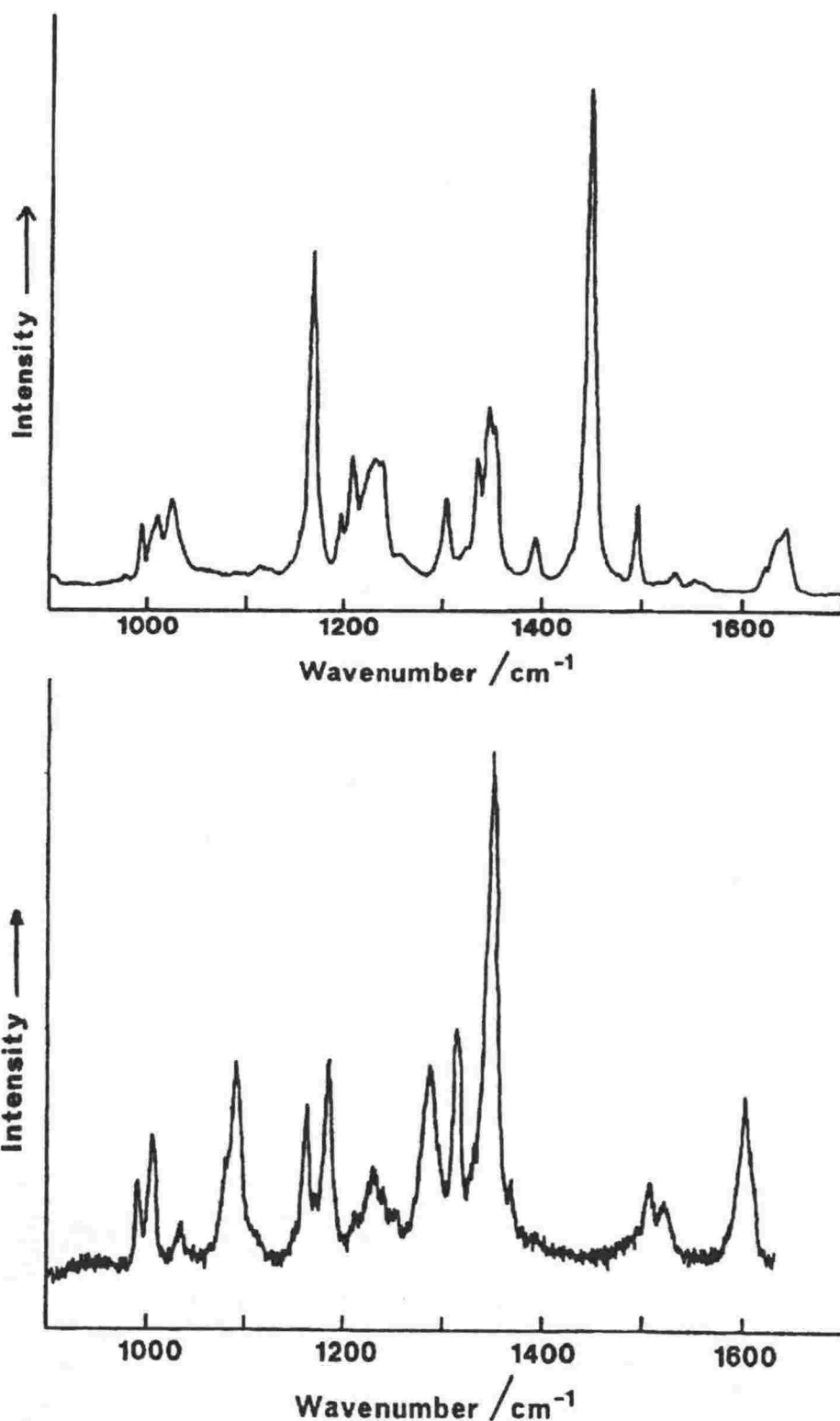
Further evidence for the existence of an equilibrium for (1) comes from the electronic absorption spectra shown in Figure 8. These spectra clearly demonstrate that both an orange and a red form are present in differing concentrations in all solvents except acetone and ethanol.

For (2) the *syn,s-cis* configuration occurs in solution in both protic and aprotic solvents and the resonances in solution closely resemble those of the solid state. The electronic absorption spectra for (2) are shown in Figure 9. There is no change in absorption maximum for the solvents studied confirming that there is no appreciable contribution from an orange conformer for (2).



Figures 8 and 9. The Ultra violet-visible Absorption Spectra of 3-methyl-1,5-diphenylformazan (1), left, and 3-tertiary-butyl-1,5-diphenylformazan (2), right.

Raman Spectra: The band centre wavenumbers for the normal modes of vibration of (1) and (2) are listed in Table 10 and typical Raman spectra are shown in Figures 10 and 11. Comparison of the two spectra



Figures 10 and 11. The Raman Spectra of 3-methyl-1,5-diphenylformazan (1), top, and 3-tertiary-butyl-1,5-diphenylformazan (2) bottom.

Table 10: Band Centre Wavenumbers for the Raman Spectra of 3-methyl-1,5-diphenylformazan (1) and 3-*tertiary*-butyl-1,5-diphenylformazan (2).

(1) solid 647.1 nm	(1) solid 422 nm [ref. 21]	(2) solid 647.1 nm
1598	1605	1601
1590		
1580		
1511		1522
1494	1500	1505
1456	1464	
1413	1412	1344
1359	1370	1363
1321	1320	1310
1315		
1306		
1273	1282	1279
1206	1208	1222
1185	1196	1176
1172		1169
1145	1148	1159
	1018	1085
1011	1010	1030
996		1001
981		984

is useful as they exemplify orange *anti,s-trans* and red *syn,s-cis* formazans. The Raman spectrum has previously been reported [21] for 3-methyl-1,5-diphenylformazan at a different exciting wavelength and is included for comparison. No Raman spectra have been reported for (2).

The Raman spectrum of (1) closely resembles that already reported for the orange isomer of 3-ethyl-1,5-diphenylformazan (3). While it is clear that there is a considerable degree of mixing, the two most intense bands at 1413 and 1145 cm^{-1} in (1) can be assigned to $\nu_{\text{N=N}}$ and $\nu_{\text{N-N}}$ respectively (1411 and 1147 cm^{-1} in (3)). The bands at 1321, 1315 and 1306 cm^{-1} are a reflection of the C-N bond order in (1). The corresponding bands appear at 1331, 1321 and 1306 cm^{-1} in (3) which has

a longer C=N bond and a shorter C-N bond length but which has an average C-N bond order equal to (1).

Weaker scattering is observed for (2) due to the increased self absorption of the sample. The lower stability of (2) also requires the use of decreased laser powers. It is still evident that the Raman spectrum of (2) differs significantly from that of (1). The most intense band at 1363 cm^{-1} has shifted from 1413 cm^{-1} in (1) as the N=N bond length increases from 1.264 \AA in (1) to 1.279 and 1.282 \AA in (2). The band at 1159 cm^{-1} is assigned to the $\nu_{\text{N-N}}$ normal mode but does not have the intensity of the corresponding band in (1). The band at 1601 cm^{-1} is assigned to vibrations of the phenyl ring and is relatively more intense than the corresponding bands in (1) which are weaker and are centred at 1598 , 1590 and 1580 cm^{-1} .

Conclusion.

3-Methyl-1,5-diphenylformazan exists in the *anti,s-trans* configuration in the solid state. In methanol solution this form is maintained. However, in aprotic solvents this form is in equilibrium with the *syn,s-trans* configuration. This behaviour closely parallels that of 3-ethyl-1,5-diphenylformazan and would seem to be characteristic of orange 3-substituted-1,5-diphenylformazans in general.

The methyl substituent is clearly the feature which determines the conformation of (1) allowing the open configuration in the solid which is further stabilised by an intermolecular hydrogen bond. In solution the formation of an equilibrium involving the closed structure is evidenced by the absorption and magnetic resonance spectra. The red form of (1) is clearly *syn,s-trans* and not *syn,s-cis*, which is seen when the 3-substituent is bulky. While the red form of (1) becomes increasingly important in CDCl_3 and C_6D_6 solutions the orange form is still apparent in appreciable concentration even in aprotic solvents in the dark. It has been shown [22,23] that red forms are promoted by traces of acid but destabilised by exposure to light.

3-Tertiary-butyl-1,5-diphenylformazan exists in the *syn,s-cis* configuration in the solid state. This form is maintained in solution as the tertiary-butyl substituent does not favour the formation of a *trans* arrangement around the C=N double bond.

The tertiary butyl substituent is clearly the feature which determines the conformation of the formazan due to its steric effect at position three. The effect of intra- or inter-molecular hydrogen bonding would appear to play a secondary role. The stabilising influence of an all-planar ring system would also appear to play a role.

The combined techniques of nuclear magnetic resonance and Raman spectroscopies make it possible to monitor changes in the formazan

structure due to simple 3-substitution. Differences in the C=N bond orders are reflected in the solid-state ^{13}C nmr spectral shifts of the C3 signals. The Raman active phonons of formazans are sensitive to conformational differences in the system. The band centre wavenumber for the normal modes based mainly on the N=N function shows a marked shift depending upon the configuration of the formazan. Solution nmr allows the straightforward characterisation of the equilibrium configurations of the formazan in different solvents, in particular the red *syn,s-trans* form has a characteristic pattern of signals compared with the more symmetric forms.

Acknowledgements.

One of the authors, CWC, is grateful to the Maori Education Foundation for the granting of a Queen Elizabeth II Post Graduate Scholarship during the research for this paper. We are also grateful to Dr R.H. Newman and Dr K. Morgan of the DSIR for recording solid-state magnetic resonance spectra.

References.

1. Bamberger, E. and Wheelwright, E.W. *Chem. Ber.*, **25**, 3201 (1892).
2. von Pechmann, H., *Chem. Ber.*, **25**, 3175 (1892).
3. Silversmith, E.F., *J. Chem. Ed.*, **65**(1), 70 (1988).
4. Otting, W. and Neugebauer, F.A., *Chem. Ber.*, **102**, 2520 (1969).
5. Otting, W. and Neugebauer, F.A., *Z. Naturforsch., Teil B*, **23**, 1064 (1968).
6. Dijkstra, E., Hutton, A.T., Irving, H.M.N.H. and Nassimbeni, L.R., *Acta Crystallogr., Sect B*, **38**, 535 (1982).
7. Preuss, J. and Gieren, A., *Acta Crystallogr., Sect B*, **31**, 1276 (1975).
8. Hutton, A.T., Irving, H.M.N.H., Nassimbeni, L.R. and Gafner, G., *Acta Crystallogr., Sect B*, **35**, 1354 (1979).
9. Omel'chenko, Yu., Kondrashev, Yu. D., Ginsburg, S.L. and Neiganz, M.G., *Kristallografiya*, **19**, 522 (1974).
10. Laing, M., *J. Chem. Soc., Perkin Trans. 2*, **1977**, 1248.
11. Guillerez, J., Pascard, C. and Prange, T., *J. Chem. Res.*, (S) 308, (1978); (M), 3934 (1978).
12. Hutton, A.T., Irving, H.M.N.H. and Nassimbeni, L.R., *Acta Crystallogr., Sect B*, **36**, 2071 (1980).
13. Burns, G.R., Cunningham, C.W. and McKee, V., *J. Chem. Soc., Perkin Trans. 2*, **1988**, 1274.
14. Nineham, A.W., *Chem. Rev.*, **55**, 355 (1955).
15. Kuhn, R. and Weitz, H.M., *Chem. Ber.*, **86**, 1199 (1953); Langbein, H., *J. Prakt. Chem.*, **321**, 655 (1979); Fischer, P.V., Kaul, B.L. and Zollinger, H., *Helv. Chim. Acta*, **51**, 1449 (1968); Grummt, U.W. and Langbein, H., *J. Photochem.*, **15**, 329 (1981); Lewis, J.W. and Sandorfy, C., *Can. J. Chem.*, **61**, 809 (1983); Kovalenko, M.F., Kurapov, P.B. and Grandberg, I.I., *Zh. Org. Khim.*, **23**, 1070 (1987).
16. Hutton, A.T., Irving, H.M.N.H., Koch, K.R. and Nassimbeni, L.R., *J. Chem. Soc., Chem. Commun.*, **1979**, 57.
17. Irving, H.M.N.H., Gill, J.B. and Cross, W.R., *J. Chem. Soc.*, **1960**, 2087.
18. Neugebauer, F.A. and Trischmann, H., *Leibigs Ann. Chem.*, **706**, 107 (1967).
19. Burke-Laing, M. and Laing, M., *Acta Crystallogr., Sect B*, **32**, 3216 (1976).
20. Bondi, A., *J. Phys. Chem.*, **68**(3), 441 (1964).
21. Kukushkina, I.I., Yurchenko, E.N., Arkhipenko, D.K. and Orekhov, B.A., *J. Phys. Chem.*, **46**(7), 963 (1972).
22. Hutton, A.T. and Irving, H.M.N.H., *J. Chem. Soc., Perkin Trans. 2*, **1982**, 1117.
23. Sueshi, Y. and Nishimura, N., *Bull. Chem. Soc. Jpn*, **56**, 2598 (1983).

Chapter 3.4

3-Halogenated-1,5-diphenylformazans.

In this chapter the results of a study of the following three 3-halogenated-1,5-diphenylformazans are presented:

3-bromo-1,5-di- <i>para</i> -bromophenylformazan	(3)
3-chloro-1,5-diphenylformazan	(4)
3-iodo-1,5-diphenylformazan	(5)

The first section of this chapter consists of the preparation and characterisation of the tribromoformazan derivative as well as a second product of the reaction: di(3-bromo-1,5-diphenyltetrazolium)-decabromide. The results have been submitted to the *Journal of the Chemical Society, Perkin Transactions 2*.

The second section of this chapter consists of preliminary results on the preparation and characterisation of the 3-chloro- and 3-iodo- formazan derivatives.

Proofs to: Dr Gary R. Burns,
Chemistry Department,
Victoria University of Wellington,
P.O. Box 600,
Wellington, New Zealand.

**The Reaction of 1,5-Diphenylformazan with Bromine:
The X-Ray Crystal Structure and Raman Spectrum of
Di(3-bromo-1,5-diphenyltetrazolium)-decabromide
and
The X-Ray Crystal Structure of
3-bromo-1,5-di-*para*-bromophenylformazan.**

Christopher W. Cunningham,
Chemistry Department,
Victoria University of Wellington,
P.O. Box 600,
Wellington, New Zealand.

and

Vickie McKee,
Department of Chemistry,
University of Canterbury,
Christchurch 1, New Zealand.

Abstract

1,5-Diphenylformazan (1) reacts with bromine in solution in a single reaction to give di(3-bromo-1,5-diphenyltetrazolium)-decabromide (2) and 3-bromo-1,5-di-*para*-bromophenylformazan (3) which have both been identified by an X-ray crystal analysis. $C_{13}H_{10.6}N_4Br_{5.3}$ (2) belongs to the triclinic space group $P\bar{1}$ [$a=8.572(1)$, $b=9.711(1)$, $c=14.166(3)$ Å, $\alpha=75.18(1)$, $\beta=89.84(1)$, $\gamma=70.42(1)^\circ$, $Z=2$]. Stacks of antiparallel pairs of 1,5-diphenylformazan cations are interleaved by isolated Br_{10}^{2-} ions. The polybromide anion represents a new type of polyhalogen network for bromine, Br_{10}^{2-} , the Raman spectrum of which has been recorded for

the first time. $C_{13}H_9N_4Br_3$ (3) belongs to the orthorhombic space group *Pnma* [$a=7.343(2)$, $b=32.793(12)$, $c=5.912(1)$ Å, $Z=4$]. The formazan adopts the *anti,s-trans* configuration common to orange formazans.

Introduction.

In a continuing study [1] on the structures and properties of photochromic formazans² we have prepared and characterised several 3-substituted 1,5-diphenylformazans in an attempt to correlate photochromic behaviour with the nature of the 3-substituent. During the preparation and characterisation of *tribromoformazan* (3-bromo-1,5-di-*para*-bromophenylformazan) we were also able to isolate and determine the structure of di(3-bromo-1,5-diphenyltetrazolium)-decabromide. Organic cations of this type are not new, formazans are known to oxidise reversibly to tetrazolium salts as first described by von Pechmann [2] in 1894. However, the polybromide cation represents a new type of polyhalogen network for bromine.

Irving and Ramakrishna [3] obtained a *black crystalline compound of metallic lustre* from the reaction of S-methyl-dithizone³ and molecular diiodine in chloroform. The product was described simply as a non-stoichiometric compound of S-methyl-dithizone without further definition. Herbstein and Schwotzer [4] subsequently determined the structure, or more correctly structures, of the products of this reaction. They found that two products were formed in a single reaction and the x-ray analyses gave the structures as S-methyl-dithizone hydrogen triiodide and 2,3-diphenyl-5-methylthiotetrazolium triiodide-chloroform. The existence of *syn* and *anti* isomers of S-methyl-dithizone suggested that the energy barrier between them is small in solution and was held to account for the two observed products.

Herbstein and Schwotzer [5] have also reported, in a paper on the interaction of molecular diiodine with thiones, the structures of the two dithizone⁴ diiodine charge transfer molecules, dithizone-diiodine and bis(dithizone)-heptakis(diiodine).

In the present study, a similar reaction between 1,5-diphenylformazan and bromine has resulted in a substituted formazan and a tetrazolium compound and has yielded a unique anion, the structure of which has been unequivocally determined and its Raman spectrum observed.

2 Compounds containing the characteristic -N=N-C=N-NH- grouping.

3 IUPAC: 3-methylthio-1,5-diphenylformazan.

4 3-mercapto-1,5-diphenylformazan.

Experimental.

Synthesis: 1,5-diphenylformazan [6,7] (4.5 g, 1 mol) mixed in acetic acid (25 ml, glacial) was treated gradually with bromine (9.6 g, 2 mol) in the cold. A dark solid separated immediately and was collected and washed with cold ethanol. The product was air dried until the characteristic bromine odour lessened, and then dried *in vacuo* over silica gel in the dark.

Red crystals suitable for x-ray analysis, were provided without the necessity of further purification. Recrystallisation from aqueous dioxane did not result in the formation of *minute orange crystals*, as was the experience of Irving and Bell [8], neither did the analyses fit their results. However, separation of the product on a column (silica gel, 1:2 dichloromethane petroleum) gave three fractions other than starting material (one fraction for the formazan and two for the tetrazolium salt, which is disordered in bromine). Detailed elemental analyses were not made as the compositions of the crystal emerged from the crystal structure analyses. Subsequent recrystallisation, after filtration through silica gel, yielded a further crop of red crystals whose structure was also determined.

Crystal Structure Determination of (2) and (3): Essentially similar methods were used in both determinations. Crystal data were collected at -100°C with a Nicolet R3m four-circle diffractometer using graphite-monochromated $\text{Mo-K}\alpha$ radiation.

(2): A red crystal of dimensions $0.26 \times 0.38 \times 0.14$ mm was used and found to belong to the triclinic space group $P\bar{1}$, $a=8.572(1)$, $b=9.711(1)$, $c=14.166(3)$ Å, $\alpha=75.18(1)$, $\beta=89.84(1)$, $\gamma=70.42(1)^{\circ}$, $V=1092.2(3)$ Å³, $F(000)=607$, $Z=2$. 1.4° ω -scans at $7.3^{\circ}\text{min}^{-1}$ were used to collect 2863 unique reflections in the range $4 < 2\theta < 45^{\circ}$ and, of these, 2540 having $I < 3(\sigma I)$ were used for the structural analysis.

(3): A red crystal of dimensions $0.31 \times 0.31 \times 0.06$ mm was used and found to belong to the orthorhombic space group $Pnma$, $a=7.343(2)$, $b=32.793(12)$, $c=5.912(1)$ Å, $V=1426.6(7)$ Å³, $F(000)=880$, $Z=4$. 2.4° ω -scans at $4.88^{\circ}\text{min}^{-1}$ were used to collect 856 unique reflections in the range $4 < 2\theta < 45^{\circ}$ and, of these, 446 having $I < 3(\sigma I)$ were used for the structural analysis.

Cell parameters were determined by least-squares refinement of 21 for (2) and 22 for (3) accurately centred reflections in the range ($23 < 2\theta < 34^{\circ}$) and ($18 < 2\theta < 31^{\circ}$) respectively. Crystal stability was monitored by recording three check reflections every 100 reflections and no significant variations were observed. The data were corrected for Lorentz and polarisation effects and an empirical absorption correction, based on ψ -scan data was applied for (2) and a correction based on ψ -scan data and

indexed crystal faces was applied for (3).

For (2), a Patterson synthesis revealed the positions of three bromine atoms and the remaining non-hydrogen atoms were located from difference Fourier maps. The bromine atom Br1 was found to be disordered and was refined with a site occupancy factor of 0.33. Hydrogen atoms were inserted at calculated positions using a riding model with thermal parameters equal to 1.2 U of their carrier atoms. Anisotropic thermal parameters were assigned to all non-hydrogen atoms and the refinement, on 121 least-squares parameters, converged with $R = 0.0467$, $R' = 0.0796$ and a maximum shift/error ratio of 0.05. The final difference map showed no significant features. The function minimised in the refinement was $\sum w(|F_o| - |F_c|)^2$ where $w = [\sigma^2(F_o) + g F_o^2]^{-1}$ and $g = 0.00048$.

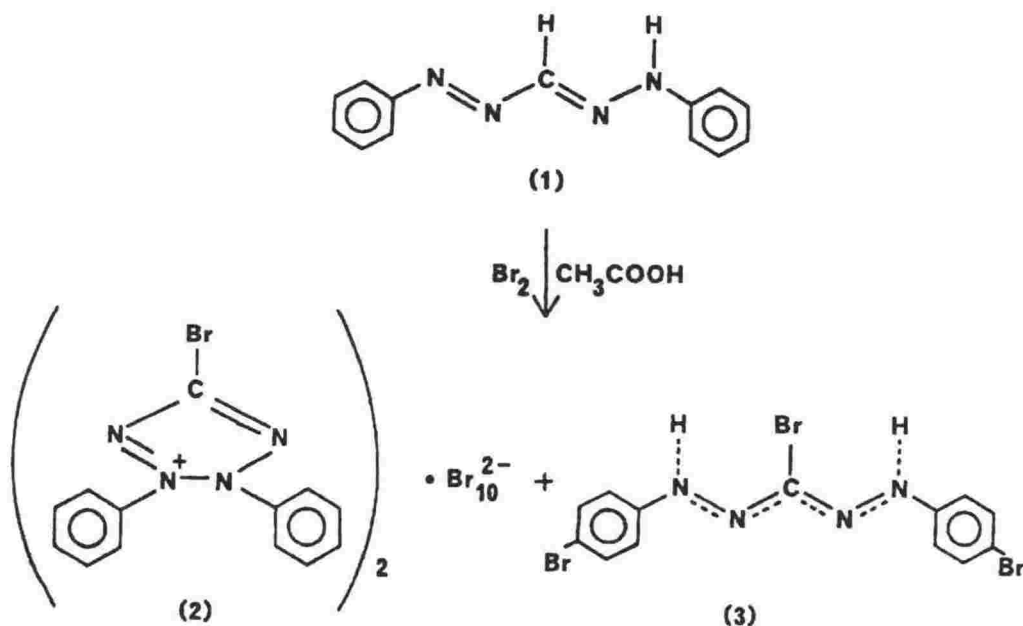
For (3) a Patterson calculation revealed the positions of the two independent bromine atoms and the remaining non-hydrogen atoms were located from difference Fourier maps. The structure was refined by blocked-cascade least-squares techniques and converged with $R = 0.0725$, $wR = 0.1074$. Owing to the paucity of data, only the bromine atoms were refined anisotropically; hydrogen atoms on the phenyl groups were inserted at calculated positions using a riding model with thermal parameters equal to 1.2 U of their carrier atoms. The hydrogen atom which must, for symmetry reasons, be disordered between N2 and N2' was not located and has not been included. The function minimised was as above with $g = 0.00375$. The final difference map showed no significant features. All programs used for the data collection and structure solution are contained in the SHELXTL (Version 4.0) package⁵.

Raman Spectra: Raman spectra were recorded using a Spex 1401 spectrometer equipped with a Thorn EMI 6256 photomultiplier tube used in the photon counting mode. A Spectra-Physics 164-01 Krypton Ion laser was used as the Raman scattering source, operating at a wavelength of 647 nm. Band wavenumbers were calibrated using the emission spectrum of neon and typical slit widths of 200 μm were employed, giving a bandpass of 2 cm^{-1} at 647 nm. Samples were studied as crystals or in capillary tubes. Spectra were also recorded at room temperature using laser powers of less than 50 mW at the sample to avoid photo-decomposition.

5 G.M.Sheldrick, SHELXTL User Manual, Revision 4, Nicolet XRD Corporation, Madison, Wisconsin, 1984.

Results.

The overall chemical reaction may be represented by Scheme A. For (2) only partial bromination of the formazan has occurred at the C3



Scheme A.

position and no evidence for the bromination of either of the phenyl rings has been observed. 1,5-Diphenylformazan has the *anti,s-trans* configuration in the solid state [10]. Formation of the tetrazolium ring requires isomerisation about the C=N double bond and rotation about the C-N single bond. This gives the *syn,s-cis* configuration seen for formazans and described elsewhere [1], which can then give the tetrazolium ring by hydrogen elimination. For (3) direct substitution of the C3 proton by bromine and *para*-substitution of the phenyl rings accounts for the product. The original preparation report details that no bromo-formazan without phenyl substitution could be synthesised.

Di(3-bromo-1,5-diphenyltetrazolium)-decabromide: Atomic nomenclature and numbering for the tetrazolium cation is given in Figure 4 and for the decabromide anion assembly is given in Figure 5. Bond lengths and bond angles are given in Tables 1 and 2.

Table 1: Bond Lengths (Å) and Bond Orders* for the Anion and Cation of Di(3-bromo-1,5-diphenyltetrazolium)-decabromide (2).

	Length	Order		Length	Order
C(11)-C(12)	1.395(20)	1.55	C(11)-C(16)	1.369(16)	1.70
C(11)-N(1)	1.448(18)	1.00	C(12)-C(13)	1.409(21)	1.45
C(13)-C(14)	1.376(17)	1.80	C(14)-C(15)	1.424(24)	1.35
C(15)-C(16)	1.427(22)	1.30	C(21)-C(22)	1.366(19)	1.80
C(21)-C(26)	1.381(14)	1.80	C(21)-N(4)	1.462(19)	1.00
C(22)-C(23)	1.372(22)	1.70	C(23)-C(24)	1.369(16)	1.70
C(24)-C(25)	1.353(22)	1.95	C(25)-C(26)	1.409(25)	1.45
N(1)-N(2)	1.333(18)	1.40	N(1)-N(4)	1.368(14)	1.20
N(2)-C(1)	1.348(18)	1.50	C(1)-Br(1)	1.643(16)	
C(1)-N(3)	1.370(19)	1.35	N(3)-N(4)	1.323(17)	1.50
Br(2)-Br(3)	2.906(2)		Br(3)-Br(4)	2.943(2)	
Br(5)-Br(6)	2.744(1)				

*Bond Orders have been calculated following the method of Burke-Laing and Laing [13].

Table 2: Bond Angles (°) for the Anion and Cation of Di(3-bromo-1,5-diphenyltetrazolium)-decabromide (2).

C(12)-C(11)-C(16)	124.9(13)	C(12)-C(11)-N(1)	119.4(9)
C(16)-C(11)-N(1)	115.8(12)	C(11)-C(12)-C(13)	117.5(11)
C(12)-C(13)-C(14)	118.5(14)	C(13)-C(14)-C(15)	124.4(15)
C(14)-C(15)-C(16)	116.0(12)	C(11)-C(16)-C(15)	118.6(14)
C(22)-C(21)-C(26)	125.8(14)	C(22)-C(21)-N(4)	118.5(10)
C(26)-C(21)-N(4)	116.7(12)	C(21)-C(22)-C(23)	115.9(11)
C(22)-C(23)-C(24)	121.2(14)	C(23)-C(24)-C(25)	121.6(16)
C(24)-C(25)-C(26)	120.0(12)	C(21)-C(26)-C(25)	115.4(13)
C(11)-N(1)-N(2)	122.7(10)	C(11)-N(1)-N(4)	127.6(12)
N(2)-N(1)-N(4)	109.7(10)	N(1)-N(2)-C(1)	103.5(11)
N(2)-C(1)-Br(1)	123.1(11)	N(2)-C(1)-N(3)	113.5(13)
Br(1)-C(1)-N(3)	123.4(10)	C(1)-N(3)-N(4)	103.1(10)
C(21)-N(4)-N(1)	125.6(10)	C(21)-N(4)-N(3)	124.3(10)
N(1)-N(4)-N(3)	110.1(11)	Br(2)-Br(3)-Br(4)	177.2(1)

In the cation, all of the rings are planar, however the phenyl rings are inclined at 52° (C11-C16) and 48.9° (C21-C26) to the five membered ring and are at 53.5° to each other. The tetrazolium cation is disordered at the three-position. In the anion, the Br_{10}^{2-} unit is not planar and there are no significant interactions with neighbouring boxes.

The Crystal Structure: Atomic coordinates and isotropic thermal parameters are given in Table 3. Anisotropic thermal parameters and hydrogen atom coordinates with isotropic thermal parameters have been given as supplementary data (submitted to the Cambridge Crystallographic Centre).

Table 3: Atomic Coordinates ($\times 10^4$) and Temperature Factors ($\text{\AA}^2 \times 10^3$) for Di(3-bromo-1,5-diphenyltetrazolium)-decabromide (2).

	x	y	z	U
C(11)	99(14)	-2719(14)	-3341(9)	51(3)
C(12)	1066(17)	-3696(17)	-3850(11)	69(4)
C(13)	623(16)	-3379(16)	-4858(10)	66(4)
C(14)	-677(18)	-2089(18)	-5292(12)	80(4)
C(15)	-1645(18)	-1063(18)	-4783(11)	76(4)
C(16)	-1191(18)	-1426(18)	-3759(11)	77(4)
C(21)	561(13)	-5746(13)	-1771(9)	48(3)
C(22)	-771(15)	-5638(15)	-2324(10)	58(3)
C(23)	-794(15)	-6969(14)	-2480(10)	57(3)
C(24)	443(15)	-8315(16)	-2088(10)	65(4)
C(25)	1726(17)	-8395(18)	-1519(11)	71(4)
C(26)	1859(15)	-7061(14)	-1365(10)	58(3)
N(1)	469(11)	-3038(11)	-2296(7)	52(2)
N(2)	688(12)	-2022(12)	-1882(8)	57(3)
C(1)	1034(15)	-2776(15)	-923(10)	54(3)
Br(1)	1424(4)	-2018(4)	-81(3)	50(2)*
N(3)	1051(12)	-4238(13)	-722(8)	62(3)
N(4)	671(11)	-4362(11)	-1593(7)	53(3)
Br(2)	3491(1)	-365(1)	1296(1)	33(1)*
Br(3)	4225(1)	2263(1)	1485(1)	27(1)*
Br(4)	5045(1)	4837(1)	1774(1)	33(1)*
Br(5)	5057(1)	2178(1)	6241(1)	41(1)*
Br(6)	4775(1)	3372(1)	4246(1)	38(1)*

* Equivalent isotropic U defined as one third of the trace of the orthogonalised U_{ij} tensor

A description of the unit cell is given in Figure 1.

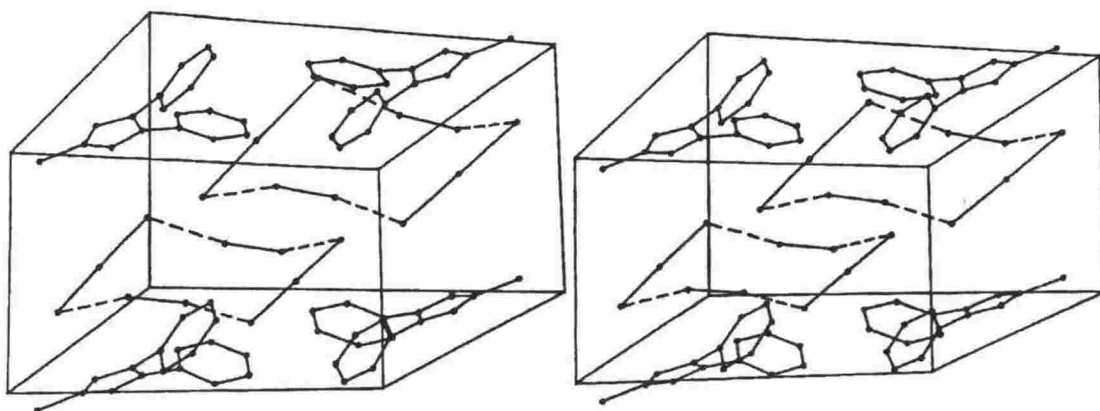


Figure 1: A Stereoview of the Unit Cell of Di(3-bromo-1,5-diphenyltetrazolium)-decabromide (2).

There are boxes of Br_{10}^{2-} anions interleaved between layers of pairs of antiparallel cations resulting in isolated decabromide moieties.

The Raman Spectrum: The Raman spectrum for the crystals is given in Figure 2. We believe this to be the first solid state Raman spectrum for Br_{10}^{2-} . The polybromide is only weakly scattering and gives rise to Raman bands between 50 and 200 cm^{-1} . In Table 4 we have compared the Raman bands with those for Br_2 and for some other symmetric and asymmetric Br_3^- anions and Br_5^- .

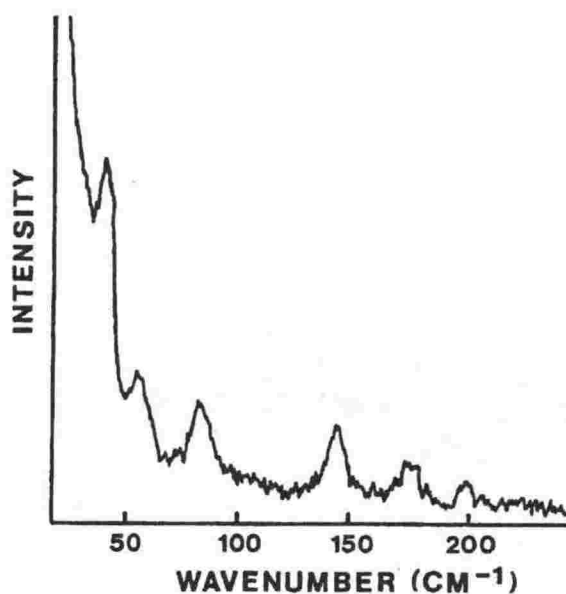


Figure 2: Raman Spectrum of Br_{10}^{2-} .

Table 4:
Raman Bands (Wavenumbers) Observed for Bromine, and Some Crystalline Di-, Tri- and Penta- bromides.

Raman Bands					Reference
Br_2	Band centred at 310				11
Cation Br_3^+ :	ν_1	ν_2	ν_3	Others	
NMe_4	161		184	22,43,169	27
NEt_4	163		200	29,75,106	27
NBu_4	167		194	24,33,49,71	27
Macrocyclc	156	97	198	31,40,105,234	27
Cetrimide	153		205	30,44,51	27
Thiuram	157		221		27
Ce	140		201,215	66,78,105,120,125, 264,342	23
PBr_4	135	94	251	247	28
Cation Br_5^+ :					
$(\text{TMA.H}_2\text{O})_{10}\text{H}^+$	265,160				23
Oxyacid	broad band <i>ca.</i> 250				12
Br_{10}^{2-}	144	94	175	54,67,193	This Work

3-Bromo-1,5-di-*para*-bromophenylformazan: Atomic nomenclature and numbering are given in Figure 6. Bond lengths and bond angles are given in Tables 5 and 6. Atomic coordinates and isotropic thermal parameters

**Table 5: Bond Lengths (Å) for
3-Bromo-1,5-di-*para*-bromophenylformazan (3).**

Br(1)-C(1)	1.859(35)	C(1)-N(1)	1.386(33)
C(1)-N(1')	1.386(33)	N(1)-N(2)	1.274(35)
N(2)-C(11)	1.398(34)	C(11)-C(12)	1.391(40)
C(11)-C(16)	1.381(37)	C(12)-C(13)	1.433(42)
C(13)-C(14)	1.298(36)	C(14)-C(15)	1.436(38)
C(14)-Br(2)	1.909(26)	C(15)-C(16)	1.362(40)

**Table 6: Bond Angles (°) for
3-Bromo-1,5-di-*para*-bromophenylformazan (3).**

Br(1)-C(1)-N(1)	123.3(16)	Br(1)-C(1)-N(1')	123.3(16)
N(1)-C(1)-N(1')	111.9(32)	C(1)-N(1)-N(2)	116.6(24)
N(1)-N(2)-C(11)	114.4(23)	N(2)-C(11)-C(12)	118.2(24)
N(2)-C(11)-C(16)	122.6(24)	C(12)-C(11)-C(16)	119.1(26)
C(11)-C(12)-C(13)	118.0(27)	C(12)-C(13)-C(14)	122.0(27)
C(13)-C(14)-C(15)	120.2(25)	C(13)-C(14)-Br(2)	122.1(21)
C(15)-C(14)-Br(2)	117.6(19)	C(14)-C(15)-C(16)	118.0(25)
C(11)-C(16)-C(15)	122.1(27)		

**Table 7: Atomic Coordinates ($\times 10^4$) and Temperature Factors ($\text{\AA}^2 \times 10^4$) for
3-Bromo-1,5-di-*para*-bromophenylformazan (3).**

atom	x	y	z	U
Br(1)	477(7)	7500	6039(7)	20(2)*
C(1)	657(51)	7500	2902(58)	3(9)
N(1)	940(39)	7150(8)	1638(42)	30(7)
N(2)	742(31)	6811(7)	2667(40)	11(6)
C(11)	1049(35)	6467(8)	1322(42)	3(6)
C(12)	524(39)	6089(10)	2161(55)	24(8)
C(13)	788(36)	5739(9)	748(45)	12(7)
C(14)	1430(34)	5769(8)	-1290(41)	5(6)
C(15)	2072(35)	6154(8)	-2122(49)	11(8)
C(16)	1775(38)	6492(9)	-828(46)	15(7)
Br(2)	1679(4)	5306(1)	-3223(5)	19(1)*

* Equivalent isotropic U defined as one third of the trace of the orthogonalised U_{ij} tensor

are given in Table 7. Anisotropic thermal parameters and hydrogen atom coordinates with isotropic thermal parameters are given as supplementary data. The molecule is not planar. The phenyl rings are each inclined at

8.8° to the mean plane of the molecule and at about 16° to each other. There is no evidence of any significant intermolecular interactions as can be seen in the description of the unit cell (Figure 3).

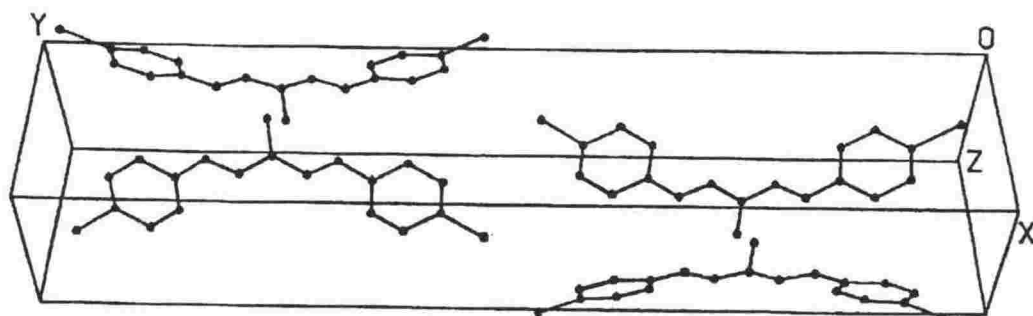


Figure 3: A Description of the Unit Cell for 3-Bromo-1,5-di-*para*-bromophenylformazan (3).

Discussion

Di(3-bromo-1,5-diphenyltetrazolioum)-decabromide:

The Cation: The cation which has resulted can be represented as a conventionally covalently bonded structure as in Scheme A, the structure

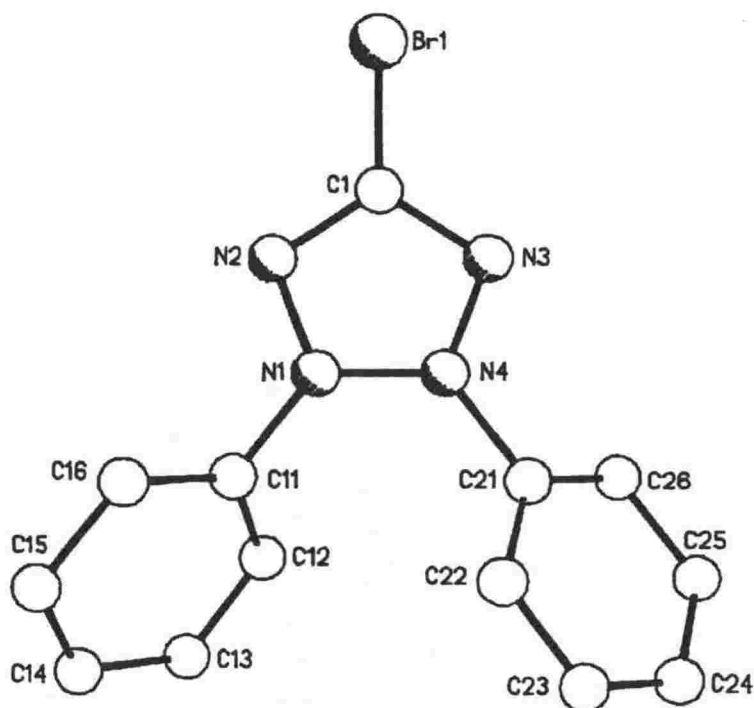


Figure 4: Molecular Structure and Atomic Nomenclature for Di(3-bromo-1,5-diphenyltetrazolioum)-decabromide (2).

is not meso-ionic [9]. There are no true single or double bond distances in the tetrazole ring [of the structure described above]. Bond orders have been calculated following the method of Burke-Laing and Laing [13]. The only single bond distance in the molecule is from the nitrogen atom in the tetrazole ring N4 to the carbon atom of the phenyl ring C21. The N-N distances in the tetrazole ring are not identical; neither are the C-N distances equal. The ring is planar and is an irregular pentagon. The bromine atom Br1 also lies in the plane of the tetrazole ring. The bond distances indicate that there is considerable electron delocalisation in the ring and the exocyclic bromine atom. The Br1-C1 bond length at 1.643 Å is considerably shorter than the corresponding bond in tribromoformazan (1.859 Å) and in other simple organo-bromine compounds (C-Br bond length in CBrCl_3 , 1.93 Å [14]; CH_3Br , 1.91 Å [15]; BrCN , 1.79 Å [15]) due to the apparent disorder found at the 3-position. It is of interest that several tetrazole structures have been reported [16] and they all exhibit a similar ring structure.

The bond distances, bond angles and bond orders in the phenyl rings are normal within experimental error. There appears to be little or no conjugation between the two ring systems. This is confirmed by the two C(phenyl)-N bond distances which are clearly single bond in character. Delocalisation over both the tetrazolium and the phenyl ring systems would seem to be precluded by the fact that the rings are not co-planar. The intense orange/red colour of the compound must be ascribed, therefore, to the delocalisation of electrons over the tetrazole ring and the exocyclic bromine atoms, paralleling a similar observation seen for related tetrazolium salts and sydnone [16].

The Anion: The decabromide anion again demonstrates the structural diversity of polyhalogen anions. A survey [17] of the many structural determinations of polyhalide anions summarises the major characteristics of the structures observed. The angles within the halogen networks are almost entirely either 90° or 180° (approximately) and the bond lengths may be longer than the sum of the covalent radii [18]. In many salts the structure of the anion is dependent upon the size and symmetry of the counter-ion.

It is a feature of all polyiodide anions that the iodine-iodine distances are intermediate between the normal covalent I-I bond length and the interlayer I...I bond lengths observed for crystalline iodine. The bromine-bromine distances in the Br_{10}^{2-} anion follow this trend of intermediacy.

In Table 8 we have listed all of the bromine-bromine bond lengths found for the Br_{10}^{2-} anion and these are compared with the values found for crystalline bromine and in tribromide and tetrabromide anions. Although the best description of the anion we have determined seems to be units containing two Br_3^- ions associated with two Br_2 molecules, it is clear that the Br5-Br6 bond length in the dibromide unit differs markedly from the value found for crystalline bromine and the tetrabromide anion.

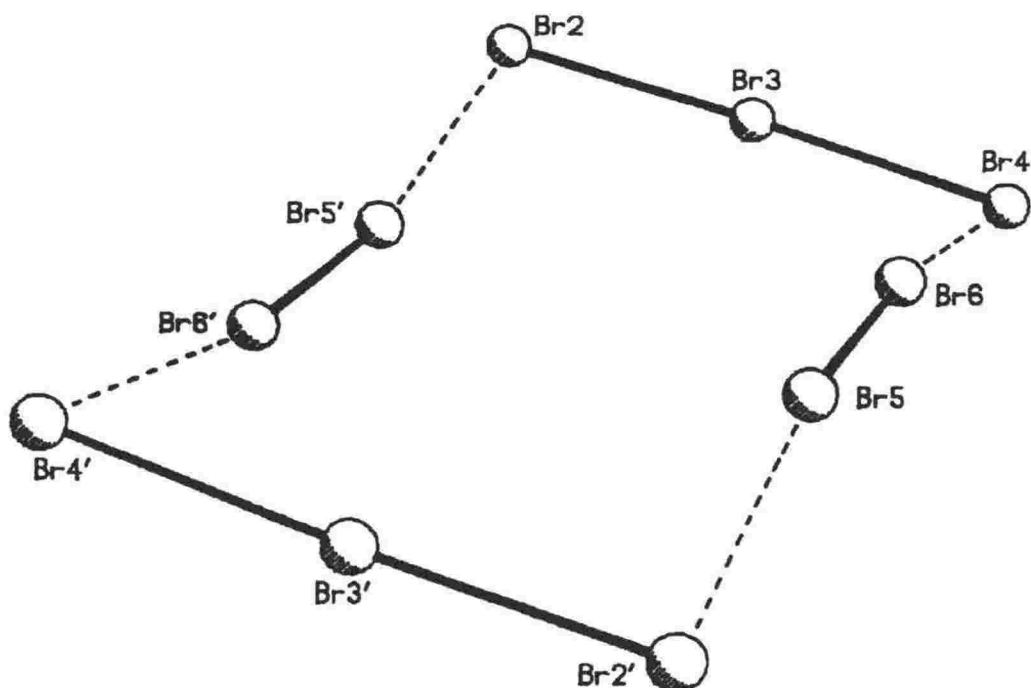


Figure 5: Molecular Structure and Atomic Nomenclature for the Decabromide of 3-Bromo-1,5-di-*para*-bromophenylformazan (3).

There is also a significant difference between the bond lengths found for the symmetric Br_3^- anions present in the decabromide and the often much shorter bond lengths found for other symmetric Br_3^- anions. The tribromide bond length in the decabromide is unusually long and while it equals the longest bond length in the most asymmetric tribromide crystal, PBr_7 , it results in a total bond distance of 5.85 Å between the terminal bromine atoms Br2-Br4 which is 0.5 Å longer than previously seen. The Br6-Br4 distance is 3.50 Å which is less than the sum of van der Waals radii (3.70 Å [24]). The significance of this intramolecular distance, the unusually long dibromide unit and the long but symmetric tribromide should be reflected in the vibrational spectra. The bonding and structure exhibited is in accord with the observations for all other halogen compounds of the type known so far, and is in remarkable agreement with the polyiodide anion I_{16}^{4-} [21] formed with theobromine. Herbstein and Kapon have [21] published a crystal structure analysis for the $(\text{theobromine})_2 \cdot \text{H}_2\text{I}_8$ which also has alternating layers of anions and cations. The I_{16}^{4-} anions are S-shaped, centrosymmetric, discrete units which are explicitly formulated as $(\text{I}_3 \cdot \text{I}_2 \cdot \text{I}_3 \cdot \text{I}_3 \cdot \text{I}_2 \cdot \text{I}_3)$. The first tri-iodide unit is symmetric and has bond lengths of 2.76 Å; the second tri-iodide unit

8 Theobromine = 3,7-dimethylxanthine.

Table 8. Br-Br Distances for Br₂ and Some Br₃⁻ and Br₄²⁻ Anions.			
Example	Br-Br / Å	Br....Br / Å	References
Br ₂ (s)	2.27	3.31, 3.79, 3.99	11
((CH ₃) ₃ NH) ₂ Br.Br ₃	2.54, 2.53		17
(CS ₃ N ₂ Br)Br ₃	2.72, 2.42		19
CeBr ₃	2.44, 2.70	3.73, 3.80	17
PBr ₄ .Br ₃	2.39, 2.91	3.66	33
(Paraquat)Br.Br ₃	2.89, 2.97	3.04	20
(W ₆ Br ₈)Br ₄ (Br ₄) ₂	2.98, 2.43		17
(C ₇ H ₁₃ NH) ₄ (SbBr ₆) ₂ Br	3.02, 2.28		17
[(CH ₃)N] ₃ Sb ₂ Br ₉ .Br ₂	2.89, 2.31		17
Br ₁₀ ²⁻	2.74, 2.91, 2.94	3.47, 3.50	This Work

is asymmetric with bond lengths of 3.03 and 2.84 Å and the iodine-iodine distances between these three sub-units are 3.35, 3.42 and 3.45 Å respectively. The structure then repeats according to the centrosymmetric symmetry which it possesses. The shortest distance between I₁₆⁴⁻ units is 3.84 Å which is of the order of van der Waals contacts (3.9 Å [24]). We have recorded the Raman spectrum of this polyiodide anion and the spectrum shows weak scattering for the tri-iodide and di-iodine sub-units at 107, 153, 171 and 205 cm⁻¹.

Raman Spectra: To date no penta- or decabromide anions have been isolated and had their structures determined, however, several spectral studies have alluded to their existence. Evans and Yo [12] in a vibrational

study presume the existence of Br_5^- to assign spectral features which they observed for salts of the oxy-anions of bromine. Hecquet and Landais [22] concluded that similar spectral features they observed in the Raman spectra of brominated acetic acid could also be ascribed to penta- and hepta-bromide anions. Evans and Yo were inconclusive about the Br_5^- anion as they were only able to observe one polarised Raman band and neither it nor any other band ascribable to the Br_5^- anion was observed in the infrared spectrum of the solution which gave the full line Raman spectrum. The band was solvent dependent and broad, centred between 250 and 257 cm^{-1} . The band centre wavenumber and the indication that other bands were of considerably lower wavenumber suggested that Br_5^- was not merely a loose $\text{Br}_2\cdot\text{Br}_3^-$ complex but was a more symmetric $[\text{Br}_2\text{BrBr}_2]^-$ anion in which the two outer bonds were considerably stronger than the two inner bonds. An L-assemblage was thought probable. The later paper of Hecquet and Landais offered no prediction of the structure of the pentabromide anion. Kalina *et al.* [23] in a paper on resonance Raman structure-spectra correlations for polybromides have predicted vibrational stretching frequencies for Br_2 , symmetric and asymmetric Br_3^- and Br_5^- . Their metrical parameters for Br_5^- were estimated from corresponding I_5^- data [25,26] giving $\text{Br}-\text{Br} = 2.38 \text{ \AA}$ and $\text{Br}\dots\text{Br} = 2.82 \text{ \AA}$. Calculated wavenumbers for the Raman active stretching vibrations for Br_5^- were 155 and 235 cm^{-1} . These calculated Raman shifts corresponded with their observed bands at 157 and 245 cm^{-1} for $\text{M}(\text{dpg})_2\text{Br}_x$ where $\text{M} = \text{Ni}, \text{Pd}$. Their predicted pentabromide was linear ($D_{\infty h}$) with $\text{Br}-\text{Br} 2.38 \text{ \AA}$ and $\text{Br}\dots\text{Br} 2.82 \text{ \AA}$.

Our observed Raman spectrum is in agreement with our determined structure which indicates an assemblage of ten bromine atoms as two tribromide ions and two dibromide molecules. There is no significant coupling between these sub-units resulting in Raman bands for penta- or decabromide, rather the loose arrangement found would be expected to give the weak but reproducible spectrum with bands between 50 and 200 cm^{-1} . While the bands at 54 and 67 cm^{-1} can probably be ascribed to lattice modes of vibration, the bands which are centred at 94, 144, 175 and 193 cm^{-1} are assigned to the decabromide anion.

The dibromide unit is considerably elongated at 2.74 \AA when compared with molecular dibromine (2.27 \AA) and a concomitant band shift is seen from *ca.* 310 cm^{-1} in Br_2^0 to 193 cm^{-1} in this structure. The Br_3^- unit is effectively symmetric with bond lengths of 2.91 and 2.94 \AA and gives rise to the bands observed at 175 and 144 cm^{-1} respectively for the ν_3 asymmetric and ν_1 symmetric stretching vibrations of tribromide. The band centred at 94 cm^{-1} is attributable to the bond deformation mode, ν_2 ,

9 Molecular dibromine has Raman bands centred at 316.8 cm^{-1} in the gas phase and 306.6 cm^{-1} in the liquid phase [15]; crystalline dibromine Raman bands have been measured at 310 cm^{-1} [12].

of the Br_3^- unit.

3-bromo-1,5-di-*para*-bromophenylformazan:

Crystal Structure: The protonation site in the formazan chain has not been located directly, however it is possible to write two tautomeric structures for the formazan. There is a mirror plane running through Br1 and C1, which means that the imino proton is necessarily disordered between N2 and N2' and that the formazan bond length will appear averaged. The calculated values are not especially accurate due to the

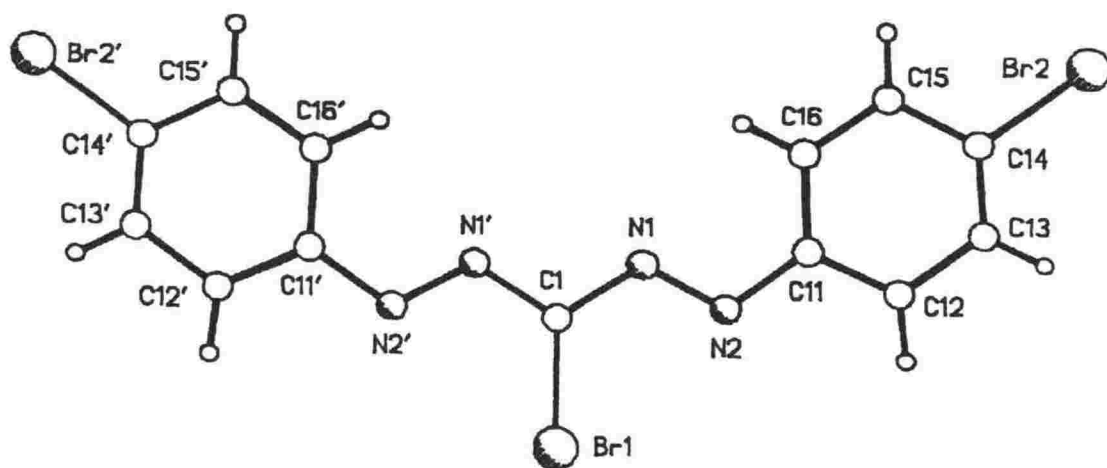


Figure 6: Molecular Structure and Atomic Nomenclature for 3-bromo-1,5-di-*para*-bromophenylformazan.

presence of the bromine atoms.

The formazan assumes the *anti,s-trans* configuration also seen for 3-chloro-1,5-diphenylformazan [29], other yellow/orange formazans [1,10,31,32] and dithizone [30]. The structural determination parallels that for dithizone in that the protonation site is not directly seen. Unlike dithizone and related structures [30] the formazan is not planar (the maximum deviations from the mean plane for atoms of the backbone are 0.57 Å for Br1 and 0.11 Å for N1). The N2-C(phenyl) bond lengths are 1.40 Å which represent bond orders of *ca.* 1.2 [13] indicating some degree of delocalisation between the N-N-C-N-N backbone and the phenyl rings. The C1-Br1 bond length of 1.86 Å is clearly a single bond; delocalisation does not extend to the 3-substituent. The accuracy of the bond lengths is not high with the result that accurate bond orders for C-N and N-N can not be deduced. However it is evident that there are no localised single or double bonds in the formazan backbone.

Preliminary investigations have revealed that the tribromoformazan is photochromic in solution as are several other formazans of the same configuration [29]. These results together with the structures of other halogen-formazans will be reported in a subsequent paper.

Acknowledgement.

One of the authors, CWC, is grateful to the Maori Education Foundation for the granting of a Queen Elizabeth II Post Graduate Scholarship during the research for this paper.

References.

- 1 Burns, G.R., Cunningham, C.W. and McKee, V., *J. Chem. Soc., Perkin Trans 2*, **1988**, 1275.
- 2 von Pechmann, H., *Chem. Ber.*, **29**, 2161 (1894).
- 3 Irving, H.M.N.H. and Ramakrishna, P.S., *J. Chem. Soc.*, **1972**, 1961.
- 4 Herbstein, F.H. and Schwotzer, *J. Chem. Soc., Perkin Trans 2*, **1984**, 1917.
- 5 Herbstein, F.H. and Schwotzer, *J. Am. Chem. Soc.*, **106**, 2367 (1984).
- 6 Irving, H.M.N.H., Gill, B. and Cross, W.R., *J. Chem. Soc.*, **1960**, 2087.
- 7 von Pechmann, H., *Chem. Ber.*, **25**, 3175 (1892).
- 8 Irving, H.M.N.H. and Bell, C.F., *J. Chem. Soc.*, **1953**, 3538.
- 9 Kushi, Y. and Fernando, Q., *J. Am. Chem. Soc.*, **92**, 1965 (1970).
- 10 O'melchenko, Yu. A., Kondrashev, Yu.D., Ginzburg, S.C. and Neigauz, M.G., *Kristallografiya*, **19**, 522 (1974); *Sov. Phys. Crystallogr.*, **19**, 323 (1974).
- 11 Wells, A.F., "Structural Inorganic Chemistry", 4th Edition, Clarendon Press, Oxford (1975), p336.
- 12 Evans, J.C. and Yo, G.Y-S., *Inorg. Chem.*, **6**(8), 1483 (1967).
- 13 Burke-Laing, M. and Laing, M., *Acta Crystallogr., Sect. B.*, **32**, 3216 (1976).
- 14 Weast, R.C. (Ed.), *Handbook of Chemistry and Physics*, 63rd Edition, CRC Florida, USA, pF183.
- 15 Gordy, W., *J. Chem. Phys.*, **14**, 305 (1946).
- 16 Kushi, Y. and Fernando, Q., *J. Am. Chem. Soc.*, **92**, 1965 (1970), and references therein.
- 17 Tebbe, K.F., "Homatmic Rings, Chains, Macromolecules of Main Group Elements," Rheingold, A.L. (Ed.), Elsevier Scientific (1972).
- 18 Wiebenga, E.H. and Kracht, D., *Inorg. Chem.*, **8**, 738, (1969).
- 19 Wolmershauser, G., Kruger, C. and Tsay, Y.-H., *Chem. Ber.*, **115**, 1126 (1982).
- 20 Robinson, W.T., Personal Communication.
- 21 Herbstein, F.H. and Kapon, M., *J. Chem. Soc., Chem. Commun.*, **1975**, 677.
- 22 Hecquet, B. and Landais, J., *C. R. Acad. Sc. Paris*, **274**, 1353 Series C (1972).
- 23 Kalina, D.W., Lyding, J.W., Ratajack, M.T., Kannewurf, C.R. and Marks, T.J., *J. Am. Chem. Soc.*, **102**, 7854 (1980).
- 24 Bondi, A., *J. Phys. Chem.*, **68**, 441 (1964).
- 25 Cowie, M.A., Gleizes, A., Grynkewich, G.W., Kalina, D.W., McClure, M.S., Scaringe, R.P., Teitelbaum, R.C., Ruby, S.C., Ibers, J.A., Kannewurf, C.R. and Marks, T.J., *J. Am. Chem. Soc.*, **101**, 2921 (1979).
- 26 Herbstein, F.H. and Kapon, M., *Acta Crystallogr., Sect. A*, **28**, S74 (1972).
- 27 Burns, G.R., Cunningham, C.W. and Renner, R.M., *Conf. Proceedings, International Conference on Raman Spectroscopy XI*, London, 1988.
- 28 Gabes, W. and Gerding, H., *Recl. Trav. Chim. Pays-Bas.*, **90**, 157 (1971). The band at 249 cm⁻¹ is split by small solid state effects.
- 29 Cunningham, C.W., Burns, G.R. and McKee, V., Paper in preparation.

- 30 Laing, M., *J. Chem. Soc., Perkin Trans*
2, 1248 (1977).
 - 31 Guillerez, J., Pascard, C. and Prange, T.,
J. Chem. Res., (S) 308; (M) 3934
(1978).
 - 32 Hutton, A.T., Irving, H.M.N.H. and
Nassimbemi, L.R., *Acta Crystallogr.*
Sect B, 36, 2071 (1980).
 - 33 Breneman, G.L. and Willett, R.D., *Acta*
Crystallogr., 23, 467 (1967).
-

3-Chloro-1,5-diphenylformazan and 3-iodo-1,5-diphenylformazan.

Introduction.

Very few studies on the 3-halogenated-1,5-diphenylformazans have been published in the literature. Lozinski and Pel'kis [34] have studied symmetrical and unsymmetrical 1,5-diaryl-3-chloroformazans and have transformed the 3-chloro derivatives into 3-amino, 3-morpholino and other substituents by treatment with nucleophiles. Foffani and Stuparich [35] have studied the ultra violet absorption spectra of formazans including the 3-chloro and 3-iodo derivatives. No comprehensive study of the structures or spectroscopy of the two formazans has appeared.

Properties.

The formazan (4) crystallises as small orange needles from ethanol. Dark red lustrous needles from benzene have been reported in the literature.

The formazan (5) crystallises as thin red needles from xylene or acetone.

Experimental.

Syntheses: (4) was prepared following the method of Irving and Bell [36].

Diethylmalonate (50 g) and sulphuryl chloride (45.6 g) were heated under reflux for 1 hour. Fractionation gave diethylchloromalonate (boiling point 113° C/10 mm Hg).

A solution of diethylchloromalonate (25 g) in ethanol (30 ml) was treated in the cold with potassium hydroxide (16.6 g) dissolved in ethanol (70 ml). Potassium chloromalonate rapidly separated in excellent yield as a white precipitate which was washed well with cold ethanol and dried *in vacuo*.

Potassium chloromalonate (22 g), water (100 ml) and sodium acetate (40 g) were treated at 0° C with a diazonium solution made from aniline hydrochloride (0.25 mol). The product precipitated in the fridge as a terracotta coloured solid. Recrystallisation from ethanol gave small orange needles in good yield. Melting Point: 147-149° C. (Lit.: 153-154° C).

(5) was prepared by the iodination of 3-chloro-1,5-diphenylformazan.

(4) was dissolved in methanol and several crystals of elemental iodine were added. After stirring at room temperature for two hours the solution had changed from orange to a dark brown/red. Deep red crystals separated from the solution in excellent yield. Melting Point: 140-142° C.

Deep red crystals were also obtained from the reaction of 3-chloro-1,5-diphenylformazan and NaI in warm acetone.

X-Ray Crystal Structures: The x-ray crystal structure of 3-chloro-1,5-diphenylformazan (4) has been determined in this study. Preliminary results are reported.

The molecular structure and atomic nomenclature for (4) are shown in Figure 9. Preliminary bond lengths and bond angles are listed in Table 9. The formazan assumes the *anti,s-trans* configuration characteristic of orange formazans. The molecule tends towards planarity although the attitude of the phenyl rings is slightly twisted. The N1-H1 proton has not been located directly. The formazan backbone shows some delocalisation of electrons and this extends into the phenyl rings.

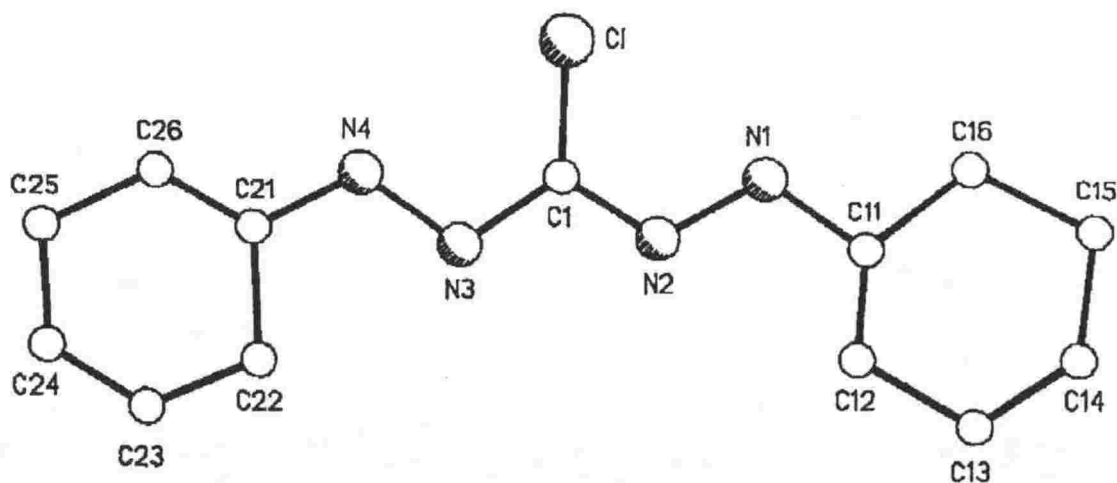


Figure 9: Molecular Structure and Atomic Nomenclature for 1-chloro-1,5-diphenylformazan (1).

Table 9: Bond Lengths (Å) and Bond Angles (°) for 3-chloro-1,5-diphenylformazan.

C1-Cl	1.567	N2-C1-Cl	120.9
C1-N2	1.324	N3-C1-Cl	126.3
C1-N3	1.415	N2-C1-N3	112.8
N1-N2	1.435	N1-N2-C11	114.0
N1-C11	1.415	N1-N2-C1	117.8
N2-C1	1.324	N4-N3-C1	109.3
N3-N4	1.402	N3-N4-C21	116.2
N4-C21	1.410		

The structure of this 3-chloro- derivative differs from the corresponding 3-bromo- derivative in that the phenyl rings are unsubstituted. They both, however, assume the same configuration. A description of the unit cell is given in Figure 10.

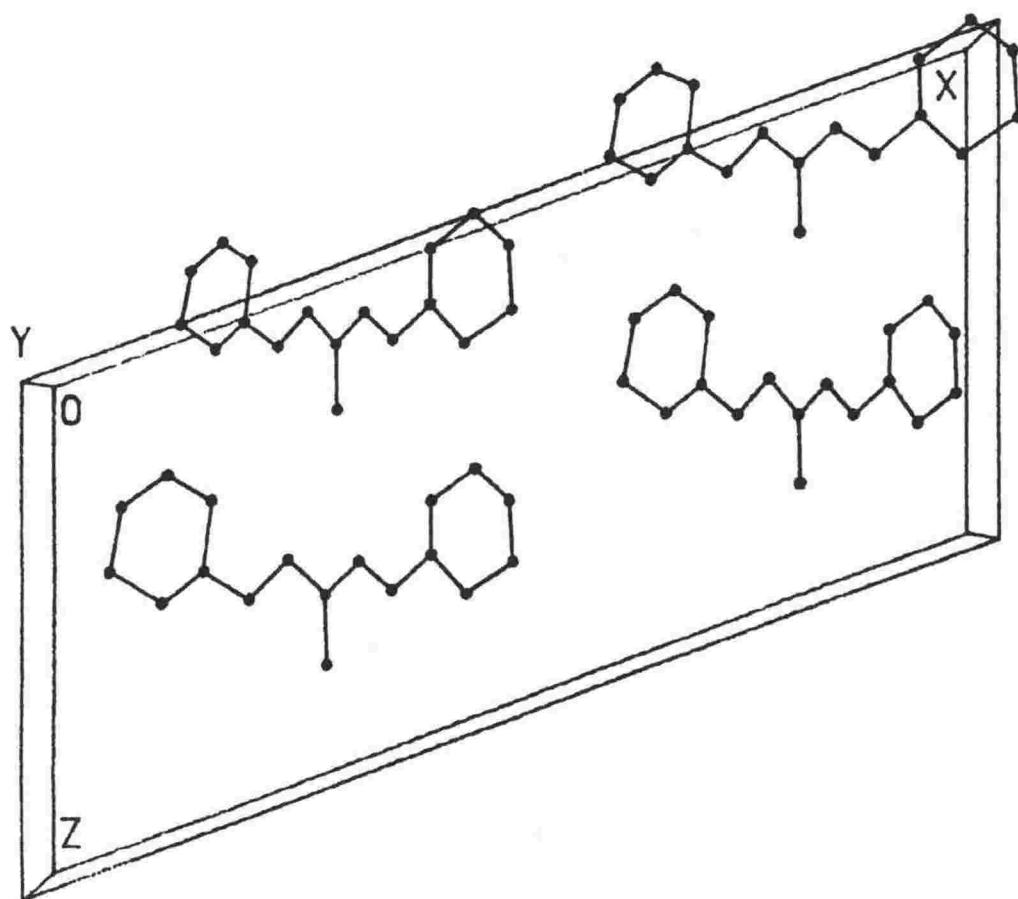


Figure 10: A Description of the Unit Cell for 3-chloro-1,5-diphenylformazan (1).

Further observations regarding the structure await the results of the full refinement [37].

References.

- | | | | |
|----|---|----|---|
| 34 | Lozinskii, M.O. and Pel'kis, P.S., <i>Zh. Obshch. Khim.</i> , 30 , 4002 (1960);
Lozinskii, M.O. and Pel'kis, P.S., <i>Zh. Obshch. Khim.</i> , 31 , 1621 (1961);
Lozinskii, M.O. and Pel'kis, P.S., <i>Zh. Obshch. Khim.</i> , 32 , 526 (1962);
Lozinskii, M.O. and Pel'kis, P.S., <i>Ukr. Khim. Zh.</i> , 29 , 414 (1963). | 35 | Foffani, A. and Stuparich, A., <i>Gazz. Chim. Ital.</i> , 83 , 508 (1953). |
| | | 36 | Irving, H.M.N.H. and Bell, C.F., <i>J. Chem. Soc.</i> , 1953 , 3538. |
| | | 37 | Cunningham, C.W., Burns, G.R. and McKee, V., Paper in Preparation. |
-

Chapter 3.5

3-Alkylthio-1,5-Diphenylformazans.

In this chapter the results of the study of the following five formazans will be given:

- | | |
|---|------|
| 3-mercapto-1,5-diphenylformazan, dithizone | (1) |
| 3-methylthio-1,5-diphenylformazan | (2) |
| 3-ethylthio-1,5-diphenylformazan, orange isomer | (3) |
| 3-ethylthio-1,5-diphenylformazan, red isomer | (4) |
| 3-isopropyl-1,5-diphenylformazan | (5). |

The chapter consists of the preparation and characterisation of the parent dithizone and its four derivatives.

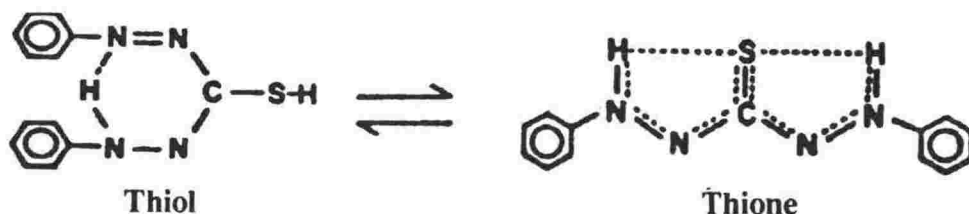
Introduction.

The black formazan (1) is commonly called dithizone (diphenylthiocarbazone) and has been formulated variously as:

NN'-diphenyl-*C*-mercaptoformazan;
NN'-diphenylformazylmercaptan;
 1,5-diphenylthiocarbazone;
 3-mercapto-1,5-diphenylformazan;
 and 1,5-diphenyl-3-thiolformazan.

The formazan is listed in the *Chemical Abstracts* under the systematic, if unfamiliar, pseudonym phenylazothioformic acid 2-phenylhydrazide.

The 3-mercapto- and thiol- formazan descriptions are largely



misleading as the formazan is now known to exist in the thione and not the thiol form in the solid state, nevertheless use of the names still persists.

Dithizone ((1) $R=H$) and the 3-alkylthiolated-1,5-diphenylformazans ((2)-(5) $R=CH_3, CH_2CH_3, CH(CH_3)_2$) (S-alkyl dithizones) (Figure 1) have been studied for many years.

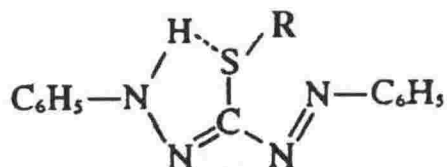


Figure 1: S-Alkyl-Dithizones.

3-alkylthio-1,5-diphenylformazans are known to exhibit colour changes in solution. The colour of a freshly prepared solution of (2) is permanganate pink. On standing in the dark or in diffused light at ambient temperatures, the colour slowly changes to yellow. This process is greatly accelerated on illumination with green light, but is reversed with light of shorter wavelength. Solutions of (5) also exhibit a colour change

upon standing, however in this case the change is opposite to that observed for (2): a fresh solution is yellow and gradually changes to brown.

It is generally accepted that these colour changes are due to thermal and photochemical isomerisations.

Ignoring isomers which are unlikely to occur due to serious steric crowding there are eight probable configurations in the 3-alkylthio-system

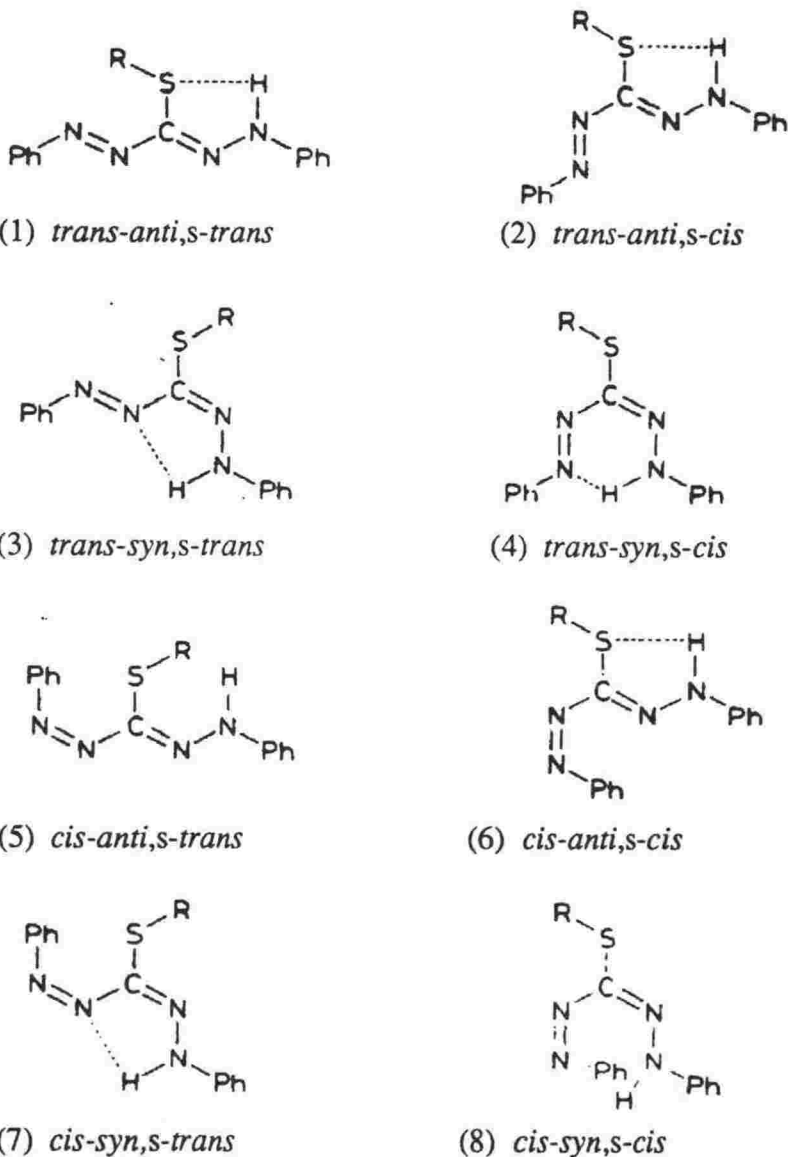


Figure 2: The Eight Principal Configurations of 3-thioalkylated-1,5-diphenylformazans.

due to *cis/trans* and *anti/syn* isomerisation around the C=N and N=N double bonds and isomerisation about the C-N single bond designated *s-cis/s-trans* (Figure 2 (1)-(8)).

Properties.

The formazan (1) crystallises as violet/black needles with a metallic reflex from chloroform solution and is a well known reagent in analytical chemistry [1]. It forms stable complexes with many metals and the crystal structures of several have been reported [2-8]. All show that the bonding to the metal involves the sulphur atom and a nitrogen atom adjacent to a phenyl group.

The formazan (2) crystallises as deep crimson red crystals by the slow evaporation of *n*-hexane solution [9,10]. In solution an equilibrium between violet and yellow forms is displayed and many authors have speculated on the structures of these forms and the mechanism of interconversion.

3-ethylthio-1,5-diphenylformazan may be crystallised in two forms closely paralleling the behaviour of 3-ethyl-1,5-diphenylformazan. (3) is given as orange needles from ethanol and (4) is given as red needles from *n*-hexane, both in excellent yield.

The formazan (5) crystallises as deep red crystals from acetonitrile. Investigations of the configuration of (5) in solution have shown that the equilibrium lies largely in favour of the yellow form.

Experimental.

Syntheses: (1) is available commercially as diphenylthiocarbazone. Solid dithizone keeps well provided it is protected from the effects of air, heat and light. Finely powdered dithizone decomposes more quickly to form phenylthiosemicarbazide and aniline [1]. As the purity of commercial samples was found by Irving to range from "94 - 37.6 %" [1] the formazan requires purification before use.

Dithizone may be purified as follows: A concentrated solution in carbon tetrachloride was filtered through a medium porosity sintered glass funnel and extracted into *ca.* 2 molar ammonia solution. After extracting the aqueous phase with several portions of CCl_4 (which are rejected) it was acidified with sulphuric acid and the purified dithizone was collected and dried *in vacuo*. Recrystallisation from acetone resulted in fine black needles.

(2) was prepared following the method of Neugebauer and Fischer [9]. A solution of dithizone (3.0 g), triethylamine (5.0 ml) and methyl iodide (3 ml) in methanol (20 ml) was mixed and left to stand at room temperature for several hours. The precipitate which formed was recrystallised from cyclohexane to give black/brown crystals. Melting Point: 122-123° C.

(3) and (4) were prepared following the method above. A solution of dithizone (2.6 g), triethylamine (1.2 g) and ethyliodide (1.0 g) in

methanol (20 ml) was heated under reflux for 30 minutes, cooled and precipitated by the addition of water. The crude product was recrystallised from *n*-hexane to give red needles and from methanol to form orange needles, both in excellent yield.

(5) was prepared following the method of Neugebauer and Fischer [9]. A solution of dithizone (2.6 g), triethylamine (1.2 g) and 2-iodopropane was heated under reflux for 30 minutes, cooled and precipitated by the addition of water. The crude product was recrystallised from ethanol to give red needles. Melting Point: 128-129° C.

Nuclear Magnetic Resonance Spectra: Solid state ^{13}C nmr spectra were recorded at 50.3 MHz with a Varian Associates XL-200 spectrometer using a standard CP/MAS probe. Powdered samples (*ca.* 300 mg) were packed in Kel-F rotors and spun using MAS frequencies between 2 and 3 kHz for (1) and at 10 kHz for (2). The combined techniques of high power proton decoupling and single contact cross polarisation (CP) were employed. Typical contact times of 50 ms were used, with recycle delays of 1.2 s. The number of transients acquired was of the order of 1000.

^{13}C nmr solution spectra were recorded at 20.00 MHz with a Varian Associates FT-80A spectrometer employing proton decoupling. In all cases either deuterated solvents or D_2O capillary tubes provided the spin lock. Typical spectral parameters employed were: spectral width 5000 Hz, acquisition time 1.023 s, pulse width 4 μs . Samples of *ca.* 200 mg were used in 5 mm o.d. tubes with tetramethylsilane as the internal standard. Precautions were taken to protect the spectroscopic solutions from the effect of light.

Vibrational Spectra: Raman spectra were recorded using a Spex 1401 spectrometer equipped with a Thorn EMI 6256 photomultiplier tube used in the photon counting mode. A Spectra-Physics 164-01 Krypton Ion laser was used as the Raman scattering source, operating at a wavelength of 647 nm. Band wavenumbers were calibrated using the emission spectrum of neon and typical slit widths of 200 μm were employed, giving a bandpass of 2 cm^{-1} at 647 nm. Samples were studied as crystals or in capillary tubes. Pressed discs diluted in potassium bromide were also used effectively to eliminate fluorescence. Spectra were recorded at room temperature using laser powers of less than 50 mW at the sample to avoid photo-decomposition.

Electronic Absorption Spectra: Ultra violet-visible spectra were recorded with a Shimadzu Model 160 ultra violet-visible spectrophotometer. Solvents were either spectroscopic grade or purified by standard methods.

Analyses: Microanalyses were performed by Professor A.D. Campbell and Dr R.G. Cunninghame and associates of the University of Otago.

Results and Discussion.

X-Ray Crystal Structures: The crystal structures of three of the

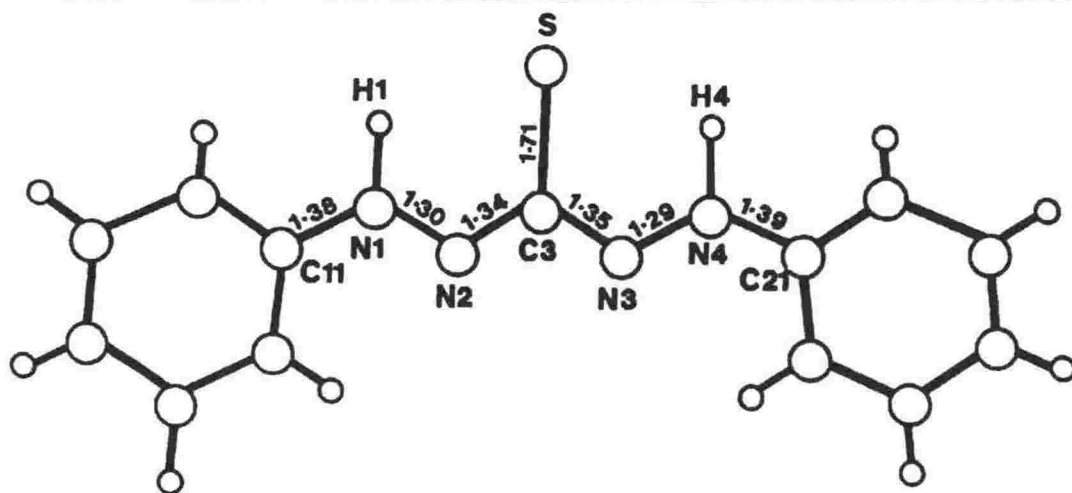


Figure 3: The X-ray Crystal Structure of Dithizone (1) as shown by Laing. [12]

formazans have been solved by other authors and are briefly described below.

The x-ray crystal structure of (1) has been determined twice, initially by Alsop in his Ph.D. thesis [11] and subsequently by Laing [12]. The initial work was of a lower precision than was desirable - crystals of (1) are very thin laths susceptible to twinning. The crystal chosen by Alsop was twinned so that the β -angle could not be determined properly. He showed that the molecule was approximately planar with an extended formazan chain. He concluded that conjugation extended into the phenyl rings. Laing subsequently chanced upon a good crystal and managed to accurately determine the structure.

$C_{13}H_{12}N_4S$ crystallises in the monoclinic space group $P21/n$, $a=4.70(1)$, $b=22.25(3)$, $c=11.95(2)$ Å, $\beta=98.03^\circ$, $V=1238$ Å³, $Z=4$. The formazan adopts the *anti,s-trans* configuration in the solid state. A description of (1) is given in Figure 3. The molecule is near planar of approximately C_{2v} symmetry with the N-N-C-N-N chain extended and the C-S bond lying on the intersection of the mirror planes. Two unique H atoms are bonded to N1 and N4, however there are no intermolecular hydrogen bonds. The formulation of alternating charge distribution along the dithizone backbone results in four relatively strong electrostatic interactions between the four nitrogen atoms in adjacent molecules (N...N) and two other interactions between (C(phenyl)...N) in adjacent molecules. It is evident that the π -electrons in the N-N-C-N-N chain are delocalised. The π -electrons on nitrogen in a C-N chain are delocalised if this atom is involved in 3 σ -bonds (especially if one is to hydrogen) [12].

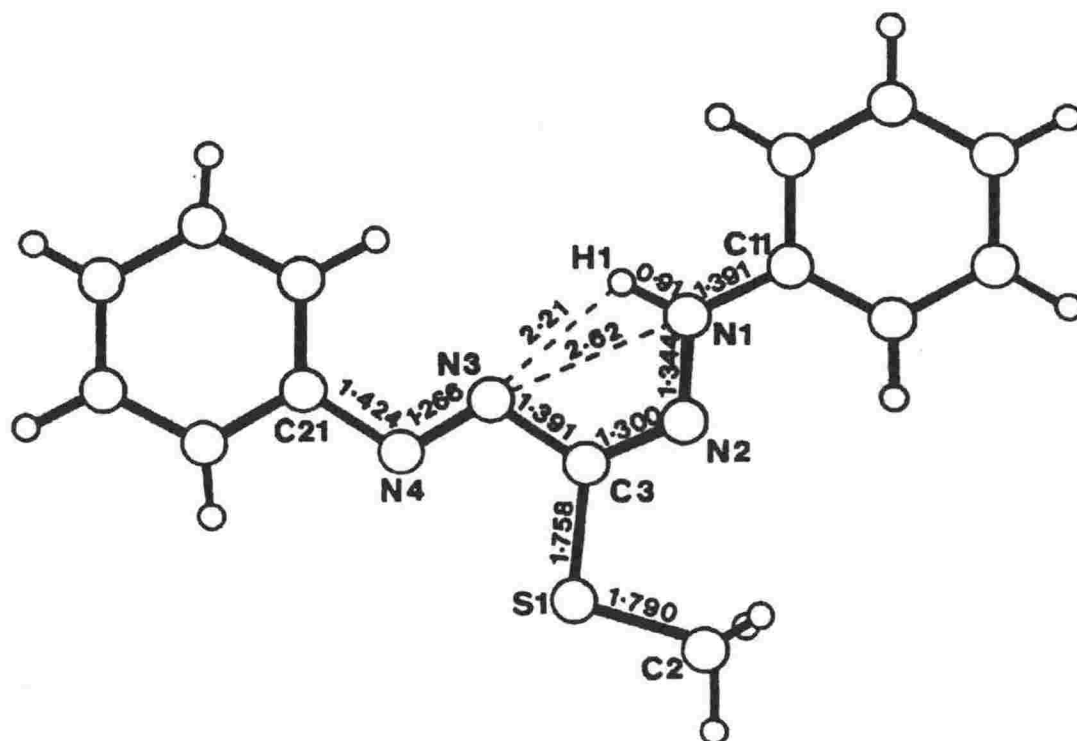


Figure 4: The X-ray Crystal Structure of 3-methylthio-1,5-diphenylformazan (2) as shown by Preuss and Gieren. [13]

The crystal structure of (2) has been determined by Preuss and Gieren in 1975 [10]. $C_{14}H_{14}N_4S$ crystallises in the orthorhombic space group $P2_12_12_1$, $a=25.48(0)$, $b=10.01(4)$, $c=5.33(4)$, $Z = 4$. The formazan assumes the *syn,s-trans* configuration in the solid state. The molecule is essentially planar and there is a significant intramolecular hydrogen bond between H1 and N3. There is considerable delocalisation of electrons along the formazan backbone. A description of the molecule is given in Figure 4.

The crystal structure of (3) has been determined by us in this study. Preliminary results are reported. An orange prism with dimensions 0.12 x 0.25 x 0.10 mm was used. $C_{15}H_{16}N_4S$ belongs to the monoclinic space group $P2_1/a$, $a = 11.027(6)$, $b = 8.627(7)$, $c = 15.487(8)$ Å, $\beta = 93.70(5)^\circ$, $U = 1470$ Å³, $Z = 4$. Intensity data were collected at -100° C with a Nicolet R3m four-circle diffractometer using graphite monochromated Mo-K α radiation. 1.8° ω -scans at a scan rate of 5.9° min⁻¹, and a background to scan ratio of 0.1, 2189 reflections were collected for $4 < 2\theta < 45^\circ$. Of these reflections, 811 having $I > 3\sigma(I)$ were ultimately used for the structure determination.

Cell parameters were determined by least-squares refinement of 25

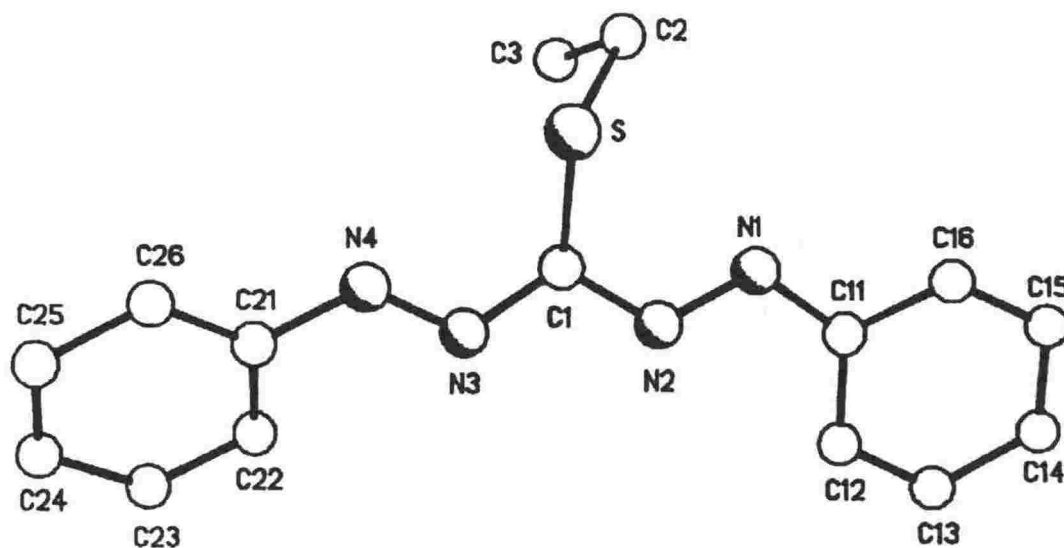


Figure 5: Molecular Structure and Atomic Nomenclature for the Orange Isomer of 3-ethylthio-1,5-diphenylformazan (3).

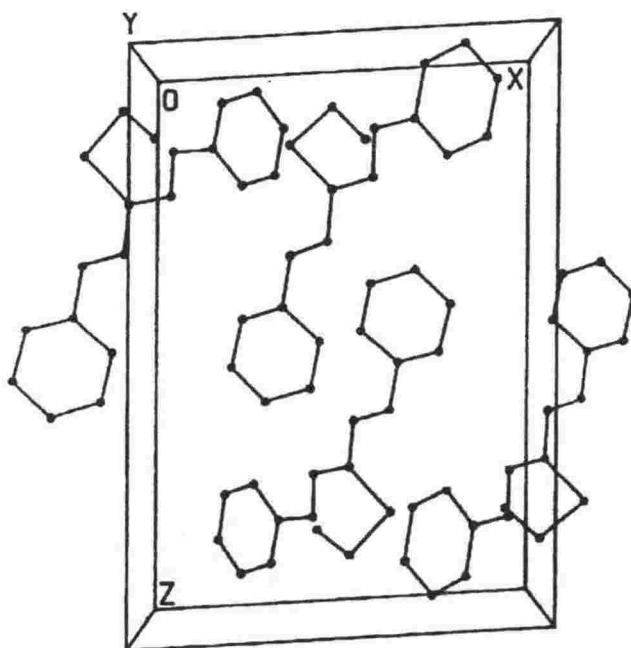


Figure 6: A Description of the Unit Cell for the Orange Isomer of 3-ethylthio-1,5-diphenylformazan.

**Table 1: Bond Lengths (Å) and Bond Angles (°)
for the Orange Isomer of
3-ethylthio-1,5-diphenylformazan.**

C1-S1	1.760	N2-C1-S1	123.7
C1-N2	1.437	N3-C1-S1	125.2
C1-N3	1.360	N3-C1-N2	110.5
S1-C2	1.860	C1-S1-C2	100.5
C2-C3	1.501	C3-C2-S1	111.3
N1-N2	1.296	C11-N1-N2	108.7
N3-N4	1.344	C1-N1-N2	111.6
N4-C21	1.425	C1-N3-N4	114.8
N1-C11	1.418	C21-N3-N4	121.6

monitored by recording 3 check reflections every 100 reflections and no significant variations were observed. The data set was corrected for Lorentz and polarisation effects but no absorption corrections were applied.

The structure was solved by direct methods, using the program SOLV, and refined by blocked-cascade least squares methods, revealing the positions of all the non-hydrogen atoms. Hydrogen atoms were inserted at calculated positions using a riding model with a common thermal parameter. Anisotropic thermal parameters were assigned to all the non-hydrogen atoms, except the phenyl ring carbon atoms, and the refinement of (3) converged with $R = 0.0562$ and $R' = 0.0567$. The function minimised in the refinement was $\sum w(|F_o| - |F_c|)^2$ where $w = [\sigma(F_o) + gF_o]$ and $g = 0.000295$. Final difference maps showed no features greater than ± 0.3 electron Å⁻³.

All programs used for data collection and structure solution are contained in the SHELXTL (Version 4) package.

The molecular structure and atomic nomenclature for (3) are shown in Figure 5. The formazan assumes the *anti,s-trans* configuration characteristic of orange formazans. The molecule tends towards planarity and there is considerable delocalisation of electrons along the formazan backbone and into the phenyl rings. A description of the unit cell is given in Figure 6. Further observations regarding the structure await the full refinement.

The crystal structure of (4) remains as yet undetermined.

The x-ray crystal structure of (5) has been determined by Guillerez *et al.* [13]. C₁₆H₁₈N₄S crystallises in the orthorhombic space group *Pca*2₁, $a = 19.782(4)$, $b = 17.321$, $c = 9.325$, $Z = 2$. The formazan adopts the *anti,s-trans* configuration in the solid state and is shown in Figure 7. The whole molecule has an essentially flat attitude. There is a short intramolecular N-H...S hydrogen bond indicating a firmly stabilised five membered ring.

There is considerable delocalisation of electrons along the formazan backbone and the bond lengths closely parallel those in 3-methylthio-1,5-diphenylformazan, with the exception that the N-H bond length of 0.91 Å in the latter is extended to 0.97 or 0.99 Å in (5).

The x-ray crystal structures which have been solved again demonstrate that the formazans have many features in common. The molecules are almost entirely planar, there exist either significant inter- or intra-molecular hydrogen bonds, there is a large degree of delocalisation of

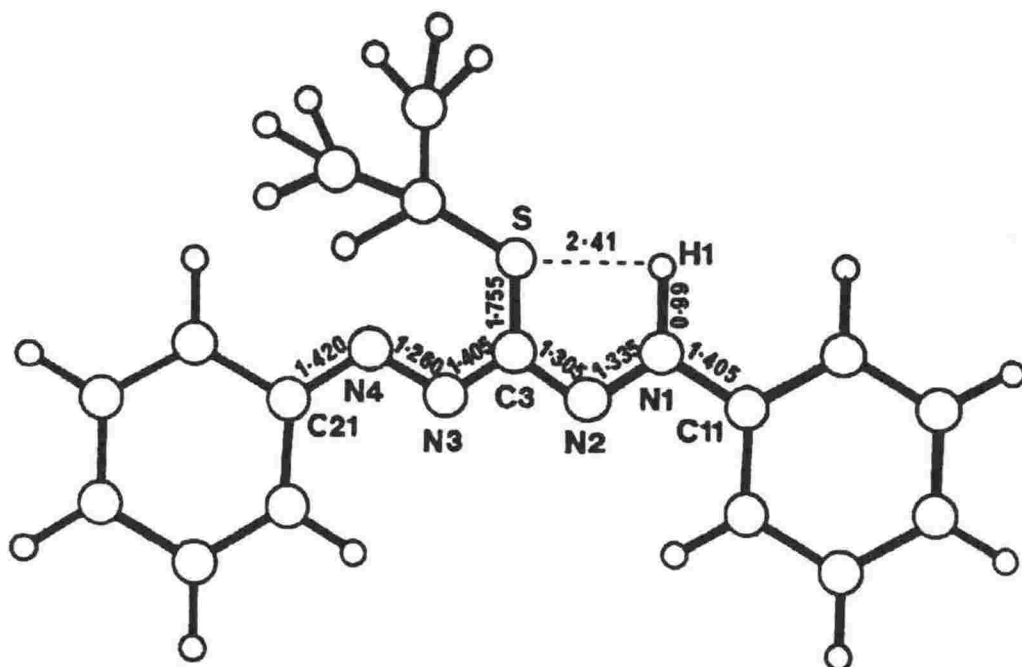


Figure 7: The X-ray Crystal Structure of 3-isopropyl-1,5-diphenylformazan (5) as shown by Guillerez *et al.* [14]

electrons along the formazan backbone and into the phenyl rings but not into the 3-substituent and the phenyl rings are "normal" in respect of their bond lengths and bond angles.

Raman Spectra: The wavenumbers for the Raman active phonons of the formazans (1)-(5) are listed in Table 2.

The Raman spectrum of (1) has been determined many times and our spectrum is in excellent agreement. Pemberton and Buck [14] have shown that significant differences are apparent in the Raman spectra of neutral dithizone (H_2Dz) as well as the conjugate acid (H_3Dz)⁺ and the corresponding anion (HDz)⁻. Their results also conclude that the solution species is the *anti,s-trans* thione isomer established in the solid state. The Raman spectra for (2)-(5) have been recorded recently by Takahashi *et al.* [15]. Our spectra are also in excellent agreement with those published.

**Table 2: Raman Bands (cm⁻¹) for
3-Alkylthio-1,5-Diphenylformazans.**

-SH	-SCH ₃	-SCH ₂ CH ₃ Orange	-SCH ₂ CH ₃ Red	-SCH(CH ₃) ₂
1592	1600	1600	1603	1601
	1597		1598	
1522	1528	1520	1527	1520
		1505	1505	1500
1459	1461	1474	1460	1458
		1433		
1382	1383	1376	1390	1389
1305	1310	1300	1310	1309
1252	1264	1265	1263	1254
1234		1214		1212
1220				
1184	1188	1172	1185	1175
1164	1155		1154	1155
1146	1146	1138	1146	1131
	1108		1115	
1021				
1001	1004	998	1000	999

The Raman spectra show that the configurationally sensitive bands apparent in other 1,5-diphenylformazans also occur in 3-alkylthio-1,5-diphenylformazans. For (1) the Raman spectrum compares favorably with that for 1,5-diphenylformazan whose structure is similar. In both formazans the C-N bond lengths are comparable (1.35 and 1.34 Å for (1) and 1.35 and 1.31 Å for 1,5-diphenylformazan) resulting in the observation of the most intense band in the spectra at 1382 and 1379 cm⁻¹ respectively. This band has previously been assigned to a vibration of the N-C=N group. While we cannot counter this exact assignment it is certain that the vibrations of the formazan backbone are intimately coupled and so it is more appropriate to assign the band as a coupled vibration involving the N-C=N group as well as the N-N and N=N function to an extent. The position of the band is at the lower-most extreme seen for *anti,s-trans* formazans and while the C3 sulphur substituent and intramolecular N-H...S hydrogen bond can be held to account for this, the similarity in the azomethine bond lengths with 1,5-diphenylformazan as described above would appear to be the over-riding factor. The bands at 1592 and 1001 cm⁻¹ are assigned to vibrations of the phenyl rings. These bands are relatively sharp and intense which is characteristic of the symmetric *anti,s-*

trans configuration.

For (2) the most intense band occurs at 1383 cm^{-1} . This band has been shown to move to 1408 cm^{-1} for the yellow isomer in solution. The position of this band compares favorably with other red *syn,s-trans* formazans. The asymmetric *syn,s-trans* configuration is reflected in the relatively weak and broad phenyl group vibrational bands which occur at *ca.* 1603 , 1597 and 1004 cm^{-1} .

For (3) the most intense band occurs at 1376 cm^{-1} while in (4) the same band is seen at 1391 cm^{-1} . These shifts must be as a result of different configurations for the orange and red isomers, but they are the reverse of that previously seen for the red/orange isomerisation in 3-ethyl-1,5-diphenylformazan. The intramolecular N-H...S hydrogen bond must be held to account for the observation of this peak at a lower wavenumber than expected in the spectrum of (3). Again the phenyl group resonances reflect the respective configurations. The phenyl bands in the spectrum of the red isomer are broader and less intense at 1603 , 1598 and 1000 cm^{-1} than the corresponding bands of the orange isomer at 1600 and 998 cm^{-1} . This is in keeping with our proposal of the *syn,s-trans* configuration for the red isomer.

For (5) the most intense band occurs at 1389 cm^{-1} . This band also occurs at a lower wavenumber than expected due to the effects of the sulphur substituent at C3 and the intramolecular hydrogen bond. The phenyl group bands are relatively intense at *ca.* 1601 and 999 cm^{-1} . These observations are in keeping with the established *anti,s-trans* configuration.

The Raman spectra show the most intense peak observable due to coupled vibrations of the formazan backbone occur at slightly lower wavenumber than has been observed for 3-alkyl substituted 1,5-diphenylformazans. The change in the position of this band seen for different configurations is moderately subtle, although the 15 cm^{-1} difference seen between the two 3-ethylthio- isomers, (3) and (4), is a little greater than the corresponding difference seen for the two 3-ethyl-1,5-diphenylformazan isomers (1411 and 1408 cm^{-1}).

All of the formazans (1) - (5) are intramolecularly hydrogen bonded. The phenyl group resonances are seen to accurately reflect the configurations of the formazans.

Table 3: Resonances for the Solid state ^{13}C MAS Nmr Spectra of the 3-Alkylthio-1,5-diphenylformazans.

Substituent	C3	C11	C21	C-phenyl	C3-subst.
-SH	170.0	140.3		129.0 124.2 119.3	
-SCH ₃	151.3	147.3	143.8	133.7 130.2 126.3 120.3 115.4 111.5	14.4
-SCH ₂ CH ₃ orange	153.0	144.8		129.8 122.7 116.0	28.1 15.4
-SCH ₂ CH ₃ red	151.4	146.5	144.4	136.0 131.7 126.3 120.7 115.2 111.5	24.9 13.3
-SCH(CH ₃) ₂	153.3	147.4	142.6	130.8 124.5 116.8 113.9	38.7 24.8 22.2

Nuclear Magnetic Resonance Spectra: The resonances for the solid state ^{13}C MAS nmr spectra for the five formazans are listed in Table 3. Assignments in the solid state are based on the use of short contact times to identify quaternary carbon signals, TOSS experiments, and multiple and fast spinner speeds to remove the influence of spinning sidebands.

In the solid state signals are observed for quaternary carbon, phenyl carbon and alkyl carbon.

The spectrum for (1) is shown in Figure 8. It can be seen that only

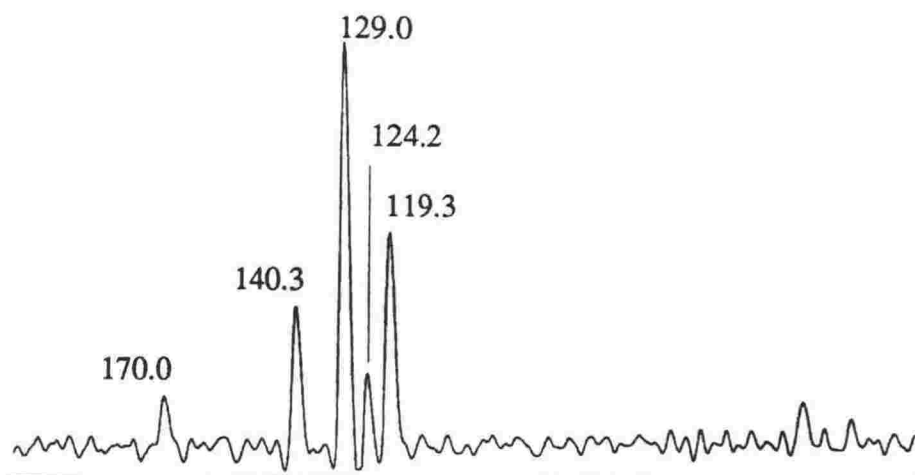


Figure 8: The Solid State ^{13}C MAS Nmr Spectrum for Dithizone.

one signal is observed for the C11 and C21 carbon nuclei coincident at 140.3 ppm. This confirms the equivalence of these carbon atoms implicit in the totally symmetric *anti,s-trans* configuration structurally identified for (1). The C3-S signal is at a relatively high 170.0 ppm. This is characteristic of C=S bonds in general [16]. The phenyl carbon resonances also reflect the exact equivalence of the 1- and 5- phenyl rings implicit in the structure.

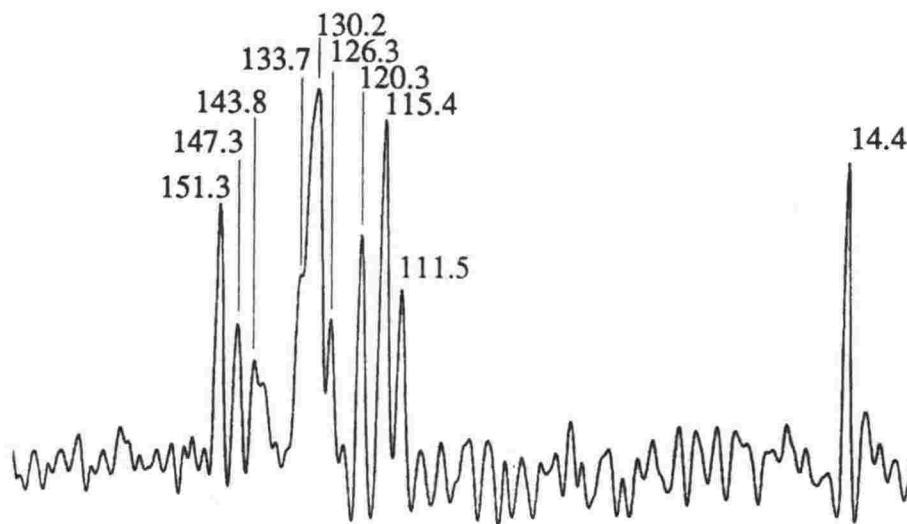


Figure 9: The Solid State ^{13}C MAS Nmr Spectrum for 3-methylthio-1,5-diphenylformazan (2).

The spectrum for (2) is shown in Figure 9. It can be seen that two signals are observed for the quaternary phenyl carbon atoms at 147.3 and 143.8 ppm for C11 and C21 respectively. This is characteristic of the

syn,s-cis configuration. The C3 resonance is observed at 151.3 ppm. Six phenyl carbon resonances are observed between 133.7 and 111.5 ppm. Only one substituent carbon signal is seen for the methyl group at 14.4 ppm. This confirms that there is only one configuration present.

The spectrum for (3) is shown in Figure 10.

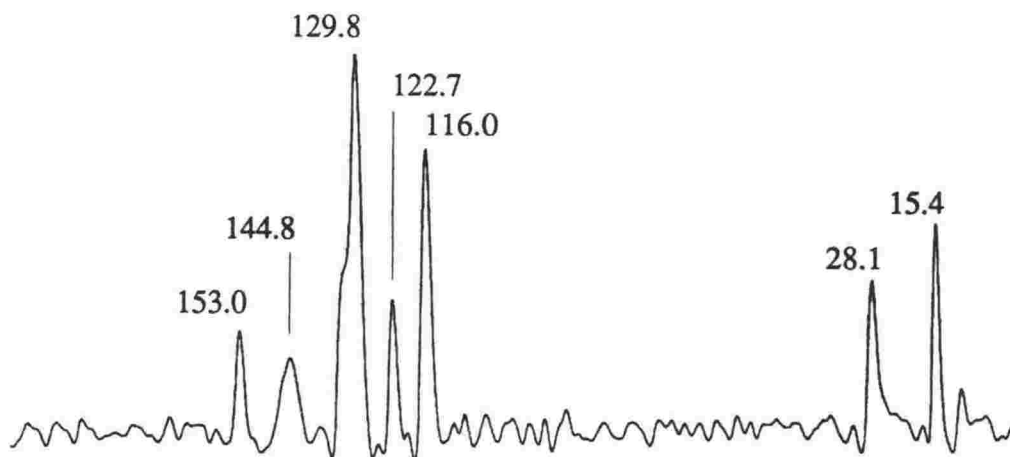


Figure 10: The Solid State ^{13}C MAS Nmr Spectrum of orange 3-ethylthio-1,5-diphenylformazan (3).

Only one signal is observed for the C11 and C21 carbon atoms coincident at 144.8 ppm. The C3 signal occurs at 153.0 ppm and the phenyl carbon resonances occur at 129.8, 122.7 and 116.0 ppm. These signals confirm the symmetric *anti,s-trans* configuration. Two substituent carbon resonances are observed at 28.1 and 15.4 ppm for the ethyl substituent.

The spectrum for (4) differs significantly from the spectrum of (3) and this is shown in Figure 11.

Two quaternary phenyl resonances are observed at 146.5 and 144.4

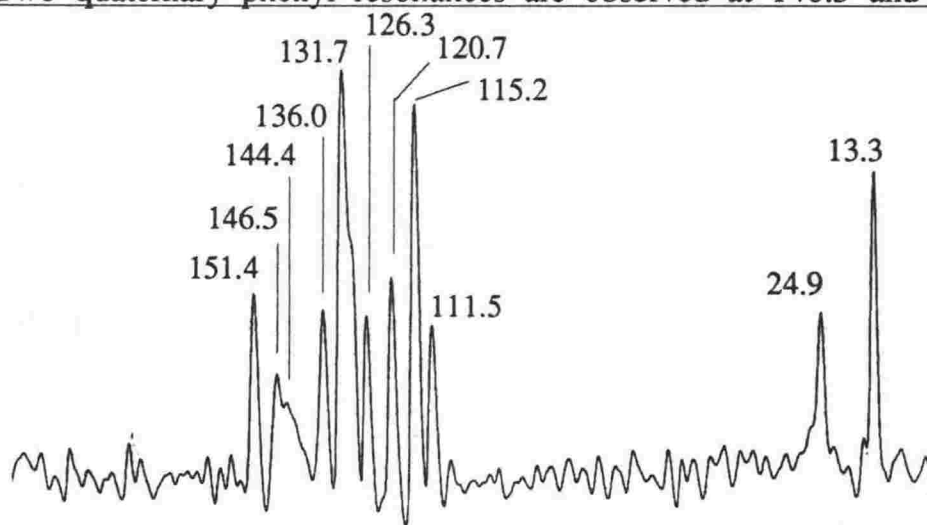


Figure 11: The Solid State ^{13}C MAS Nmr Spectrum of red 3-ethylthio-1,5-diphenylformazan (4).

ppm respectively for C11 and C21. The C3 signal is observed at 151.4 ppm. This is some 1.5 ppm lower than the corresponding resonance in (3) and may reflect an increased C=N bond length. Six phenyl carbon signals are observed between 136.0 and 111.5 ppm, indicating the non-equivalence of the two phenyl rings and therefore indicating the *syn,s-trans* configuration. Two substituent carbon signals are seen at 24.9 and 13.3 ppm. These are both slightly lower than the equivalent resonances in (3).

The spectrum for (5) is shown in Figure 12.

Two quaternary phenyl resonances are observed at 147.4 and 142.6 ppm. This is unusual for a formazan in the *anti,s-trans* configuration.

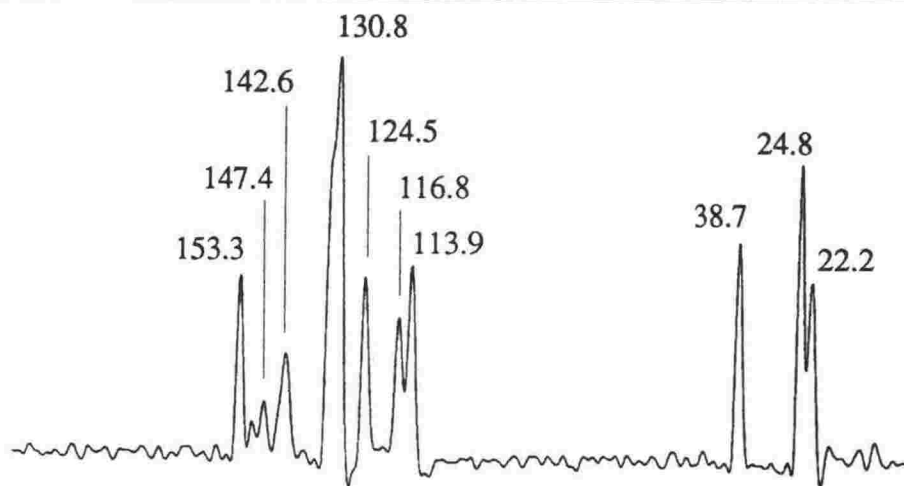


Figure 12: The Solid State ^{13}C MAS Nmr Spectrum of 3-isopropylthio-1,5-diphenylformazan (5).

However, in this case the effect of the intramolecular N-H...S hydrogen bond and the large isopropyl substituent is to cause the phenyl rings to be in significantly different chemical environments. The C3 resonance occurs at 153.3 ppm. The phenyl carbon signals occur at 130.8, 124.5, 116.8 and 113.9 ppm. This pattern of resonances indicates that the phenyl groups are in only slightly different environments. Three substituent carbon signals are observed for the isopropyl substituent, as the CH_3 groups are split by the CH function.

Resonances for the formazans (1) - (5) in various solvents are listed in Tables 4-7. Assignments in solution have been made on the basis of DEPT pulse sequences to identify quaternary, tertiary, and secondary carbon.

The spectrum for (1) in CDCl_3 shows a resonance for the C3 carbon at 171.38 ppm, only one signal coincident at 139.59 ppm for the C11 and C21 quaternary phenyl carbons and three phenyl carbon signals at 130.00, 128.73 and 118.97 ppm. These signals are consistent with the formazan assuming the *anti,s-trans* thione structure in solution paralleling the observation of this configuration in the solid state. The solution spectrum is almost identical to the solid state spectrum.

Table 4: Resonances (δ ppm) for the Solution ^{13}C Nmr Spectra of 3-mercapto-1,5-diphenylformazan (1).

Solvent	C3	C11	C21	C-phenyl
CDCl_3	171.38		139.59	130.00 128.73 118.97

The spectra for (2) have been recorded in three solvents. The resonances for the methyl substituent provides a means of establishing the

Table 5: Resonances (δ ppm) for the Solution ^{13}C Nmr Spectra of 3-methylthio-1,5-diphenylformazan (2).

Solvent	C(3)	C(11)	C(21)	C-phenyl	C(subst.)
CDCl ₃	152.50	147.96 147.00 143.13	130.69	130.10	15.75
			129.48	129.31	13.33
			129.02	126.73	
			123.01	118.44	
			114.90		
(CD ₃) ₂ CO	153.29	149.09 146.95 143.73	131.45	131.23	15.77
			130.17	130.12	13.24
			127.40	127.36	
			123.39	119.34	
			115.65		
C ₆ D ₆	153.13	148.29 142.66	130.78	129.68	15.30
			129.44	129.36	13.12
			126.75	123.37	
			123.01	118.74	
			114.96		

solvent dependence of the any equilibrium. Two signals are observed for the methyl group in all of the solvents studied. In CDCl_3 the C3 resonance occurs at 152.50 ppm, the quaternary carbon signals at 147.96, 147.00 and 142.13 ppm, nine phenyl resonances between 130 and 114 ppm and two methyl resonances, one for each isomer present, at 15.75 and 13.33 ppm respectively. These signals indicate an equilibrium

Table 6: Resonances (δ ppm) for the Solution ^{13}C Nmr Spectra of 3-ethylthio-1,5-diphenylformazan (3,4).

Solvent	C3	C11	C21	C-phenyl	C-subst.
CDCl_3	152.30		147.74	130.75 129.51	27.45
			146.17	129.34 129.03	15.75
			141.84	126.73 123.02	
				118.38 114.82	
C_6D_6	153.05		148.24	130.73 129.65	27.38
			146.51	129.41 129.32	24.47
			142.58	126.71 123.30	15.68
				122.98 118.98	14.53
				114.95	
$(\text{CD}_3)_2\text{CO}$	153.28		149.06	131.39 130.13	27.55
			146.31	130.08 127.31	24.61
			143.60	123.41 123.35	15.83
				119.25 115.62	14.80

involving two species, the *syn,s-trans* of the solid state and a symmetric yellow formazan - clearly the *anti,s-trans* configuration. Such a combination of isomers would result in the three quaternary carbon signals and nine phenyl carbon signals seen. In all the solvents studied the ratio of the two isomers, as evidenced by the relative intensities of the methyl signals, is almost equal.

For (3) and (4) the spectra in solution are identical for each isomer in the respective solvents if they are allowed to equilibrate in the dark. The ethyl signals provide a means of establishing the solvent dependence of the equilibrium between the two isomers. In all of the CDCl_3 , C_6D_6 and $(\text{CD}_3)_2\text{CO}$ solutions one signal assigned to the C3 carbon is observed; three signals attributable to quaternary phenyl carbon, nine phenyl carbon signals and four ethyl substituent signals are also seen. These observations are in keeping with an equilibrium involving two configurations - the *anti,s-trans* of the orange isomer and the *syn,s-trans* of the red isomer. The hexadeuteroacetone solution would appear to favour the orange formazan in the equilibrium and the deuteriochloroform and deuterobenzene solutions would seem to favour the red formazan. This is in keeping with the results of the absorption spectra.

For (5), a clear solvent dependence is indicated from the solution nmr spectra. The formazan adopts the *anti,s-trans* configuration in hexadeuteroacetone as evidenced by the single quaternary carbon signal coincident at *ca.* 147 ppm and the simple, three peak phenyl multiplet between 130 and 119 ppm. Two signals are observed for the *isopropyl*

Table 7: Resonances (δ ppm) for the Solution ^{13}C Nmr Spectra of 3-isopropylthio-1,5-diphenylformazan (5).

Solvent	C3	C11	C21	C-phenyl	C-subst.
CDCl_3	152.31	147.73 141.82	130.65 129.45 129.30 128.98 126.68 122.98 122.93 118.34 114.79	38.39 23.86	
C_6D_6	153.20	148.32 147.01 142.61	130.72 129.39 129.46 129.34 126.73 123.38 122.98 118.69 114.97	38.26 34.87 23.82 23.30	
$(\text{CD}_3)_2\text{CO}$	152.51	147.05	130.15 127.38 119.32	38.40 23.86	

substituent at *ca.* 38 and 24 ppm, which indicate that the two methyl groups are now equivalent contrasting the observation of a splitting in the solid state. In CDCl_3 there would also appear to be largely one configuration present, and from the positions of the *isopropyl* group resonances it would again seem to be the *anti,s-trans* configuration. However, the phenyl groups would now not seem to be equivalent as evidenced by two quaternary carbon signals and nine phenyl group signals. This apparent contradiction between the deuterochloroform and the hexadeuteroacetone spectra may be explained if the intramolecular N-H...S hydrogen bond is in competition with a hydrogen bond to the solvent available only in "protic" solvents with an effect on tautomerism in solution. The equivalence implicit in a compound tautomerising rapidly in solution must be brought into question in chloroform solution therefore.

Further evidence for the existence and characterisation of the solution equilibria come from the electronic absorption spectra.

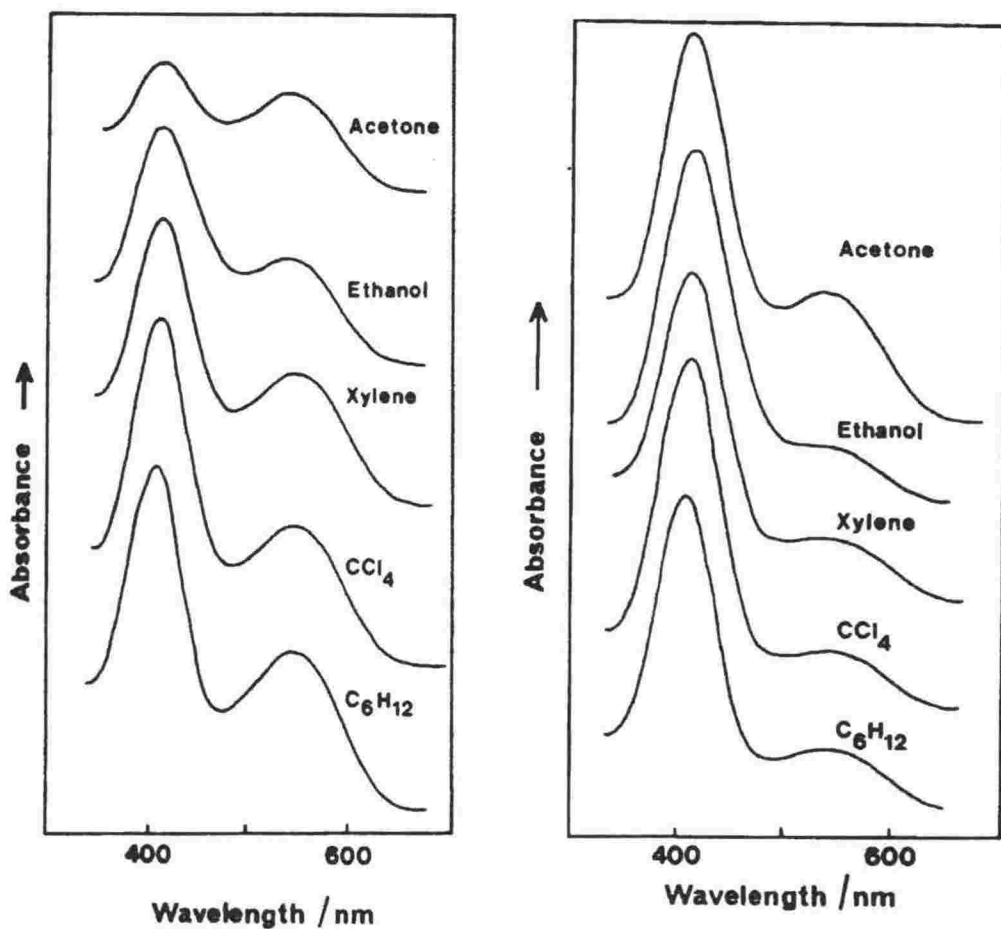
Absorption Spectra: Ultra violet-visible absorption spectra for the alkylthio-1,5-diphenylformazans have been recorded in several solvents and are shown in Figures 13-16.

For (1) the spectra vary greatly depending upon the solvent. However, unlike the other formazans where changes in the absorption spectra may be attributed to configurational changes, dithizone may lose or gain a proton in solution and form the ions HDz^- and H_3Dz^+ . The H_2Dz species is the *anti,s-trans* configuration of the solid state with two N-H

protons located.

For (2) - (5) the absorption spectra do reflect the configurations in solution and are invaluable in assigning the solution species of the nmr spectra.

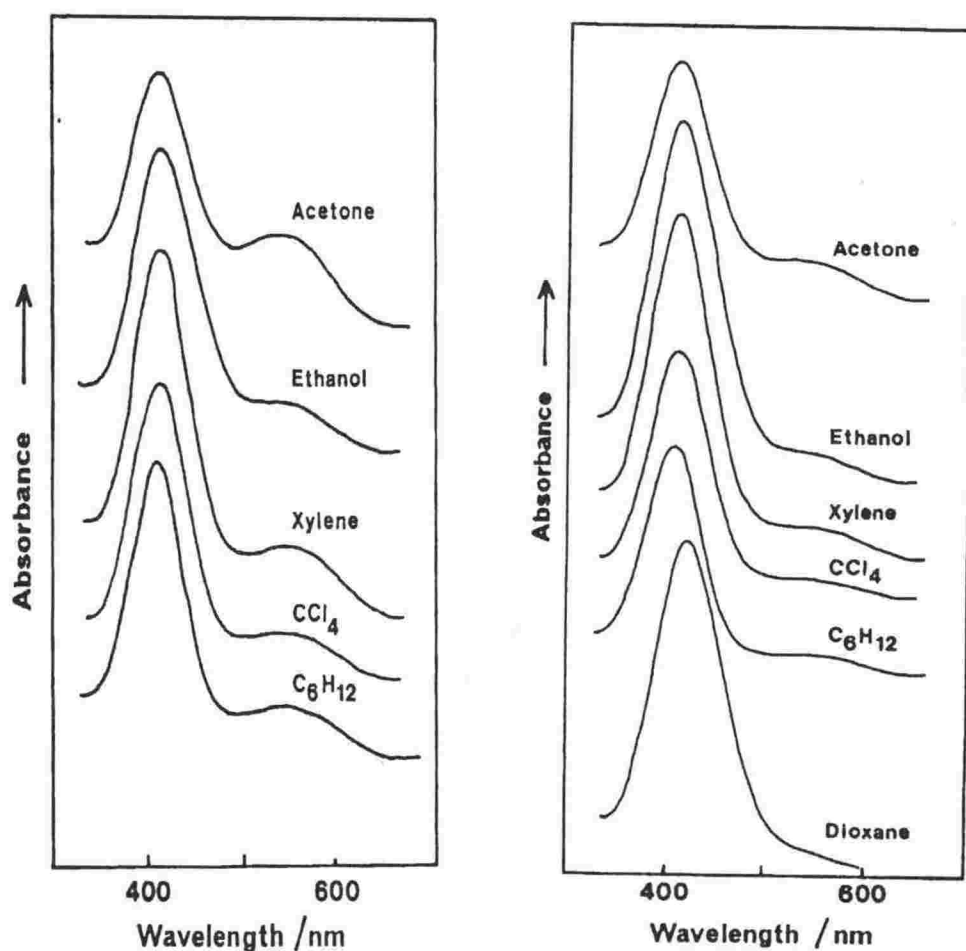
For (2) the absorption spectra confirm that two isomers are significantly present in all of the solvents studied. For (3) and (4) it is



Figures 13 and 14: The Ultra Violet-visible Absorption Spectra of 3-methylthio-1,5-diphenylformazan(2), (left), and Orange 3-ethylthio-1,5-diphenylformazan(3), (right).

evident that the absorption spectra of the equilibrated dark-stable species are the same and this parallels the same observation seen in the solution nmr spectra. Again there is a significant contribution by both the red and orange isomers in the solvents studied.

For (5) the contribution from the red isomer of the equilibrium would appear to be less significant in the solvents studied and this too is reflected in the solution nmr spectra.



Figures 15 and 16: The Ultra Violet-visible Absorption Spectra of Red 3-ethylthio-1,5-diphenylformazan (4), (left), and 3-isopropylthio-1,5-diphenylformazan (5), (right).

Conclusion.

The 3-mercapto-formazan, dithizone, exists in the *anti,s-trans* thione form in the solid state. This configuration is maintained for the dithizone species in CDCl_3 solution. The symmetry of this thione form is indicated by both the solid state and solution nmr spectra. The small C3 substituent and the two intramolecular N-H...S hydrogen bonds would seem to be the features which determine the configuration of the formazan.

3-Methylthio-1,5-diphenylformazan exists in the *syn,s-trans* configuration in the solid state. This red formazan is in equilibrium with the orange *anti,s-trans* configuration in solution and this is reflected in the solution nmr and absorption spectra. The ratio of the two isomers would seem to be approximately equal in solution.

3-Ethylthio-1,5-diphenylformazan exists in two configurations in the solid state. These are the orange *anti,s-trans* and red *syn,s-trans* forms. The former has been identified by an x-ray analysis and the latter has been identified from its solid state nmr spectrum. Both isomers result in the same equilibrium mixture in solution in the dark.

3-Isopropylthio-1,5-diphenylformazan exists in the *anti,s-trans* configuration in the solid state. In solution an equilibrium with the *syn,s-trans* configuration has been identified from the absorption and solution nmr spectra. The equilibrium would seem to lie in favour of the solid state structure.

The formazans which result in the solid state would seem to be as a result of three competing factors. Firstly, there is the steric effect at the C3 position which is less crowded than in other formazans due to the C-S-R arrangement of the C3 substituents and this would seem to favour the *anti,s-trans* and *syn,s-trans* configurations. Secondly, there is the possibility of an intramolecular hydrogen bond of the N-H...S type which is unavailable in other formazans and thirdly, the *syn,s-trans* configuration may be stabilised by more efficient packing in the crystal lattice. The electron donating ability of the alkyl substituent increases from (1) - (5) and therefore the electron density at the sulphur atom bridging between these substituents and the electron-delocalised formazan backbone increases in the same order. The intramolecular N-H...S hydrogen bond becomes more favourable from (1) - (5).

The combined techniques of nuclear magnetic resonance, vibrational and electronic spectra again demonstrate the viability of identifying the solid state and solution species of formazan equilibria even in the absence of definitive structural information in the solid state.

References.

- 1 Nineham, A.W., *Chem. Rev.*, **55**, 355 (1955).
- 2 Hutton, A.T., Irving, H.M.N.H. and Nassimbeni, L.R., *Acta Crystallogr., Sect. B*, **36**, 2064 (1980).
- 3 Niven, M.L., Irving, H.M.N.H. and Nassimbeni, L.R., *Acta Crystallogr., Sect. B*, **38**, 2140 (1982).
- 4 Noda, H., Engelhardt, L.M., Harrowfield, J. MacB., Pakawatchai, C., Patrick, J.M. and White, A.H., *Bull. Chem. Soc. Jpn.*, **58**, 2385 (1985).
- 5 Harrowfield, J. MacB., Pakawatchai, C. and White, A.H., *J. Chem. Soc., Dalton Trans.*, **1983**, 1109.
- 6 Laing, M. and Alsop, P.A., *Talanta*, **17**, 242 (1970).
- 7 Harding, M.M., *J. Chem. Soc.*, **1958**, 4136.
- 8 Harrowfield, J. MacB., Pakawatchai, C. and White, A.H., *Aust. J. Chem.*, **36**, 825 (1983).
- 9 Neugebauer, F.A. and Fischer, H., *Chem. Ber.*, **107**, 717 (1974).
- 10 Preuss, V.J. and Gieren, A., *Acta Crystallogr., Sect. B*, **31**, 1276 (1975).
- 11 Alsop, P.A., University of London, Ph.D. Thesis, 1971.
- 12 Laing, M., *J. Chem. Soc., Perkin Trans. 2*, **1977**, 1248.
- 13 Guillerez, J., Pascard, C. and Prange, T., *J. Chem. Res.*, (S) 308 (1978); (M) 3934 (1978).
- 14 Pemberton, J.E. and Buck, R.P., *J. Raman Spectrosc.*, **12**, 76 (1982).
- 15 Takahashi, H., Yamada, O., Isaka, H., Igarashi, T. and Kaneko, N., *J. Raman Spectrosc.*, **19**, 305 (1988).
- 16 Werhli and Wirthlin, "¹³C Nuclear Magnetic Resonance Spectroscopy".

Chapter 3.6

1-Methyl-1,5-Diphenylformazan.

In this chapter the results of the study of 1-methyl-1,5-diphenylformazan are given. The basis of this chapter is a paper entitled "Photochromic Formazans: X-ray Crystal Structure, Magnetic Resonance and Raman Spectra of 1-Methyl-1,5-diphenylformazan." which has been submitted to the *Journal of the Chemical Society, Perkin Transactions 2*, 1989.

Proofs to: Dr Gary R Burns,
Chemistry Department,
Victoria University of Wellington,
P.O. Box 600,
Wellington, NEW ZEALAND.

**Photochromic Formazans: X-ray Crystal Structure,
Magnetic Resonance and Raman Spectra of
1-Methyl-1,5-diphenylformazan.**

Christopher W. Cunningham and Gary R. Burns,
Chemistry Department,
Victoria University of Wellington,
P.O.Box 600,
Wellington, New Zealand.,

and

Vickie McKee,
Department of Chemistry,
University of Canterbury,
Christchurch 1, New Zealand.

Abstract

The X-ray crystal structure of one of a series of photochromic formazans has been determined. 1-methyl-1,5-diphenylformazan belongs to the monoclinic space group $I2/a$, $a = 28.402(7)$, $b = 5.640(1)$, $c = 15.688(4)$ Å, $\beta = 97.34^\circ$, $U = 2493(1)$ Å³, $Z = 8$ and adopts the *anti,s-trans* configuration common to orange formazans. Nuclear magnetic resonance and Raman spectra in both the solid state and in solution have been studied confirming that the formazan retains its configurational integrity in solution in both protic and aprotic solvents. The excitation profiles of the Raman active phonons based mainly on the N=N function indicate a maximum corresponding to the electronic absorption band both in the solid state and in solution.

Introduction.

Formazans have been known since the late nineteenth century when they were discovered and studied independently by Bamberger and his co-workers [1] and von Pechmann [2]. As a class of photochromic compound, formazans provide both organic and inorganic examples with the latter being the more widely investigated to date. Hg(II)dithizonate remains one of the few commercially exploited photochromes while 3-alkyl-1,5-diphenylformazans are recommended as yellow filters in photographic processing [3].

Formazans can in principle adopt four structures ((a)-(d) Figure 1) ignoring isomers which are unlikely to occur due to serious steric crowding. This is as a result of *syn-anti* isomerisation about the C=N double bond and isomerisation about the C-N single bond (*s-cis/s-trans*). Otting and Neugebauer [4] have concluded that in solution the red and yellow formazans are, respectively, *syn,s-cis* and *anti,s-trans* isomers. In the solid state the formazans crystallise as either red or orange-yellow solids, with the *syn,s-cis* [5] configuration if red and the *anti,s-trans* [6,8] or *syn,s-trans* [7,8] configuration if orange-yellow. These structures are characterised by significant inter- or intra-molecular hydrogen bonds ((a), (b) Figure 1) which have been held to account for the stability of the particular configurations adopted.

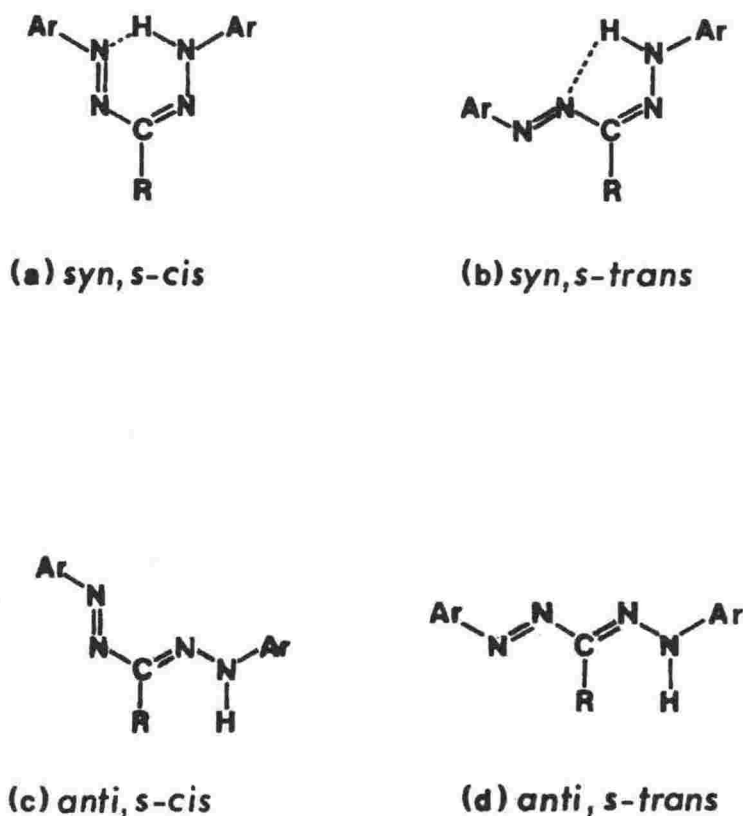


Figure 1: The Principal Isomers in the Formazan System.

During a continuing study of the structures of several isomeric formazans [8], we have determined the x-ray crystal structure of 1-methyl-1,5-diphenylformazan (1). The replacement of the 1-H atom by a methyl group removes the possibility of hydrogen bonding as seen in many 3-substituted 1,5-diphenylformazans. The formazan (1) crystallises as an orange formazan and provides a useful comparison for other orange formazans as we seek to explain why they adopt particular configurations on the basis of substitution of the formazan backbone in the absence of substitution of the phenyl rings or at the C3 position.

We present the x-ray crystal structure as well as the results of the Raman and nuclear magnetic resonance spectral investigations of (1).

Experimental.

Synthesis: 1-methyl-1,5-diphenylformazan (1): This was prepared following the method of McConnachie and Neugebauer [9]. The formazan was recrystallised from hot methanol giving orange crystals in good yield. Melting Point: 93-94° C. (Analysis: Found: C, 70.5; H, 5.8; N, 23.9; $C_{14}H_{14}N_4$ requires: C, 70.6; H, 5.9; N, 23.5 %).

Nmr Spectra: Solid state ^{13}C nmr spectra were recorded at 50.3 MHz with a Varian Associates XL-200 spectrometer using a standard CP/MAS probe. Powdered samples (*ca.* 300 mg) were packed in Kel-F rotors and spun using MAS frequencies up to 10 kHz. The combined techniques of high power proton decoupling and single contact cross polarisation (CP) were employed. Typical contact times of 50 μs were used, with recycle delays of 1.2 s. The number of transients acquired was of the order of 1000.

Solution ^{13}C nmr spectra were recorded at 20.00 MHz with a Varian Associates FT-80A spectrometer employing proton decoupling. In all cases either deuterated solvents or D_2O capillary tubes provided the spin lock. Typical spectral parameters employed were: spectral width 5000 Hz, acquisition time 1.023 s, pulse width 4 μs . Samples of *ca.* 200 mg were used in 5 mm o.d. tubes with tetramethylsilane as the internal standard.

Vibrational Spectra: Raman spectra were recorded using Spex 1401 and 14018 double monochromators in conjunction with Spectra Physics Model 164-01 Krypton ion laser, Coherent Radiation Models CR12 argon ion and CR500K krypton ion lasers. Laser excitation ranging from 476 to 753 nm was used with the power at the sample restricted to < 50 mW so as to avoid sample decomposition. Detection of the scattered radiation was by standard photon-counting techniques employing RCA C31034 photomultipliers. Band wavenumbers were calibrated using the emission spectrum of neon and typical slit widths of 200 μm were employed, giving a bandpass of 2 cm^{-1} at 647 nm. Samples were studied as crystals or in capillary tubes. Pressed discs diluted in potassium bromide were also used effectively to eliminate fluorescence. Divided disks were prepared including KClO_4 as an internal standard. Spectra were recorded both at 80 K and at room temperature.

Electronic Absorption Spectra: Ultra violet-visible spectra were recorded with a Shimadzu Model 160 ultra violet-visible spectrophotometer. Solvents were either spectroscopic grade or purified by standard methods. Diffuse reflectance spectra were recorded with a Pye Unicam SP700 spectrometer using MgCO_3 as a reference.

Analysis: The microanalysis was performed by Professor A.D. Campbell, Dr R.G. Cunninghame and associates of the University of Otago.

Crystal Data: Crystal data were collected at with a Nicolet R3m four-circle diffractometer using graphite-monochromated $\text{Mo-K}\alpha$ radiation. An orange crystal of dimensions 0.8 x 0.5 x 0.3 mm was found to belong to the monoclinic space group $I2/a$, $a = 28.402(7)$, $b = 5.640(1)$, $c = 15.688(4)$ Å, $\beta = 97.34^\circ$, $U = 2493(1)$ Å³, $Z = 8$, $F(000) = 1008$. Using 1.6° ω -scans at a scan rate of $5.86^\circ \text{ min}^{-1}$, 1625 unique reflections were collected in the range $4 < 2\theta < 45^\circ$ at 130 K. Of these, 1172 which had $I > 3\sigma(I)$ were used in the structure refinement.

Cell parameters were determined by a least-squares refinement of 22

accurately centred reflections in the range $13 < 2\theta < 32$). Crystal stability was monitored by recording three check reflections every 100 reflections and no significant variations were observed. The data were corrected for Lorentz and polarisation effects and an empirical absorption correction, based on ϕ -scan data, was applied.

The structure was solved by direct methods, using the program SOLV, which revealed the positions of all the non-hydrogen atoms, and refined by blocked-cascade least squares techniques. All the non-hydrogen atoms were assigned anisotropic temperature factors and hydrogen atoms were inserted at fixed positions using a riding model with thermal parameters equal to 1.2 U of their carrier atoms. The refinement, on 166 least-squares parameters, converged with $R = 0.0370$, $R' = 0.0489$ and a maximum shift/error ratio of 0.004. The final difference map showed no features greater than $0.2 \text{ e } \text{\AA}^{-3}$. The function minimised in the refinement was $\Sigma w(|F_o| - |F_c|)^2$ where $w = [\sigma^2(F_o) + 0.0013F_o^2]^{-1}$.

Results and Discussion.

Crystal Structure: The molecular structure and atomic nomenclature for (1) are shown in Figure 2. The final fractional coordinates and lists of bond lengths and bond angles are given in Tables 1 and 2. The

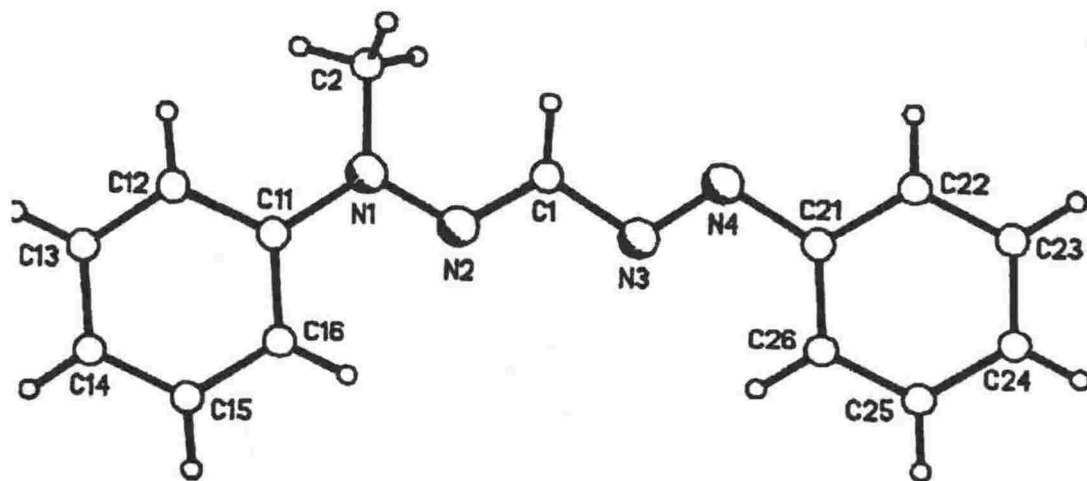


Figure 2: Molecular Structure and Atomic Nomenclature for 1-Methyl-1,5-diphenylformazan (1).

formazan assumes the *anti,s-trans* configuration characteristic of orange formazans. The molecule is almost planar with only small deviations from the plane of the two phenyl rings. The angle between the planes by the two phenyl rings and the backbone equals 2.3°. The phenyl bond lengths and angles are all "normal" within standard deviation. While the single and double bond character of the formazan backbone is clearly evident there is significant delocalisation of electrons along the backbone and into the phenyl rings. This delocalisation does not extend into the 1-methyl substituent. The C-N distances are all shorter than the "normal" single bond (1.43 Å [10]).

The 1-methyl substituent does not impose any significant alteration to the classic *anti,s-trans* configuration due to a steric effect at position 1, although the phenyl ring attached to N1 is shifted 2° away from the methyl group to accommodate it when compared with other orange formazans.

Table 1: Fractional Atomic Coordinates ($\times 10^4$) and Temperature Factors ($\text{\AA}^2 \times 10^3$) for 1-methyl-1,5-diphenylformazan (1).

	x	y	z	U
N(1)	1429(1)	4075(3)	8215(1)	24(1)*
N(2)	1742(1)	5789(3)	8471(1)	25(1)*
C(1)	2183(1)	5528(4)	8365(1)	27(1)*
N(3)	2482(1)	7360(3)	8680(1)	29(1)*
N(4)	2910(1)	6953(3)	8566(1)	29(1)*
C(2)	1585(1)	1824(4)	7891(1)	34(1)*
C(11)	958(1)	4487(4)	8375(1)	23(1)*
C(12)	596(1)	2918(4)	8069(1)	28(1)*
C(13)	139(1)	3262(4)	8265(1)	32(1)*
C(14)	34(1)	5156(4)	8758(1)	33(1)*
C(15)	387(1)	6766(4)	9041(1)	32(1)*
C(16)	847(1)	6458(4)	8856(1)	26(1)*
C(21)	3232(1)	8754(4)	8907(1)	26(1)*
C(22)	3702(1)	8450(4)	8764(1)	29(1)*
C(23)	4044(1)	10066(4)	9083(1)	31(1)*
C(24)	3922(1)	11986(4)	9551(1)	32(1)*
C(25)	3453(1)	12304(4)	9692(1)	33(1)*
C(26)	3111(1)	10703(4)	9376(1)	30(1)*

* Equivalent isotropic U defined as one third of the trace of the orthogonalised U_{ij} tensor

**Table 2: Bond Lengths (Å) and Bond Angles (°)
for 1-methyl-1,5-diphenylformazan (1).**

N(1)-N(2)	1.340(2)	N(1)-C(11)	1.414(2)
N(2)-C(1)	1.295(2)	C(1)-N(3)	1.388(3)
N(3)-N(4)	1.273(2)	N(4)-C(21)	1.427(3)
C(11)-C(12)	1.394(3)	C(11)-C(16)	1.403(3)
C(12)-C(13)	1.388(3)	C(13)-C(14)	1.376(3)
C(14)-C(15)	1.384(3)	C(15)-C(16)	1.386(3)
C(21)-C(22)	1.393(3)	C(21)-C(26)	1.392(3)
C(22)-C(23)	1.379(3)	C(23)-C(24)	1.379(3)
C(24)-C(25)	1.389(3)	C(25)-C(26)	1.373(3)

N(2)-N(1)-C(11)	115.8(2)	N(1)-N(2)-C(1)	
N(2)-C(1)-N(3)	115.3(2)	C(1)-N(3)-N(4)	
N(3)-N(4)-C(21)	113.4(2)	N(1)-C(11)-C(12)	
N(1)-C(11)-C(16)	120.6(2)	C(12)-C(11)-C(16)	
C(11)-C(12)-C(13)	120.3(2)	C(12)-C(13)-C(14)	
C(13)-C(14)-C(15)	119.3(2)	C(14)-C(15)-C(16)	
C(11)-C(16)-C(15)	119.7(2)	N(4)-C(21)-C(22)	
N(4)-C(21)-C(26)	124.8(2)	C(22)-C(21)-C(26)	
C(21)-C(22)-C(23)	120.3(2)	C(22)-C(23)-C(24)	
C(23)-C(24)-C(25)	119.9(2)	C(24)-C(25)-C(26)	
C(21)-C(26)-C(25)	119.9(2)		

A projection of the unit cell is shown in Figure 3. It can be seen

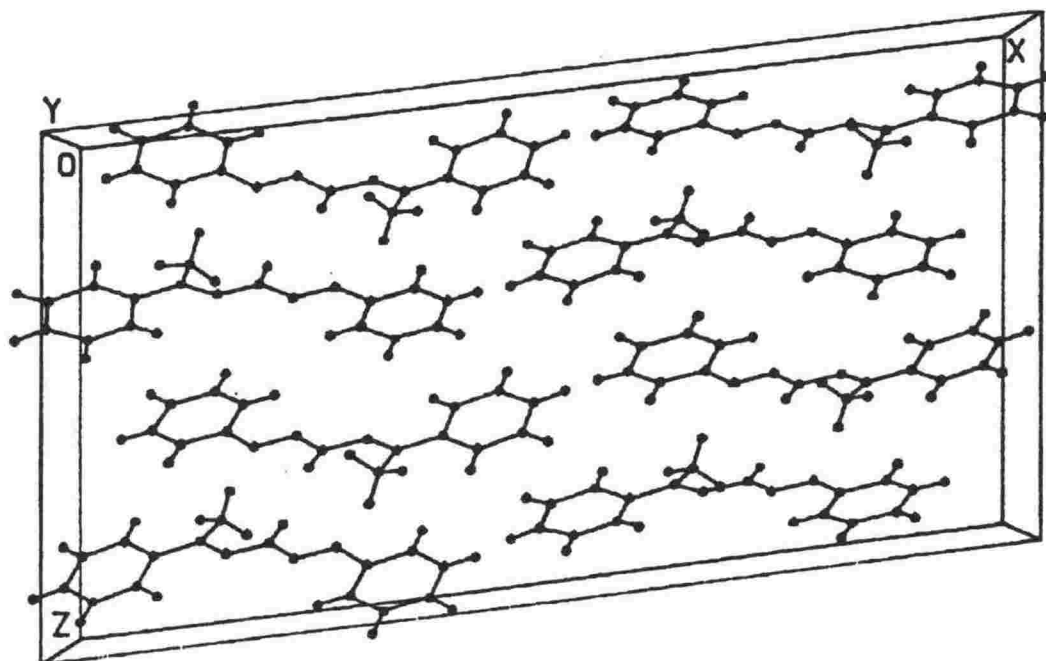


Figure 3: A Projection of the Unit Cell for 1-methyl-1,5-diphenylformazan (1).

that there are no significant inter or intra-molecular interactions. The orientation of the individual molecules is similar to the structure solved for 1,5-diphenylformazan which was seen to obey the "principle of densest packing".

Raman Spectra: The formazan (1) is a highly scattering sample lending itself to Raman spectroscopy. Diluted and pure powder samples afforded the use of very low laser powers. Representative Raman spectra are shown in Figure 4 and the band centre wavenumbers for the Raman active phonons are listed in Table 3. Bands are assigned on the basis of the symmetry coordinate whose contribution to the normal coordinate is greatest.

In the solid state at 80 K, the most intense band in the spectrum occurs at 1398 cm^{-1} . This is seen for all the exciting wavelengths studied. This band is based largely upon coupled vibrations of the formazan backbone, the $\text{N}=\text{C}-\text{N}$ and $\text{N}=\text{N}$ functions. The occurrence of this band at this wavenumber is characteristic of orange formazans in general and may be considered as a 'marker' band. The band at 1595 cm^{-1} is asymmetric, having a shoulder at 1582 cm^{-1} and is assigned to vibrations of the phenyl rings. This asymmetry is also characteristic of formazans where the 1- and 5-phenyl groups are slightly differently bonded to the backbone. The major difference of the spectrum from other orange formazans, however,

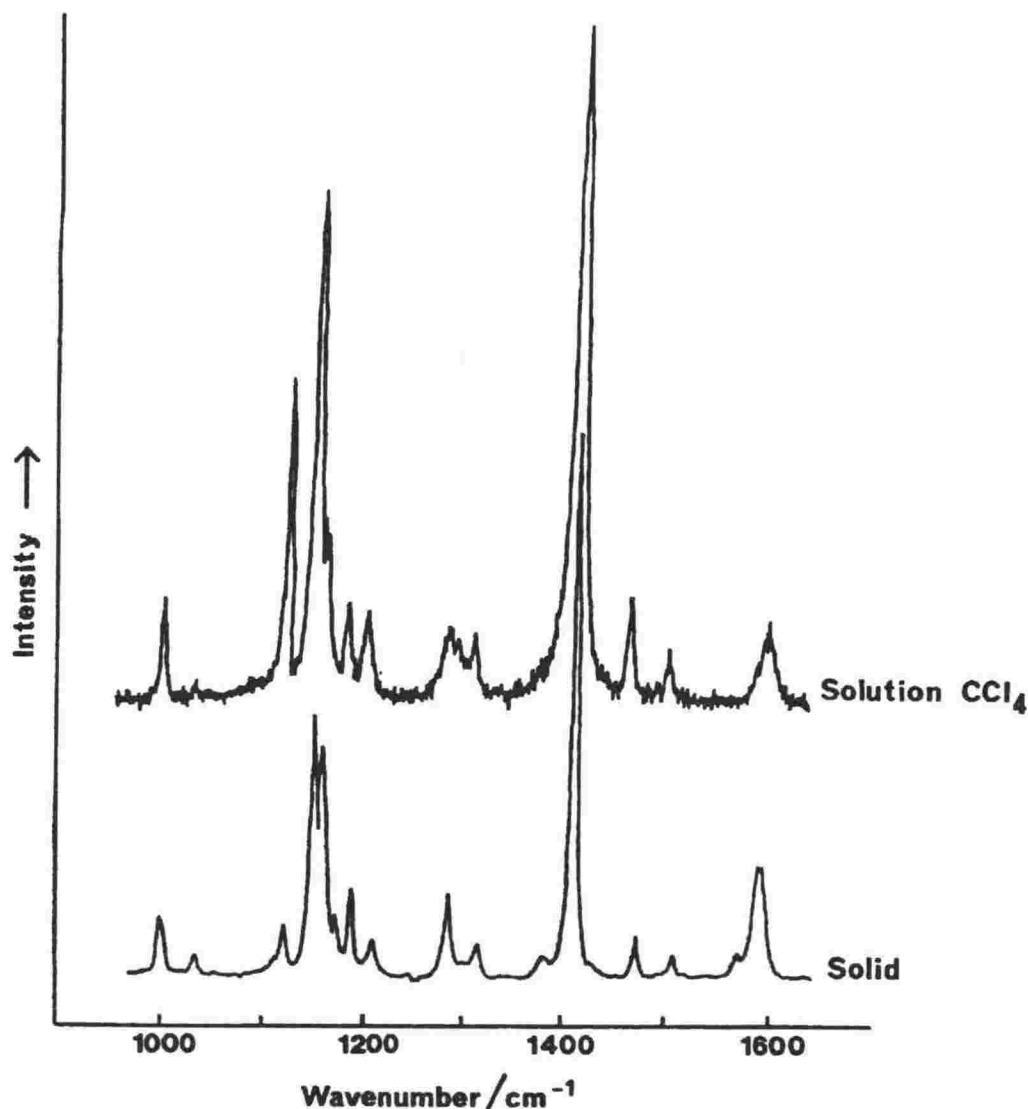


Figure 4: The Raman Spectra of Crystalline and Solution Samples of 1-methyl-1,5-diphenylformazan (1).

is the splitting of the band at 1150 cm⁻¹. Although the bands which result are from the strong coupling of the vibrations of the formazan backbone, this band has been assigned to a vibration involving the N-N function. Substitution at the 1-position by a methyl group would seem to result in the appearance of a doublet which may be assigned to the coupled vibrations of the C1-N2-N1 and C2-N1-N2 fragments of the backbone.

Table 3: Band Centre Wavenumbers (cm⁻¹) for the Raman Spectra of 1-methyl-1,5-diphenylformazan (1).

647.1 nm	568.2 nm	647.1 nm
CCl ₄ solution	solid 80 K	solid
1597	1595	1597
1585	1582	1583
1502	1498	1498
1464	1462	1462
1407	1398	1399
	1371	1371
1309	1307	1305
1285	1280	1280
1205	1204	1212
1185	1183	1184
	1167	1171
1151	1152	1156
1143	1144	1148
1126	1117	1120
1030	1033	1035
1001	997	1002

By using the ν_2 band of $\text{K}[\text{ClO}_4]$ as an internal standard we have constructed the excitation profile for the 1398 cm^{-1} band of (1) using laser excitation in the range 476 to 765 nm. Although no maximum can be explicitly determined the band intensity increases by 8 - 10 times towards the blue. This increase coincides with the band edge observed in the diffuse reflectance spectrum of (1) shown in Figure 5.

The Raman spectrum of (1) has also been recorded in CCl_4 solution at room temperature. The most intense band is observed at 1407 cm^{-1} and this corresponds with the 1398 cm^{-1} band in the solid state. Major bands are also observed at 1600 cm^{-1} and the doublet at 1150 cm^{-1} is still evident. Band centre wavenumbers are listed in Table 3. The excitation profile for the 1407 cm^{-1} band has been constructed and again indicates a maximum corresponding closely with the observed absorption spectrum in CCl_4 solution shown in Figure 5.

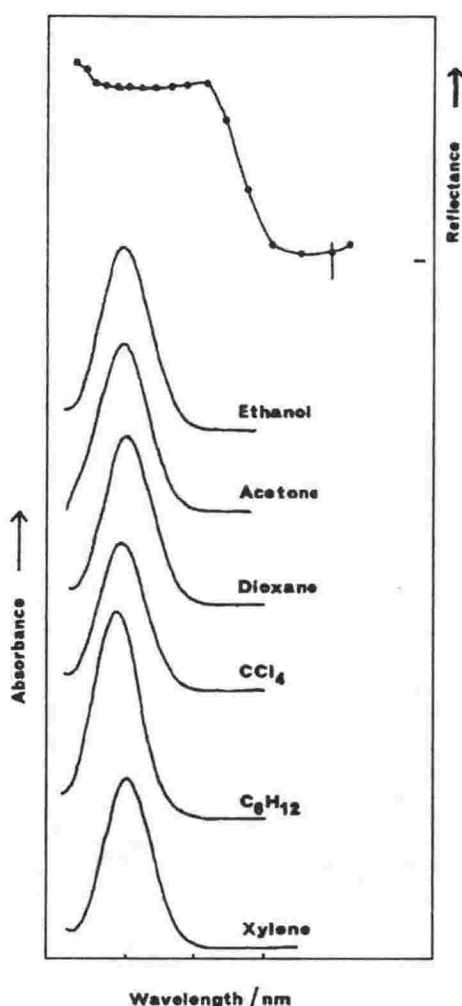


Figure 5: The Ultra violet-visible Electronic Absorption Spectra and Diffuse Reflectance Spectrum of 1-methyl-1,5-diphenylformazan (1).

Nuclear Magnetic Resonance Spectra: Resonances for ^{13}C nmr spectra recorded in the solid state and in several solvents are listed in Table 4 together with their assignments.

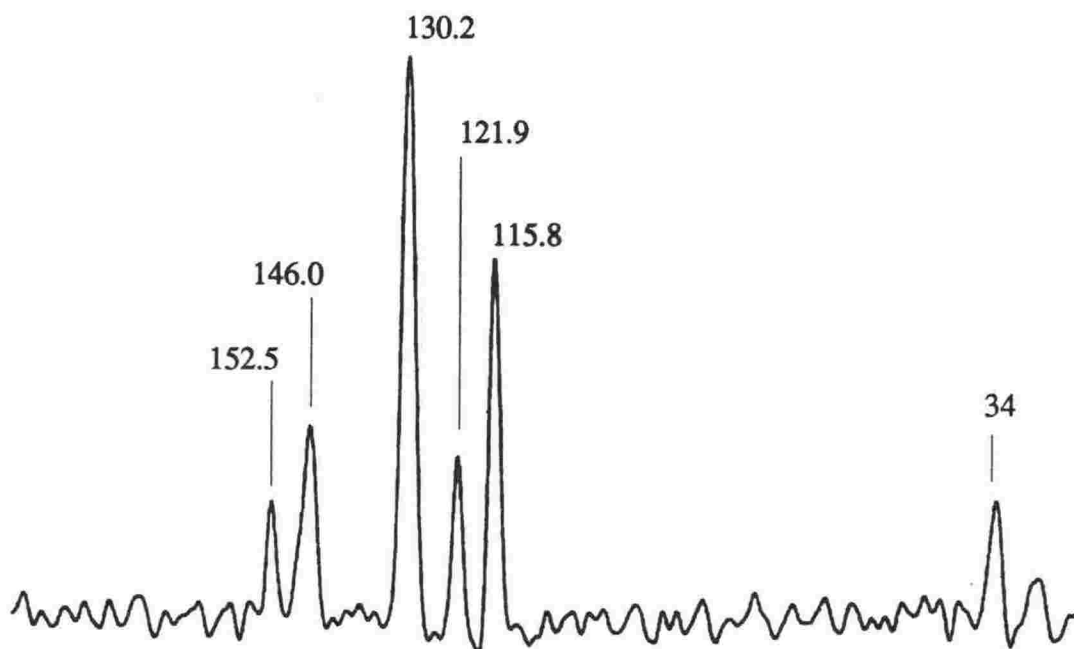


Figure 6: The Solid State ^{13}C MAS Nmr Spectrum for 1-methyl-1,5-diphenylformazan (1).

Six peaks are observed in the solid state MAS ^{13}C nmr spectrum of (1) and this is shown in Figure 6. One peak appears for the 1-methyl group at *ca.* 34 ppm and, although being of lower intensity and slightly broadened due to the quadrupolar effects of the N1 nucleus, this indicates one pure configuration. Three phenyl carbon signals are observed at *ca.* 130, 122 and 116 ppm indicating that the phenyl rings are in, more or less, equivalent chemical environments. This is characteristic of orange *anti,s-trans* formazans and the effect of the 1-methyl substituent is not manifest. Two signals at higher field are observed, one for the C1 at 152.5 ppm and the other for the C11 and C21 atoms coincident at 146.0 ppm. This latter signal is also slightly broadened due to the effect of nitrogen at N1 and N5 as well as the coincidence of signals.

It can be seen from the electronic absorption spectra (Figure 5) that there is no solvent dependent change in absorption maximum indicating an appreciable orange-red equilibrium in this system. The resonances for the ^{13}C nmr spectra recorded in solution also reflect this maintenance of configurational integrity in both protic and aprotic solvents. The formazan (1) differs in this respect from other orange formazans; 1,5-diphenyl-, 3-methyl- and 3-ethyl-1,5-diphenylformazan all exhibit a solvent dependent

Table 4: ^{13}C Nmr Resonances (δ ppm) for 1-methyl-1,5-diphenylformazan (1).

State	C3	C11	C21	C-phenyl	1-methyl
solid	152.5	146.0	146.0	130.2 121.9 115.8	34.5
CDCl_3	152.80	146.80	146.59	130.61 129.19 129.07 123.22 122.68 117.07	35.62
$(\text{CH}_3)_2\text{SO}$	153.77	148.25	147.66	132.21 130.97 130.76 124.43 123.50 117.90	36.75
C_6D_6	154.06	147.19		130.79 129.60 129.46 123.33 123.00 117.21 116.89	34.10
$(\text{CD}_3)_2\text{CO}$	152.90	147.70		131.30 130.07 129.97 123.54 123.12 117.36	35.50

equilibrium which is reflected in both their electronic and nuclear magnetic resonance spectra.

The pattern of resonances, as much as their actual positions, may be regarded as markers in the nmr spectra of (1). The solution spectra are exemplified, for example, by the CDCl_3 solution spectrum. The resonance at *ca.* 36 ppm is assigned to the 1-methyl group. Five non-quaternary phenyl carbon resonances are observed between *ca.* 117 and 131 ppm indicating the non-equivalence of the two phenyl groups. Formazans which assume the *anti,s-trans* configuration often exhibit the exact equivalence of the two phenyl rings due to the rapid tautomerism of the N1-proton, and in these cases only three non-quaternary phenyl carbon resonances are observed in this region. However, in the case of (1), the effect of the 1-methyl substituent is to split the signals for all of the non-quaternary phenyl carbons, with the exception of the *p*-carbon atoms which are too remote. The effect of the 1-methyl substituent is also to bring together the resonances for the quaternary C11 and C21 phenyl carbon atoms at 146.59 and 146.80 ppm. The C1 resonance is observed at 152.80 ppm closely paralleling the behaviour of other orange formazans (1,5-diphenylformazan, 152.1; 3-methyl-1,5-diphenylformazan, 153.8 ppm [7]).

It can be seen from these nmr spectra and the ultra violet-visible absorption spectra that only one configuration is evident in solution and that this is the *anti,s-trans* configuration of the solid state. However, unlike other orange *anti,s-trans* formazans, (1) does not undergo rapid tautomerism in solution at ambient temperatures. The presence of the 1-methyl substituent must be held to account for this difference.

Conclusion.

1-methyl-1,5-diphenylformazan exists in the *anti,s-trans* configuration in the solid state. There are no significant inter- or intra-molecular interactions. This configuration is maintained in solution in both protic and aprotic solvents. No marked photochromic effect is evidenced.

The hydrogen substituent at the C3 would seem to be the feature which determines the configuration of the formazan both in solution and in the solid-state. The formazan closely parallels the behaviour of 1,5-diphenylformazan in this respect. While the 1-methyl substituent does not significantly alter the classic *anti,s-trans* configuration characteristic of orange 1,5-diphenylformazans, it does disfavour the equilibrium involving the *syn,s-trans* or *syn,s-cis* configurations. These latter configurations can not accomodate the 1-methyl substituent and an all planar ring system, neither can they be afforded the extra stabilisation of the intramolecular hydrogen bond. The marker bands in both the Raman and nuclear magnetic resonance spectra both accurately reflect the configuration of the formazan and are reliable even in the presence of the 1-substituent.

Acknowledgement.

C.W.C. is grateful to the Maori Education Foundation for the granting of a Queen Elizabeth II Post Graduate Scholarship. G.R.B. is grateful to the Council of Victoria University for the granting of a sabbatical leave.

References.

1. Bamberger, E. and Wheelwright, E.W., *Chem. Ber.*, **25**, 3201 (1892).
 2. von Pechmann, H., *Chem. Ber.*, **25**, 3175 (1892).
 3. Ilford Patents.
Ger: 1 146 753 (1963).
Brit: 908 299 (1961).
Brit: 884 494 (1900).
Brit: 2 107 882 (1970).
 4. Otting, W. and Neugebauer, F.A., *Z. Naturforsch., Teil B*, **23**, 1064 (1968).
 5. Dijkstra, E., Hutton, A.T., Irving, H.M.N.H. and Nassimbeni, L.R., *Acta Crystallogr., Sect.B*, **38**, 535 (1982).
 6. Preuss, J. and Gieren, A., *Acta Crystallogr., Sect.B*, **31**, 1276 (1975);
Hutton, A.T., Irving, H.M.N.H., Nassimbeni, L.R. and Gafner, G., *Acta Crystallogr., Sect.B*, **35**, 1354 (1979).
 7. Omel'chenko, Yu., Kondrashev, Yu. D., Ginsburg, S.L. and Neiganz, M.G., *Kristallogafiya*, **19**, 522 (1974).
Laing, M., *J. Chem. Soc., Perkin Trans 2*, **1977**, 1248; Guillerez, J., Pascard, C. and Prange, T., *J. Chem. Res., (S)* 308 (1978); *(M)* 3934 (1978); Hutton, A.T., Irving, H.M.N.H. and Nassimbeni, L.R., *Acta Crystallogr., Sect. B*, **36**, 2071 (1980).
 8. Burns, G.R. and Cunningham, C.W., *J. Chem. Soc., Perkin Trans. 2*, **1988**, 1275.
 9. McConnachie, G. and Neugebauer, F.A., *Tetrahedron*, **31**, 555 (1975).
 10. Burke-Laing, M., and Laing, M., *Acta Crystallogr., Sect B*, **32**, 3216 (1976).
-

Chapter 3.7

Metal Dithizonates.

In this chapter some preliminary results concerning the photochromism of primary metal dithizonates are presented.

The first section of the chapter concerns the published observations on the photochromic behaviour of the complexes, particularly concerning the importance of the ligand and the representative x-ray crystal structures of several metal dithizonates which have been identified.

The second section of this chapter details a summary of the results we have obtained during a flash photolysis study of the photochromic change of a series of ten metal dithizonates. The work represents an important preliminary to a more comprehensive study of the systems which is envisaged.

The formazan, 3-mercapto-1,5-diphenylformazan (dithizone, H_2Dz) has long been used as a reagent for the colorimetric determination of trace metals [1-3]. Dithizone may exist in thiol or thione forms as shown in Figure 1. The thione structure has been established in the solid state by an x-ray analysis.

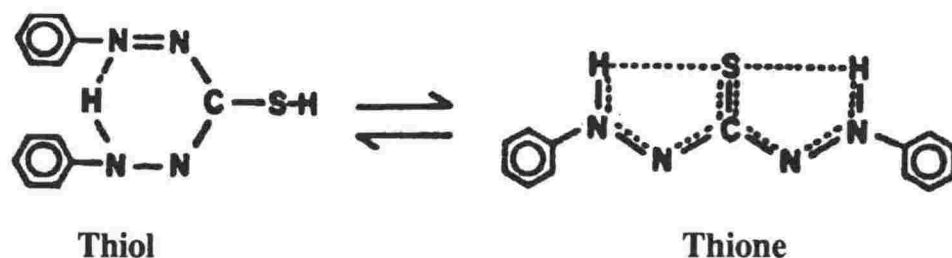


Figure 1: The Thiol - Thione Equilibrium for Dithizone.

It was not until the mid 1960s that evidence began to accumulate on the structures and properties of the complexes formed by dithizone and various metals [4-10]. Although several workers [1-3,11] have commented on the light sensitivity of the compounds formed it was not until around 1950 that Irving *et al.* [12] and Webb *et al.* [13] reported independently that the $Hg(II)$ complex is photochromic. When benzene or chloroform solutions of $Hg(II)(Hdz)_2$ were irradiated they changed from their normal orange-yellow colour to an "intense royal blue". They found that the orange-yellow colour returned slowly in the absence of light and that the cycle could be repeated many times. Apparently these unusual observations were not followed up for more than a decade until a detailed study on the photochromism of metal dithizonates led to the discovery of a large number of photochromic dithizonates.

Dithizone is known to form two types of metal complex, the so-called "primary" and "secondary" dithizonates [2]. The former are those formed with the monoanion $(HDz)^-$:



whereas the latter are formed from the dianion $(Dz)^{2-}$:



The Structures of Dithizonate Complexes: X-ray crystal structure determinations of metal dithizonates are few in number, however mono-, bis- and tris- complexes have been identified. In almost every case the

dithizone ligand behaves as a bidentate chelating agent coordinating through both S and N to give a five membered ring:

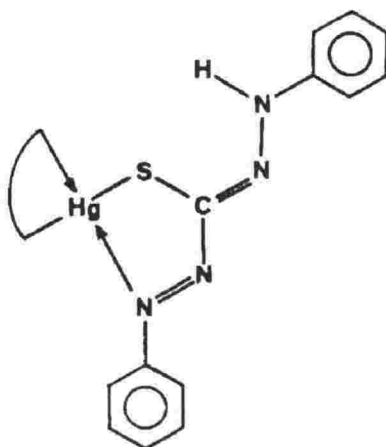


Figure 2: Mercury(II) Dithizonate Complex.

The first dithizonate to be structurally identified was Hg(II)(Hdz)_2 (2) by Harding in 1958 [4]. She showed that the mercury was bonded to one sulphur atom of each of two dithizone groups and that a nitrogen atom from each azo group is weakly coordinated to the mercury atom making a rather distorted tetrahedron. The dithizone groups are in an extended arrangement with no intramolecular hydrogen bonding. Alsop, in 1971 [5], also investigated the x-ray crystal structure of (2). Unfortunately, the crystal chosen for the study was recrystallised from pyridine and retained about 2 mol of solvent per mol of complex which are clearly not coordinated and are lost on storage of the compound over sulphuric acid.

Laing and Alsop [6] have shown that Ni(Hdz)_2 is essentially square planar and that the whole molecule is almost planar.

Alsop [5] has also shown that Pt(Hdz)_2 and Pd(Hdz)_2 are isostructural.

Zn(Hdz)_2 has been studied independently by three groups (Math and Freiser [7]; Mawby and Irving [8]; Harrowfield, Patawatchai and White [9]). It has been shown that two polymorphs are formed. When crystallised from chloroform the α -polymorph is isolated and this has been structurally identified by the first two groups of workers whose results are concordant. The two almost planar dithizonate ligands act as bidentate ligands and are tetrahedrally coordinated to zinc through sulphur and nitrogen. However, when crystallised from benzene a second β -polymorph was obtained. This β -polymorph, structurally identified by the last group of researchers above, is very similar to $\alpha\text{-Zn(HDz)}_2$ with regard to its internal molecular geometry, the major difference is that the axial lengths

angles between the conjugated formazan backbone nevertheless remain "pseudo co-planar" with it in both polymorphs. Only minor differences are seen in the bond lengths and angles between the two phases, except in regard to the interligand S-Zn-N angles which are asymmetric in the α -phase.

The structure of the potassium salt of the monoanion, K^+HDz^- [10], has been established. The pseudo planar anion is extensively delocalised and the structure is essentially ionic.

$Bi(HDz)_3$ [11] consists of discrete molecules containing three dithizone residues all acting as bidentate ligands coordinating through sulphur and nitrogen. The configuration is all *cis* i.e. the three sulphur atoms are facially arranged on one side of the bismuth coordination sphere. Steric considerations and in particular the phenyl rings, whose attitude is remarkably co-planar with the rest of the formazan backbone, were held to account for this observation. The Bi^{3+} is in a pseudo-octahedral coordination sphere. The overall planarity of each dithizone moiety allows extensive delocalisation of electrons. Intramolecular hydrogen bonding, N-H...S, occurs, the concomitant orientation on one of the lone pairs of electrons on each of the sulphur atoms towards the respective hydrogen atom then effectively locks the dithizone residues into the *anti,s-trans* configuration.

Comparisons of the ligand geometries in all of the complexes above show little or no change in those parameters not directly involving the central metal.

Only one example of a dithizonate complex of a metal ion in a high oxidation state has been identified. $In(Hdz)_3$ was structurally identified by Harrowfield *et al.* [12] in 1983. In spite of a large indium atom, the coordination array of the complex was found to be sparse - being five coordinate trigonal bipyramidal. Two of the ligands are bidentate coordinating through sulphur and nitrogen while the third is unusually unidentate by way of sulphur. The ligands span equatorial and axial sites but the In-S and In-N sets of bond lengths in the three ligands are surprisingly uneven, although, in keeping with the low coordination sphere the metal-ligand bond lengths are short. The phenyl ring attitude in the three ligands is substantially co-planar with the rest of the ligand. The C-N distances change quite markedly in the three ligands as do the N-N distances.

The Dithizone Residue: The coordination of the dithizone molecule to various metals results in the formation of several types of complexes. However, the dithizone moiety apparently retains much of its formazan character in respect of the attitude of the phenyl rings, some delocalisation of electrons along the backbone and in to the rings and the possibility of hydrogen bonding, all combining to effectively lock the formazan into the *anti,s-trans* configuration in the solid state.

Photochromism.

Although several authors [1-3,11] had commented upon the sensitivity of metal dithizonates to light, this curious phenomenon was not followed up in depth until the American Cyanamid Company recognised the potential use of the complexes in solar batteries, sun glasses and car windscreens [13].

Meriwether, Breitner and Sloan [14] have investigated 24 primary dithizonates in sixteen solvents both at room temperature and at -80°C . They found nine primary but no secondary dithizonate complexes to be photochromic in solution. Only Hg(II)(HDz)_2 was found to be photochromic in the solid state.

Independent of the metal ion the colour change was usually from orange to red, blue or violet indicating the primary importance of the dithizone ligand. The rate of return to the normal colour, however, was seen to depend enormously upon the metal. Return rates ranged from *ca.* 30 s for mercury down to < 1 s for cadmium.

This, and a subsequent study by Meriwether *et al.* [15], both of which studied the photochromic property by ultra violet-visible absorption spectroscopy, led the authors to propose a generic reaction scheme. They proposed a *cis-trans* isomerisation about the azomethine group with a rate determining proton shift.

Meriwether and his co-authors [14,15] observed that the return reaction for Hg(II)(HDz)_2 in benzene at 25°C follows primary kinetics. The photochromism occurs independently in each ligand and is unaffected by the presence of a second or third ligand.

"...further evidence must await the flash-photolysis studies."

Geosling, Adamson and Gutierrez [16] followed this definitive study by an investigation to determine the formal kinetics of the approach to the photostationary state using laser-pulse or flash-photolysis.

While they could not confirm some of Meriwether's results they did observe that B, the photostationary product, was not itself photosensitive. They also observed, as did Meriwether, that the return rates were always strictly first order. However, these latter authors also observed that the exact return rates were not reproducible from one preparation to the next, there even seemed to be some dependance on the exact cleaning preparation of the glassware used!

Hg(II)(HDz)_2 and Ag(HDz) in tetrahydrofuran solvent were examined for evidence of a delayed appearance of the photo-product, which might occur if it was derived from an excited state of a few nano-second lifetime, or if some intermediate was formed; no such effect was detected.

"We conclude that at least for Hg(II)(Hdz)₂, both ligands isomerise essentially simultaneously following light absorption... The high quantum yields and the lack of delay in the appearance of a photoproduct indicates a very prompt excited state reaction."

In this study the kinetics of the return rate of a number of photochromic primary metal dithizonates have been investigated by flash photolysis. The study is restricted to one solvent, benzene, which provides a medium in which:

- i) the metal dithizonates are largely soluble;
- ii) the water content could be estimated.

The strongest photochromic effects are found in dry, non-polar solvents (benzene, toluene, chloroform, carbon tetrachloride). Hydroxylic solvents and organic acids and bases are poor media, greatly accelerating the return reactions.

The photochromism of the primary metal dithizonates of the following metals:

Pd, Pb, Sb, Bi, Tl, Ni, Cu, Zn, Cd, Hg
have been investigated by flash photolysis.

Experimental.

Samples: The primary metal dithizonates used in this study were all prepared using standard methods. Typically, a chloroform solution of dithizone was shaken with an aqueous solution of the metal ion. The metal dithizonate was then isolated and purified from the organic phase. All of the samples used in this study were kindly supplied by Dr Gary R. Burns.

Flash Photolysis: Flash photolysis was carried out with the use of an amplified and frequency-doubled Neodymium laser, which produced 153 kV, 20 ns pulses at 527 nm. The solution of the dithizonate complex was held in a 1 cm square, four-faced quartz cuvette, with the monitoring beam arranged at right angles to the photolysing pulse. Monitoring was by means of a DC quartz-halogen or xenon arc lamp, suitably focussed and collimated.

The monitoring beam was seen by a photomultiplier preceded by a grating monochromator, set to accept only the monitoring wavelength by the use of appropriate filters. The output from the photomultiplier

controlled the beam of a storage oscilloscope triggered from the laser. It was possible to photograph the trace to show either the rise-time of the photo-excited species or, at longer sweep rates, the decay of the photo-product as it returned to the normal form.

Results.

A summary of the observed half lives ($t_{1/2}$) for the dithizonate complexes studied and a comparison with literature values is given in Table 1. The observed results compare well with most of the previously measured half lives with the exception of the Pd(II)(HDz)_2 complex which we found had a much longer half life than Geosling *et al.* found [16]. An interesting observation was that many of the dithizonates studied appeared to have two distinct decays. For example, Zn(II)(HDz)_2 and Hg(II)(HDz)_2 in ethanol, as well as AgHDz in benzene all yield a very fast initial decay (half life of the order of a few milliseconds) as well as a reasonably slow one (of the order of hundreds of milliseconds). This paralleled an earlier observation for 1,3,5-triphenylformazan studied under the same conditions [17].

The order of increase in the observed return rate is:



compared with Meriwether's



although it should be noted that Meriwether did not specify a unique solvent for this comparison.

The Effect of Water: Meriwether [14,15] and Geosling [16] have both commented on the effect of water on the return rates of the dithizonates. The rates were seen to decrease with increasing water content. For all of our measurements we attempted to standardise the water content by saturating the benzene solutions with water. The solubility of water in benzene at 25° C is 0.04 mol dm⁻³ and the benzene was allowed to stand over water for 24-48 hours. Even following these precautions many of the return rates were not reproducible leading to errors of up to 20 % in Table 1.

Table 1: Half Lives for Metal Dithizonates.

Dithizonate in benzene	Observed ($t_{1/2}$ /s)	Literature [14]. ($t_{1/2}$ /s)	Solvent
Tl(I)HDz	0.150	0.030 0.018	benzene benzene
Ni(II)(HDz) ₂	0.030		benzene
Pd(II)(HDz) ₂	1 - 2	0.150	CH ₂ Cl ₂
Pt(II)(HDz) ₂	1 - 5		benzene
Cu(II)(HDz) ₂	0.020	0.096	acetone
Zn(II)(HDz) ₂	10.0	9.500 0.016	CH ₂ Cl ₂ THF
Cd(II)(HDz) ₂	1.0	0.308 0.008	THF acetone
Hg(II)(HDz) ₂	0.010 long	0.0014	pyridine benzene
Pb(II)(HDz) ₂	0.16	0.110	CH ₂ Cl ₂
Sb(III)(HDz) ₃	0.8		benzene
Bi(III)(HDz) ₃	2.0	0.335	CH ₂ Cl ₂

Errors and Uncertainties in the longer ($t_{1/2}$)s determined are large due to the limitations of the oscilloscope used. Errors are up to 20 %.

Discussion.

The flash photolysis study has confirmed many of the findings of the two previous studies. The observed half lives for the ten photochromic primary dithizonate complexes studied compare favourably with those in the literature. The return rates are strictly first order, although the exact rate was difficult to reproduce exactly. Errors up to 20 % were thought reasonable under the conditions. The reasons for the variation were unclear, but it is certain that the water content has an effect and the physical problems of convection currents in the cuvettes and other experimental factors (e.g. photolysis by the monitoring beam) may have introduced further inconsistencies.

One reproducible finding, not previously reported, was the observation of two decay rates for some of the dithizonate complexes. It is apparent that a short lived species, with a half life of the order of milliseconds occurs for the mercury, thallium and silver species, and that a much longer lived species was also present. Both species absorbed at a similar wavelength as the monitoring beam was filtered as was appropriate to the individual dithizonate complex. Absorption spectra had been measured prior to the flash photolysis experiments.

The significance of these observations for the dithizone ligand and ultimately to the 1,5-diphenylformazans is equally uncertain at this time. The observation that a similar double decay is seen for some formazans and some dithizonates leads to the conclusion that it is the same effect seen in both cases. The dithizonate complexes behave similarly to the formazans excepting that the chelation to a metal ion limits the possible *cis/trans* isomerisations to the one involving the azomethine group.

There are still many questions left unanswered by this study which must be left for further investigation. The effect of the water content of both the solvent and the solute upon the return rate is not yet well understood. The forward reaction may be more than single-specied and it may be that the two species have the same absorption spectrum characteristics.

The results of other studies of formazans (nmr, ultra violet-visible, Raman) may be applicable to this system. The identification of the solution species by these combined techniques is possible and would certainly assist in explaining some of the findings above.

References.

- 1 Fischer, H., *Wiss. Veroffentlich. Siemens-Werken*, **4**, 158 (1925); Allport, N.L. and Skrimshire, G.H., *Analyst*, **57**, 440 (1932); Allport, N.L. and Skrimshire, G.H., *J. Pharm. Pharmacol.*, **5**, 461 (1932); Ross, J.R. and Lucas, C.C., *Canad. Med. Assoc.*, **29**, 649 (1933); Bohnenkamp, H. and Linneweh, W., *Deut. Arch. Klin. Med.*, **175**, 157 (1933); Irving, H., *Z. Analyt. Chem.*, **263**, 264 (1973); LAutenschlager, W., Pahlík, S. and Tolg, G., *Z. Analyt. Chem.*, **260**, 203 (1972); Ruzicka, J. and Stary, J., *Talanta*, **8**, 228 (1961); Ruzicka, J. and Stary, J., *Talanta*, **9**, 617 (1962); Spevaackova, V. and Krivanek, M., *J. Radioanalyt. Chem.*, **21**, 485 (1974).
- 2 Nineham, A.W., *Chem. Rev.*, **55**, 355 (1955).
- 3 Sandell, E.B., "Colorimetric Determination of Trace Metals", Interscience, New York, 1959; Iwantscheff, G., "Das Dithizon und seine Anwendung in der Mikro- und Spuren-analyse", 1st edn., Verlag Chemie, Weinheim (1958); 2nd (and revised) edn., Verlag-Chemie, Weinheim (1972); Venturello, G. and Ghe, A.M., *Ann. Chim. (Italy)*, **45**, 1054 (1955); Webb, J.L.A., Bhatia, I.S., Corwin, A.H. and Sharp, A.G., *J. Am. Chem. Soc.*, **72**, 91 (1950).
- 4 Harding, M., *J. Chem. Soc.*, **1958**, 4136.
- 5 Alsop, P.A., University of London, Ph.D. Thesis (1971).
- 6 Laing, M. and Alsop, P.A., *Talanta*, **17**, 243 (1970).
- 7 Math, K.S. and Feiser, H., *Talanta*, **18**, 435 (1971).
- 8 Mawby, A. and Irving, H.M.N.H., *J. Inorg. Nucl. Chem.*, **34**, 109 (1972).
- 9 Harrowfield, J. MacB., Pakawatchai, C. and White, A.H., *Aust. J. Chem.*, **36**, 825 (1983).
- 10 Harrowfield, J. MacB., Pakawatchai, C., Patrick, J.M. and White, A.H., *Bull. Chem. Soc. Jpn.*, **58**, 2358 (1985).
- 11 Reith, J.F. and Gerritsma, K.W., *Rec. Trav. Chim.*, **64**, 41 (1945).
- 12 Irving, H., Andrew, G. and Risdon, E.J., *J. Chem. Soc.*, **1949**, 541.
- 13 Webb, J.L.A., Bhatia, I.S. Corwin, A.H. and Sharp, A.G., *J. Am. Chem. Soc.*, **72**, 91 (1950).
- 14 Irving, H.M.N.H., "Dithizone, Analytical Sciences Monographs 5", John Wright and Sons, London (1977).
- 15 Meriwether, L.S., Breitner, E.S. and Sloan, C.L., *J. Am. Chem. Soc.*, **87**, 4441 (1965).
- 16 Meriwether, L.S., Breitner, E.S. and Colthup, N.B., *J. Am. Chem. Soc.*, **87**, 4448 (1965).
- 17 Geosling, C., Adanson, A.W. and Guitierrez, A.R., *Inorg. Chim. Acta*, **29**, 279 (1978).
- 18 Cunningham, C.W., Victoria University of Wellington, B.Sc.(Hons.) Thesis, 1982.

SUMMARY OF RESULTS

In the following chapter the major results of the previous chapters are summarised. Conclusions are drawn on the solid state and solution structures of individual formazans and the trends evident in the series are explained.

The basis of this chapter is a preprint of a paper entitled "The Recent Structural Chemistry of 1,5-Diphenylformazans".

Proofs to: Dr Gary R. Burns,
Chemistry Department,
Victoria University of Wellington,
P.O. Box 600,
Wellington, NEW ZEALAND.

The Recent Structural Chemistry of 1,5-Diphenylformazans.

Christopher W. Cunningham and Gary R. Burns
Chemistry Department,
Victoria University of Wellington,
P.O.Box 600,
Wellington, New Zealand.

Abstract

Raman and nuclear magnetic resonance spectra have been recorded for a series of thirteen isomeric 1- or 3-substituted 1,5-diphenylformazans. Identification of solid state configurations by these combined techniques has been substantiated by an X-ray crystallographic determination of ten of these structures. The configuration of the solid state has been shown to depend upon the nature of the substituent at the 3-position. The effect of inter- or intra-molecular hydrogen bonding is seen to play a secondary role. Solution equilibria for the series have been studied. Nuclear magnetic, Raman and electronic absorption spectra allow the identification of the configurations of formazans in solution and show

that the *anti,s-trans* configuration of orange formazans is in equilibrium with either the *anti,s-cis* or *syn,s-trans* configurations, both of which are red formazans.

Introduction.

The photo- and thermal interconversions of the *syn*- and *anti*- isomers of imines (Schiff's Bases) are a subject of long standing interest. Attempts to elucidate the mechanisms of individual isomerisations continue to challenge the ingenuity of various research groups. Photochemical *syn-anti* isomerisations are also seen in other groups of compounds containing the C=N moiety including oximes and hydrazones.

The coupling of hydrazones with diazo compounds results in the synthesis of formazans in alkaline media. Formazans are compounds containing the characteristic -N=N-C=N-NH- grouping. The aromatic formazans, 1,5-diphenylformazan and 1,3,5-triphenylformazan were first described by von Pechmann [1] and Bamberger in 1892 [2]. These are usually brightly and intensely coloured compounds, and, following the observation that 1,3,5-triphenylformazan readily formed some metal complexes, considerable effort was devoted to developing formazan dyestuffs.

As a class of photochromic compound, the formazans provide both organic and inorganic examples, with the latter being the more widely investigated to date. Hg(II)dithizonate remains one of the few commercially exploited photochromes while 3-alkyl-1,5-diphenylformazans are recommended as yellow filter dyestuffs for improved colour reproduction of colour photographic materials [3].

Aspects of the chemistry of formazans have been reviewed previously. A comprehensive and definitive review on the formazans and related tetrazolium salts was given by Nineham in 1955 [4]. These two groups of compounds have been historically reviewed together as formazans provide the only synthetic route to tetrazolium salts. Mester reviewed the formazan reaction in carbohydrate chemistry in 1958 [5] and this was followed by a review of the recent chemistry of formazans and tetrazolium salts by Hooper in 1969 [6]. An important addition appeared in 1975 when Bednyagina *et al.* [7] reviewed hetarylformazans - formazans with heteroaromatic substituents. This latter work also summarised much of the hitherto unrecognised Russian work.

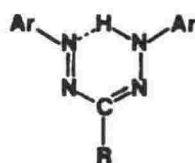
Since this most recent review much progress has been made. Many new formazans have been synthesised. X-ray crystallographic structural analyses have been published for the first time and the new analytical

techniques (solid state nuclear magnetic resonance, Raman spectroscopy) to detect and determine molecular configurations have been developed.

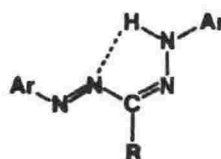
X-ray crystallography is the definitive technique for the solid-state when single crystals are available. However, the major value of nmr, infrared, Raman and electronic spectroscopies is the ability to span the phases and in particular bridge the gap between solid state and solution structures. Fewer than 1% of the known formazans have had their x-ray crystal structures solved and, of these, many are unrepresentative of 1,5-diphenylformazans. This is due to the fact that those which have had their structures solved are very often highly substituted within the 1,5-diphenyl rings and at the C3 position making attempts to correlate isomerism with the structural nature of the backbone, the inter- or intramolecular hydrogen bond or the all-planar ring systems difficult. We have therefore chosen to study 3-substituted 1,5-diphenylformazans free from the influence of substitution of the phenyl rings and to establish the configurationally-sensitive Raman active phonons and the configurationally-sensitive nuclear magnetic resonances.

Isomerism in Formazans.

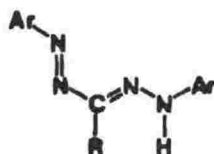
Apart from isomers which are unlikely to occur due to serious steric crowding, the formazans can in principle adopt any of four possible



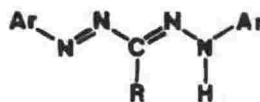
(a) *syn, s-cis*



(b) *syn, s-trans*



(c) *anti, s-cis*



(d) *anti, s-trans*

Figure 1: The Principal Configurations of Isomeric 1,5-Diphenylformazans.

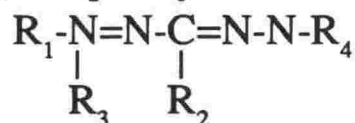
structures (Figure 1 (a) - (d)) corresponding to *syn-anti* isomerisation about the C=N double bond and isomerisation about the C-N single bond (*s-cis/s-trans*). Otting and Neugebauer [8] have concluded that in solution the red and yellow formazans are, respectively, *syn,s-cis* and *anti,s-trans* isomers.

The photo- and thermal interconversions of the isomers have been studied several times [9]. Although three major mechanistic studies have been published the interpretation of the colour changes in formazans still remains the subject of some controversy.

Attempts to correlate photochromic behaviour with the nature of the substituents on N1, C3 or N5 have suffered from the absence of definitive structural information in the solid state. Neither has the link between solid state and solution structures been confirmed by a convenient or routine spectroscopic method.

We shall present the results of the structural and spectroscopic studies of the compounds listed in Table 1.

Table 1: 1,5-Diphenylformazans Studied.



No	R ₁	R ₂	R ₃	R ₄	1,5-diphenylformazan
I	Ph	H	H	Ph	
II	Ph	Me	H	Ph	
III	Ph	Et	H	Ph	orange 3-ethyl
IV	Ph	Et	H	Ph	red 3-ethyl
V	Ph	Bu ^t	H	Ph	
VI	Ph	Ph	H	Ph	triphenyl
VII	Ph	H	Me	Ph	
VIII	Ph	SH	H	Ph	dithizone
IX	Ph	SMe	H	Ph	
X	Ph	SEt	H	Ph	orange 3-ethylthio
XI	Ph	SEt	H	Ph	red 3-ethylthio
XII	Ph	SPri ^t	H	Ph	
XIII	Ph	S	H	Ph	potassium dithizonate

Experimental.

A summary of the elemental analyses and synthetic methods used for the formazans studied is given in Table 2.

Nuclear Magnetic Resonance Spectra: Solid state ^{13}C nmr spectra were recorded at 50.3 MHz with a Varian Associates XL-200 spectrometer using a standard CP/MAS probe. Powdered samples (*ca.* 300 mg) were packed in Kel-F rotors and spun using MAS frequencies up to 10 kHz. The combined techniques of high power proton decoupling and single contact cross polarisation (CP) were employed. Typical contact times of 50 μs were used, with recycle delays of 1.2 s. The number of transients acquired was of the order of 1000.

Solution ^{13}C nmr spectra were recorded at 20.00 MHz with a Varian Associates FT-80A spectrometer employing proton decoupling. In all cases either deuterated solvents or D_2O capillary tubes provided the spin lock. Typical spectral parameters employed were: spectral width 5000 Hz, acquisition time 1.023 s, pulse width 4 μs . Samples of *ca.* 200 mg were used in 5 mm o.d. tubes with tetramethylsilane as the internal standard.

Vibrational Spectra: Raman spectra were recorded using Spex 1401 and 14018 double monochromators in conjunction with Spectra Physics Model 164-01 Krypton ion laser, Coherent Radiation Models CR12 argon ion and CR500K krypton ion lasers. Laser excitation ranging from 476 to 753 nm was used with the power at the sample restricted to < 50 mW so as to avoid sample decomposition. Detection of the scattered radiation was by standard photon-counting techniques employing a RCA C31034 photomultiplier. Band wavenumbers were calibrated using the emission spectrum of neon and typical slit widths of 200 μm were employed, giving a bandpass of 2 cm^{-1} at 647 nm. Samples were studied as crystals or in capillary tubes. Pressed discs diluted in potassium bromide were also used effectively to eliminate fluorescence. Divided disks were prepared including KClO_4 as an internal standard. Spectra were recorded both at 80 K and at room temperature.

Fourier transform infrared spectra were recorded using a Digilab FTS-60 Fourier transform infra-red spectrometer equipped with a globar source, KBr beamsplitter and a TGS pyroelectric detector. The bench was purged with air recycled through a molecular sieve air drier. Samples were prepared as KBr disks.

Electronic Absorption Spectra: Ultra violet-visible spectra were recorded with a Shimadzu Model 160 ultra violet-visible spectrophotometer. Solvents were either spectroscopic grade or purified by standard methods. Diffuse reflectance spectra were recorded with a Pye Unicam SP700 spectrometer using MgCO_3 as a reference.

Table 2: Elemental Analyses and Synthetic Methods.

No.	Formula	M_R g mol ⁻¹	Calculated %				Found %				MP °C	Synthetic Method. /[Ref.]
			C	H	N	Other	C	H	N	Other		
I	$C_{13}H_{12}N_4$	224.27	69.6	5.4	25.0		69.8	5.6	25.2		115-117	Irving, Gill & Cross./[10]
II	$C_{14}H_{14}N_4$	238.29	70.6	5.9	23.5		70.7	5.8	23.7		124-126	Irving, Gill & Cross./[10]
III	$C_{15}H_{16}N_4$	252.3	71.4	6.4	22.2		71.1	6.5	22.5		96-98	Burns & Cunningham./[11]
IV	$C_{15}H_{16}N_4$	252.3	71.4	6.4	22.2		71.1	6.5	22.5		73-74	Burns & Cunningham./[11]
V	$C_{17}H_{20}N_4$	280.37	72.8	7.2	20.0		72.	7.2	19.6			Neugebauer & Trischmann./[12]
VI	$C_{19}H_{16}N_4$	300.36	76.0	5.4	18.7		75.8	5.3	18.0			Todd./[13]
VII	$C_{14}H_{14}N_4$	238.29	70.6	5.9	23.5		70.5	5.8	23.9			Commercial (BDH).
VIII	$C_{14}H_{12}N_4S$	256.33	60.9	4.7	21.9	12.5	61.0	4.5	21.7		168-170	Neugebauer & Fischer./[15]
IX	$C_{14}H_{14}N_4S$	270.35	62.2	5.2	20.7	11.9	70.5	5.8	23.9		109-110	McConnachie & Neugebauer./[14]
X	$C_{15}H_{16}N_4S$	284.37	63.4	5.7	19.7	11.2	63.5	5.9	19.9			Noda, Engelhardt <i>et al.</i> /[16]
XI	$C_{15}H_{16}N_4S$	284.37	63.4	5.7	19.7	11.2	63.5	5.9	19.9			Noda, Engelhardt <i>et al.</i> /[16]
XII	$C_{16}H_{18}N_4S$	298.40	64.4	6.1	18.8	10.7	64.9	6.3	18.9		128-129	Guillerez <i>et al.</i> /[17]
XIII	$K^+ C_{13}H_{11}N_4^-$	286.29	54.5	3.9	19.6	11.2	-	-	-			Noda, Engelhardt <i>et al.</i> /[16]

X-ray Crystal Structures.

The first reported crystal structure for a formazan was that published by Omel'chenko *et al.* [18] for 1,5-diphenylformazan in 1973, more than eighty years after the first reported synthesis of formazans. The structure was determined by photographic methods as part of an investigation of proton transfer in the crystalline state at room temperature. Since that first structure four other 1,5-diphenylformazans have had their structures determined over the past fifteen years. These include three S-alkyl-dithizones and dithizone itself [19-23]. As no comprehensive study of the structures of 1,5-diphenylformazans has ever been undertaken we have recently determined the structures of 3-methyl-, the orange and red isomers of 3-ethyl-, 3-*tertiary*-butyl and 1-methyl- 1,5-diphenylformazans as well as the structure of tribromoformazan.

A summary of the known crystal structures, together with a summary of the important determined parameters of 1,5-diphenylformazans is given in Table 3.

Several striking similarities are evident when comparing the known crystal structures. The molecules show a tendency to planarity of the backbone with the phenyl rings and the 1- and 3-substituents. While the phenyl groups are all 'normal' there is considerable delocalisation of electrons along the formazan backbone and into the phenyl rings. This delocalisation of electrons does not generally extend into 1- or 3-substituents. The N-N and C-N bond lengths in the backbone are all intermediate between a single and double bond.

While there are changes in the bond lengths in the backbone for different formazans there is no clear reflection of the particular configuration assumed. The azo, azomethine and hydrazinyl bond lengths do not vary from the average by more than 0.03 Å in any of the formazans with the exception of dithizone in which two protons are located. The stability of the preferred configuration therefore is not markedly affected by these bond lengths.

It appears that in the majority of formazans the steric effect of the C3 substituent is the most important factor in determining the configuration of the particular formazan. The ethyl and ethylthio substituents clearly represent borderline functional groups in that for formazans with small C3 substituents, such as -H, -CH₃ and =S, the orange *anti,s-trans* configuration is favoured whereas for formazans with the bulkier C3 substituents, -Bu^t, -Ph and -SMe, either the *syn,s-trans* or *syn,s-cis* configurations are thermodynamically more stable in the solid state at room temperature.

Table 3: Crystal Structure Data for 1,5-Diphenylformazans.

No.	Crystals/ Colour	Configuration	Space Group	Z	$\frac{a \quad b \quad c}{\text{\AA}}$			$\begin{array}{c} \\ \text{---N}_4\text{=N}_3\text{---C}_3\text{=N}_2\text{---N}_1\text{H---} \\ \text{Bondlengths / \AA} \end{array}$										Ref.
I	not stated	<i>anti,s-trans</i>	$C2/c$	8	25.278 ₅	7.085 ₂	20.645 ₅	1.41 ₅	1.26 ₂	1.35 ₀	1.31 ₀	1.32 ₁	1.39 ₂					[18]
II	orange	<i>anti,s-trans</i>	$P2_1/c$	4	8.133 ₁	19.085 ₄	9.364 ₂	1.423 ₄	1.264 ₃	1.400 ₄	1.302 ₃	1.339 ₃	1.402 ₃					[24]
III	orange	<i>anti,s-trans</i>	$P2_12_12_1$	4	9.281 ₁	17.986 ₂	8.474 ₁	1.422 ₃	1.269 ₂	1.403 ₂	1.298 ₂	1.337 ₂	1.400 ₂					[11]
IV	red	<i>syn,s-trans</i>	$P2_1/n$	4	5.211 ₁₁	9.835 ₁₂	25.95 ₆	1.417 ₁₅	1.265 ₁₃	1.379 ₁₅	1.308 ₁₅	1.361 ₁₃	1.389 ₁₅					[11]
V	red	<i>syn,s-cis</i>	$P2_1/c$	8	11.235 ₃	20.117 ₅	14.176 ₃	1.422 ₇	1.279 ₇	1.404 ₇	1.316 ₇	1.310 ₇	1.386 ₈					[24]
VI	deep red	-	-	-	-	-	-	1.431 ₈	1.282 ₇	1.405 ₈	1.305 ₈	1.334 ₇	1.402 ₈					
VII	orange	<i>anti,s-trans</i>	$I2/a$	8	28.402 ₇	5.640 ₁	15.688 ₄	1.427 ₃	1.273 ₂	1.388 ₃	1.295 ₂	1.340 ₂	1.414 ₂					[25]
VIII	black	<i>anti,s-trans</i>	$P2_1/n$	4	4.70	22.25	11.95	1.39	1.29	1.35	1.34	1.30	1.38					[19,20]
IX	dark red	<i>syn,s-trans</i>	$P2_12_12_1$	4	25.48	10.01	5.33	1.424	1.266	1.391	1.300	1.344	1.391					[21]
X	orange	<i>anti,s-trans</i>	$P2_1/a$	4	11.027 ₆	8.627 ₇	15.487 ₈	1.418	1.296	1.437	1.360	1.344	1.425					[26]
XI	dark red	-	-	-	-	-	-	-	-	-	-	-	-					
XII	deep red	<i>anti,s-trans</i>	$Pca2_1$	2	19.782	17.321	9.325	1.42	1.26	1.405	1.305	1.335	1.404					[22]
XIII	metallic brown	<i>anti,s-trans</i>	$Pbca$	8	28.942	13.247	7.163	1.434	1.276	1.410	1.320	1.346	1.382					[16]

subscripts denote uncertainties.

Two isomers have been structurally identified for 3-ethyl-1,5-diphenylformazan (Figure 2). When recrystallised from methanol/water,

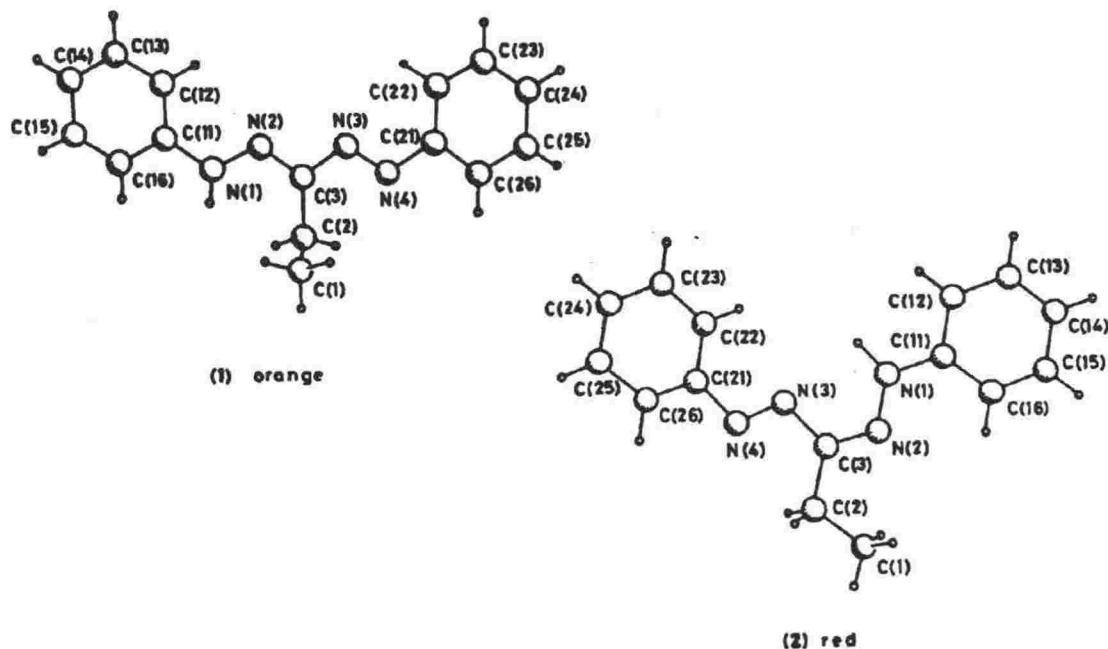


Figure 2: The Orange and Red Isomers of 3-ethyl-1,5-diphenylformazan [11].

orange needles are given in excellent yield. However, when pure orange 3 ethyl- is dissolved in cyclohexane and allowed to equilibrate in the dark an intense red solution is attained which gives red needles in low yield. However, this formazan is not unique in yielding two isomers in the solid state, 3-ethylthio-1,5-diphenylformazan also gives rise to two isomers although both of these have yet to be structurally identified.

A third pair of formazan isomers has been structurally determined. Espenbetov *et al.* [27] have recently published results on the x-ray analysis of the two crystalline forms of (1,3-diphenyl-5-(1',2'-dihydro-2'-methyl-4'-chloro-1'-phthalazinylidene) formazan) (Figure 3). The structural analysis confirms the *E* (*anti,s-trans*) and *Z* (*syn,s-cis*) relationship of the two isomers. In this case the configurations assumed are clearly a result of the very large substituent at the 5-position. This group forces the 1 and 3

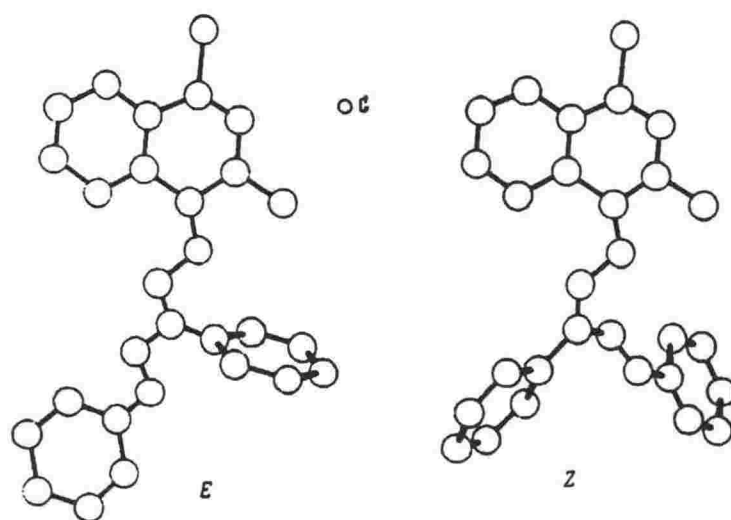


Figure 3: The *E* and *Z* Isomers of (1,3-diphenyl-5-(1',2'-dihydro-2'-methyl-4'-chloro-1'-phthalazinylidene) formazan) as shown by Espenbetov *et al.* [27]

phenyl rings out of the plane of the molecule and therefore delocalisation of electrons over the backbone is lost.

Five crystal structures are available for 3-thioalkylated-1,5-diphenyl formazans (-SH, -SCH₃, -S(CH₃)₂CH, -SCH₂COOH and potassium dithizonate) [16,19-23]. These are all either *anti,s-trans* or *syn,s-trans* configurations. No *syn,s-cis* configurations have been established.

The configurations of the thioalkylated 1,5-diphenylformazans may be interpreted in terms of three competing effects. Firstly, the steric effect at C3 is lessened due to the S-bridge between the formazan backbone and the alkyl substituent. This tends to favour the *anti,s-trans* and *syn,s-trans* configurations over the *syn,s-cis*. Secondly, the *anti,s-trans* configuration can be stabilised by an intramolecular hydrogen bond, N-H...S, unavailable in other formazans. Thirdly, the *syn,s-trans* configurations may be stabilised by more favourable packing in the crystal lattice.

The electron donating ability of the alkyl substituent increases from methyl to ethyl to *isopropyl* and therefore the electron density at the sulphur atom bonded between these alkyl substituents and the delocalised formazan backbone increases in the same order. The intramolecular hydrogen bond N-H...S becomes more favourable from -SCH₃ to -SCH₂CH₃ and -S(CH₃)₂CH.

The 3-methylthio assumes the *anti,s-trans* configuration in the solid state. The steric effect and, perhaps, the efficient crystal packing over-

rides the influence of the intramolecular hydrogen bond. On the other hand, this situation is reversed for the 3-isopropylthio which assumes the *anti,s-trans* configuration. For 3-ethylthio these effects are in balance allowing the isolation of two isomers in the solid state.

This interpretation is consistent with the fact that 3-SCH₂COOH assumes the *syn,s-trans* configuration. The CH₂COOH is electron withdrawing so the electron density at the sulphur atom is even less than that for 3-methylthio.

All of the 3-substituted formazan structures which have been determined are characterised by inter- or intramolecular hydrogen bonds. The *anti,s-trans* configuration has an intermolecular hydrogen bond. The *syn,s-trans* and *syn,s-cis* configurations have intramolecular hydrogen bonds and this difference is reflected in the generally lower melting point of these last red formazans.

While it appears that the steric effect of the C3 substituent is the most important factor in determining the configuration adopted by a particular formazan in the solid state, the effects of intra or intermolecular hydrogen bonding and the maintenance of an all planar molecule is also seen as important. The electronic properties of the C3 substituents would appear to play a secondary role.

Unequivocal solid-state structures of three of the four principle isomers (Figure 1) makes identification of these isomers by other spectroscopic methods viable. The availability of solid state and solution nmr and Raman spectroscopies bridges the gap between the solid state and solution structures.

¹³C Solid State Nuclear Magnetic Resonance Spectra.

Solid-state, high resolution ¹³C nmr spectroscopy involving a combination of cross polarisation, high power proton decoupling and magic angle spinning, has been applied to many systems. In solid state nmr some of the motional degrees of freedom are quenched. The application of this technique to the formazan system allows both the identification of individual isomers and the identification of particular configurations [11], even in the absence of single-crystal x-ray analyses. A study of the chemical shifts provides a quantitative structural probe.

In the solid state, assignments are based on the use of short contact times to identify quaternary carbon signals, TOSS experiments and multiple and fast spinner-speeds to reduce the influence of spinning-sidebands. Representative spectra for three formazans in each of the characterised structures are shown in Figure 4 and the resonances for all the formazans studied are given in Table 4.

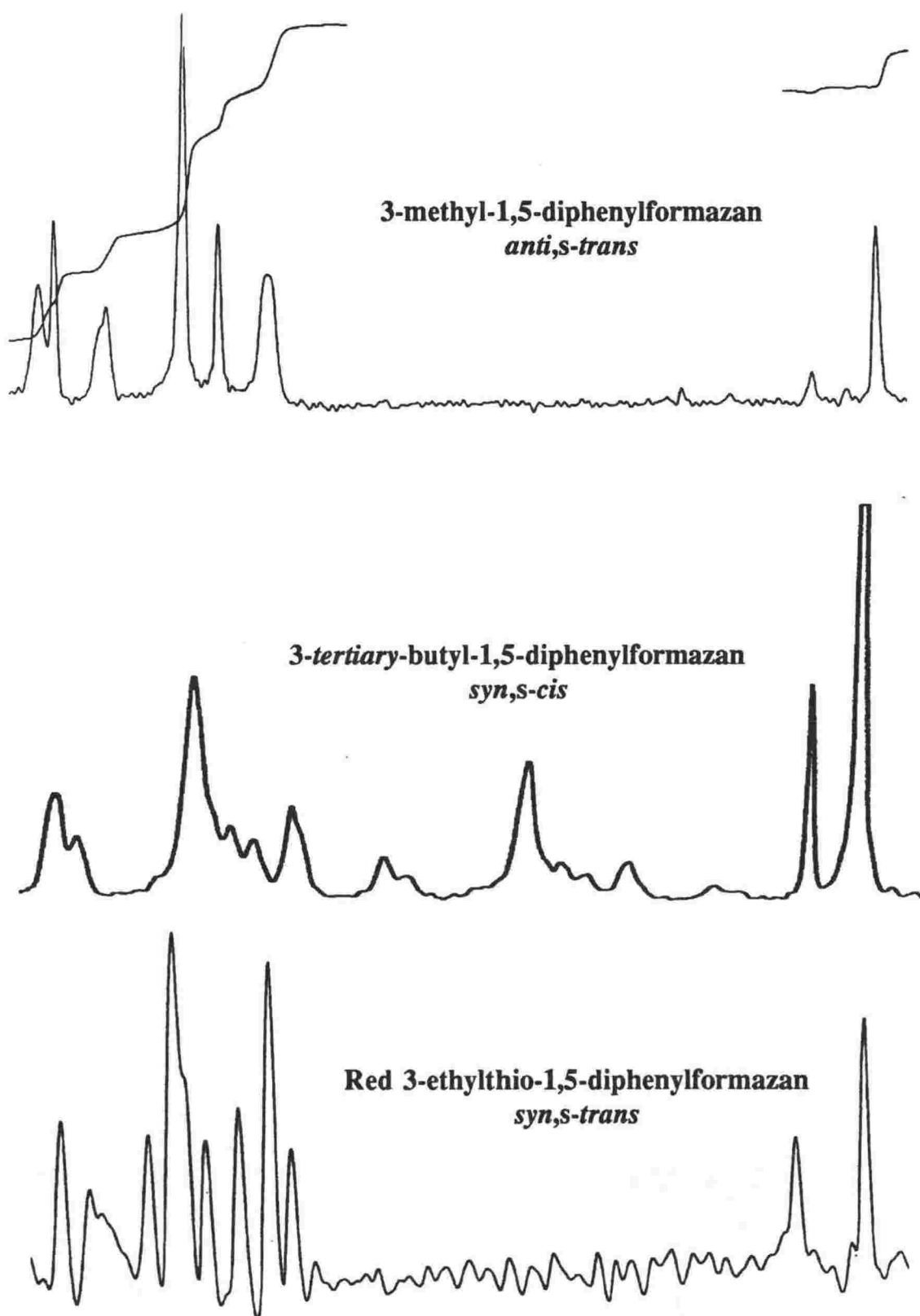


Figure 4: Solid state ^{13}C MAS Nmr Spectra for 3-methyl-, 3-*tertiary*-butyl- and the Red Isomer of 3-ethylthio-1,5-diphenylformazan.

In the solid state the ^{13}C nmr spectra are characterised as follows. Three groups of signals are observed: those for quaternary carbon at high field (ca. 150 ppm); those for phenyl carbon at mid field (ca. 120 ppm) and those for 1- or 3-substituents at low field (alkyl) or mid field (aryl).

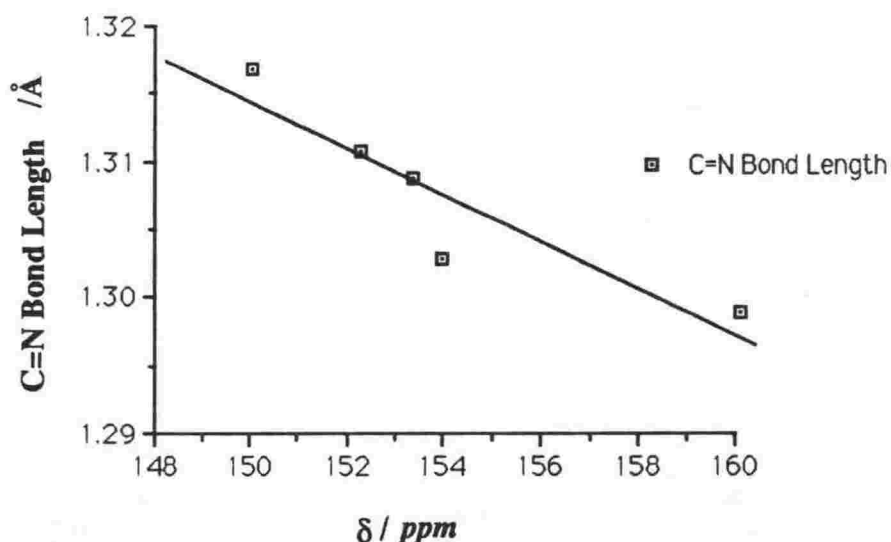
Quaternary carbon is identified by the use of short contact times and exact assignments are based on judicious 1- and 3-substitution and the use of model compounds.

Phenyl carbon signals characteristically appear between 130 and 110 ppm. Equivalent and non-equivalent 1- and 5-phenyl rings are resolvable.

1- or 3-substituent carbon is readily identified and the position and relative intensities of these peaks is invaluable when two isomers are present (e.g. 3-ethyl, 3-S-ethyl) in assigning the corresponding solution spectra.

The signal observed for the C3 carbon itself is seen to be dependent both upon the substituent (hydrogen, alkyl, aryl, sulphur, halogen) and the resulting chemical environment. When the substituents provide the same chemical environment, for example alkyl substituents, the corresponding signals for the C3 carbon are seen to reflect the C=N bond length. A plot of the chemical shift versus the C=N bond length is shown in Figure 5 for 3-alkyl-1,5-diphenylformazans.

Figure 5: Chemical Shift vs C=N Bond Length



The shorter double bond and concomitant increase in electron density are reflected in the upfield resonance of orange 3-ethyl-1,5-diphenylformazan when compared with red 3-*tertiary* butyl-1,5-diphenylformazan.

Signals are observed for each of the quaternary phenyl carbons when they are in different chemical environments. The *anti,s-trans* and *syn,s-trans* configurations both result in the observation of discrete signals for

Table 4: Resonances /ppm for the Solid State ^{13}C MAS Nmr Spectra of Isomeric 1,5-Diphenylformazans.

Compound	C3	C11	C21	C-phenyl	C-subst.
I	152.1	147.9	144.9	130.6 123.3 114.8	
II	155.8	153.2	144.0	130.2 124.1 114.7	7.80
III	159.9	152.9	144.8	131.2 124.2 122.9 121.2 115.8 114.8	15.4 10.6
IV	153.2	148.2	144.2	132.0 122.1 117.12 114.0	22.5 10.1
V	149.8	146.5		129.4 123.8 120.3 114.6	38 31
VI	147.1	137.9		129.0 113.5	129.0 113.5
VII	152.5	146.0		130.2 121.9 115.8	34
VIII	170.0	140.3		129.0 124.2 119.3	
IX	151.3	147.1	143.3	133.2 131.5 129.7 120.4 115.2 111.8	14.3
X	153.0	144.8	142.8	129.8 122.7 116.0	28.1 15.4
XI	151.4	146.5	144.4	136.0 131.7 126.3 120.7 115.2 111.5	24.9 13.3
XII	153.3	147.4	142.6	130.8 124.5 116.8 113.9	38.7 24.8 22.2

the C11 and C21 carbon atoms. However, the *syn,s-cis* configuration results in the observation of only one signal. The intramolecular hydrogen bond between the N1-H1 and N5 must be held to account for bringing together the two expected resonances.

Vibrational Spectroscopy.

A study of the Raman active phonons of a molecular crystal has been shown to be important for an understanding of the intra- and inter-molecular interactions operating in a system. A study of microcrystalline and powdered samples retains much of this information.

In previous infrared and Raman studies [28] it has been suggested that the various forms of the substituted formazans, both chelated and unchelated, were spectroscopically distinguishable. In these cases it may be countered that substitution and/or ^{15}N labelling of one or more of the nitrogen atoms perturbs the system to the extent that one resonance form becomes the preferred one. Infrared studies are of limited value in the examination of a variety of formazans as the comparatively weak (NH) band, which may be used to distinguish the respective configurations is obscured by the (CH) vibrations. Raman spectroscopy, however, can be shown to accurately reflect the configuration of the formazan and give detailed information on the nature of the chromophore.

Assignment of the Raman Bands.

A list of the Raman active phonons for the series of isomeric 1,5-diphenylformazans is shown in Table 5. Several Raman spectroscopic studies of formazans and metal dithizonates have been published in the literature [29]. Even with the aid of isotopic substitutions, low temperature solid and solution samples, the assignments of the individual bands still remain the subject of some uncertainty. A normal coordinate analysis is appropriate but the complexity of such a task precludes its inclusion in this study. Although we have accurately determined the wavenumbers of the Raman active phonons we have refrained from assigning individual bands, preferring instead to relate the overall pattern of bands with the established solid state structures. This, then, allows us to establish the configurationally sensitive phonons.

The Raman spectra, representative examples of which are described in Figures 6-8, are characterised by two types of band: those which arise from vibrations of the 1- and 5- phenyl rings, generally occurring at *ca.* 1600 cm^{-1} and at *ca.* 1000 cm^{-1} and those which arise from vibrations of the formazan backbone, observed between 1600 and 1000 cm^{-1} . The assignments of the former type of bands are rather more straightforward

Table 5: Band Centre Wavenumbers (cm⁻¹) for the Raman Spectra of Isomeric 1,5-Diphenylformazans

-H	-CH ₃	CH ₂ CH ₃	-CH ₂ CH ₃	-Bu'	-C ₆ H ₆	-SH	-SCH ₃	SCH ₂ CH ₃	SCH ₂ CH ₃	SOH(CH ₃) ₂	N-CH ₃	K ⁺ HDz ⁻
1600	1598	1603	1600	1601	1598	1592	1600	1600	1603	1601	1597	1598
1592	1590	1591	1590						1598		1583	1584
	1580	1583										
1557	1511	1519		1522	1510	1522	1528	1520	1527	1520		
1487	1494	1500	1504	1505				1505	1505	1500	1498	1510
1450	1456	1461	1461			1459	1461	1474	1460	1458	1462	1424
1379	1413	1411	1408	1344	1349	1382	1382	1433	1390	1389	1399	1349
	1359	1373	1359	1363				1376			1371	-159.
	1321	1331	1339		1334							
	1315	1324	1322		1321		1324					
	1306	1306	1306	1310	1305	1305	1310	1300	1310	1309	1305	1311
1275	1273	1242	1285	1279	1271	1252	1264	1265	1263	1254	1280	1301
1234		1208	1192	1222	1204	1234						
1218	1206	1179	1170	1176	1181	1220		1214		1212	1212	1213
1178	1185	1172	1141	1169		1184	1188	1172	1185	1175	1184	
	1172	1147		1159	1147	1164	1155		1154	1155	1171	1168
1159	1145	1076	1062	1085		1146	1145	1138	1146	1131	1156	1127
1151		1059		1030		1021	1108		1115		1148	
1023	1011	1051									1120	
1000	996	998	1004	1001	983	1001	1004	998	1000	999	1035	997
995	981	994	985	984								991

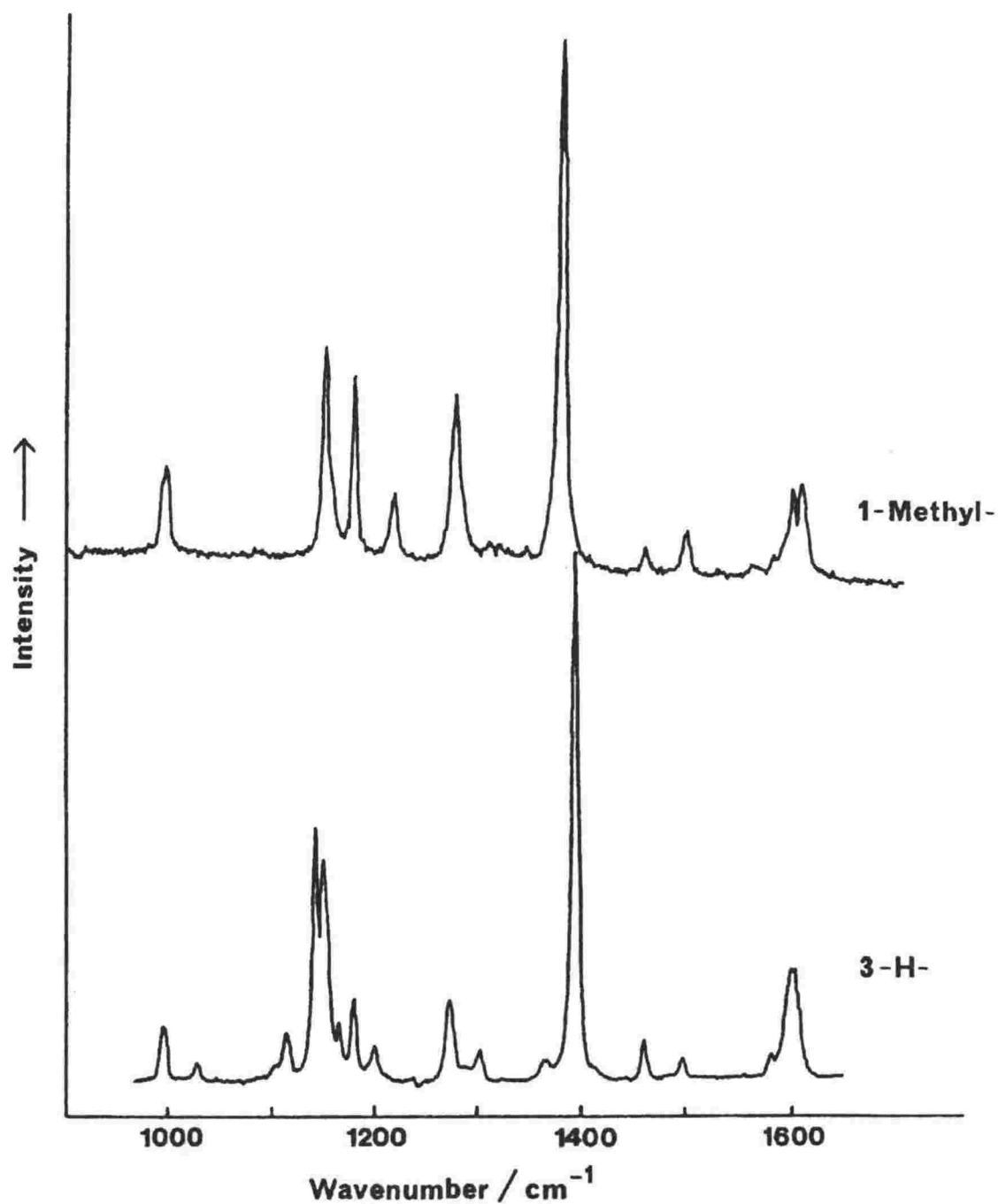


Figure 6: The Raman Spectra of 1,5-diphenylformazan (I) and 1-methyl-1,5-diphenylformazan (VII).

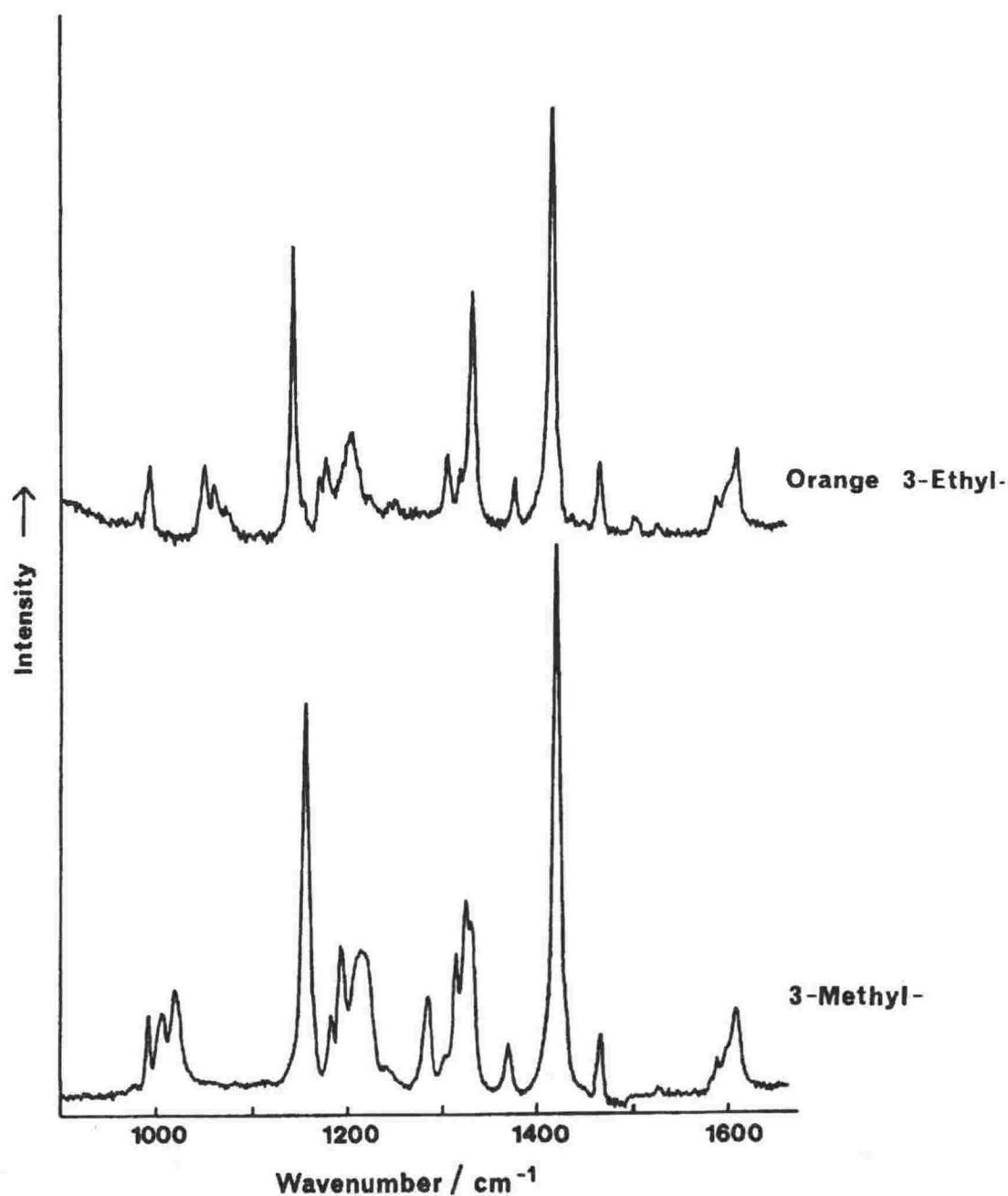


Figure 7: The Raman Spectra of 3-methyl-1,5-diphenylformazan (II) and the Orange Isomer of 3-ethyl-1,5-diphenylformazan (III).

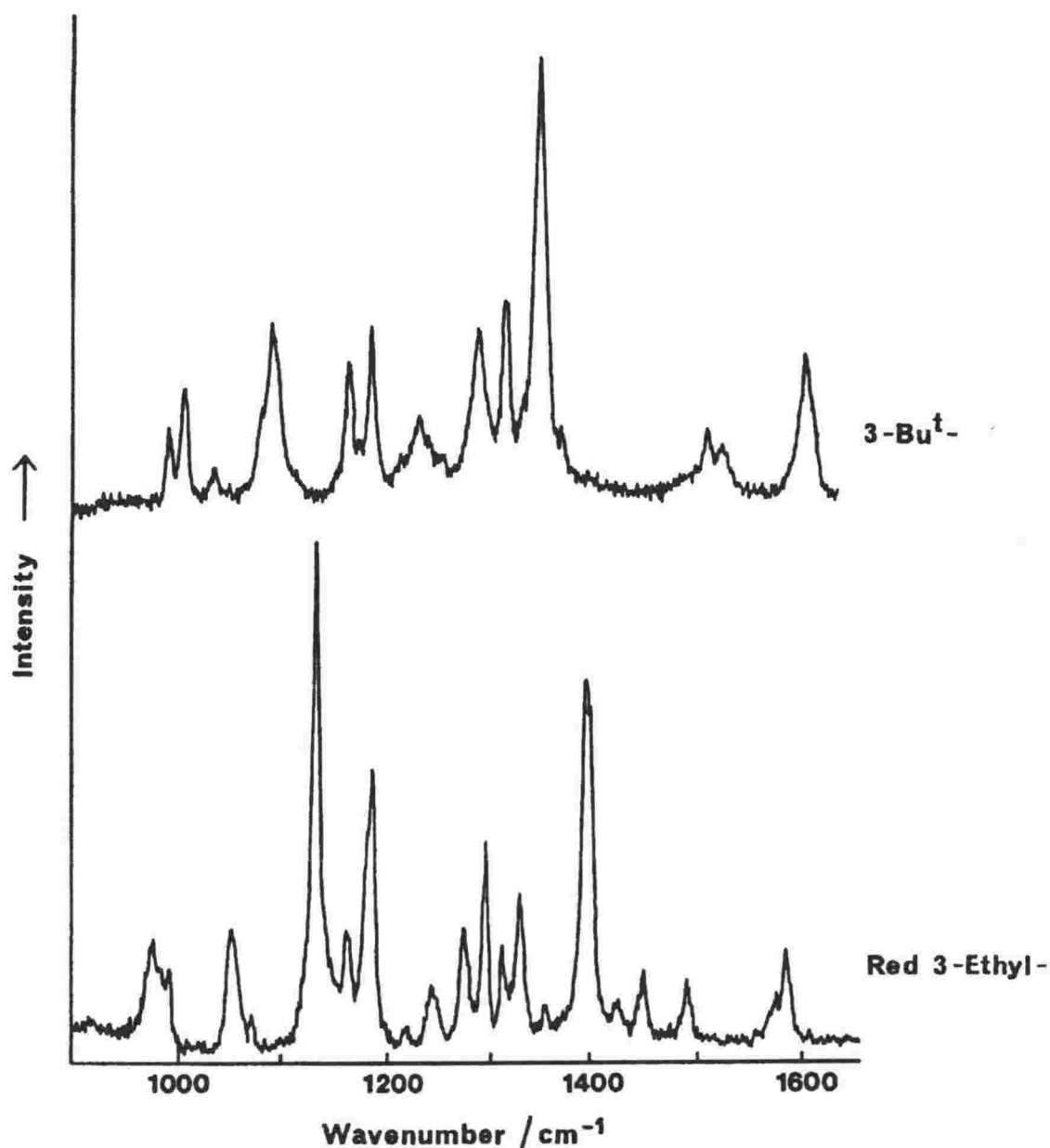


Figure 8: The Raman Spectra of the Red Isomer of 3-ethyl-1,5-diphenylformazan (IV) and 3-*tertiary*-butyl-1,5-diphenylformazan (V).

than the assignment of the latter. The vibrational assignments of Bright-Wilson [30] have been applied to the formazans recently. These assignments are both reasonable and appropriate.

It is a feature of these phenyl vibrations that they reflect the equivalence or non-equivalence of the 1- and 5- phenyl groups in the formazans. Symmetric configurations, such as *anti,s-trans* and *syn,s-cis*, result in the observation of narrower bands of higher intensity than do asymmetric *syn,s-trans* formazans. These latter formazans result in less intense bands for the phenyl groups which are broader and often resolvable into more than one distinct band. This observation is invaluable in assigning configurations.

The assignment of the remainder of the peaks observed between *ca.* 1600 and *ca.* 1000 cm^{-1} is more difficult. These vibrations are largely ascribable to the formazan backbone and, to a lesser extent, the 3-substituent. It is certain that considerable coupling of the N-N and C-N units in the formazan backbone occurs. To what extent awaits the results of a normal coordinate analysis.

The most intense peaks in the spectra occur at *ca.* 1400 and *ca.* 1150 cm^{-1} . Various authors have assigned these to vibrations of the N=N, N-N or N-C=N fragments. Less intense bands have been assigned to NH-Ph or N-Ph vibrations [29].

The appearance of the most intense band at *ca.* 1400 cm^{-1} does correspond with the configurations observed in the solid state. In formazans with the *anti,s-trans* configuration, this most intense band generally occurs at higher wavenumber than the corresponding band in the spectra of *syn,s-trans* and *syn,s-cis* formazans. This effect would seem to be the result of the intramolecular hydrogen bonds seen in the *syn,s-trans* and *syn,s-cis* formazans and this adds support to the assignment of the vibrations as largely coupled. Further, for orange *anti,s-trans* formazans the C-N and C=N bond lengths directly relate to the position of the peak. The band appears at lower energy as the C=N bond lengthens and the C-N bond shortens, both approaching the *aromatic* distance of 1.31 Å. This trend is not so apparent in red formazans whose solid state structures are less well known.

It is the overall pattern of resonances that indicate the configuration of the respective formazan in the solid state. The symmetry or asymmetry of the configuration is indicated, from the phenyl group vibrations, as is the overall configuration by the position of the most intense band in the spectra. For orange formazans the position of this latter band also indicates the C-N and C=N bond lengths.

Mass Spectra.

Studies of the mass spectra of dithizone and the primary dithizonate complexes of Cu(II), Ni(II) and Co(III) have exhibited similar splitting schemes [31]. The mass spectra of isomeric formazans have been collected to ascertain if the splitting scheme shown was configuration dependent. The mass spectra of *cis* and *trans* isomers are generally very similar if not identical.

The principal peaks and the relative intensities are shown in Table 6. The following splitting schemes apply:

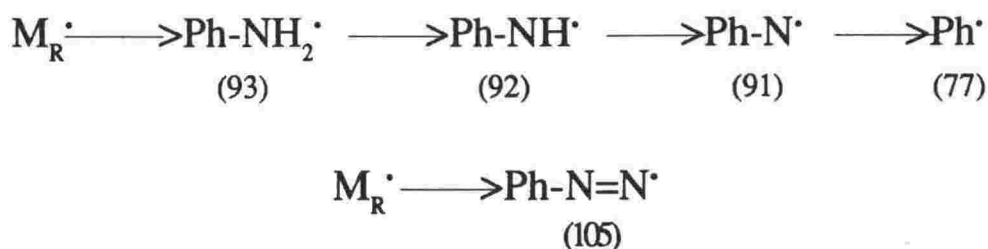


Figure 9: Splitting Scheme for 1,5-diphenylformazans.

Table 6: Ion Abundances for 1,5-diphenylformazans.

No.	Mass						$M_R \cdot$	$M_R - 77 \cdot$	$M_R - 105 \cdot$
	77	91	92	93	105	106			
I	27	10	100	14	6	1	22	58	10
II	47	50	100	34	3	-	37	6	55
III	46	52	100	39	3	3	32	9	-
IV	17	100	-	13	4	-	1	-	17
V	25	32	100	28	2	-	15	-	65
VI	9	8	100	12	2	-	11	1	34
VII	89	26	12	33	18	100	13	11	19
VIII	75	5	100	70	15	5	15	-	12
IX	31	16	100	12	4	-	9	-	24

It can be seen that while there is some correlation of splitting scheme with the configuration of the formazan the effect is by no means clear-cut. The mass spectra do not accurately reflect the configuration of the formazan in the solid state.

Solution Nmr and Absorption Spectra.

Solution nmr has been shown [11,32] to be of value in the study of many systems including formazans, although the studies which have been published to date have largely concerned sugar formazans.

In this study nmr spectra have been observed in a number of solvents including CDCl_3 , C_6D_6 , $(\text{CD}_3)_2\text{CO}$ and $(\text{CD}_3)_2\text{SO}$. In solution three groups of resonances are observed, similar to the solid state spectra, for quaternary, phenyl and 1- or 3-substituent carbon. The resonances in solution are expected to be the same as those observed in the solid state and this greatly assists in the assignment of the peaks.

Important differences are observed in the solution spectra when compared with the solid state spectra, and these are directly attributable to solvent effects, tautomerism and equilibration in solution. Equilibration can be further observed and monitored by following the absorbance spectra of the spectroscopic solutions used for nmr. These solvent dependent equilibria may result in the observation of overlapping signal-patterns for each of the configurations present.

Tautomerism in solution at ambient temperatures produces changes in the observed spectra. The tautomeric shift of the N1-H1 proton is fast on the timescale of the nmr experiment and therefore the averaging of some resonances are observed.

By careful selection of the solvent (protic/aprotic) and by the protection of the spectroscopic solution from the influences of temperature and light, known to promote the formation of orange formazans, high relative concentrations of the configuration of interest are possible.

The resonances for a selection of representative nmr spectra in several solvents are listed in Table 7. The interpretation of the following trends have allowed the characterisation of the individual formazan isomers present in solution. The *anti,s-trans* configuration results in the observation of one resonance at *ca.* 145 ppm attributable to C3 carbon, although this is dependent upon the 3-substituent to a certain extent. One signal only is observed for C11 and C21 carbons coincident at *ca.* 135 ppm due to the tautomerism of the N1-H1 proton. A three peak multiplet is observed for the 1- and 5- phenyl carbon nuclei, again due to the exact equivalence of the chemical environment. The *syn,s-cis* configuration is

Table 7: Resonances for ^{13}C Nmr Spectra of Some 1,5-Diphenylformazans in Various Solvents.

Solvent	C3	C11	C21	C-phenyl	C-subst.
3-Methyl-1,5-diphenylformazan					
CDCl_3	154.2	149.5	149.5	129.3 126.3 118.3	6.60
	152.1	147.1	143.2	130.5 129.0 122.9 122.1 114.4	16.06
$(\text{CD}_3)_2\text{CO}$	155.0	149.5	149.5	129.9 126.9 114.7	7.35
		147.5	147.5	weak bands	15.50
C_6D_6	154.1	148.7	148.7	129.4 126.5 118.8 130.5	6.05
	153.9	147.1	144.1	127.5 123.3 122.2 114.6	16.23
1,3,5-Triphenylformazan					
CDCl_3	147.88	141.09	137.43	129.43 128.41 127.65 127.50 125.82 118.79	
$(\text{CD}_3)_2\text{CO}$	148.87	138.05	138.05	129.28 128.57 128.49 126.80 119.75	
C_6D_6	148.24	141.65	138.09	129.62 129.51 129.05 128.72 128.34 128.13 128.02 127.87 127.70 127.53 126.41 119.16	
3-Tertiary -butyl-1,5-phenylformazan					
CDCl_3	150.2	148.2	148.2	118.4 129.3 126.7	38.05 29.88
$(\text{CD}_3)_2\text{CO}$	150.9	149.4	149.4	119.2 130.2 127.7	38.56 30.01

3-Ethylthio-1,5-diphenylformazan

CDCl ₃	152.30	147.74	147.74	130.75	129.51	27.45	15.75
			146.17	129.34	129.03		
			141.84	126.73	123.02		
				118.38	114.82		
(CD ₃) ₂ CO	153.05	148.24	148.24	130.73	129.65	27.38	24.47
			146.51	129.41	129.32	15.68	14.53
			142.58	126.71	123.30		
				122.98	118.98		
				114.95			
C ₆ D ₆	153.28	149.06	149.06	131.39	130.13	27.55	24.61
			146.31	130.08	127.31	15.83	14.80
			143.60	123.41	123.35		
				119.25	115.62		

also a symmetric system and this results in the observation of one C3 resonance, one signal for C11 and C21, again coincident, and three phenyl resonances. These two symmetric formazans can only be distinguished with the assistance of the uv-visible absorption spectra. The *syn,s-trans* configuration results in the observation of one C3 resonance, two quaternary phenyl carbon resonances for C11 and C21, with the C11-N1H1 resonance being downfield and relatively more intense than the C21 resonance, and up to six phenyl signals due to the non-equivalence of the chemical environment for the two phenyl groups.

Conclusion.

The results of the Raman, nuclear magnetic resonance and ultra violet investigations have allowed the identification of the solid state and solvent-dependent structures of the 1,5-diphenylformazans studied. All of the predicted solid state structures agree with the known x-ray crystal data. The results are summarised below.

1,5-diphenylformazan is known to assume the *anti,s-trans* configuration in the solid state [18]. The solid state Raman and nmr studies confirm this configuration. The solution nmr and ultra violet-visible spectroscopic studies show that the *anti,s-trans* configuration is preferred in protic solvents but the *syn,s-cis* is in equilibrium with the *anti,s-trans* configuration in aprotic solvents. This differs from the expected *syn,s-trans* configuration and the near-aromatic formazan backbone bond lengths are held to account for the stability of the *syn,s-cis* configuration in aprotic solvents.

3-methyl-1,5-diphenylformazan assumes the *anti,s-trans* configuration

in the solid state. The Raman and solid state nmr investigations confirm this configuration. In methanol solution the *anti,s-trans* is the only species present. However, if the solvent is changed from acetone to chloroform to benzene this *anti,s-trans* configuration is in equilibrium with the *syn,s-trans* configuration. This latter form becomes increasingly dominant in aprotic solvents.

3-ethyl-1,5-diphenylformazan exists in two isomers in the solid state [11]. These have been identified as *anti,s-trans* for the orange and *syn,s-trans* for the red isomer. The Raman and solid state nmr spectra correctly predict these two structures respectively. In solution the species present tend towards the same equilibrium mixture regardless of the starting isomer if allowed to stand in the dark for a time. The equilibrium mixture is then solely solvent dependent. In C_6D_6 the *syn,s-trans* is the dominant species. In methanol the *anti,s-trans* is the dominant species. In $CDCl_3$ and $(CD_3)_2CO$ the two species are in equilibrium.

3-tertiary-butyl-1,5-diphenylformazan assumes the *syn,s-cis* configuration in the solid state [24]. It is the only 1,5-diphenylformazan to have the structure unequivocally substantiated in the solid state. The Raman and solid state spectra correctly predict this configuration. In solution only the *syn,s-cis* form is present irrespective of the solvent chosen. The bulky tertiary-butyl substituent is held to account for the disfavouring of a *trans* arrangement around the C=N bond. There is no evidence for the existence of the *syn,s-trans* configuration in solution.

1,3,5-triphenylformazan has not been identified by a x-ray crystallographic determination. In the solid state the Raman and nmr spectra both indicate that the *syn,s-cis* and *syn,s-trans* configurations are both present. This conclusion agrees closely with the recent findings of

Veas [33] who has confirmed a thermal pathway between two red triphenylformazans, which she assumed to be the *syn,s-trans* and *syn,s-cis*. In protic and aprotic solvents these two configurations are both seen with the *syn,s-trans* form being the preferred one in the equilibrium.

3-mercapto-1,5-diphenylformazan is known to assume the *anti,s-trans* thione form in the solid state [19,20]. The Raman and solid state nmr studies confirm this exact configuration. In $CDCl_3$ the *anti,s-trans* form is also the only configuration seen.

3-methylthio-1,5-diphenylformazan is known to assume the *syn,s-trans* configuration in the solid state [21]. In the solid state Raman and nmr studies this configuration is confirmed. In solution the *syn,s-trans* configuration is in equilibrium with the *anti,s-trans* configuration. The ratio of the two species would appear to be almost equal in these solvents.

3-ethylthio-1,5-diphenylformazan may be isolated in two distinct isomers in the solid state, orange and red respectively. Preliminary x-ray studies have shown the orange isomer to assume the *anti,s-trans* configuration. The Raman and nmr studies in the solid state predict the

anti,s-trans configuration for the orange isomer and the *syn,s-trans* configuration for the red isomer. This result parallels the structural characterisation of the orange and red isomers of 3-ethyl-1,5-diphenylformazan. In solution the two isomers tend towards the same equilibrium mixture of configurations. The *anti,s-trans* form is in equilibrium with the *syn,s-trans* form in all of the solvents studied.

3-isopropylthio-1,5-diphenylformazan is known to assume the *anti,s-trans* configuration in the solid state [22]. The solid state Raman and nmr studies confirm this configuration. In solution the *anti,s-trans* form is in equilibrium with the *syn,s-trans* form, although in all the solvents the *anti,s-trans* form would seem to be the more dominant.

1-methyl-1,5-diphenylformazan exists in the *anti,s-trans* configuration in the solid state [25]. The solid state Raman and nmr studies confirm this observation. In solution this *anti,s-trans* form is also the only one seen in both protic and aprotic solvents. The 1-methyl substituent must be held to account for this observation.

We have demonstrated conclusively that the combination of Raman, nuclear magnetic resonance and ultra violet-visible absorption spectra can substantiate the solid state and solution structures for the 1,5-diphenylformazans studied.

References.

- 1 von Pechmann, H., *Chem. Ber.*, **25**, 3175 (1892).
- 2 Bamberger, E., *Chem. Ber.*, **25**, 3547 (1892).
- 3 Ilford, Brit. P.: 884 494 (1900); Brit. P.: 908 299 (1961); Ger. P.: 1 146 753 (1963); Brit. P.: 2 107 882 (1970).
- 4 Nineham, A.W., *Chem. Rev.*, **55**, 355 (1955).
- 5 Mester, L., *Adv. Carbohydrate Chem.*, **13**, 105 (1958).
- 6 Hooper, W.D., *Rev. Pure and Appl. Chem.*, **19**, 221 (1969).
- 7 Bednyagina, N.P., Postovskii, I.Ya., Garnovskii, A.D. and Osipov, O.A., *Russ. Chem. Rev. (Engl. Transl.)* **44**, 493 (1975).
- 8 Otting, W. and Neugebauer, F.A., *Z. Naturforsch., Teil B.*, **23**, 1064 (1968).
- 9 Hausser, J., Jerchel, D. and Kuhn, R., *Chem. Ber.*, **82**, 195 (1949).
Hausser, K., *Naturwissenschaften*, **36**, 313 (1949).
Kuhn, R. and Weitz, H., *Chem. Ber.*, **86**, 1199 (1959).
- 10 Kettrup, A. and Grote, M., *Z. Naturforsch., B*, **31**, 1689 (1976); Tiers, V.D., Kansas State University, Ph.D. Thesis, 1959; Tiers, V.D., Plován, S. and Searles, S., *J. Org. Chem.*, **25**, 285 (1960).
- 11 Burns, G.R., Cunningham, C.W. and McKee, V., *J. Chem. Soc., Perkin Trans. 2*, **1988**, 1275.
- 12 Neugebauer, F.A. and Trischmann, H., *Leibigs Ann. Chem.*, **706**, 107 (1967).
- 13 Todd, D., "Experimental Organic Chemistry", Prentice-Hall, Inc., New Jersey (1979), p 251.
- 14 McConnachie, G. and Neugebauer, F.A., *Tetrahedron*, **31**, 555 (1975).
- 15 Neugebauer, F.A. and Fischer, *Chem.*

- Ber.*, 107, 717 (1974).
- 16 Noda, H., Engelhardt, L.M., Harrowfield, J.MacB., Pakawatchai, C., Patrick, J.M. and White, A.H., *Bull. Chem. Soc. Jpn.*, 58, 2385 (1985).
- 17 Guillerez, J., Pascard, C. and Prange, T., *J. Chem. Res.*, (S) 308 (1978); (M) 3934 (1978).
- 18 Omel'chenko, Yu.A., Kondrashev, Yu.D., Ginzburg, S.L. and Neiganz, M.G., *Kristallografiya*, 19, 522 (1974).
- 19 Alsop, P.A., University of London, Ph.D. Thesis (1971).
- 20 Laing, M., *J. Chem. Soc., Perkin Trans. 2*, 1977, 1248.
- 21 Preuss, J. and Gieren, A., *Acta Crystallogr., Sect B*, 38, 535 (1982).
- 23 Hutton, A.T., Irving, H.M.N.H., Nassimbeni, L.R. and Gafner, G., *Acta Crystallogr., Sect B*, 35, 1354 (1979).
- 24 Cunningham, C.W., Burns, G.R. and McKee V., *J. Chem. Soc., Perkin Trans 2*, In Press.
- 25 Cunningham, C.W., Burns, G.R. and McKee V., Paper in Preparation.
- 26 Cunningham, C.W., Burns, G.R. and McKee V., Paper in Preparation.
- 27 Espebetnov, A.A., Litvinov, I.A., Struchkov, Yu.T., Bystrykh, N.N. and Buzykin, B.I., *Izv. Akad. Nauk SSSR, Ser. Khim.*, 4, 832 (1986).
- 28 Jerchel, D. and Edler, W., *Chem. Ber.*, 88, 1287 (1955); Le Fevre, R.J., Sousa, J.B. and Werner, R.L., *Aust. J. Chem.*, 9, 151 (1956); Foffani, A., Pecile, C. and Ghersetti, S., *Tetrahedron Lett.*, 16 (1956); Foffani, A., Pecile, C. and Ghersetti, S., *Adv. Mol. Spectrosc.*, 2, 769 (1962); Schiele, C., *Leibigs Ann. Chem.*, 689, 197 (1965); Schiele, C. and Arnold, G., *Tetrahedron Lett.*, 4103 (1966); Arnold, G. and Schiele, C., *Spectrochim. Acta*, 25A, 671 (1969); Arnold, G. and Schiele, C., *Spectrochim. Acta*, 25A, 685 (1969); Arnold, G. and Schiele, C., *Spectrochim. Acta*, 25A, 697 (1969); Kukushkina, I.I., Yurchenko, E.N., Ermakova, M.I. and Latosh, N.I., *Zh. Fiz. Khim.*, 46, 176 (1972), *Russ. J. Phys. Chem.*, 1 (1972) (Engl. Trans.); Kukushkina, I.I., Yurchenko, E.N., Arkhipenko, D.V. and Orekhov, B.A., *Zh. Fiz. Khim.*, 46, 1677 (1972), *Russ. J. Phys. Chem.*, 7 (1972) (Engl. Trans.); Lewis, J.W. and Sandorfy, C., *Can. J. Chem.*, 61, 809 (1983); Otting, W. and Neugebauer, F.A., *Z. Naturforsch., B*, 23, 1064 (1968). Takahashi, H., Yamada, O., Isaka, H., Igarashi, T. and Kaneko, N., *J. Raman Spectrosc.*, 19, 305 (1988).
- 29 Pemberton, J.E. and Buck, R.P., *J. Raman Spectrosc.*, 12, 76 (1982).
- 30 Bright-Wilson, E., *Phys. Rev.*, 45, 706 (1934).
- 31 Alsop, P.A. and Irving, H.M.N.H., *Anal. Chim. Acta*, 65, 202 (1973).
- 32 Kettrup, A. and Grote, M., *Z. Naturforsch., B*, 31, 1689 (1976); Tiers, V.D., Kansas State University, Ph.D. Thesis, 1959; Tiers, V.D., Plován, S. and Searles, S., *J. Org. Chem.*, 25, 285 (1960).
- 33 Veas-Arancibia, C., Louisiana State University and Agricultural and Mechanical College, Ph.D. Thesis (1986).

SUMMARY

This thesis has presented the major results of a structural and spectroscopic study of 3-substituted-1,5-diphenylformazans. The results of x-ray crystal structural analyses, solid state nuclear magnetic resonance, Raman and mass spectral analyses, together with some solution nuclear magnetic resonance, electronic absorption and kinetic studies have been presented.

The x-ray crystal structures of 3-methyl-1,5-diphenylformazan, the orange and red isomers of 3-ethyl-1,5-diphenylformazan, 3-*tertiary*-butyl-1,5-diphenylformazan, 1-methyl-1,5-diphenylformazan, 3-bromo-1,5-di-*para*-phenylformazan, di(3-bromo-1,5-diphenyltetrazolium)-decabromide, 3-chloro-1,5-diphenylformazan and the orange isomer of 3-ethylthio-1,5-diphenylformazan have been determined for the first time. All of these formazans together with 1,5-diphenylformazan, 1,3,5-triphenylformazan, 3-methylthio-1,5-diphenylformazan, the red isomer of 3-ethylthio-1,5-diphenylformazan, 3-*isopropyl*thio-1,5-diphenylformazan and the salt potassium dithizonate have been studied by solid state ^{13}C MAS nmr and Raman spectroscopy. These combined solid state techniques have allowed the unequivocal determination of the structures of these formazans. The mass spectra indicate that no discernable and reliable difference in the fragmentation patterns of the different configurations may be found.

Solution nmr and ultra violet-visible absorption spectra have allowed the identification of the solution configurations of the formazans studied and, more importantly, the dependence of said configurations upon the solvent system. These configurations are identified as the dark stable equilibrium species, as particular care to exclude the influences of heat and light was exercised.

The kinetics of the interconversions of the light and dark stable species for the metal dithizonates as well as the two isomers in the 3-ethyl-1,5-diphenylformazan equilibrium have been studied. Preliminary results have suggested that the interconversions of the dithizonates and formazans follow similar mechanisms. However, the details of the mechanisms indicated are more complicated than could be investigated in the present study.

This study has contributed largely to the structural studies of formazans and demonstrated a procedure for investigating the solution species and confidently determining the isomers present. It has demonstrated preliminary findings on the kinetics of the interconversions of the dark and light stable species and indicated appropriate areas of future study.

FUTURE STUDY

The x-ray structure determination of 1,3,5-triphenylformazan remains the most important structural result missing in the present study. Therefore, every effort should be exercised to remedy this omission. The solution behaviour of this formazan, then, could be more fully investigated as this is the most studied single formazan to date.

The interconversion schemes and mechanism of the interconversions still remain uncertain and are both appropriate areas of further study.

The exact assignments of the vibrational spectra also require explicit determination. A normal coordinate analysis for the formazans is overdue. Much Raman and infrared data is available, both in this study and in the wider literature, and while the task is by no means trivial it will be one of the more welcome results of the near future.

A significant, although serendipitous, result of this thesis was the synthesis and characterisation of the decabromide anion of the tetrazolium salt which resulted from the reaction of bromine with 1,5-diphenylformazan. Many new and interesting anions of a similar nature are possible by the reaction of halogens with formazans and this remains an area of intense interest.

Some preliminary results of Molecular Mechanics calculations on the 1,5-diphenylformazan system have been collected. The several x-ray crystal structures solved in his study make these calculations the source of much useful information, concerning the energies of the respective configurations and the barrier to interconversion between them. This area also remains one of intense interest.